NATIONAL TECHNICAL UNIVERSITY OF ATHENS
SCHOOL OF CIVIL ENGINEERING
LABORATORY OF METAL STRUCTURES

postgraduate diploma thesis

SEISMIC PERFORMANCE OF STEEL PALLET RACKS

student:

AVGERINOU STELLA

supervisors:

Vayas I._ professor, ntua

Castiglioni C. A._ professor, polimi

Athens, October 2012

EMK ME 2012/11

ΕΘΝΙΚΟ ΜΕΤΣΟΒΙΟ ΠΟΛΥΤΕΧΝΕΙΟ
ΣΧΟΛΗ ΠΟΛΙΤΙΚΩΝ ΜΗΧΑΝΙΚΩΝ
ΕΡΓΑΣΤΗΡΙΟ ΜΕΤΑΛΛΙΚΩΝ ΚΑΤΑΣΚΕΥΩΝ

μεταπτυχιακή εργασία

ΣΕΙΣΜΙΚΗ ΑΠΟΚΡΙΣΗ ΒΙΟΜΗΧΑΝΙΚΩΝ ΡΑΦΙΩΝ ΑΠΟ ΧΑΛΥΒΑ

φοιτήτρια:

ΑΥΓΕΡΙΝΟΥ ΣΤΕΛΛΑ

επιβλέποντες:

Βάγιας Ι._ καθηγητής, ΕΜΠ

Castiglioni C. A._ professor, polimi

Αθήνα, Οκτώβριος 2012

ΕΜΚ ΜΕ 2012/11

Αυγερινού Σ. (2012).
Σεισμική απόκριση βιομηχανικών ραφιών από χάλυβα
Διπλωματική Εργασία ΕΜΚ ΜΕ 2012/11
Εργαστήριο Μεταλλικών Κατασκευών, Εθνικό Μετσόβιο Πολυτεχνείο, Αθήνα.

Avgerinou S. (2012).
Seismic performance of steel pallet racks
Postgraduate Diploma Thesis EMK ME 2012/11
Institute of Steel Structures, National Technical University of Athens, Greece

national technical university of athens
school of civil engineering
laboratory of metal structures

postgraduate diploma thesis:

seismic performance of steel pallet racks

EMK ME 2012/11

author:
Avgerinou Stella

supervisors:
Vayas Ioannis_ professor, ntua, athens
Castiglioni Carlo Andrea_ professor, polimi, milano

ABSTRACT

The present thesis constitutes the final part of the author's studies in the MSc in Analysis and Design of Earthquake Resistant Structures (ADERS) in National Technical University of Athens. However, it was mostly carried out in Politecnico di Milano in the context of the Erasmus European exchange programme. The main objective of this dissertation was the investigation of the seismic performance of steel storage pallet racking systems that mainly consist of cold-formed, thin-walled members. The seismic response of these structures was approached through the use of a finite element software (Sap2000, CSI) and the application of various pushover analyses. The data used for the completion of this thesis were obtained in the context of a European research project called "Seisracks 2".

The first chapter is an introduction to the problem that had to be examined. The importance of the subject is highlighted as the use of steel storage racks is increasingly widely spread in both warehouses and stores open to the public and therefore their design must meet the requirements for strength, simplicity and adaptability in installation, economy and of course safety of the users as well as of the stored goods. In addition to this, the typical pallet rack configuration is described (in terms of geometry and connections) along with the basic properties of members with thin-walled cold formed steel profiles. It should be noted that racks have the peculiarity of carrying very large live loads (pallet weights) while having insignificant self weight. In the end of this chapter, the relevant codes as well as the design parameters concerning the seismic analysis of this type of structures are presented.

The second chapter focuses on the previous research that has been made on the subject and especially on the "SEISRACKS" research project. Its basic results are summarized regarding component tests, pallet sliding-friction models and pushover tests.

In the third chapter, the simulation procedure in Sap2000 is explained. The methodology of the simulation is presented concerning the general configuration of the models, each member

separately and each type of connection or support. The procedure of the nonlinear static analysis in Sap2000 is presented along with the options regarding material nonlinearity and geometric nonlinearity. Concluding this unit, the simulation problems, relative to the complexity of the specific structures that were encountered and had to be overcome, are mentioned.

In chapter four, the structures examined are presented. In total six models were made, obtaining data from three different companies. Each company provided drawings and a few experimental data on two types of racks: one type designed for medium or low seismicity zones and another designed for high seismicity. Each of the six models was examined separately with regard to its two main directions (down-aisle or X and cross-aisle or Y).

In the following three chapters (which means chapters five to seven), more specific information are given regarding the simulations and the interpretation of the experimental data provided by the companies (assignment of nonlinearities). The results of the analyses run are displayed, giving emphasis on the results of the pushover analyses (inelastic deformation, internal forces and capacity curves) in each direction. Chapter five refers to Company A, chapter six refers to Company B and chapter seven refers to Company C respectively.

In the final chapter eight, some conclusions and comments on the results are attempted. The results are summarized and the graphs for each case are superimposed in order to enable the comparison of the responses between the three companies. Furthermore, the importance of p-delta effects is highlighted by providing the results of the linear buckling analyses in Sap2000 as well as the different pushover curves that occur by or without taking into account the geometric nonlinearity. The effects of the different types of pushover load cases (uniform lateral loads or modal pushover/inverse triangle distribution) are also mentioned. The inter-storey drifts at the performance point (according to ATC 40) are presented for each case and compared. Finally, ductility, overstrength and q capacity factors are calculated for each case based in a bilinear approach of the obtained capacity curves. An estimation of another q factor based on the Life Safety performance level (according to FEMA 356) and a q factor for the performance point is also presented.

Since the "Seisracks 2" research project is now in progress, these comments and results remain to be updated or corrected in the future, as the experiments (full scale pushover tests and component/connection tests) along with the computational approach through a more sophisticated software, will provide valuable information both on the real properties of the structures as well as on their seismic responses.

εθνικό μετσόβιο πολυτεχνείο
σχολή πολιτικών μηχανικών
εργαστήριο μεταλλικών κατασκευών

μεταπτυχιακή εργασία:

σεισμική απόκριση βιομηχανικών ραφιών από χάλυβα

μεταπτυχιακή φοιτήτρια:
Αυγερινού Στέλλα
ΕΜΚ ΜΕ 2012/11

επιβλέποντες:
Βάγιας Ιωάννης_ καθηγητής, ΕΜΠ, αθήνα
Castiglioni Carlo Andrea_ professor, polimi, milano

ΠΕΡΙΛΗΨΗ

Η παρούσα διπλωματική εργασία έγινε στα πλαίσια του μεταπτυχιακού προγράμματος σπουδών "Δομοστατικός Σχεδιασμός και Ανάλυση Κατασκευών" του ΕΜΠ. Ωστόσο ένα μεγάλο τμήμα της εκπονήθηκε στο Politecnico di Milano. Ο βασικός της στόχος είναι η διερεύνηση της σεισμικής απόκρισης χαλύβδινων βιομηχανικών ραφιών τα οποία κατά βάση αποτελούνται από λεπτότοιχα στοιχεία ψυχρής έλασης. Η σεισμική απόκριση αυτών των κατασκευών προσεγγίστηκε μέσω της προσομοίωσης με το λογισμικό πεπερασμένων στοιχείων Sap2000 (CSI) και τη μέθοδο της στατικής ανελαστικής ανάλυσης (pushover). Τα δεδομένα που χρησιμοποιήθηκαν για την περάτωση αυτής της εργασίας, αποκτήθηκαν στα πλαίσια του ευρωπαϊκού ερευνητικού προγράμματος "Seisracks 2".

Το πρώτο κεφάλαιο αποτελεί εισαγωγή στο υπό εξέταση πρόβλημα. Η σημασία του ζητήματος υπερτονίζεται υπό το πρίσμα της σύγχρονης αυξανόμενης διάδοσης της χρήσης των βιομηχανικών ραφιών τόσο σε αποθήκες όσο και σε χώρους ανοιχτούς στο κοινό όπως π.χ. καταστήματα. Κατ' επέκταση ο σχεδιασμός τους πρέπει να ανταποκρίνεται στις απαιτήσεις για υψηλή αντοχή, απλότητα και προσαρμοστικότητα στην εγκατάσταση, οικονομία και φυσικά, ασφάλεια τόσο των χρηστών όσο και των αποθηκευμένων αγαθών. Στη συνέχεια, περιγράφεται η τυπική διάταξη και διαμόρφωση ενός συστήματος βιομηχανικών ραφιών καθώς επίσης οι βασικές ιδιότητες των λεπτότοιχων μελών ψυχρής έλασης. Θα έπρεπε σε αυτό το σημείο να προστεθεί ότι μια ακόμη από τις ιδιαιτερότητες των κατασκευών αυτών είναι το γεγονός ότι φέρουν πολύ μεγάλα κινητά φορτία ενώ έχουν ελάχιστο ίδιο βάρος (συγκριτικά αμελητέο). Τέλος, αναφέρονται οι σχετικοί Κώδικες και Κανονισμοί καθώς επίσης και οι συνήθεις σεισμικές παράμετροι σχεδιασμού.

Το δεύτερο κεφάλαιο επικεντρώνεται στην προηγούμενη έρευνα που έχει γίνει πάνω σε αυτό το θέμα και κυρίως στο ερευνητικό πρόγραμμα "SEISRACKS" τα βασικά αποτελέσματα

του οποίου, πάνω σε ζητήματα πειραματικών ελέγχων μελών, προσομοιωμάτων ολίσθησης των παλετών και pushover αναλύσεων, παρουσιάζονται.

Στο τρίτο κεφάλαιο, επεξηγείται η διαδικασία προσομοίωσης στο λογισμικό Sap2000. Η μεθοδολογία παρουσιάζεται με άξονες τη γενική διάταξη των προσομοιωμάτων, το κάθε τύπο μέλους χωριστά αλλά και τον κάθε τύπο σύνδεσης ή στήριξης. Η διαδικασία της στατικής ανελαστικής ανάλυσης στο Sap2000 παρουσιάζεται στη συνέχεια, καθώς επίσης και οι επιλογές που αφορούν τη μη γραμμικότητα των υλικών και της γεωμετρίας. Στο τέλος αυτής της ενότητας αναφέρονται τα προβλήματα που προέκυψαν και έπρεπε να επιλυθούν κατά την διάρκεια του σχεδιασμού της προσομοίωσης.

Στο τέταρτο κεφάλαιο, παρουσιάζονται οι κατασκευές που εξετάστηκαν. Συνολικά έξι προσομοιώματα φτιάχτηκαν, λαμβάνοντας δεδομένα από τρεις διαφορετικές εταιρείες. Κάθε εταιρεία παρείχε σχέδια και πειραματικά δεδομένα για δύο είδη συστημάτων ραφιών: έναν τύπο που προορίζεται για ζώνες χαμηλής ή μέσης σεισμικότητας και έναν τύπο σχεδιασμένο για υψηλή σεισμικότητα. Κάθε ένα από τα έξι προσομοιώματα εξετάστηκε χωριστά στις δύο κύριες διευθύνσεις του (κατά μήκος ή Χ και εγκάρσια ή Υ).

Στα επόμενα τρία κεφάλαια (από το πέμπτο μέχρι και το έβδομο), δίδονται πιο συγκεκριμένες πληροφορίες σχετικά με την προσομοίωση και την αξιοποίηση των πειραματικών δεδομένων από τις εταιρείες, κυρίως όσον αφορά τη διαχείριση των μη-γραμμικοτήτων. Παρουσιάζονται τα αποτελέσματα των αναλύσεων, με έμφαση στα αποτελέσματα των pushover αναλύσεων (ανελαστικές παραμορφώσεις, εντατικά μεγέθη μελών και καμπύλες τέμνουσας βάσης - μετατόπισης οροφής), για κάθε προσομοίωμα σε κάθε διεύθυνση. Το πέμπτο κεφάλαιο αναφέρεται στην εταιρεία Α, το έκτο κεφάλαιο στην εταιρεία Β και το έβδομο στην εταιρεία C αντίστοιχα.

Στο όγδοο κεφάλαιο διατυπώνονται κάποια ποιοτικά σχόλια και γίνεται η απόπειρα να διεξαχθούν κάποια συμπεράσματα. Τα αποτελέσματα συνοψίζονται και οι καμπύλες pushover επαλληλίζονται γραφικά προς διευκόλυνση της σύγκρισης ανάμεσα στις τρεις εταιρείες. Η σημασία των φαινομένων δευτέρας τάξης (p-delta effects) επισημαίνεται μέσω των αποτελεσμάτων που προέκυψαν από τη γραμμική ανάλυση λυγισμού του λογισμικού και τη σύγκριση των αποτελεσμάτων της pushover ανάλυσης με ή χωρίς γεωμετρική μη-γραμμικότητα. Επίσης παρουσιάζονται τα αποτελέσματα της επιβολής διαφορετικού τύπου πλευρικού φορτίου κατά την ανάλυση pushover (ομοιόμορφο ή ανεστραμμένο τριγωνικό με βάση τις ιδιομορφές). Επιπλέον παρουσιάζονται για κάθε κατασκευή οι πλευρικές μετατοπίσεις ανά όροφο, στο σημείο επιτελεστικότητας (performance point κατά τον κανονισμό ATC 40). Τελικά, η πλαστιμότητα, η υπεραντοχή και ο συντελεστής συμπεριφοράς $q_{capacity}$ υπολογίζονται για κάθε περίπτωση, με βάση τη διγραμμική προσομοίωση της εκάστοτε pushover καμπύλης. Συμπληρωματικά, γίνεται ο υπολογισμός ενός επιπλέον δείκτη συμπεριφοράς q με βάση τη στάθμη επιτελεστικότητας "Προστασία Ζωής" (σύμφωνα με τον FEMA 356) καθώς επίσης και ο υπολογισμός του δείκτη q στο σημείο επιτελεστικότητας.

Καθώς το ευρωπαϊκό ερευνητικό πρόγραμμα "Seisracks 2" βρίσκεται σε εξέλιξη, τα παραπάνω σχόλια και συμπεράσματα μένει να επικαιροποιηθούν ή να διορθωθούν στο μέλλον. Τα πειράματα που θα διεξαχθούν (pushover σε πραγματική κλίμακα και επιπλέον έλεγχοι των μελών και των συνδέσεων) σε συνδυασμό με την αναλυτική επεξεργασία του προβλήματος με πιο εξειδικευμένο λογισμικό, αναμένεται να δώσουν πολύτιμες πληροφορίες σχετικά με τις ιδιότητες των κατασκευών, τη σεισμική τους απόκριση και κατ΄ επέκταση τον βέλτιστο σχεδιασμό τους.

Acknowledgements

I feel the need to thank all those people who helped and supported me while working on this thesis.

Firstly I would like to thank my supervisors, professor Vayas Ioannis for the opportunity he gave me and his continuous scientific guidance and professor Castiglioni Carlo for his constant and great support both while I was in politecnico di Milano and after my return in NTUA.

Secondly, I would like to thank Adamakos Constantinos, PhD candidate, for his valuable support and collaboration during all these months.

I would also like to thank professor Degee Herve for his kind support regarding software issues and Alper Kanyilmaz, research assistant, for his help.

Last but not least I would like to express my gratitude towards my parents, my sister Charis and my friends Christos, Dafni, Giannos, Eleana, Angeliki, Lazaros and all the others that supported me in so many ways in both Milano and Athens while working on this thesis.

Index

Chapter 6: simulation and results_ company B

Chapter 7: simulation and results_ company C

Chapter 8: conclusions

References

Introduction

The scope of this thesis is the analysis of the earthquake response of a pallet storage rack made of thin-walled steel products. This project is the final part of the studies of the MSc in Analysis and Design of Earthquake Resistant Structures, under the supervision of professor I. Vayas of National Technical University of Athens and professor C. Castiglioni of Politecnico di Milano. This dissertation was completed in the context of the Erasmus European exchange programme.

The data used for the completion of this thesis were obtained in the context of a European research project called "Seisracks 2", whose subject is the seismic behaviour of steels storage pallet racking systems and which takes place under the collaboration of the following universities: Politecnico di Milano, National Technical University of Athens, University of Liege and RWTH Aachen University with the participation of the following industrial partners: Stow, Nedcon, Modulblock, SSI-Schaefer.

Note: In the following chapters, the companies will be referred to as Company A, B and C. These names are the equivalents of Company 1, 2 and 4 in "Seisracks 2" respectively.

Chapter 1 description of the problem

1.1. Introduction - Description of the problem

Over the years the evolution as far as the design and function of storage warehouses is concerned, has been determined by the lack of space, the high labour cost and the demands of modern production methods. The goods are no longer stored in one level only and they have to be easy to access and transfer. Storage racking systems are the structures that answer exactly these needs. They are thin metallic structures used to store goods in height. Amongst their special characteristics is that they have to be standardized and adaptive. The design of their elements is an outcome of optimization as well as of the combination of experimental and computational methods, given the fact that every reduction of the total weight, every increase of the strength and every simplification of the installation procedure can significantly affect the economy of the whole structure.

The wide use of racks started in the decade of 1930. At that point they were composed by slotted/perforated angles in order to facilitate the connections and the adaptability as far as the various forms were concerned. Their main disadvantages, however, was that the bolting procedure was difficult and expensive apart from the fact that the vertical bracing was necessary. Nowadays, the use of slotted angles is no longer the case since the extreme adaptability to different structural shapes is no longer a prerequisite. Instead a limited number of standard profiles for beams and columns is used that can be combined in an appropriate way in order to meet the usual needs. The columns are still perforated but the beams are not. The beam-to-column connections are hooked, thus quick and inexpensive. These connections have the additional advantage that they can undertake moments, so stability is provided in the longitudinal direction (frame action) and the need for vertical bracings is limited.

In contrast with usual civil engineering structures, storage racking systems made of thin-walled cold formed steel products are able to carry very high live load (many times larger than their dead load) and can also raise considerable height. The behaviour of these systems is affected by the geometry of their structural components (high slenderness elements, open-section profiles hence prone to buckling problems) as well as by the nonlinear behaviour of their joints (beam-to-upright and base-plate), therefore many difficulties arise in the prediction of their structural behaviour, such as instabilities (global, local and distortional) or modeling problems (beam-upright connection stiffness, base plate anchorages).
Things become even more complicated when a storage rack is installed in a seismic zone where it has to be able to withstand horizontal dynamic forces. In that case, apart from the usual seismic global and local mechanisms, an additional limit state of the system is the fall of pallets with subsequent damages to goods, people and to the structure itself.
The phenomenon of sliding of the pallets (as well as their consequent fall) depends on the dynamic friction coefficient between the pallet and the steel beam, and represents a serviceability limit state. If, however, the horizontal forces acting on the pallets during an earthquake, exceed the friction resistance and cause a sliding movement whose amplitude is

small enough for the pallets to remain on the rack, this effect can be beneficial for the structure, due to component energy dissipation.

Apart from the scientific point of view, the study of the seismic behaviour of steel storage racks has a large economic as well as a social impact. Racks are widely used in warehouses were they are loaded with tons of more or less valuable goods, the loss of which during an earthquake could mean to the owner a very large economic loss. Racks are increasingly adopted in supermarkets and shopping centres as well, in areas open to the public. In this case, occupant safety depends on both the structural performance of the building and on the performance of the storage racks. Earthquake ground motions can cause storage racks to collapse or overturn, if not properly designed. In addition to this, the falling of pallets may endanger the life of the clients and/or the employees, involving a life-safety risk as well as Civil and Penal Right considerations.

Figure 1.1: Collapses with goods spilled over the fork lift trucks

Figure 1.2: Cross-aisle collapse

Figure 1.3: The "Domino-effect" collapse

1.2. Typical Pallet Rack configuration

Steel pallet storage racks are particular structures formed with specially designed cold-formed steel elements which allow easy installation and reconfiguration. As mentioned before, they are and widely used in many warehouses to store various kinds of goods. Typical storage pallets have plan areas of about one square meter and can weight up to approximately 8 to 15 kN. The Euro pallet for example has dimensions (L*W*H) 800*1200*144 mm and it is a four-way pallet made of wood (Figure 1.4).

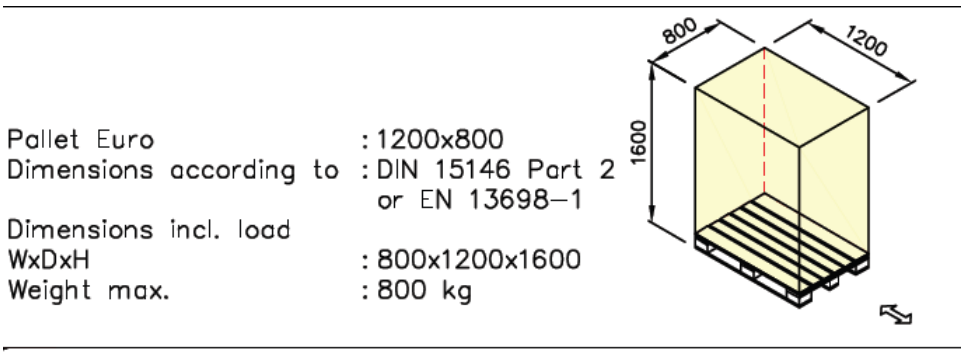

Figure 1.4: Dimensions and weight of a typical Euro-pallet

The longitudinal direction of a racking system is called down-aisle, whereas the transversal is called cross-aisle direction.
The term bay refers to the space between two upright frames, spanning as many load levels as allowed.
The number of pallet loads on each shelf between uprights is generally specified by the operator of the warehouse. In a typical storage rack system, there are two or three pallet loads between uprights. The storage rack bays are typically 1.0 to 1.1 meter deep and 1.8 to 2.7 meters wide.
The shelf elevations are determined by functionality needs such as the height of the loads, the shelf beam size as well as the clearances required for storing and removing the load. The shelves may be spaced regularly for the full height of the rack system if all the loads are the same height or the spacing may be varied to accommodate different height loads in an economic way. The overall height of the racking system is based on the limitations imposed by the handling/lifting equipment and the building height. For example, the overall height of a typical pallet racking system found in retail warehouses varies between 5 and 6 meters, while in industrial warehouse facilities it can reach heights up to 12-15 meters.

The main structural elements of the racking system are:
_ Upright frames:
The vertical components of the racks are called upright frames and they consist of two columns (front and rear) of thin gauge cold formed profiles linked together by a system of diagonal trusses. The diagonal bracings can be working in tension or both in tension and compression, depending on the configuration of the structure. The profile of the columns is defined by the need for high strength and easy connections in the two perpendicular vertical levels. The increase of their resistance to local buckling is achieved through stiffeners. The columns are

perforated in order to facilitate the links, usually with oblique slots for the beams and circular holes for the diagonal trusses.

The strength of the columns is affected by phenomena such as local buckling (with or without warping) and global flexural bending. Furthermore the presence of holes complicates the application of analytical calculation and therefore their design is often based on experiments.
As far as the base plates are concerned, they are usually welded to the columns and bolted to the either concrete or steel deck.

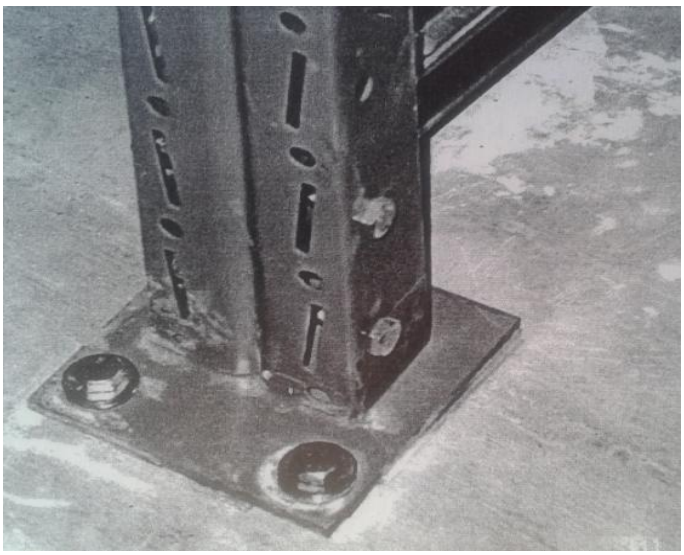

Figure 1.5: Upright and base plate detail

_ Beams:
The adjacent uprights are linked in the down-aisle (longitudinal) direction of the racks through horizontal members referred to as pallet beams. They have closed built up sections made of cold formed elements. Usually they are composed by two U-shaped members, thus forming a box cross section with increased torsional stiffness. Their connection to the uprights is performed with hooking connectors at their endpoints which engage in the holes of the uprights. These hooking connectors are usually angles welded to the beams' ends.

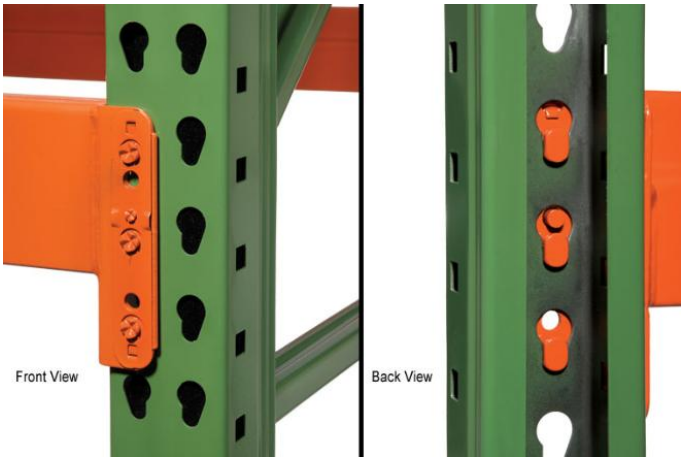

Figure 1.6: Beam end connector detail (front and back view)

The behaviour of the beam-to-column connection is crucial for the stability of the whole structure since it provides the frame action longitudinally. The connection is semi-rigid and can be described with a moment-rotation diagram defined by experiments. The behaviour of this link could be approached as a rotational spring with stiffness derived by the aforementioned moment-rotation diagram.
The failure of the beam elements is usually due to yielding and local buckling of the flange under compression.

_ Spine bracings (vertical bracing): [not present in every racking system]
Sometimes bracing in the vertical plane in the down-aisle direction is placed, thus linking adjacent upright frames. Nowadays, these vertical bracings are usually in the rear plane of the rack, thus spoiling structural regularity in plan. They stiff the rack against horizontal loads, in particular seismic forces.
Spine bracing is usually made of vertical uprights, transverse members (mainly compressed) and diagonal members working in tension only.

_ Plan bracings (horizontal bracing): [not present in every racking system]
Horizontal diagonal bracings on the level of the shelves are also used occasionally, placed between beams, in order to transfer the horizontal actions from the unbraced vertical plane of upright to the braced vertical plane.

Figure 1.7: Storage rack with two bays and three levels

All of the racking systems examined in this dissertation consist of six bays and four floors. The storage rack bays are 1.10 m deep and their length is approximately 2.70 m. Their heights range from 8.10 to 8.21 m with the "ground floor" always being slightly taller than the rest. In the storage rack systems used for the analysis, there are three pallet loads between uprights. The typical unit load is considered to be a pallet with dimensions 800x1200x1500 mm (L*W*H) and a weight of 8kN.

1.3. Thin-walled, cold formed steel profiles

Thin-walled cold formed products are increasingly met in many aspects of modern life and serve various as well as different needs ranging from beverage cans to bearing elements in structures.
Thin walled cold formed elements are very efficient as far as strength and stiffness are concerned. Furthermore, they are very light, given the fact that their thickness can be even less than 1mm. Usually their thickness ranges between 1-6 mm.

Regarding structural elements, their profiles can be either constant or variable, open type simple or composite, closed type and composite. Through cold formation it is much easier to achieve more complicated profiles, which are usually symmetric in an axis or a point, and are reinforced through the use of stiffeners. However, these complicated profiles can lead to designing issues that are not covered by the so far applying Regulations. The use of numerical methods such as the Finite Elements Method is possible but can also lead to serious simulation problems due to the peculiarity of the forms and of the various connections in the structures. As a result, for this kind of cases many Regulations suggest the application of experimental methods apart from the analytical ones.

The yield limit of the steel used is usually between 250-550 MPα, but higher strength steels are increasingly used. The types of steel used must be suitable to undergo the cold forming procedure. Moreover they have to be suitable for welding and galvanizing. These types are defined by European and international regulations which also define their yield limit and their tensional strength.

Regulation	Quality	F_{yb} [N/mm^2]	F_{ub} [N/mm^2]
EN 10025	S 235	235	360
	S 275	275	430
	S 355	355	510
EN 10113 Part 3	S 275 M	275	360
	S 355 M	355	450
	S 420 M	420	500
	S 460 M	460	530
prEN 10149 Part 2	S 315 MC	315	390
	S 355 MC	355	430
	S 420 MC	420	480
	S 460 MC	460	520
	S 500 MC	500	550
	S 550 MC	550	600
EN 10147	Fe E 220 G	220	300
	Fe E 250 G	250	330
	Fe E 280 G	280	360
	Fe E 320 G	320	390
	Fe E 350 G	350	420

Table 1.1: Types of cold formed steel and respective limit stresses

In general, the difference between cold formed and hot formed steel, as far as stress-strain diagrams are concerned, is that the latter has a specific yield limit defined by tension tests under controlled deformation. After the yielding zone, where stresses remain constant and deformations increase, hardening occurs where the stresses increase until failure. On the other hand, in cold formed steel there is not a specific yield limit and therefore it is conventionally defined as the limit of 0.2%, which means the stress beyond which any unloading would result in a remaining deformation of 0.2%.

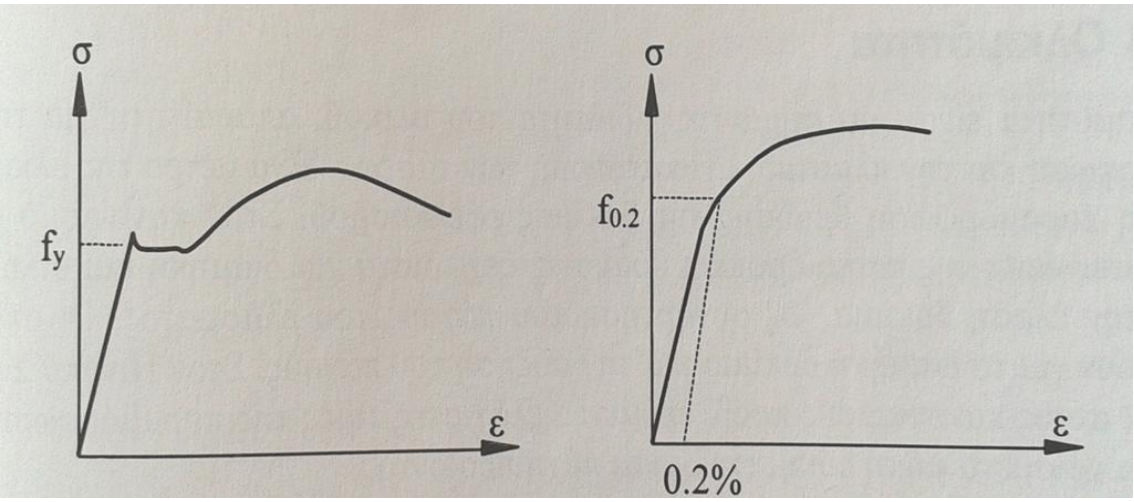

Figure 1.8: Stress-strain diagrams with and without specific yield limit

The special weight is γ=78.5 kN/m^3 ,the modulus of elasticity is E=210000 N/mm^2, the Poisson's ratio is v=0.3 and the shear modulus is G= E/2(1+v) = 80770 N/mm^2.

The use of thin-walled profiles and high-strength steel arises questions and problems in the calculating procedure that did not normally occur in common steel structures. Stability problems are much more frequent due to the reduced resistance against local buckling of the members.

Cold formed steel profiles have the following advantages when used in structures:
_ lighter bearing members
_ more complicated types of profiles manufactured in an economic way as far as the ratio of bearing capacity/weight is concerned
_ easier storage and transportation
_ the bearing sheets can withstand forces not only normal to their plane but also in their plane, thus working as diaphragms, if formed accordingly.
The producing procedure of these profiles largely determines their local buckling behaviour. To start with, it modifies the stress-strain diagram of steel. In comparison to the initial material, through the cold forming procedure the yield stress limit is increased and sometimes even the tensile strength of the flanges and the corners is increased whereas through the compression procedure the flanges' properties do not change.
The aforementioned increase in the yield stress limit is due to the hardening of the material and it depends on the quality of the steel. On the contrary, the increase in the tensile strength is related with the ageing of the material due to deformation.

In cold formed profiles the residual stresses are mostly due to bending and do not really affect the buckling strength.

Stability

The behaviour of steel members is defined by four factors/types of potential instabilities: local buckling, global buckling, distortional buckling and shear buckling. The cold formed profiles are very sensitive against local buckling (warping) which is characterized by a relatively small wave length of the mode of buckling. On the contrary, the wave length in the case of global buckling (which can either be flexural buckling or torsional flexural) is very long. In global buckling the profiles remain undeformed as if rigid/stiff diaphragms. In local buckling with distortion of the profile, the instability is caused by the relative displacement of the edges of the cross section. Its wave length is between those of local and global buckling. This type of buckling is the most common in the more complicated profiles.

The resistance to torsion of thin walled profiles is very small. The cross sections are usually characterized by simple symmetry, therefore their shear centre does not coincide with their centre of gravity. As a result every loading, whose axis does not cross the shear centre, also causes torsional deformations apart from the bending ones. Thus, the members in compression run the risk of torsional flexural buckling.

Ductility

Due to the local buckling risk, the cold formed profiles have cross sections that usually belong to category/class 4 (or sometimes even 3). Apart from this, the ductility of the cold formed materials is reduced due to their producing procedure, so the plastic design is not allowed. The inelastic capacity is very limited. However the Regulations allow for a tolerance margin as far as the tensile inelastic resistance in members under bending is concerned.

Due to their limited ductility the structures with thin walled members cannot absorb energy in the case of an earthquake and therefore should be designed with a q factor equal to 1.00. Despite of this, the economic aspect of this kind of structures is not adversely affected, thanks to their small weight and the increased strength of their members.

Resistance to fire

The fire resistance of these profiles is very limited, due to the small value of the ratio of the perimeter (exposed to heating) over the section's area.

Regulations regarding structures from thin-walled cold-formed elements

_ AISI Specification, Edition 1996, [1.3]

_ North American Cold-formed steel specification, Edition 2001, [1.5]

_ Australian/New Zeeland Annex , AS/NZS 4600, Edition 1996, [1.11],[1.12]

_ German directive, DASt-Richtlinie 016, [1.8]

_ ENV and EN 1993-1-3:Eurocode 3, study and design of steel structures, part 1.3- thin-walled cold formed elements.

1.4. Codes and Regulations

Racking systems are not "buildings" neither "ordinary steel structures". Their differences lie on their use, their loads, their geometry as well as their steel components (cold formed steel and thin gauge profiles). The aforementioned peculiarities influence significantly the seismic response of these structures and the question is whether or not it is possible to apply the "general design rules" and how to correctly modify them in order to achieve the desired safety level. The live loads of racks such as pallet loads often represent more than 95% of their total mass, therefore the load presence and distribution on racking systems affect very much the response of these structures under seismic action. As far as safety is concerned, it is also very important to take into account the potential movements of the stored goods regardless of the strength of the racking systems against the earthquake.
The above parameters highlight the complexity of the problem of the seismic design of racking systems. As a result, untill recently very few Codes dealing with this problem were available.

Research and Codes in the US

The situation in the US was better than in Europe. Even since the early 1970s in the US, the Rack Manufacturers Institute (RMI) has sponsored many analytical and experimental storage rack research projects conducted at Cornell University. Major research projects were also undertaken, during the late 1970s and early 1980s, at Stanford University and at the University of California/Berkeley, with funding from RMI as well as from the National Science Foundation (NSF).
Consequently, rack manufacturers very often had to refer to the Rack Manufacturers Institute (R.M.I) Specifications (R.M.I a and b, 2002). What is more, storage racks are typically made of cold-formed steel members. Therefore their design depends on the thorough understanding and application of the American Iron and Steel Institute's (AISI) "Specification for the Design of Cold-Formed Steel Structural Members".
The Canadian Standards Association has also developed two storage racks standards: A344.1 "User Guide for Steel Storage Racks" and A344.2 "Design and Construction of Steel Storage Racks". The RMI has also supported these efforts.

Research and Codes in Europe

The Fédération Européenne de la Manutention (FEM) is the European Federation of Materials Handling Associations, was formed in 1953 and today is the largest Mechanical Engineering Sector in the EU. The FEM Product Group "Racking & Shelving" was established in 1970 as a Section of FEM and today operates as the European Racking Federation (ERF).
The first attempt to create a European Code of Practice happened in the beginning of the eighties, as part of a research program funded by the European Community. However it was not adopted by the national associations of racking and shelving manufacturers at that time and it was retried in the nineties.

In an attempt to create e European Code of practice regarding racking structures, ERF/FEM funded the development of FEM Codes of Practice which resulted in 2000 in the publication of the following Manufacturers' Design Recommendations:

_ FEM 10.2.02: Design of Static Steel Pallet Racking
_ FEM 10.2.03: Specifiers Guidelines
_ FEM 10.2.04: Users Code
_ FEM 10.2.05: Guidelines for working safely with lift trucks in pallet racking installations (Draft)
_ FEM 10.2.06: Design of Static Steel Shelving
_ FEM 10.3.01: Pallet racking: Tolerances, Deformations and Clearances

The main difference between a Standard and a Manufacturers Code is the involvement of- in principle- all parties involved. In case of storage systems this means for instance: manufacturers, users, governmental bodies (like the office for health, safety and building authorities), scientist (universities, R&D institutes) and contractors.

In 2002, CEN (Comité Européen de Normalisation) activated a Technical Committee in order to develop a set of Eurocodes dedicated to racking and shelving, CEN/TC 344 N 57 (2006), "Steel static storage systems". ERF/FEM also funded this project in order to convert its Manufacturers Code's of Practice into formal European EN Standards. The FEM Industry Code's of Practice became a starting point for the CEN/TC 344 working groups.
Furthermore, the European Federation of Maintenance performed Standard development research activities for the European Union (EU) which resulted in 2005 in the FEM seismic Design Standard, Pr FEM 10.2.08: "The Seismic Design of Static Steel Pallet Racks".

An important number of standards has been recently published or is being currently developed and a review is given in the following Tables.

REVIEW OF STANDARDS IN THE EN - SERIES

"STEEL STATIC STORAGE SYSTEMS"

First draft	EN Standard	Published
FEM 10.2.02	EN 15 512 : Adjustable pallet racking systems - Principles for structural design	March 2009
FEM 10.3.01	EN 15 620 : Adjustable pallet racking - Tolerances, deformations and clearances	October 2008
FEM 10.2.03	EN 15 629 : Specification of storage equipment	November 2008
FEM 10.2.04	EN 15 635 : Application and maintenance of storage equipment	November 2008
–	pr EN 15 878 : Terms and definitions	December 2008

REVIEW OF FEM CODE'S OF PRACTICE PUBLISHED, STILL WORKING ON OR INTENDED TO WORK ON		
FEM Code	**Title**	**Published**
FEM 10.2.05 Draft	Guidelines for working safely with lift trucks in pallet racking installations	October 1999 (Final: 2013)
FEM 10.2.06	The design of hand loaded static steel shelving systems	April 2001
FEM 10.2.07	The design of drive-in and drive-through racking	(Mid 2011)
FEM 10.2.08	Recommendations for the design of static steel pallet racks under seismic conditions	(Mid 2011)
FEM 10.2.09	The design of cantilever racking	(End 2011)
FEM 10.2.10	Rail dependent storage and retrieval systems – Interfaces	(Mid 2011)
FEM 10.2.11	Rail dependent storage and retrieval systems – Consideration of kinetic energy action due to a faulty operation in cross-aisle direction, in compliance with EN 528 – Part 1: Pallet racking	(Mid 2011)
FEM 10.3.01-1	Basis of calculations for storage and retrieval machines – Tolerances, deformations and clearances in the storage system – Part 1: General, Single deep and Double deep Pallet racking	(Mid 2011)

1.4.1 Design parameters concerning the seismic analysis

The FEM 10.2.08 Code of practice deals with all relevant and specific seismic design issues for racking systems such as:

_ The seismic response can be significantly different in down-aisle direction and in cross-aisle direction and can also be considerably affected by the size and the distribution of the masses

_ The natural damping of the structure without its pallet loads is very small, however in real conditions the damping can be significantly more than expected due to micro movements of the stored goods and sliding effects

_ Cyclic forces due to earthquake can progressively damage connections and/or other components thus affecting the response of the whole structure

_ In case of seismic isolation, the effectiveness of it must be guaranteed for all the loading conditions and during the whole expected life of the racking system.

The design procedures given in FEM 10.2.08 apply to all types of static pallet racks fabricated from steel members and supported by floors lying on the ground. The approach to the seismic design is based upon the philosophy of EN 1998-1 (Eurocode 8), whereas the design, tests and quality control of components and materials refer to FEM 10.2.02.

With reference to prEN1998-1, it is stated that structures in seismic regions shall be designed in such a way that the following requirements are met up to a certain point of reliability:
_ no collapse requirement (neither local nor general)
_ damage limitation requirement
_ movement of pallets

Furthermore, two elastic spectra are defined to describe the earthquake motion (Type 1 and 2). In FEM 10.2.08, the seismic response is modified by means of two coefficients that estimate the effects of phenomena of the racking systems such as energy dissipation (due to the friction between the pallets and the beams), pallet damping (due to the movements of the stored product), pallet flexibility etc:
E_{D1} = design spectrum modification factor [on $S_d(T)$, constant value c=0.8 →energy dissipation damping, or c = 1.00 → in case the movement of the pallets is prevented]
E_{D2} = pallet weight modification factor [modifies the period and the horizontal action, depends on the type of the stored goods].

As far as the importance factor is concerned, it must be at least equal to the importance factor specified for the part of the building in which the racks are located.

Importance Class	Description	Importance factor	
		reference	reduced [Note (2)]
I	Warehouses with fully automated storage operations Low warehouse occupancy (1)	0.8	0.67
II	Normal warehouse conditions, including picking areas	1.0	0.84
III	Retail areas with public access	1.2	n. a.
IV	Hazardous product storage	1.4	n. a.

Notes
1. The reduced importance factor can only be used for racking systems not located on storey of a building and/or not used for retail areas or hazardous product storage.
2. The reduced importance factor is based on design life of the rack of 30 years instead of 50.

The vertical component of the seismic action shall only be taken into account in the following cases: cantilever components and beams supporting columns. For normal racking structures it is generally neglected. However the recent experience of the earthquake in Emily Romagna (2012) with its casualties indicates that the vertical component can be larger than expected and should be taken into account ["the main reasons of the damage is the extremely high vertical ground shaking (of the order of 1.0 g) in combination with the moderate horizontal motions", Carydis et al, July 2012].

The sliding of the pallets is expected to occur when the pallets are not restrained on the beams and the horizontal seismic action on the pallets (evaluated by using the design spectrum with modification factor E_{D1}=1.0) is greater than the horizontal reaction generated by the friction between the pallet and the beams. The pallet-beam friction coefficient to be considered is the static one and it depends on the materilas in conatact and the environment (wet/dry/warehouse conditions). It ranges between 0.05 and 0.25.

The reference method for determining the seismic effects is the modal response spectrum analysis, using a linear-elastic model of the structure and the design spectrum multiplied by the modification factor E_{D1}, but also other analysis methods, according to Eurocode 8, can be used.

The seismic base shear force F_b for each main direction is: $F_b = E_{D1} \times S_d(T1) \times W_{E,tot}$, where $W_{E,tot}$ is the total seismic mass.
Furthermore, the fundamental period of vibration of the rack must be evaluated by means of modal analysis.

Design of low dissipative structures

In addition to general requirements related to materials and connections, the following specific rules are stated:
_ If ductility factor q > 1.5 is assumed, members which contribute to the seismic resistance of the structure by working in compression or bending must be of class 1, 2 and 3 according to EC3.
_ If the structure is not regular in plan or elevation, q shall not exceed 1.50.
_ K bracings, in which the tension diagonals intersection lies on a column, should not be used in seismic zones.
_ For bolted shear connections the shear strength of the bolts should be higher than 1.20 times the bearing resistance.

Structural systems withstanding the seismic action

The seismic action can in general be studied separately in the down-aisle direction and in the cross-aisle direction. The relevant load condition for the seismic design of the rack is the fully loaded rack, as the horizontal seismic action is maximized.
The rack's structural systems withstanding the seismic actions are:
_ In the cross-aisle direction: the upright frames
_ In the down-aisle direction, one of the following:
    _ The unbraced frames: stability is provided by the beam-to-column connections and horizontal bracings are provided connecting the front and the rear frames.
    _ The rear bracing made of the following elements: a rear bracing placed behind the rear frame and horizontal bracings connecting the front unbraced frame to the rear braced frame
    The vertical bracing withstand the horizontal seismic action.

Structural upright frame types and q behaviour factors

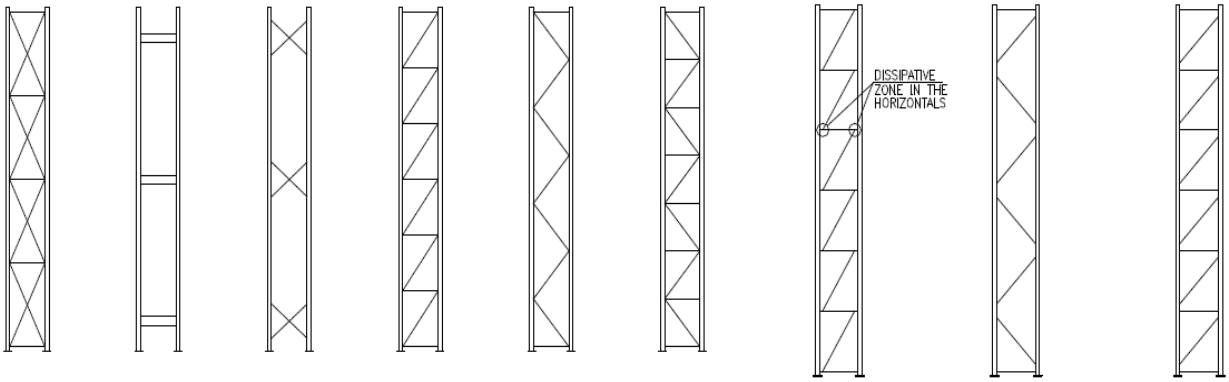

(a) Tension braced frame	(b) battened (vierendeel) frame	(c) partially braced frame	(d) Z- form braced frame	(e) D - form braced frame	(f) K - form braced frame	(d_1) Z-form dissipative braced frame	(e_1) D-form braced frame	(d_2) Z-form braced frame

Frame type	Structural type	maximum q factor	
		Regular rack	Not regular rack
a	tension diagonals	4	3.2
	tension/compression diagonals	2.5 (class DCH)* 2.0 (class DCM)*	2.0 1.6
b	dissipative battened frame can be used, provided that the requirements of moment resisting are met, otherwise q=1.5		
c		1.0	1.0
d-e-f	low dissipative	1.5	1.5
d1	eccentric bracing (energy dissipation in the horizontals)	4.0	3.2
e1-d2		1.5	1.5

***DCM**: ductility class medium, and bracing elements belonging to class 1,2 and 3
DCH: ductility class high, and bracing elements belonging to class 1 and 2.

Chapter 2 previous research_ the SEISRACKS project

2.1 Research in Europe

As mentioned previously, there have been limitations regarding the design of storage racks in seismic areas which are in principal due to lack of knowledge and hence lack of Standard Design Codes in Europe.

By 2003, little research on the dynamic behaviour of racks had been carried out, mainly in the US. Only one study was available in Europe, carried out within the ECOLEADER Research Program, for Free Access to Large scale Testing Facilities, titled "Seismic Behaviour of Pallet Rack Systems" (Castiglioni et al, 2003). In that project, four specimens were tested in full scale on the shaking table of the Laboratory for Earthquake Engineering at the National Technical University of Athens.

To solve the aforementioned limitations, the EU sponsored through the Research Fund for Coal and Steel, a research project titled "Storage Racks in Seismic Areas" (SEISRACKS) which initiated in 2004 and terminated in 2007. Its objectives were to increase knowledge on actual service conditions of storage racks, on their actual structural behaviour and to assess design rules thus constituting a scientific background document for the drafting of a European Standard.

Within the SEISRACKS project, the following activities were carried out:

_ Characterization of the component behaviour

_ Assessment of the sliding conditions of pallets on rack beams/ Experimental determination of friction properties of pallets

_ Push-over tests on two full-scale racks models

_ Pseudo-dynamic tests on one full-scale rack model

_ Assessment of the actual service loading conditions of racks (in-situ monitoring)

_ Shake table tests on six full-scale rack models/ Experimental study of the cyclic behaviour of beam-to-upright joints and of base anchor-ages

_ Numerical modeling and study of the global dynamic structural behaviour of racks subjected to earthquakes including sliding of pallets

The main outcome of the SEISRACKS project was a set of proposals included in a revised draft of prFEM10.2.08, issued in 2008. The results achieved, were considered very satisfactory especially those concerning the characterization of the friction properties of the pallets and the down-aisle behaviour of rack structures.

However, further gaps in the knowledge of the seismic performance of these structures were revealed. Therefore the project " Seismic Behaviour of Steel Storage Pallet Racking Systems" (SEISRACKS 2) initiated in 2011. Amongst its objectives is the investigation of the out-of-plane behaviour of the beams and of the beam-to-upright connections, the investigation of the behaviour in cross-aisle direction depending on the configuration and the behaviour in down-aisle direction in presence of eccentric vertical bracings, the use of a non linear analysis for the behaviour of rack structures under seismic loads based on multi modal spectral analysis, the study of the actual behaviour of the palletized goods depending on size and shape, etc.

The above issues will be investigated by means of component testing, full scale (push-over) testing and in-situ testing of racking systems in operating warehouses, as well as by numerical simulations.

2.2 The SEISRACKS project

In this chapter, some of the results of SEISRACKS are briefly presented, in an attempt to provide a clearer prospective of the subject.

2.2.1 Component tests

During the SEISRACKS project, component tests were performed in order to characterize the behaviour of both beam-to-upright and base connections. The behaviour of both components was found to be strongly influenced by the nature and geometry of the profiles (unsymmetrical cross section of the upright, thin walled sections of beams and uprights), as well as by the asymmetry of the connections (in beam-to-upright connections it is caused by the inclined hooks, in base connections it is due to the eccentric position of the upright on the base plate and to the asymmetrical disposition of the bolts)

Beam-to-upright connections

They are typically moment connections. A hooked end plate connector is welded to the beam at both ends.

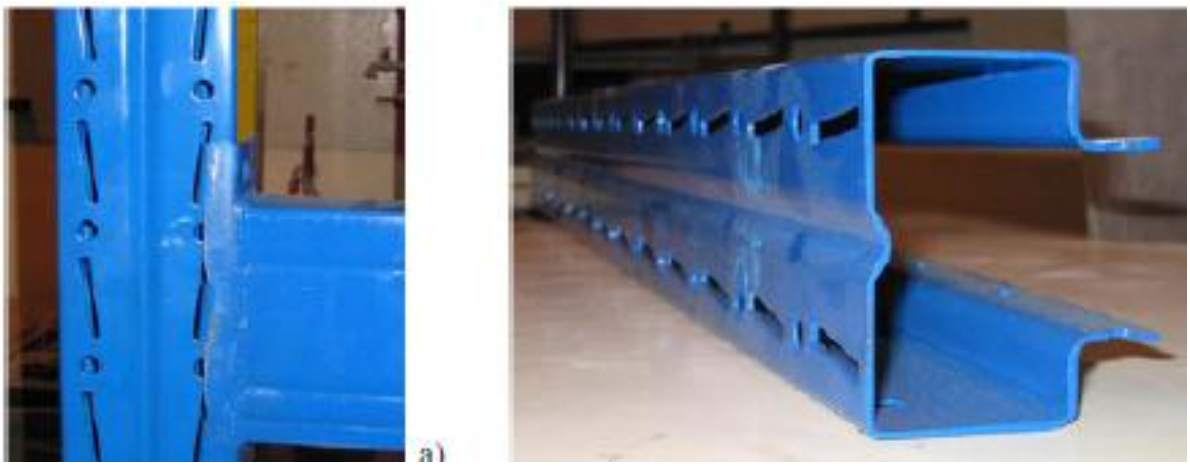

Figure 2.1: Specimens for beam-to-upright connection tests (connection and upright)

This connection is strongly non-symmetric in both vertical and horizontal planes. As a result a non-symmetric response was to be expected under hogging (MB) and sagging (MT) bending.

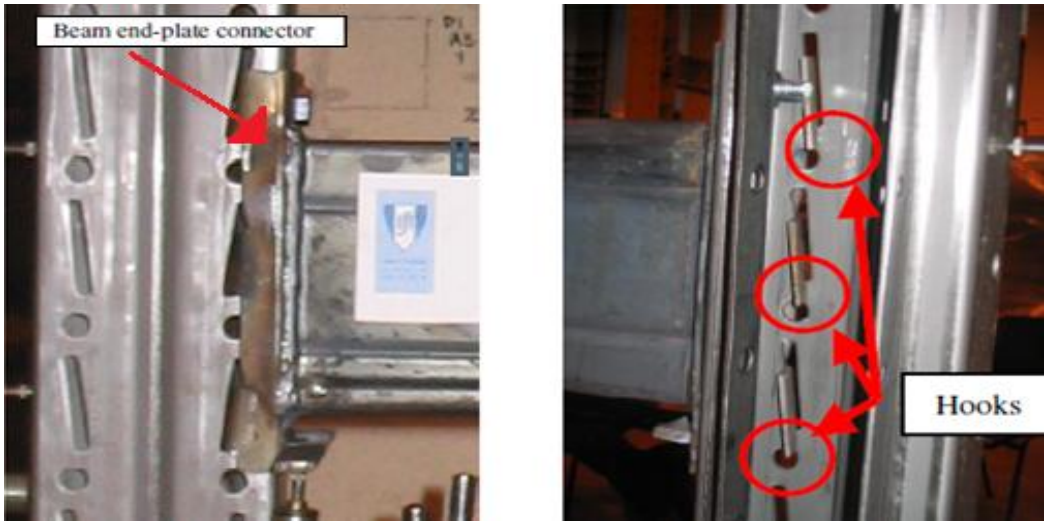

Figure 2.2: Typical beam-to-upright connection

The **monotonic tests** carried out indicated differences in the ductile behaviour: while the initial elastic stiffness was similar, the average ultimate rotation of the specimens under hogging bending was approximately 2.3 times larger than that of the specimens under sagging bending. Failure of both specimens subjected to hogging and sagging bending was due to large deformations in the beam end connector, respectively resulting in the top and bottom hooks coming out of the openings in the upright. More specifically:

_ The failure mode of specimens subjected to **hogging** (M-) bending, consisted of large deformations in the top zone of the beam end connector, leading to loosening of the hooked connection and to the hooks exiting from the holes.

2.3: Typical collapse mode under hogging bending moments

_ The failure mode of specimens subjected to **sagging** (M+) bending was governed by the failure of the hooks in the lower part of the connector. Failure was accompanied by evident cracks and the fracture of the beam close to the weld.

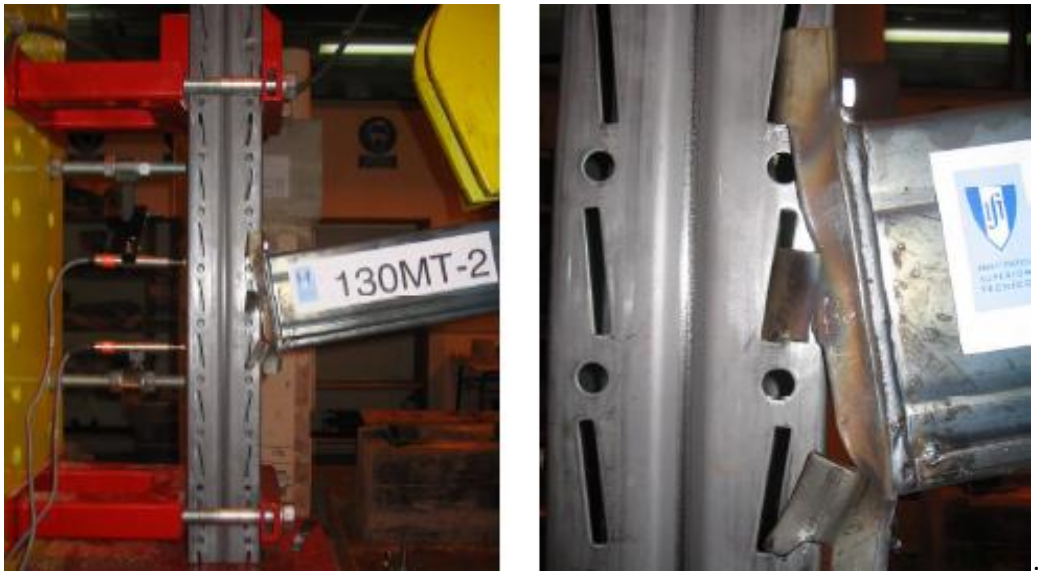

2.4: Typical collapse mode under sagging bending moments

For all tests the connection behaviour was **not influenced** by safety bolt deformation (its axial stiffness is much larger than the bending stiffness of the end-plate connector).

Column-base connections

Moment connections are typically used as column-base connections for steel pallet storage racks. In these tests, the column bases consisted of two vertical steel gusset plates fillet-welded to the base plate. The upright were connected to the base by bolting through the slotted holes in the gusset plates using two bolts for each vertical plate. The base plate was connected to the foundation surface by means of two bolts. All bolts were preloaded.

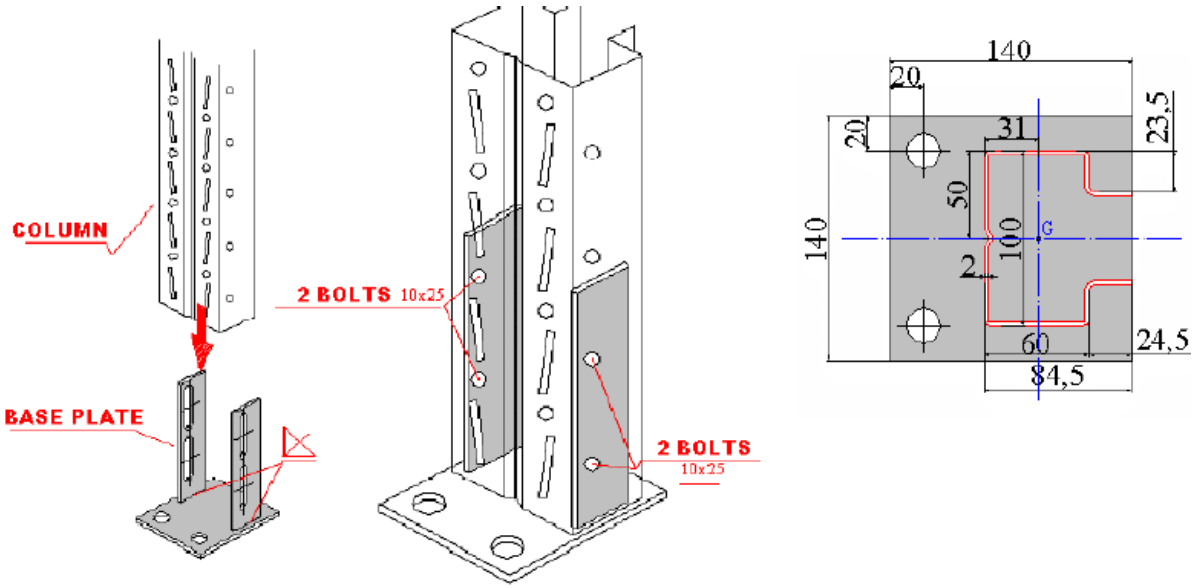

Figure 2.5: Typical column-base configuration used in the tests

This configuration is strongly non-symmetric in cross-aisle direction. A non-symmetric response was hence to be expected in cross-aisle direction under transverse load reversals, when the bolts may be either in tension or in compression.

Monotonic tests_ cross aisle direction:

In tests with bolts in tension, increasing the axial load in the column resulted in an increment of stiffness but also in a reduction of strength, ductility and energy absorption capacity of the specimens.
In tests with bolts in the compression zone, increasing the axial load in the column resulted in an increment of stiffness, strength, ductility and energy absorption capacity of the specimens bolted to a concrete deck. On the other hand, when bolted to a steel deck, there was an increment of stiffness and strength but a reduction of ductility and energy absorption capacity.

2.6: Collapse modes for specimens bent in cross-aisle direction (bolts in tension)

Monotonic tests_ down aisle direction:
In this case, the increase of axial loads results in an increment of stiffness and in a reduction of ductility and energy absorption capacity.

Failure modes
The collapse modes exhibited by the specimens were weld failure, base bending and distortional buckling of the cross section of the upright. In some tests premature weld failure caused a reduction in the rotation capacity of the connection.
The tests indicated that connecting the column base to a concrete slab or to a steel deck does not substantially change the mechanical properties or the failure mode of the connection. In both cases, however, pre-tension in the bolts should be provided.

Conclusions:
In the column base connections under cross-aisle bending, the axial compression load is beneficial when the bolts are in the compression zone (increase of the axial force → increase of resistance and stiffness but decrease of rotation capacity).
When the loading direction results in tension of the bolts, the axial force in the upright causes a reduction of resistance and stiffness of the column bases, because induces distortional buckling of the free edges of the cross-section profile.
In the cyclic tests, the higher the axial force, the bigger the difference between the resistance under positive and negative bending moments.

2.2.2 Pallet sliding-friction models

Assessment of both the static and the dynamic sliding conditions of pallets stored on steel racking systems was carried out, by means of static as well as dynamic tests performed at the Earthquake Engineering Laboratory of the National Technical University of Athens.

Static tests were carried out in both down and cross-aisle direction, by means of an “inclined plane” device, by slowly increasing the inclination of the plane.
Influence of the type of beam was investigated by adopting different types of beam specimens, with different types of surface finish. In both cross and down-aisle direction, the surface finish influenced very much the static friction factor, with differences as large as 20-30% from one type to the other, in the case of wooden pallets.
Influence of the type of pallet was investigated by adopting three different types of pallets. In both cross and down-aisle direction, the mass weight didn’t affect much the results. However, its geometry (height of the c.o.g.) and its “placement” on the pallet (centered or eccentric) resulted in small variations of the measured friction factor.

Dynamic tests were carried out with a sinusoidal excitation. A lower bound of the acceleration appeared, beyond which pallets start sliding on the steel beams. When acceleration of the mass is lower than such “lower bound”, no sliding occurs. When the “lower bound” of acceleration is exceeded, increasing the acceleration results in a lower increment in the mass

acceleration, until an “upper bound”. Beyond this, any further increase in the acceleration doesn’t affect the acceleration of the sliding mass.
In both cross and down-aisle direction lateral pallets slide systematically earlier than the central one. Dynamic behaviour in cross-aisle direction is completely different to the one in down-aisle direction: In **cross-aisle** direction, the flexural stiffness of the beams in the horizontal plane as well as their torsional stiffness influence very much the results. In **down-aisle** direction, the sliding acceleration is in general higher than the one measured in cross-aisle direction.

2.2.3 Pushover tests

Two push-over tests (one in down-aisle, the other in cross-aisle direction) were carried out at the European Laboratory for Structural Assessment of the Joint Research Center of Ispra, on full scale specimens (three levels, two bays, 6.00 m height and 3.60 m length).

Pushover test in down-aisle direction

Figure 2.4: Test set up in down-aisle direction

The specimen was brought to collapse under monotonic loading. Initially, failure occurred in the base plate connections that lost stiffness, and started behaving like hinges. Immediately afterwards, plastic hinges were formed in the uprights, at the top of the lower level, just below

the beam-to-upright connection at first level (“soft-floor” mechanism type). Finally, local buckling occurred in the uprights of the side to which the actuators were connected, between the first and the second level. This mechanism was caused by some local effect related to the concentrated load transfer mechanism between actuators and structure. In the beam-to-upright connection zones, in fact, short portions of square hollow sections were introduced inside the upright section, in order to avoid distortion of the cross section, due to the concentrated load. Local buckling occurred in the “unstiffened” portion of the upright. Collapse of the beam-to upright connection was also achieved when the transversal displacement was further increased.

Conclusion: The specimen under pushover test in down-aisle direction showed a progressive loss of stiffness associated to accumulation of plastic deformation in the column-base connections and to the large inter-storey drift of the first level. Inter-storey drifts of the upper levels were much smaller than that of the first level. This is characteristic of a “soft-floor” type of collapse mechanism that may lead to global instability due to second-order effects. In order to reduce this type of problem, the deformability of the column-base connections should be somehow limited. Therefore, the adoption of a beam at the ground level could be considered.

Figure 2.5: "soft-floor" type of collapse mechanism

Pushover test in cross-aisle direction

In the test in cross-aisle direction the base plates are subjected to bending in a direction perpendicular to the line of the bolts. Due to the eccentric position of the upright as well as of the bolt line on the base plate, under loading in cross-aisle direction, one base plate has bolts in tension (preventing bending of the plate) while the other base plate has bolts in compression (hence not preventing bending of the plate).

Furthermore, it has to be noticed that the diagonal members of the upright were positioned all in the same direction. The structure was hence positioned in such a way to resist to the applied loads with diagonals in compression, this being the most severe loading condition.

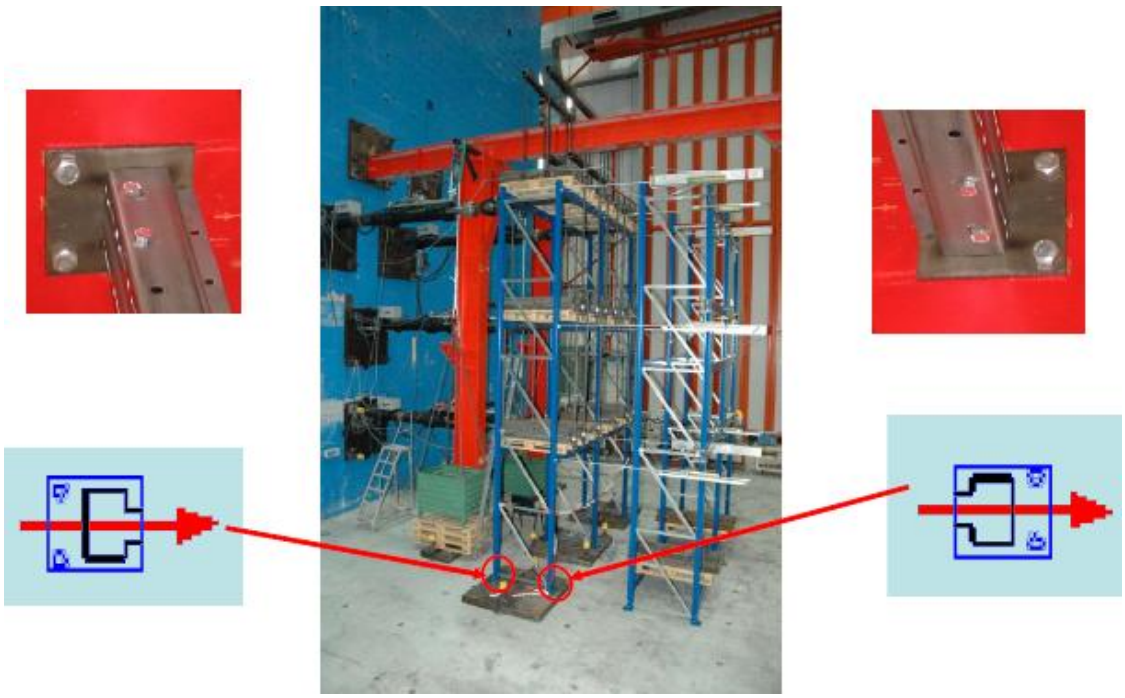

Figure 2.6: Test set-up for the pushover test in cross-aisle direction

The pushover test in the cross-aisle direction was carried out up to collapse of the specimen. Failure occurred because of buckling of the diagonal members of the transversal frames. Buckling started in the diagonals of the lower level, where the inter-storey drift is larger. The test was however continued until buckling of the diagonal members of all levels occurred. Buckling of the diagonal members did not arise simultaneously in all the transversal frames. Afterwards, the structure was subjected to torsional effects, due to difference in the stiffness of the transversal frames with and without buckled diagonals.
The structural response in the cross-aisle direction is strongly influenced by the orientation of the diagonal members of the transversal frames, by the behaviour of the base-plate connections as well as by the out-of-plane behaviour of the beam-to-upright connections.

Conclusion: Due to the bracing systems of the uprights, the specimens show a larger stiffness in cross-aisle direction that in the down-aisle. The bracing system is the most stressed structural component. Its failure leads to global collapse, accompanied by flexural-torsional

buckling of the columns. The configuration where all diagonals are inclined in the same direction should be avoided when the structure has to be erected in a seismic zone.

Figure 2.7: Deformed shape and buckling of the diagonals

Down-aisle and cross-aisle response comparison

It was observed that in **cross-aisle direction the structure was stiffer and stronger**, but more fragile than in down-aisle direction. In down-aisle direction, formation of “plastic hinges” in all the joints could be observed. In cross-aisle direction, most of the structural components remained in the elastic range, apart from the diagonal members of the bracing system of the upright frames which, beyond a certain level, could not withstand the applied compressive forces and buckled. Comparison of the absorbed energy in the two tests shows that **the behaviour in the down-aisle direction is more dissipative**, thanks to the plastic deformation of the beam-to-upright as well as of the base plate connections. In the cross-aisle direction, on the contrary, dissipation was practically due only to the plastic deformation of the diagonals of the upright frames, while most other components remained in the elastic range.

Chapter 3 simulation in Sap2000

3.1. Introduction - Methodology

The objective of this dissertation was the simulation of different racking systems through a finite element software and the comparison of the response of these models under static non linear pushover analysis. In reality, the same structures will undergo full scale pushover experiments in the future, in the context of the SEISRACKS 2 project.

The software used for this purpose is the Computers and Structures Inc' SAP2000 version 14. The main reason for which the specific programme was chosen as an analysis tool, was its popularity and circulation rather than its specification in this kind of problems. In other words, the ability of a relatively common software was also examined as far as the approach of this type of structures is concerned, thus having to overcome several simulation problems.

In total, the structures examined belong to three different companies which will be referred to as companies A,B and C due to a non disclosure agreement. For each company two structures were simulated, one designed for medium or low seismicity and the other designed for high seismicity. In general, it can be said that although the drawings of the structures were provided in detail, little additional information on the experimental behaviour of the elements and their connections was given. Therefore various parameters necessary for the non linear analysis of the models had to be assumed and remain to be examined in the future.

The purposes of this simulation were multiple: combination and comparison with future experimental data for each company, comparison between the structures of different companies for the same purposes and needs, investigation of a q behaviour factor.

For every racking configuration a 3D model was made taking into account the dimensions, the materials and the profile sections dictated by the drawings. All the members were considered as beam or truss elements and special consideration was given for the simulation of the various connections (beam to column, base plates, diagonals etc). The simulation procedure will be explained in detail in the following units. Each model was subjected to its dead and pallet loads as well as to a pushover load case in each direction (down-aisle and cross-aisle). The pushover analysis performed was displacement controlled, using one user-specified monitor node and could either have a modal shape or an acceleration form [see unit 3.3].

In each model there were assigned non linear links and plastic hinges in all the areas considered prone to exhibiting very large deformations or inelastic behaviour, as indicated by previous research, experiments and projects. More specifically, as mentioned in Chapter 2, when the specimens were subjected to pushover tests, failure occurred in the following areas:
_ base plate connections: initial stiffness loss accompanied by hinge behaviour

_ top of the lowest level of uprights: formation of plastic hinges following the failure of the base plates, thus forming a "soft-floor" type of collapse mechanism (large inner-storey drift of the first level

_ beam-to-upright connection: collapse with further increase of transversal displacement

_ diagonals: buckling of the uprights bracing starting from the lowest level and moving upwards.

As a result, the need to form four different hinge or link elements arises in order to simulate the above failures. Judging by the differences in their internal forces, these elements should be divided in the following categories:

_ elements defined by a moment-rotation diagram, with the additional ability to have fixed (with defined stiffness) or released the remaining degrees of freedom, as well as with the ability to either take into account the moment-axial force interaction or at least to control the magnitude of both moments and axial forces [useful for uprights]

_ elements controlling the moments, again defined by a moment rotation diagram though simpler than the previous ones [useful for beam ends]

_elements controlling the magnitude of the axial forces, defined by a force displacement diagram [useful for diagonals]

The simulation of the above elements of concentrated plasticity in Sap2000 can be either through the assignment of plastic hinges or through the definition of multi linear two-joint links. The advantages and disadvantages of which are explained in the following units. Both types were used in various combinations during this project and with various results that often were misleading and unrealistic. Some of these attempts will be mentioned in the following units. In general, it is difficult to specify whether and which of these elements is completely suitable for the simulation of the problem since the difficulties are related with not only the limits of the software used but also with the limits of knowledge available concerning racks and their members.

What is more, it should be reminded that in most cases the sections of the upright elements involved in racking systems belong to class 4, which means that they fail before reaching neither their plastic nor their elastic moment due to local buckling phenomena. Therefore, plasticity does not really exist for a class 4 section and these elements should be dealt with an elastic method of analysis. However the shape of the moment-rotation curves is similar for all classes, and so what is referred to as plastic hinge and plastic behaviour from this point on, actually refers to an inelastic behaviour.

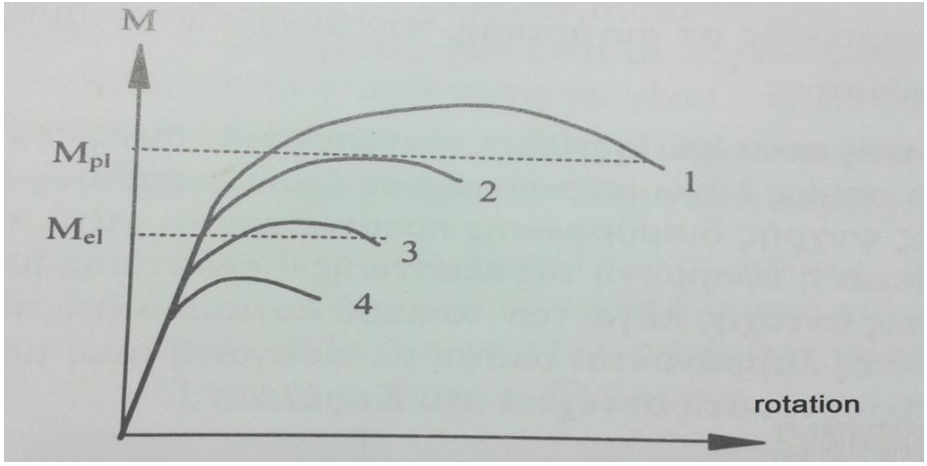

Figure 3.1: Moment-rotation curves for the different classes of sections

3.2. Simulation of structures

_ Geometry

All the configurations examined were according to a X-Y-Z grid defining six bays, a front and a rear vertical level and four floors. The grid was divided in a primary grid and a secondary grid. The primary grid described the aforementioned geometry of the structure whereas the secondary was much denser and was used for the position of the diagonals, the pallet loads and all the secondary nodes in general.

Global axes:

_ Axis X is parallel to picking bays (down-aisle direction)

_ Axis Y is parallel to upright frames (cross-aisle direction)

_ Axis Z is the vertical direction all the secondary nodes in general.

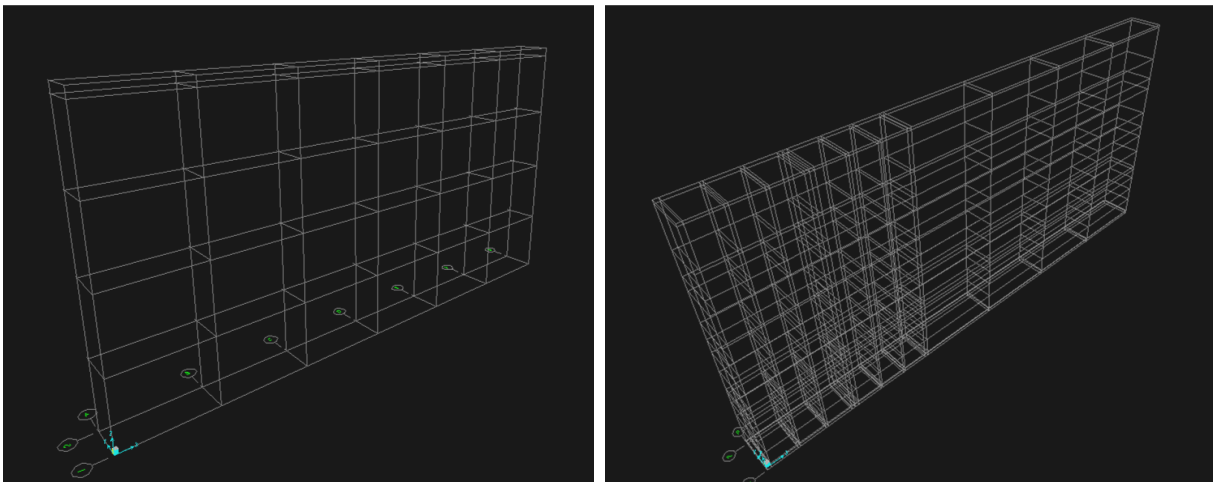

Figure 3.2: Primary and secondary grids in X,Y,Z axes

_ Elements and profiles

The uprights as well as the pallet beams of the structures were simulated as beam elements whereas all the vertical and horizontal bracings were simulated as truss elements. In Sap2000 all the above elements are referred to as Frame Sections. The profiles of the elements were defined in Sap's Section Designer tool were the geometry and the materials can be specified.

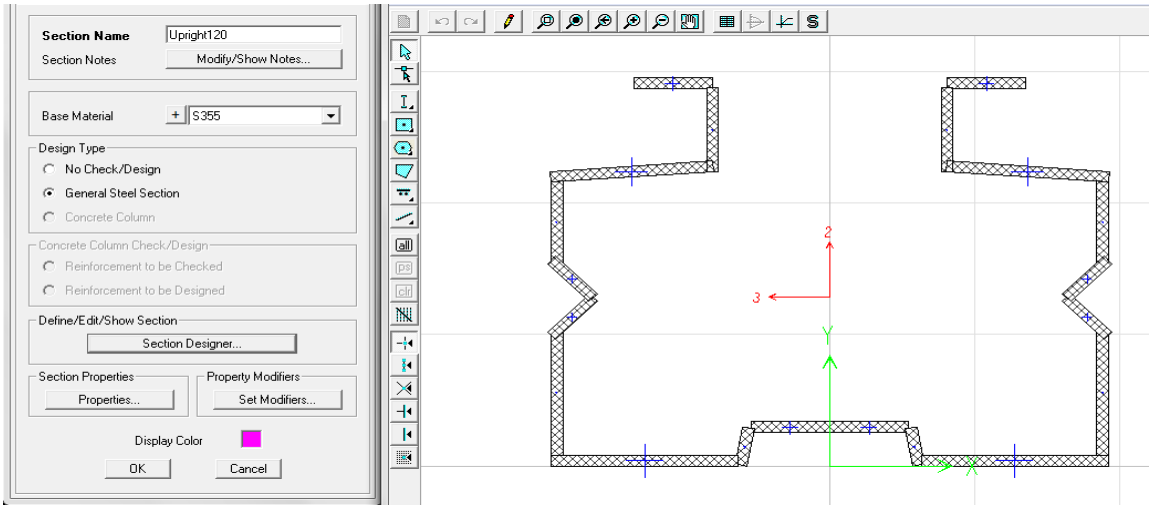

Figure 3.3: A section designer example

_ Uprights

All the uprights are considered fixed in their supports on the ground. However, between the fixed support and the upright there is assigned a multi linear plastic link which simulates the action of the base plate. Apart from the plastic links, plastic hinges were also assigned at the top of the lowest level of each column defined in order to take into account the interaction between moments and axial forces. These hinges are only activated in case the defined elastic yield limit is exceeded.

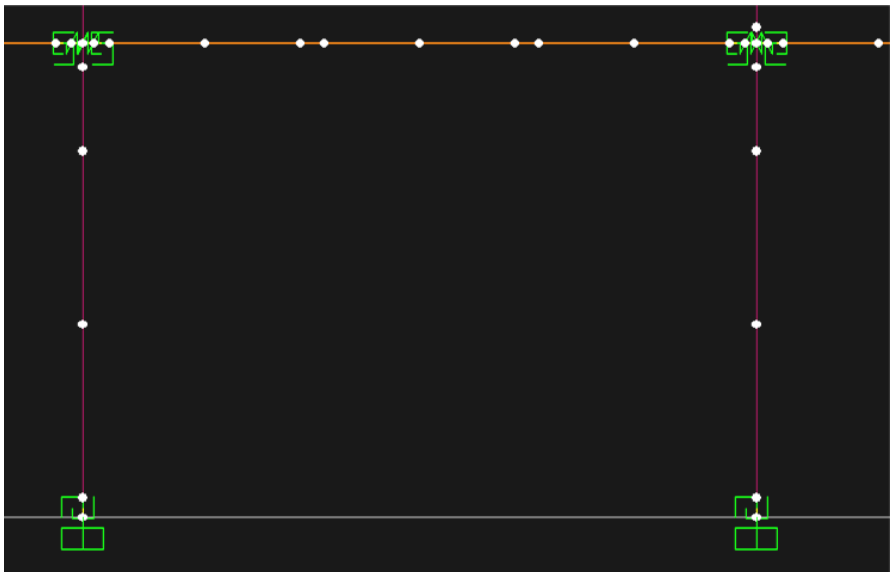

Figure 3.4: Detail of link assignments in the lowest level

As mentioned before the supports of the uprights are considered semi-rigid and could be simulated with rotational springs. These base plate links have a defined axial stiffness (E*A/L referring to the column element), a defined moment-rotation diagram around Y axis and are free to rotate around X axis. Whenever possible the moment-rotation data were taken from the experimental data provided by the construction companies.

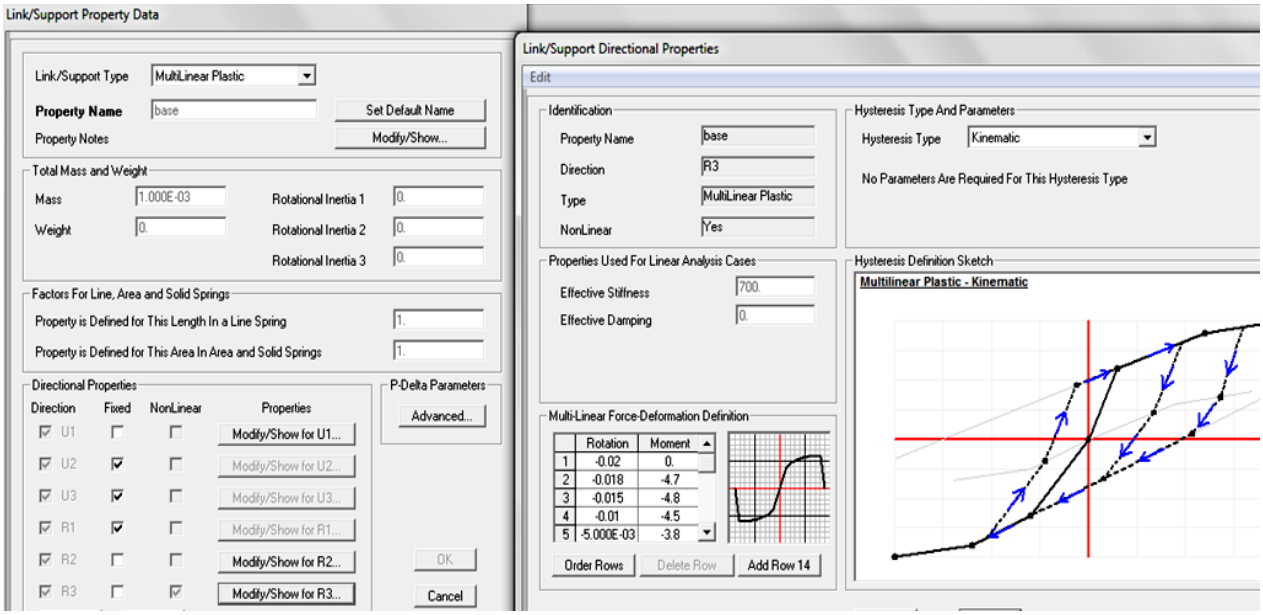

Figure 3.5: A base-plate link property example

_ Beams

Each bay has the capacity of three pallets per level and therefore the internal nodes of the beams were drawn accordingly. Each pallet was represented by three nodes, two in the ends and one in the middle. The free space between the pallets of each bay was considered equal and so the distances were evenly distributed. The pallet loads were considered as concentrated loads and were imposed according to the geometry of the pallets. As mentioned in unit 1.2 the length of the typical Euro pallet in X direction is 800 mm and the total load is 8 kN.

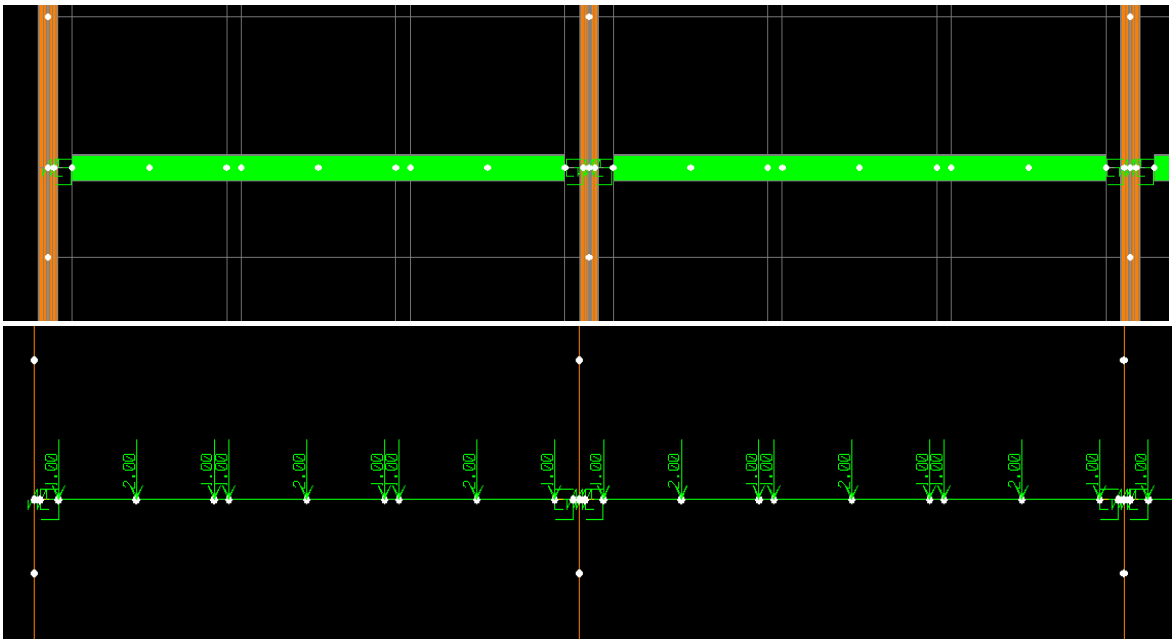

Figure 3.6: Detail of nodes, links and load assignments in beams

In the end points of the pallet beams are placed two types of links:

_ a rigid link connecting the column with the beam, representing the geometrical eccentricity between the centroid of the upright and the edge of the beam

_ a multi linear plastic link simulating the non linear behaviour of the beam-end connector.

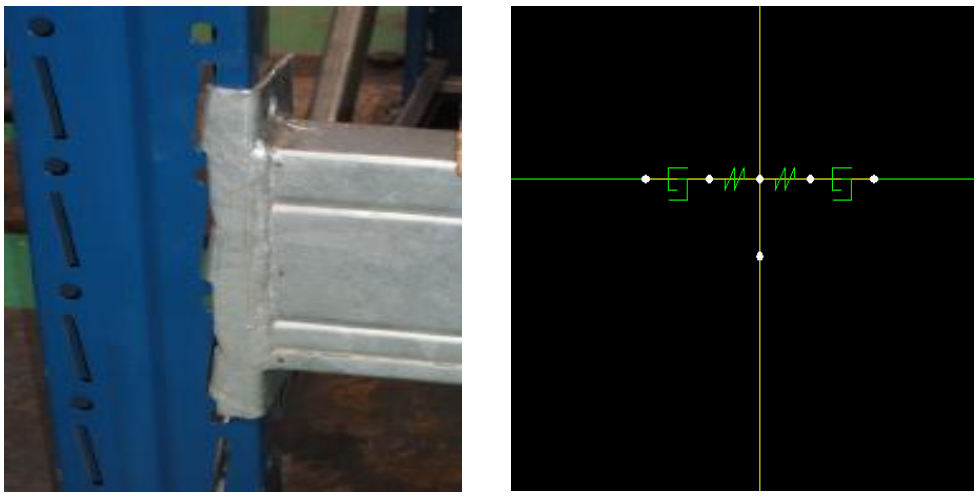

Figure 3.7: Beam-to-column connection

The properties of the multi linear plastic links are again defined using experimental data from the companies and are used to describe the moment-rotation relation regarding the rotations around Y axis.

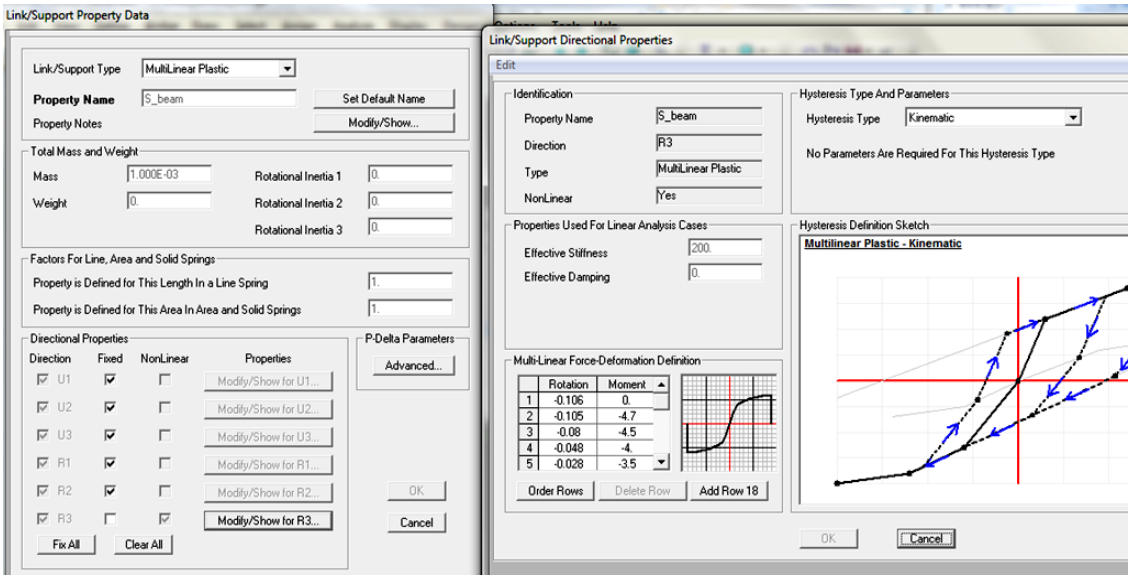

Figure 3.8: Example of beam-end connector link properties

As mentioned before, the behaviour of the beam-to-column connections is of major importance for the structure since its stability in the down-aisle direction is achieved through frame action. This connection is actually semi-rigid and could be described by a moment-rotation diagram. The behaviour of these connections can be simulated with rotations springs whose properties ought to be defined by experiments. The connection's stiffness is equal to the slope of the moment-rotation diagram. For elastic analysis this slope is considered to be constant. However the use of the initial slope value renders the connection stiffer than it really is, thus resulting in larger moments and smaller lateral deformations of the structure. In this way, the P-delta effects which jeopardize the structure's stability are underestimated and the results are not safe. For this reason, the calculations must be done using secant stiffness.

_ Diagonals

Diagonal members are truss elements of open and simply symmetric profiles. In all cases examined they were considered to have a reducing factor of about 10% multiplied with their gross area in order to simulate the experimental behaviour of the diagonals which was different than the theoretical one, as far as shear stiffness was concerned. Furthermore, in order for the diagonals to behave as trusses all the moments had to be released in both ends of the elements.

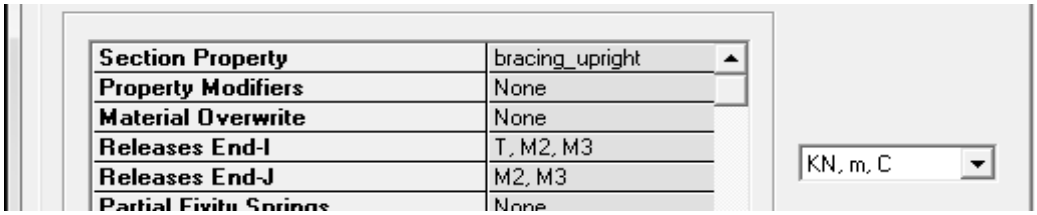

Figure 3.9: Moment releases in diagonals

As far as the hinges are concerned, they are assigned with axial force, deformation controlled type of hinges which are activated during the pushover in cross-aisle direction. The yield force used in the definition of these hinges is the minimum (critical) calculated by either the buckling check of the member or by the checks of the bolts (shear resistance and bearing resistance). In other words:

$$Ncr = \min\{ \chi * A * f_y,\ F_{v,Rd} = a_v * f_{ub} * A_S / 1.25,\ F_{b,Rd} = (2.5 * a_b * f_{u,Profile} * d * t_{Profile}) / (1.25) \}$$

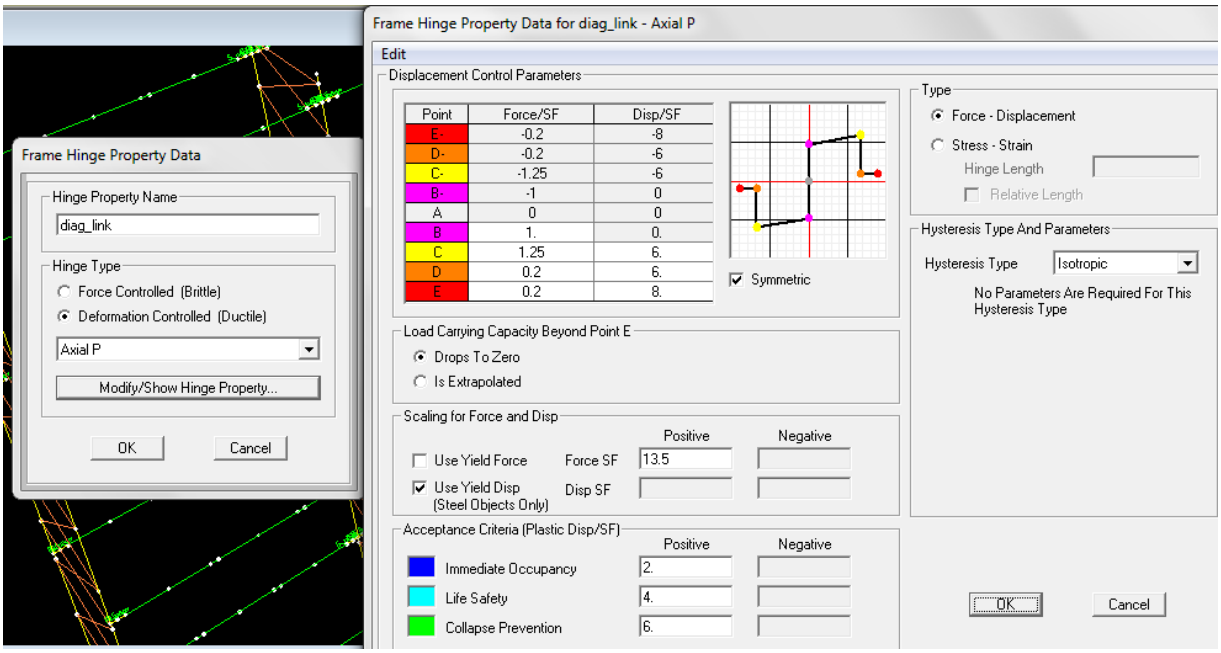

Figure 3.10: Example of diagonal hinges

3.3 Nonlinear static analysis in SAP2000

Pushover analysis is a static, nonlinear procedure in which the magnitude of the structural loading is incrementally and monotonically increased in accordance with a certain predefined pattern. With the increase in the magnitude of the loading, weak links and failure modes of the structure are found. Static pushover analysis is an attempt to evaluate the real
strength of a structure and it is therefore a useful and effective tool for performance based design. The ATC and FEMA documents define force-deformation criteria for hinges used in pushover analysis. As shown in Figure, five points labeled A, B, C, D, and E are used to define the force-deformation behavior of the hinge and three points labeled IO, LS and CP are used to define the acceptance criteria for the hinge (Immediate Occupancy, Life Safety and Collapse Prevention respectively).

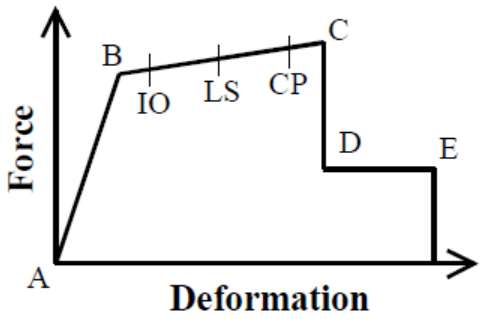

Figure 3.11: Force-deformation behaviour of hinges and characteristic points

SAP2000 is a general purpose, three-dimensional structural analysis program that can be used for performing pushover analysis, since it provides many useful tools, as briefly mentioned below.

The following **types of nonlinearity** are available in SAP2000:
_ material nonlinearity: nonlinear properties in Link/Support elements, tension/compression limits in Frame elements, Plastic hinges in Frame elements
_ geometric nonlinearity: P-delta effects, large displacement effects
_ staged construction: changes in the structure, aging, creep, shrinkage

Mathematically, nonlinear static analysis does not always guarantee a unique solution. Inertial effects in dynamic analysis and in the real world limit the path a structure can follow. But this is not true for static analysis, particularly in unstable cases where strength is lost due to material or geometric nonlinearity. Small changes in properties or loading can cause large changes in nonlinear response.

A pushover analysis may start from zero **initial conditions**, or it may start from the end of a previous nonlinear analysis.

The **pushover load** can be applied as any combination of Load Patterns, Acceleration Loads and Modal Loads. The modal load is a pattern of forces on the joints that is proportional to the product of a specified mode shape. The acceleration load is a uniform load pattern defined by uniform acceleration acting in any of the three global directions (X, Y, Z).
The loads can be applied incrementally from zero to the full specified magnitude. The loading can be controlled by monitoring the resulting displacement in a specified node in the structure.
Pushover analysis can be performed as either **force controlled** or **displacement controlled**. Force-controlled option is useful when the magnitude of the load that will be applied is known (such as gravity loading) and the structure is expected to be able to support that load.
Displacement-controlled procedure should be preferred when the target displacement of the structure is known but the load required is not known in advance. This is most useful when the structure is expected to lose strength during the analysis and become unstable. To use displacement control, a displacement component must be selected in order to be monitored. This is usually a single degree of freedom at a joint. The magnitude of the target displacement is also defined, and the programme attempts to apply loads in order to reach that displacement. The load magnitude may be increased or decreased during the analysis.

However it should be stressed out that displacement control is not the same thing as applying displacement loading on the structure. Displacement control is only used to measure the displacement at one joint that results from the applied loads, and to adjust the magnitude of the loading in an attempt to reach the predefined target displacement. The overall displaced shape of the structure will be different for different patterns of loading, even if the same displacement is controlled.

In order to see how the structure responded during loading and for the pushover curve to be designed, it is possible to save intermediate results (steps) during the analysis. In Sap2000 the **number of saved steps** is defined by the following parameters:
_ minimum number of saved steps
_ maximum number of saved steps
_ option to save positive increments only
The minimum and maximum number of saved steps define the number of points saved during the analysis. The maximum length of a step is equal to the target displacement divided by the specified Minimum Number of Saved Steps. The programme starts the analysis with this increment. If a significant event occurs at a step length less than this increment, then this step is also saved and the programme continues with the maximum increment from that point. The Maximum Number of Saved Steps controls the number of significant events that will be saved.
The option to save positive increments only, is useful in displacement controlled analysis and in the case of extreme nonlinearity when a pushover curve may show negative increments in the monitored displacement while the structure is trying to redistribute the force from a failing component.

The nonlinear equations are solved iteratively in each load step. This may require reforming and resolving the stiffness matrix. The iterations are carried out until the solution converges. If convergence cannot be achieved, the program divides the step into smaller substeps and tries

again. Several parameters are available in Sap2000 to control the iteration and substepping process such as:

_the maximum number of steps allowed in the analysis,

_the maximum of null (zero) steps allowed (when a hinge is trying to unload or when iteration does not converge and a smaller steps is attempted or when an event such as yielding occurs),

_the maximum number of iterations per step to achieve equilibrium (at first constant stiffness iteration is tried, if convergence is not achieved Newton-Raphson iteration is tried next, if both fail the step size is reduced),

_the iteration convergence tolerance (for the needs of this thesis the tolerance was reduced from default 10^{-4} to 10^{-3})

Some other useful tools and parameters for nonlinear analysis are also available in Sap2000 but in the current unit only those parameters used for the purposes of this project were mentioned. Furthermore, important display capabilities are provided in the graphical user interface in order to plot and output pushover curves, the state of hinges at each step etc.

3.4 Geometric nonlinearity in SAP2000

When the load on a structure and/or the resulting deflections are large, the load-deflection behaviour may become nonlinear. SAP2000 is capable of considering geometric nonlinearity in the form of either P-delta effects or large displacement effects. Strains within the elements are assumed to be small. Geometric nonlinearity can be considered on a step-by-step basis in nonlinear static analysis and incorporated in the stiffness matrix for linear analyses. More specifically the two options for geometric nonlinearity are as follows:

P-delta (large stress) effect: The suitable option when large stresses/forces/moments are present within the structure. The equilibrium equations take into partial account the deformed configuration of the structure.

The P-delta effect refers specifically to the nonlinear geometric effect of a large tensile or compressive stress upon transverse bending and shear behaviour. A compressive stress tends to make a structural member more flexible in transverse bending and shear, whereas a tensile stress tends to stiffen the member against transverse deformation and stiffen the structure by resisting the rotation of elements.

On the other hand, compressive forces tend to enhance the rotation of elements and destabilize the structure. If an element is in compression, it s more flexible against the axial load (moment and deflection are increased). If the compressive force is large enough, the transverse stiffness tends to zero and the deflection tends to infinity, thus the structure buckles. Only the transverse deflection is considered in the deformed configuration. Any change in moment due to a change in length of the member is neglected.

This effect requires a moderate amount of iteration. For most structures, the P-delta option is adequate, particularly when material nonlinearity dominates.

Large displacement effect: The suitable option when a structure undergoes large deformations (strains and rotations), even when the stresses are small in all elements. All equilibrium equations are written in the deformed configuration of the structure. Large displacements and rotations are accounted for but strains are assumed to be small. If the position or orientation of an element changes, its effect upon the structure is accounted for. However if the element changes significantly in shape or size this effect is ignored. This effect in SAP2000 includes only

the effects of large translations and rotations. A requirement for the elements is that the strains and relative rotations within them must be small.
This option should be used for any structure undergoing significant deformation, and for buckling analysis. It requires a large amount of iterations because it is more sensitive to convergence, Newton-Raphson iterations being usually the most effective.

It hereby should be noted that, in SAP2000 when continuing one nonlinear case from another it is recommended that they both have the same geometric nonlinearity settings.

3.5 Material nonlinearity in SAP2000

3.5.1 Frame Hinges

Plastic hinges at any number of locations along the length of any Frame element can be inserted in Sap2000. Each hinge represents concentrated post-yield behaviour in one or more degrees of freedom. These hinges only affect the behaviour of the structure in nonlinear static and nonlinear direct-integration time-history analyses.

The **types** of hinges available are: uncoupled moment, torsion, axial force and shear hinges. There is also a coupled P-M2-M3 type of hinge which yields based on the interaction of axial force and bi-axial bending moments at the hinge location. Subcategories of this type of hinge include P-M2, P-M3 and M2-M3 behaviour.

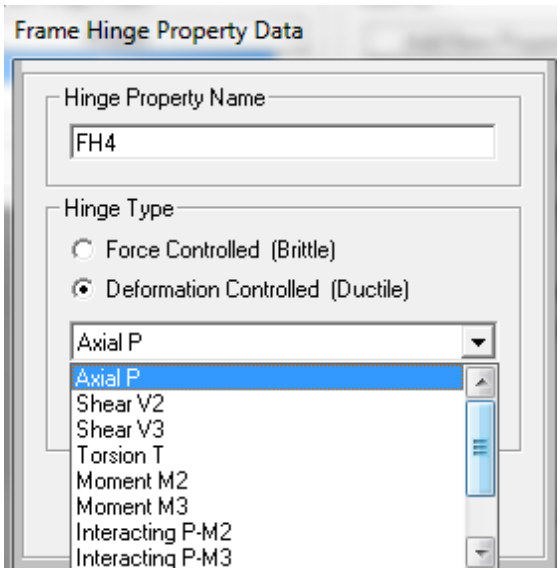

Figure 3.12: Types of deformation controlled hinges

Hinge properties can be user defined or computed automatically from the element material and section properties according to FEMA-356 (FEMA, 2000) criteria. In this project all hinges used were user defined with properties deriving from experimental results whenever possible.

Strength loss is permitted in the hinge properties and in order to help with convergence, the program automatically limits the negative slope of a hinge to be no stiffer than 10% of the elastic stiffness of the Frame element containing the hinge.
A hinge property is a named set of rigid-plastic properties that can be assigned to one or more elements. Each hinge property may have plastic properties specified for any number of the six degrees of freedom. The axial force and the two bending moments may be coupled through an interaction surface. Degrees of freedom that are not specified remain elastic.
For each force degree of freedom (axial or shear), the plastic force-displacement behaviour may be specified. For each moment degree of freedom (bending or torsion), the plastic moment-rotation behaviour may be specified. As far as the coupled P-M types of hinges are concerned, the interaction P-M curve must also be specified.

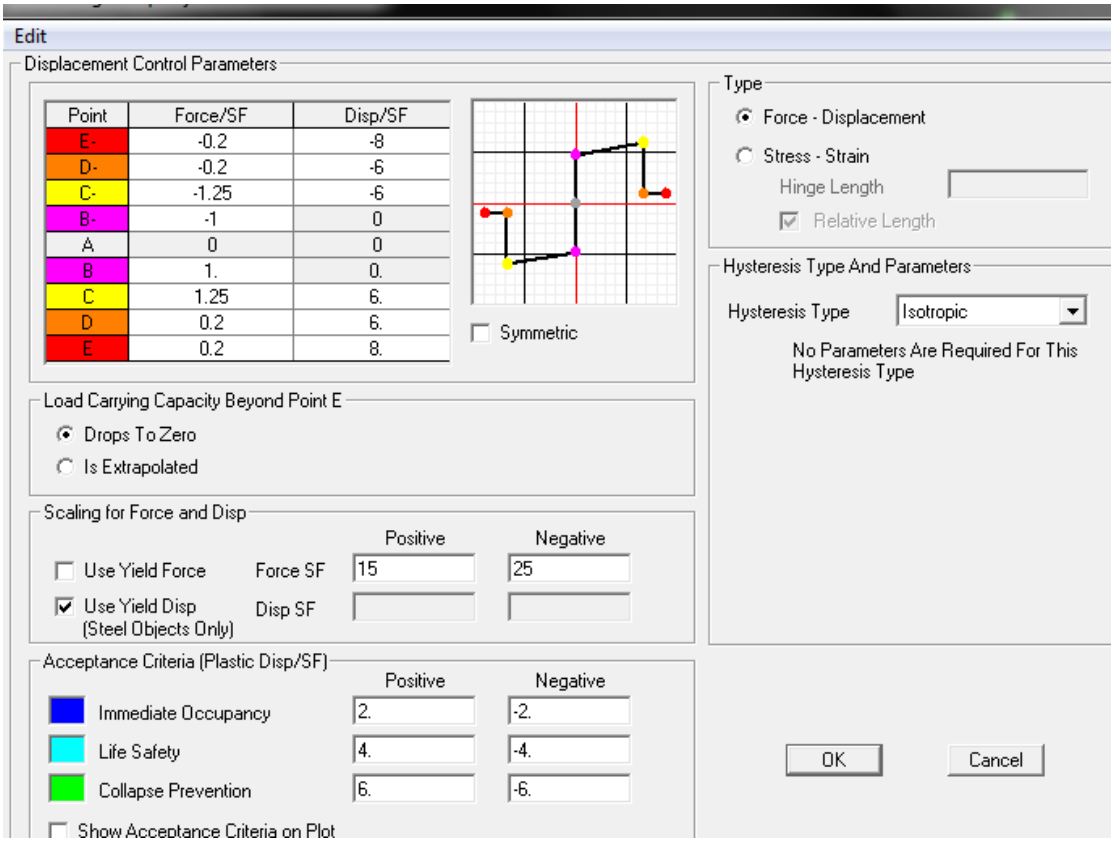

Figure 3.13: Control parameters of "axial P force" type hinges

For each degree of freedom, a force-displacement (or moment-rotation) curve must be specified, providing information on the yield value and the plastic deformation following yield. This curve has values at five characteristic points, A-B-C-D-E (see figure 3.11) and can be symmetric or not. These characteristic points are:
_ A is always the origin.
_ B represents yielding. No deformation occurs in the hinge up to point B. The displacement (or rotation) at point B is subtracted from these at points C,D and E. As a result, only plastic deformations beyond point B are exhibited by the hinge (as shown in figures 3.13 and 3.14, lines AB are always vertical). Prior to reaching point B all deformation is linear and occurs in the element. Plastic deformation beyond B occurs in the hinge in addition to any elastic deformation that may occur in the element.

_ C represents the ultimate capacity. However it is possible to specify a positive slope for C-D.
_ D represents a residual strength for pushover analysis.
_ E represents total failure. Beyond point E the hinge drops load directly to zero.
For the P-M-M type of hinge, an interaction (yield) surface is specified in a three-dimensional P-M2-M3 space that represents where yielding first occurs for different combinations of axial force P, minor moment M2, and major moment M3. The surface is specified as a set of P-M2-M3 curves, where P is the axial force (tension is positive), and M2 and M3 are the moments.
In the following figures, the frame hinge property tables are displayed for a P-M type of hinge.

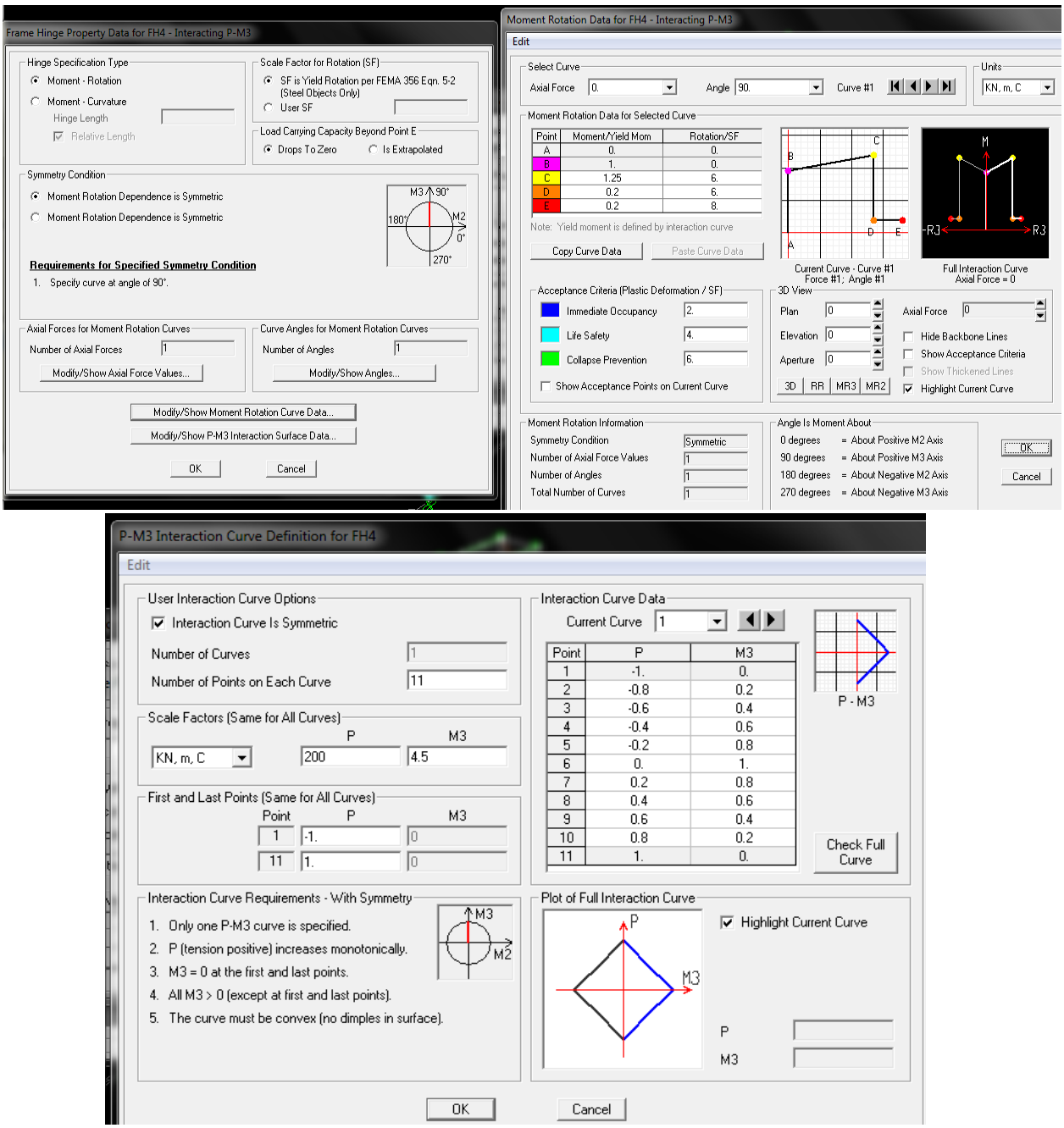

Figure 3.14: Control parameters of "P-M3" type hinges

3.5.2 Link elements

A Link element is a two-joint connecting link. Each element is assumed to be composed of six separate “springs,” one for each of six deformational degrees of freedom (axial, shear, torsion, and pure bending). Link elements can have linear or nonlinear property sets. These sets contain linear properties that are used by the element for linear analyses (and for other types of analyses if no other properties are defined). Furthermore these property sets may also contain nonlinear properties that will be used for all non linear analyses, and for linear analyses that continue from nonlinear analyses.

Amongst various other types of nonlinear behaviour that can be modeled with the link elements, is the **multi-linear uniaxial plasticity type** with several types of hysteretic behaviour. This multi-linear type was used for the purposes of this project.

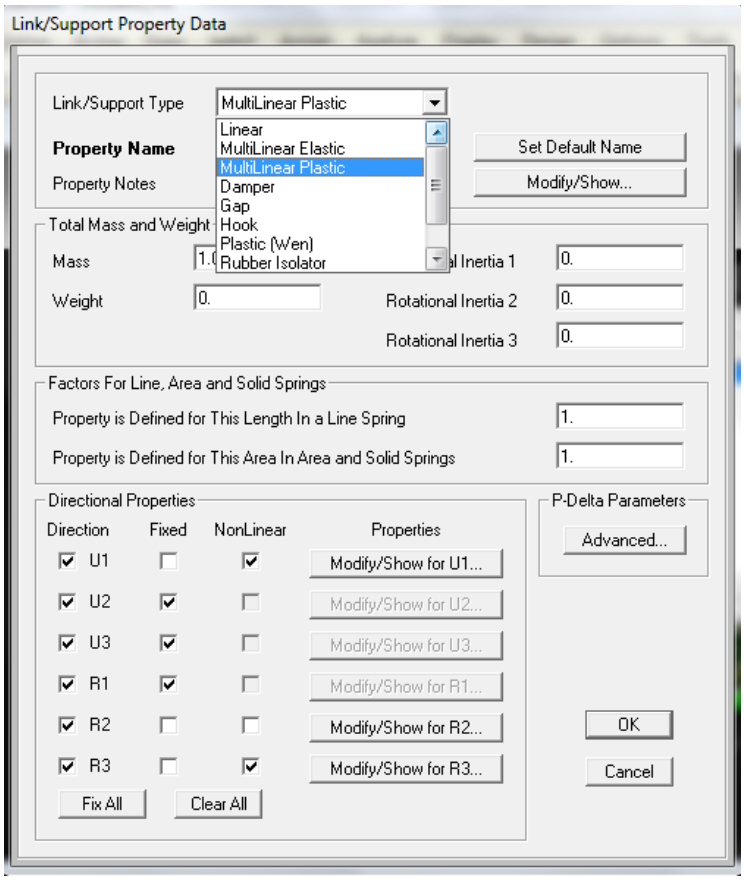

Figure 3.15: Link/Support property data

Each element has its own **local coordinate system** for defining the force-deformation properties and for interpreting output. The axes of this local system are denoted 1,2 and 3. The system is right-handed. The first axis (1) is directed along the length of the link element. The default orientation of the local 2 and 3 axes is determined by the relationship between the local 1 axis and the global Z axis. The local 1-2 plane is taken to be vertical. The local 2 axis has an upward sense (+Z) unless the elements is vertical, in which case the local 2 axis is taken to be horizontal along the global +X direction. The local 3 axis is always horizontal.

A Link/Support Property is a set of structural properties that can be used to define the behaviour of one or more Link or Support elements. Each Link/Support Property specifies the force-deformation relationships for the six internal deformations. Mass and weight properties may also be specified.

Link elements with fixed degrees of freedom should not be connected to other fixed link elements or connected to constrained joints. Otherwise, this would result in joints that are multiply constrained, which may be inaccurate for dynamics.
Every degree of freedom in a nonlinear property type must have specified a set of uncoupled linear stiffness and damping coefficients that are used instead of the nonlinear properties for linear analyses. These substitute linear properties are called “linear effective stiffness” and “linear effective damping” properties.

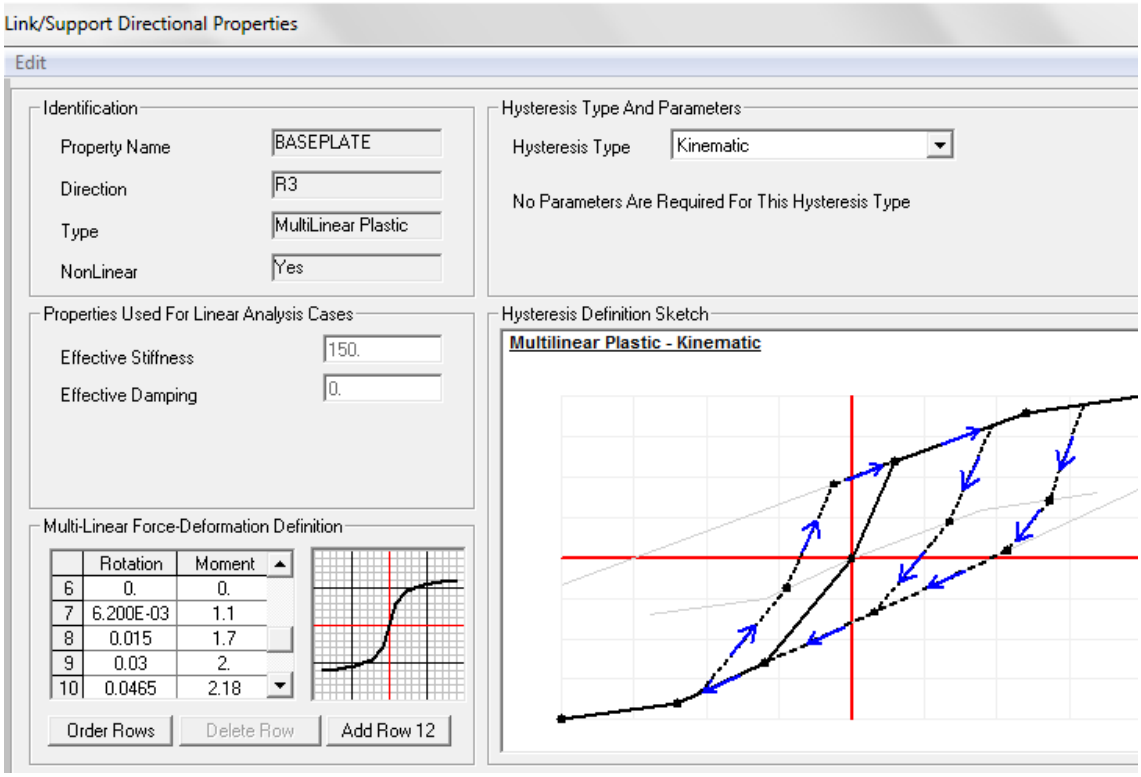

Figure 3.16: Multi-linear plastic link properties

During nonlinear analysis, the nonlinear force-deformation relationships are used at all degrees of freedom for which nonlinear properties were specified. For all other degrees of freedom, the linear effective stiffnesses are used.

As mentioned before the type of links used in this project was the multi-linear plastic Kinematic type. This is based upon kinematic hardening behaviour that is commonly observed in metals. All internal deformations are independent which means that the deformation in one degree of freedom does not affect the behaviour of any other. If no nonlinear properties are specified for a degree of freedom, then it is assumed to be linear. The nonlinear force deformation relationship is given by a multi-linear curve that is defined by a set of points and can take almost any shape, as long as it follows some restrictions:

_ one point must be the origin (0,0),
_ at least one point with positive and one point with negative deformation must be defined,
_ deformations increase monotonically,
_ forces or moments must have the same sign as the deformations (or they can be zero),
_ the final slope at each end of the curve must not be negative.

3.6 Simulation problems

After having presented the context in which the simulation was made, it is time to present the difficulties encountered during the various simulation attempts. These difficulties were either related with the nature of the problem (peculiarities of structure and lack of sufficient experimental data) or with the software chosen.

To start with, the material used in most cases was cold formed steel. As mentioned in unit 1.3 this type of steel has a different stress-strain diagram since it does not have a specific yield limit. Furthermore it is prone to instabilities (buckling) and its ductility/inelastic capacity is very limited. However when assigning materials in the frame elements of the models in SAP2000, the "Cold formed steel" option could not be chosen due to incompatibilities with the hinges that were later assigned in the same elements. As a result the materials assigned in all models are considered to be the regular (hot formed) Steel.

As far as material nonlinearity is concerned, the most basic simulation problem had to do with the non-linear behaviour of the various connections. As mentioned in the previous units of this chapter, the beam end connectors (beam-to-column connections) as well as the base plates (column base connections) have a nonlinear behaviour that is difficult to be calculated or predicted in advance. That is why the experimental results are necessary in order to define the moment-rotation diagram that better describes each connection. Unfortunately in most cases these data were either non existing or insufficient.
Apart from this, the different kinds of connections have obviously different behaviour and are prone to different kinds of failures. This means that they must be simulated with different tools, depending on their internal forces and failure modes. However in SAP2000 there are two basic tools to simulate material non linearity: plastic hinges and links. Plastic hinges are only activated when the element section is found beyond its yield limit and therefore they are very reliable as far as the elastic behaviour of the structure is concerned. However their reliability is a bit uncertain in the inelastic region because of the yield moments and rotations they take into account. On the other hand, the links are more reliable in their inelastic behaviour since everything is user defined. However they seem to affect the structure even from the first steps of the analysis and therefore attention has to be paid on the results of the static linear analyses and the modal analysis. What is more, in the structures examined it was discovered that the exclusive use of links in the columns resulted in unrealistically large values of axial loads. That happened because although links can be assigned with a very accurate diagram (e.g. moment-rotation curve) for each degree of freedom, they cannot take into account neither the interaction between their internal forces nor they can be assigned with a failure curve. That is why in the case of uprights, a combination of hinges and links had to be used in order to

achieve both control on the interacting forces and moments and on the desired inelastic behaviour.
Furthermore, the lack of experimental data rendered it quite difficult to simulate the conditions under which buckling occurred in both columns and diagonals. As a result additional programs and calculations had to be used, whereas some of the parameters input eventually had to be chosen by the users (always bearing in mind the achievement of realistic results).

As far as the simulation of pushover is concerned, SAP2000 has specific ways of simulating the application of this load case [see unit 3.3] which are not similar to the experimental set up. The pushover tests will be probably performed with the use of jacks and cables that will act on every level of the rack and will pull the specimen with an inverted triangular force distribution, always monitoring the displacements. On the other hand the pushover load cases that were used in SAP2000 were displacement controlled (using a specified monitor node) and had either the form of uniform acceleration or the form of the suitable modal shape. These two options did not lead to exactly the same results as far as the pushover curve is concerned but they did indicate similar critical force. However, the acceleration type of pushover indicated smaller deformations and larger forces and it was the type of load case used in order to plot the final diagrams in the following units. Furthermore, the pushover load cases that use modal shapes could not be applied to the models that refer to high seismicity due to their rear vertical bracings that create torsional modes which are not suitable for the simulation of the pushover test. In addition to this, apart from the type of load case, special attention should be paid concerning the target displacement assigned for the pushover and the number of steps for each analysis in SAP2000. The non linear analysis being very sensitive, the results of the pushover curves were different even after a slight change in these parameters. In order for the results to be more stable and also the computational time to be affordable, it is suggested that the number of steps are more than ten (default price) and less than sixty. It is also suggested that the target displacement is not defined as much larger than the expected limit because that could create convergence problems.

Chapter 4 models' presentation

4.1. Introduction - Presentation of models

In this chapter, the racking systems that were examined are presented. Each company provided with drawings of the general layout and the details, some of which are hereby presented in a simplified version.
For each of the companies A, B and C the following drawings are presented, whenever possible:
_ longitudinal view
_ plan view
_ cross-aisle view
_ details of the upright (cross section and view)
_ details of the base plates
_ details of horizontal bracing
_ details of upright bracing (diagonals)
_ details of beam end connections
_ view of the rear bracing and its connection to the main rack

As mentioned before, for each company, two types of structures were examined: one for medium or low seismicity and one for high seismicity.

Similarities:
_ All of the racking systems examined in this project have four levels and six bays.
_ Their height is approximately 8.00 meters, their width 1.10 meters (without the rear bracing) and their length is approximately 17.00 meters.
_ Every compartment has the capacity of three unit loads, which means that in each bay there can be up to twelve pallets and each racking system can carry up to seventy two units of palletized goods. The weight of each unit load is estimated 8kN or 800kg (Euro Pallets).

Differences:
In order to enable the comparison between the different cases examined, in the end of this chapter there is a table with summarized configurations, materials and basic section properties for each racking system.

4.2. Company A

4.2.1 Medium seismicity

_ Longitudinal view

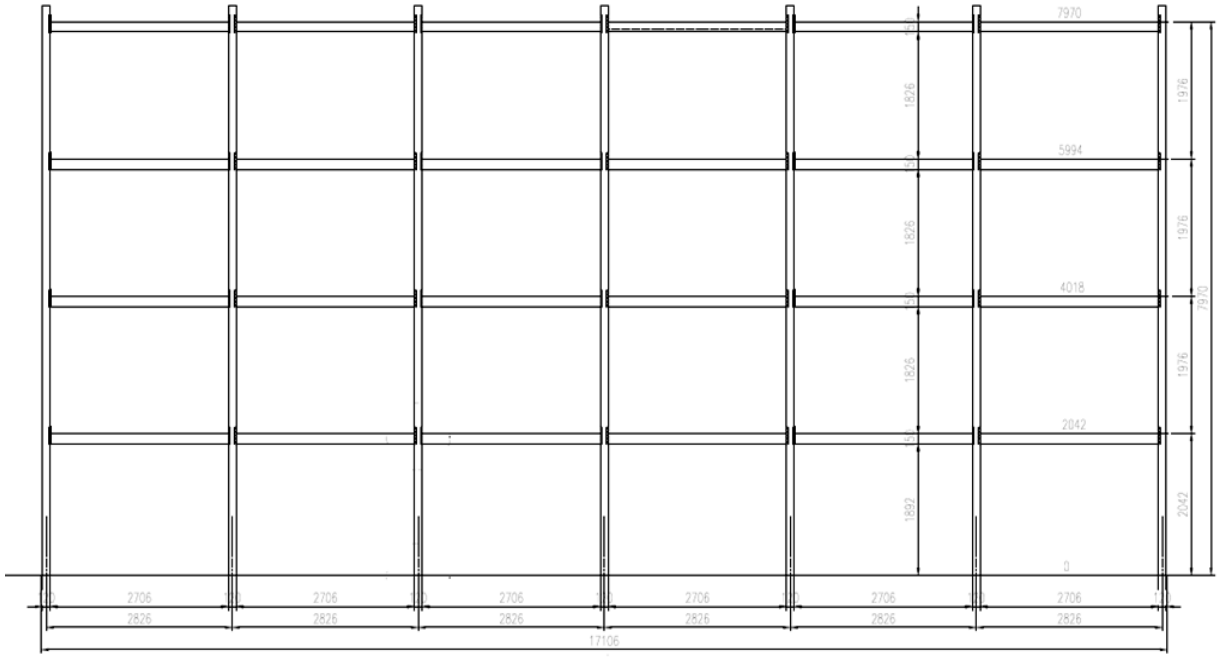

_ Plan view

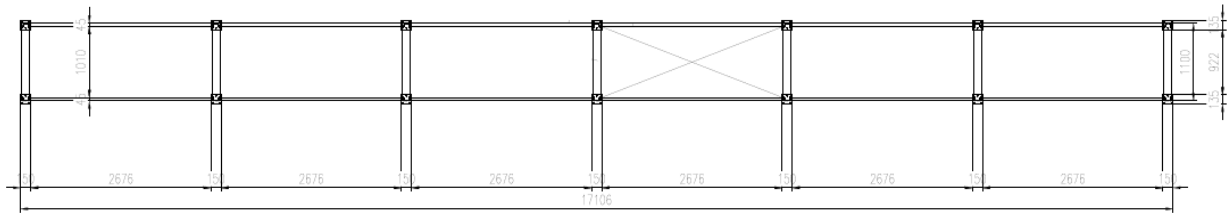

_ Cross-aisle view

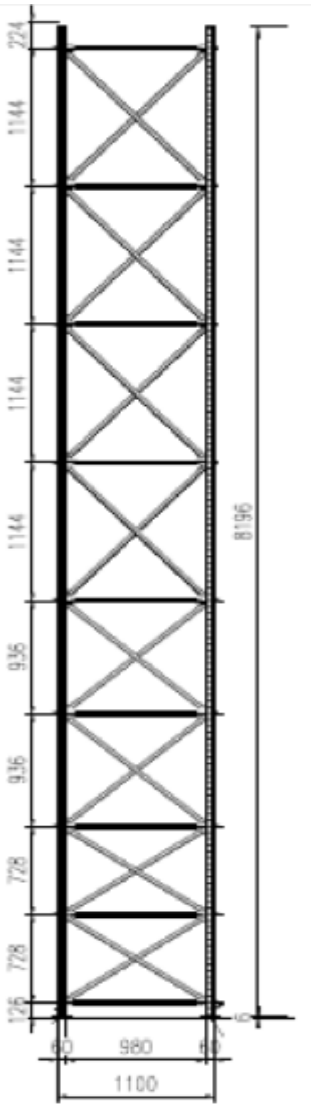

_ Details of uprights and base plates

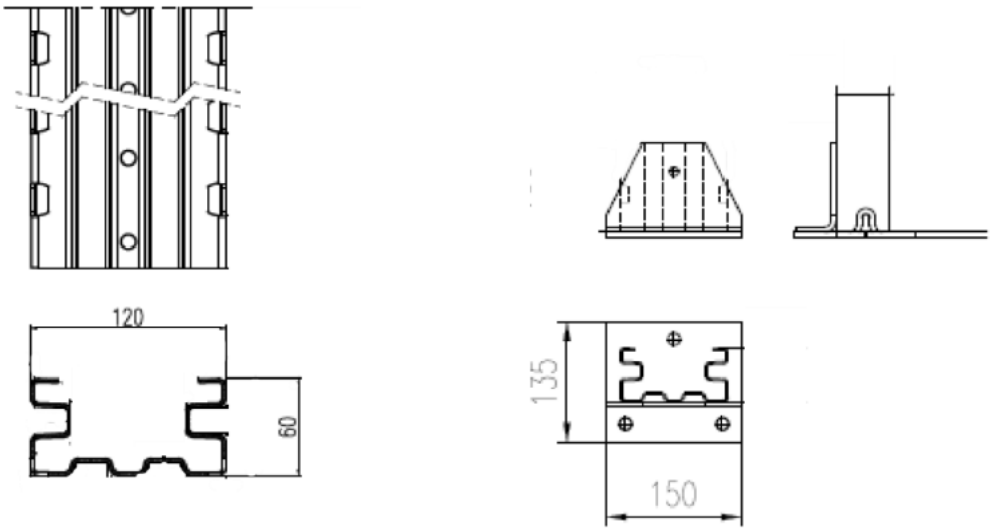

_ Beam end connections

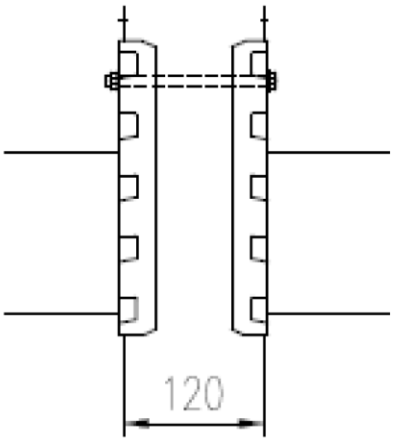

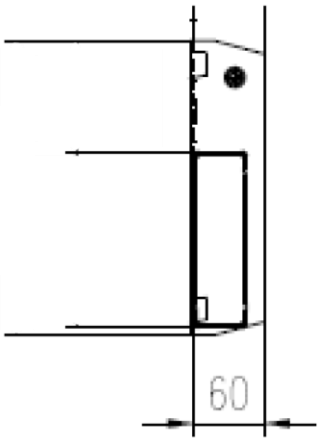

_ Diagonal connection

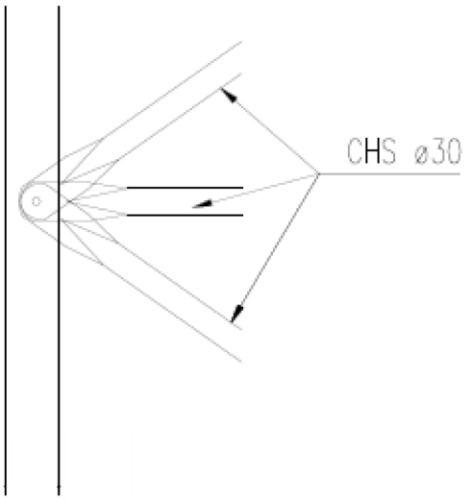

_ Horizontal bracing

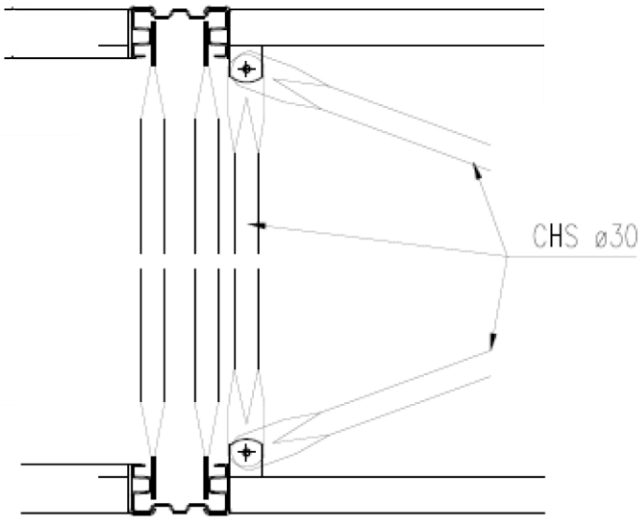

4.2.2 High seismicity

_ Longitudinal view

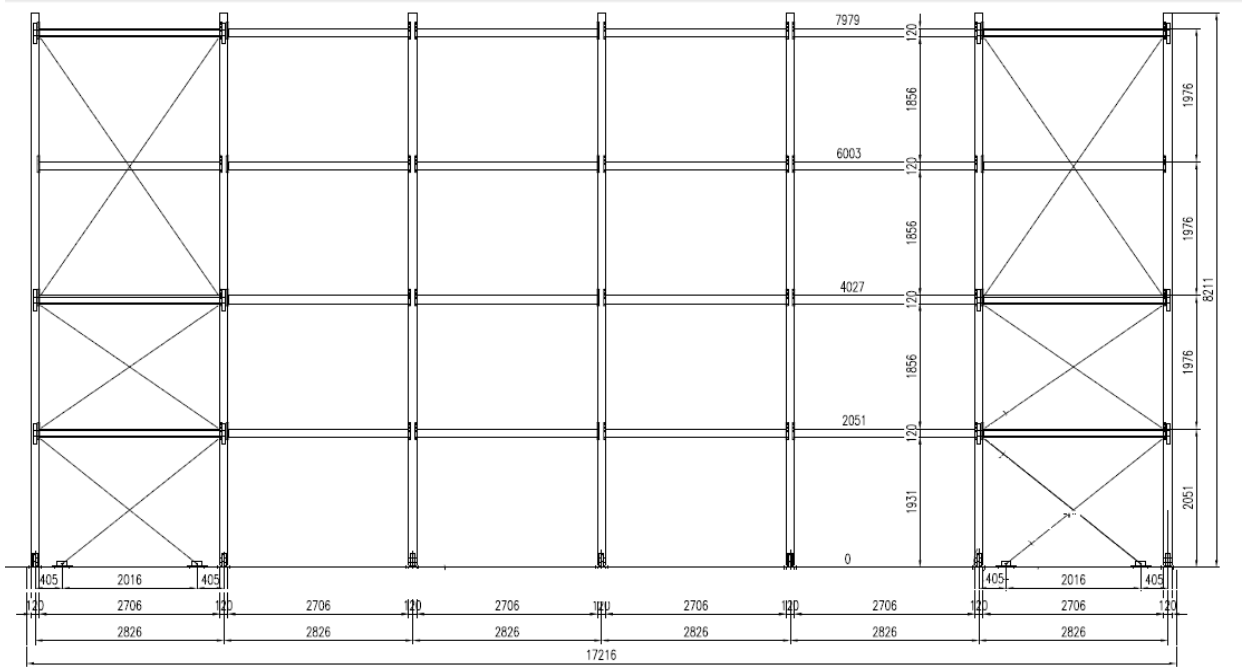

_ Plan view

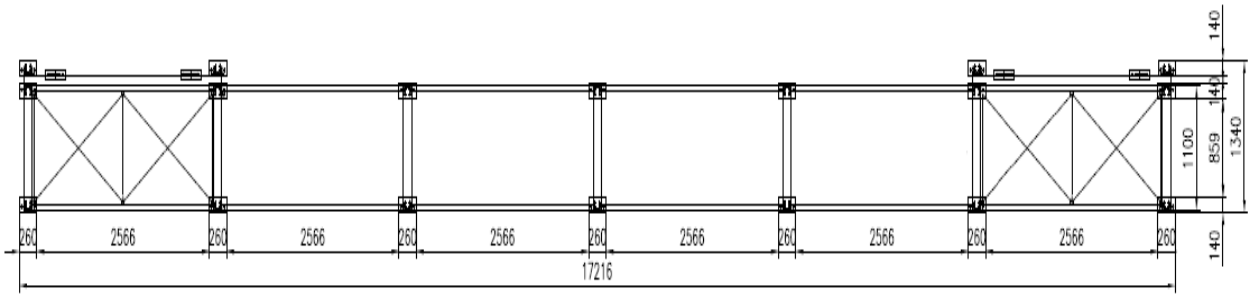

_ Cross-aisle view

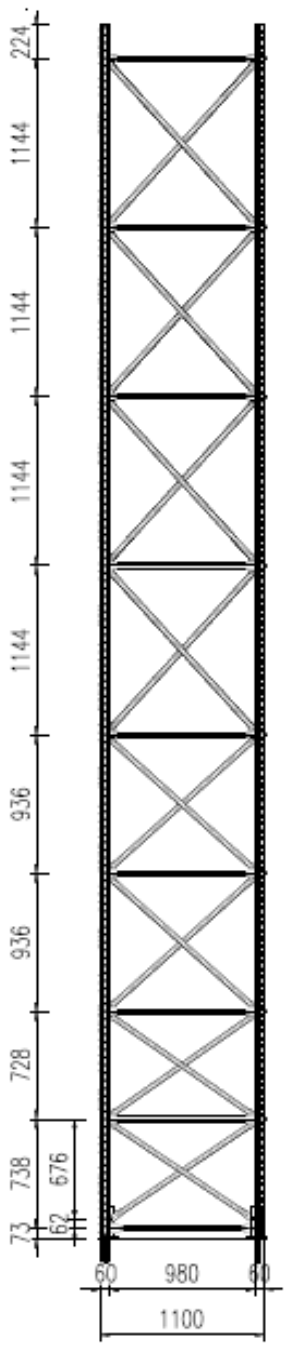

_ Rear bracing view

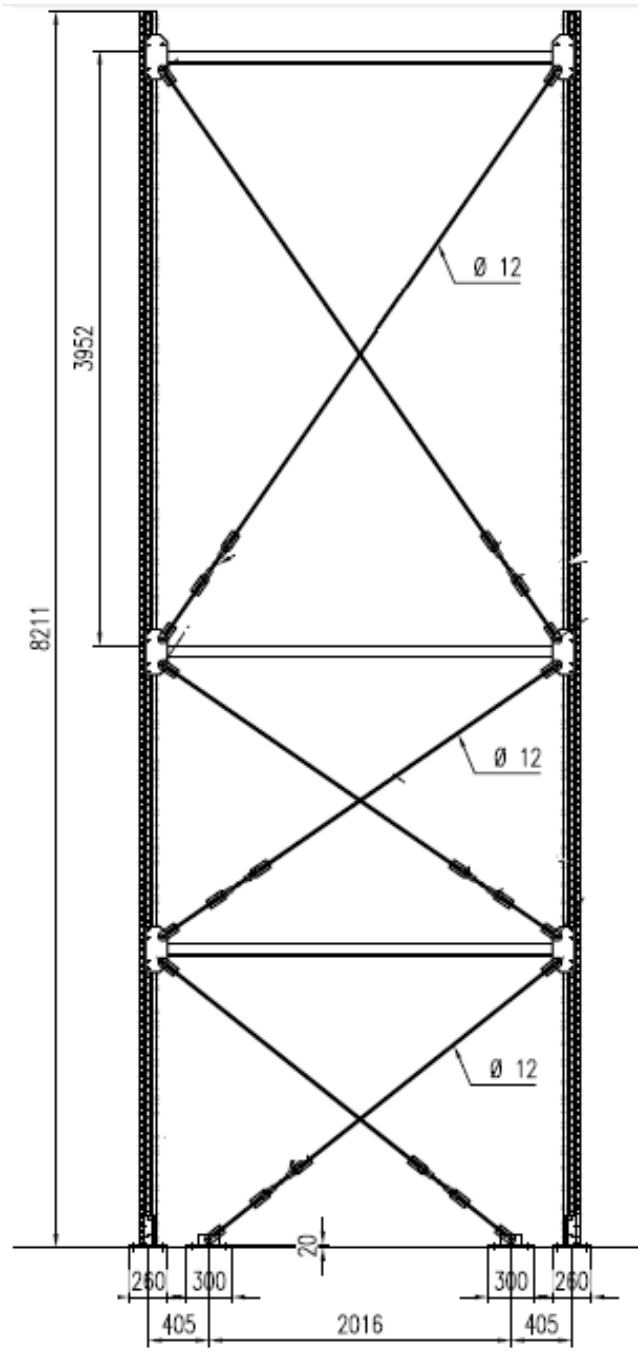

_ Uprights

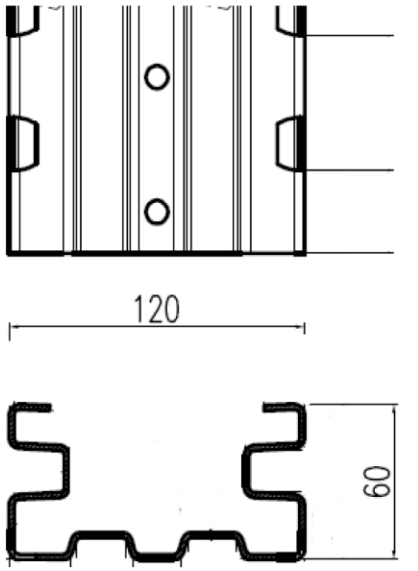

_ Base plates

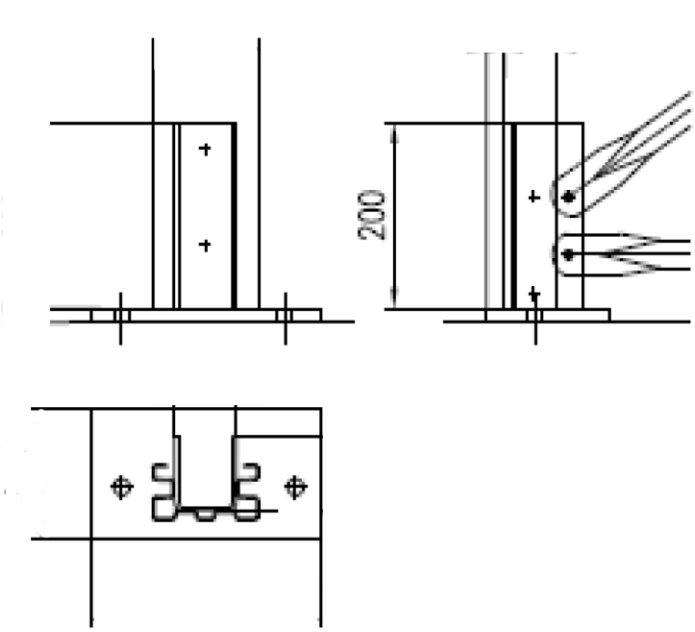

_ Beam end connections

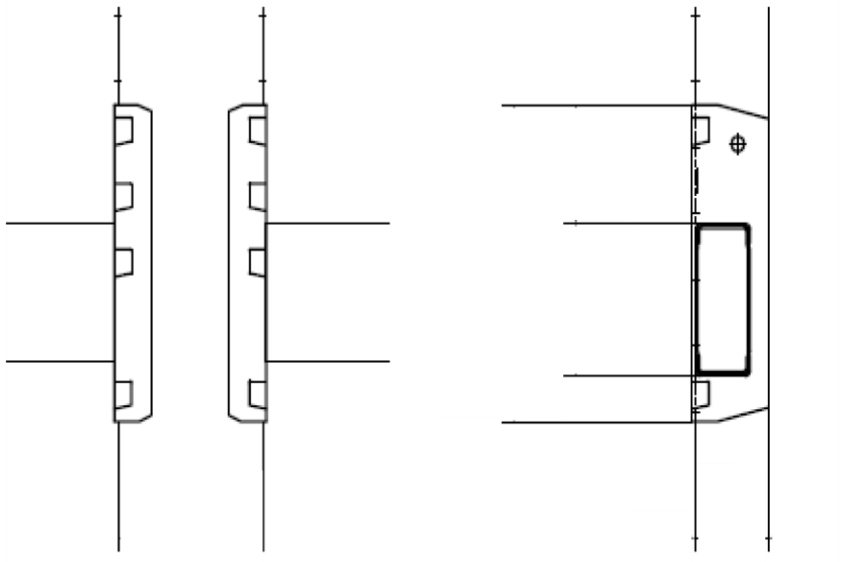

_ Diagonal connection

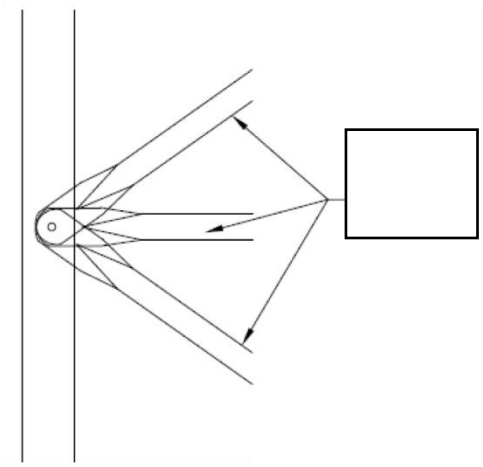

_ Horizontal bracing

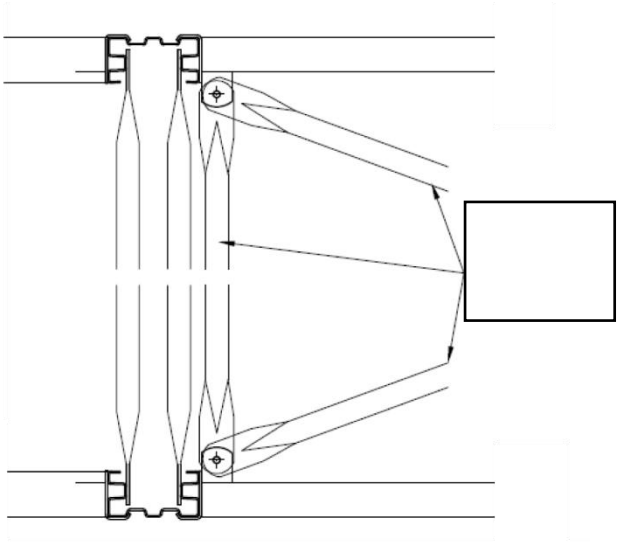

_ Vertical (rear) bracing connections

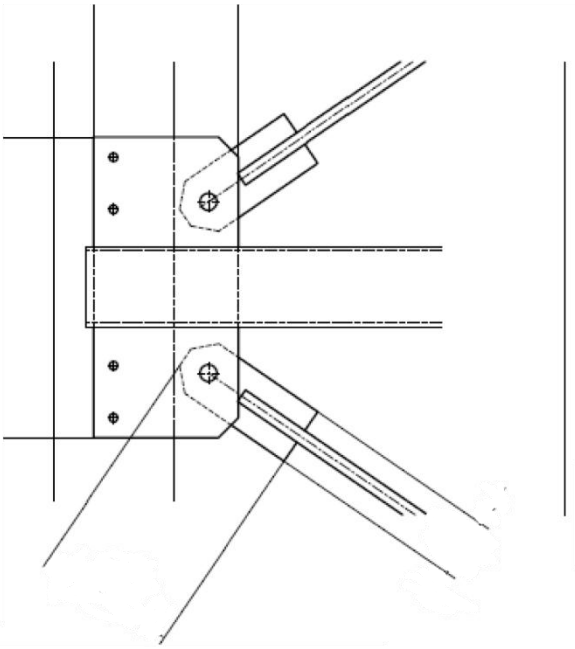

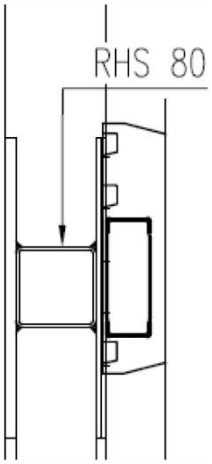

4.3. Company B

4.3.1 Medium seismicity

_ Longitudinal view

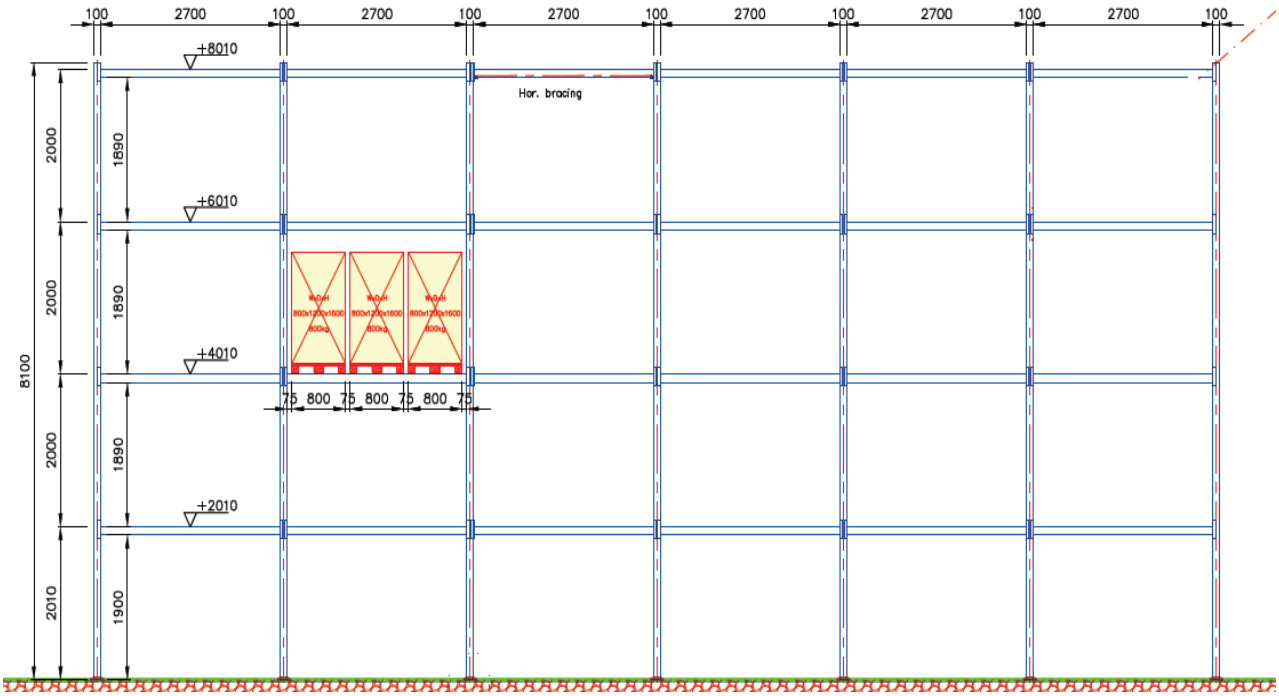

_ Plan view

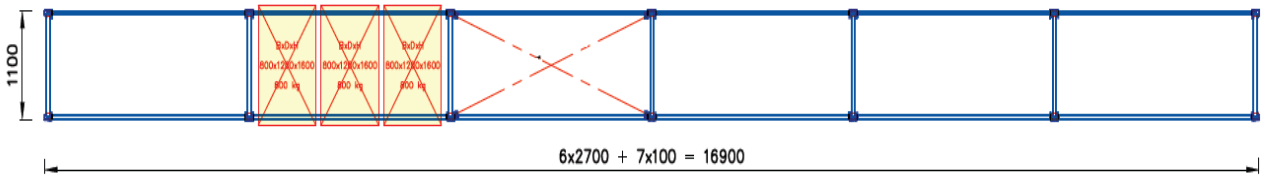

_ Cross-aisle view

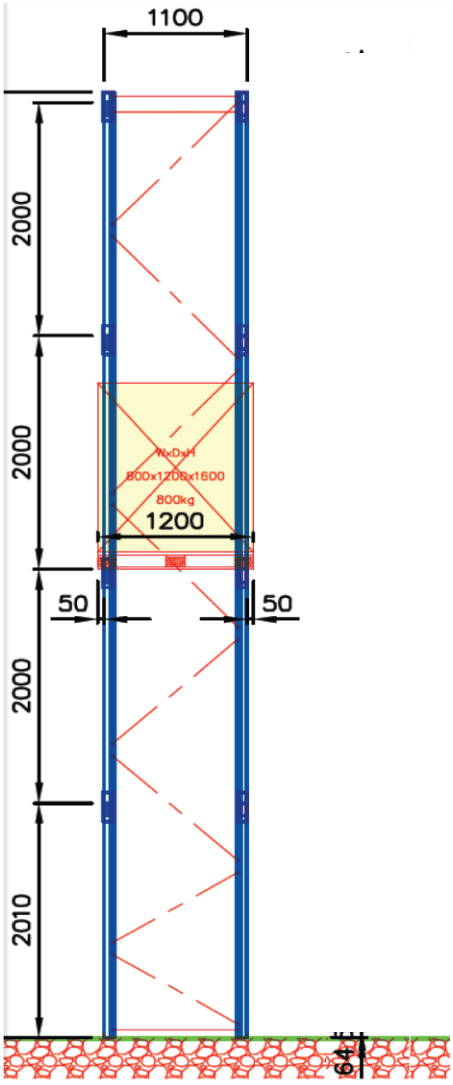

_Details of uprights and base plates

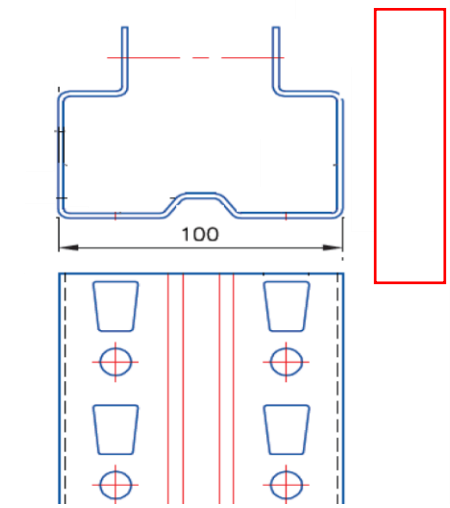

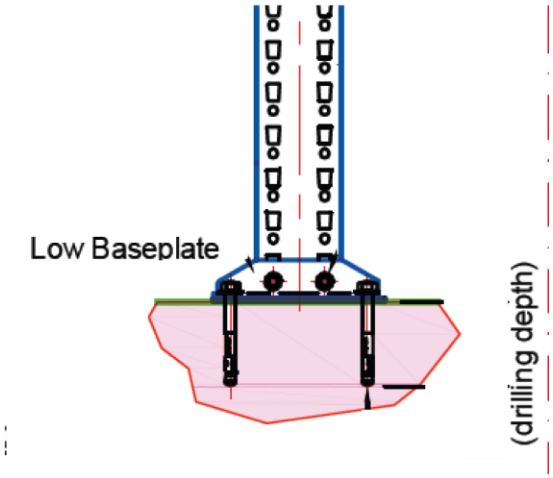

4.3.2 High seismicity

_ Longitudinal view

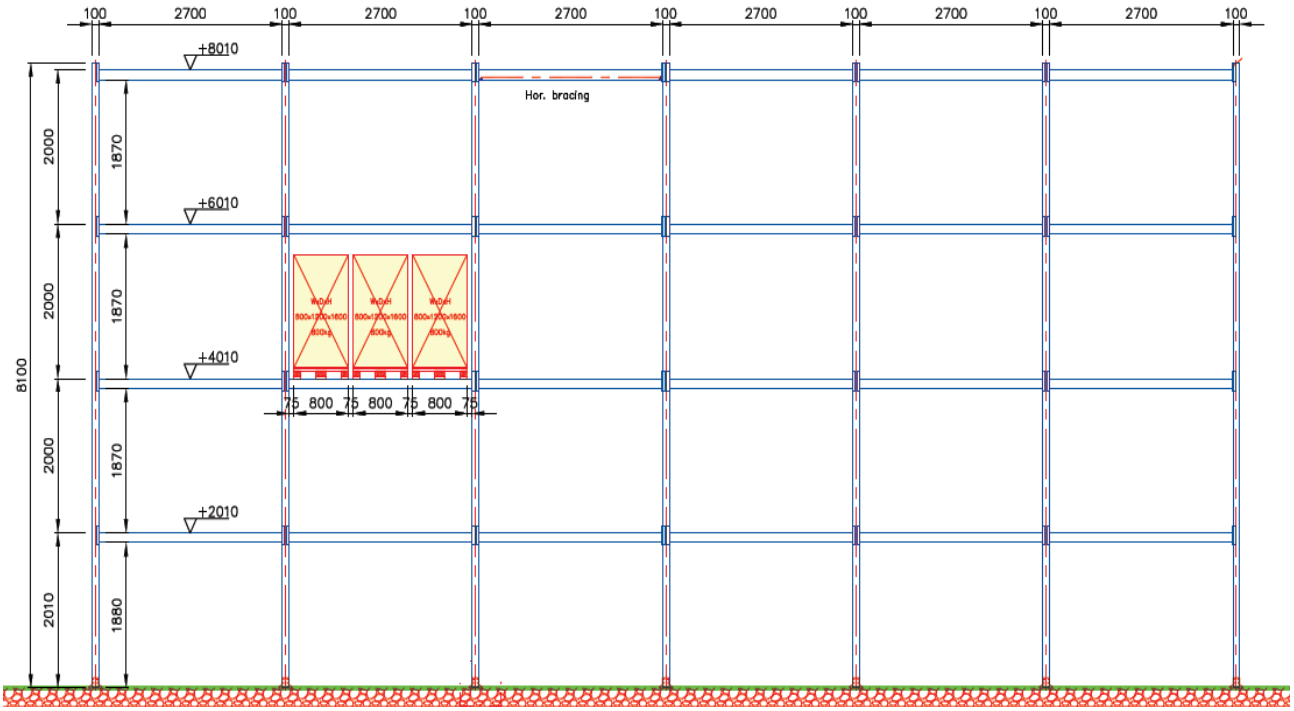

_ Plan view

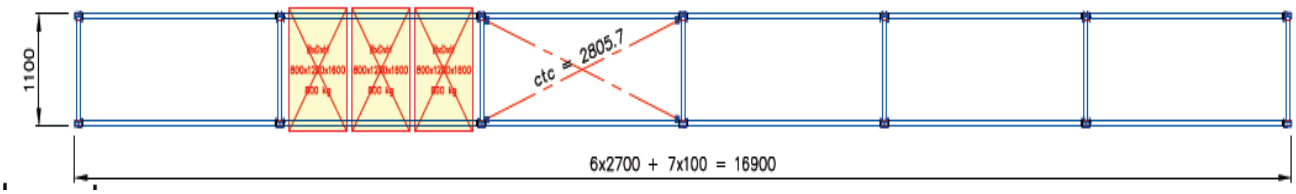

_ Cross-aisle view

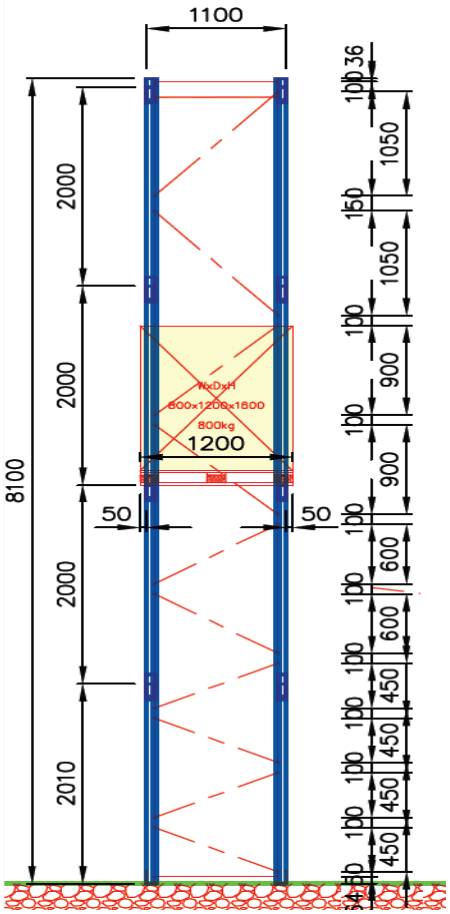

_Details of uprights and base plates

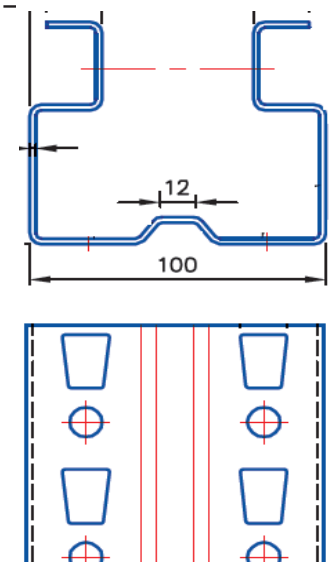

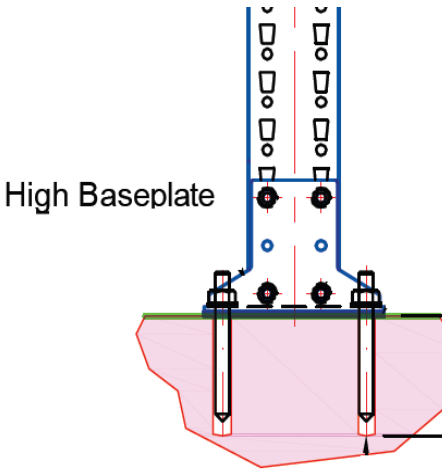

4.4. Company C

4.4.1 Medium seismicity

_ Longitudinal view

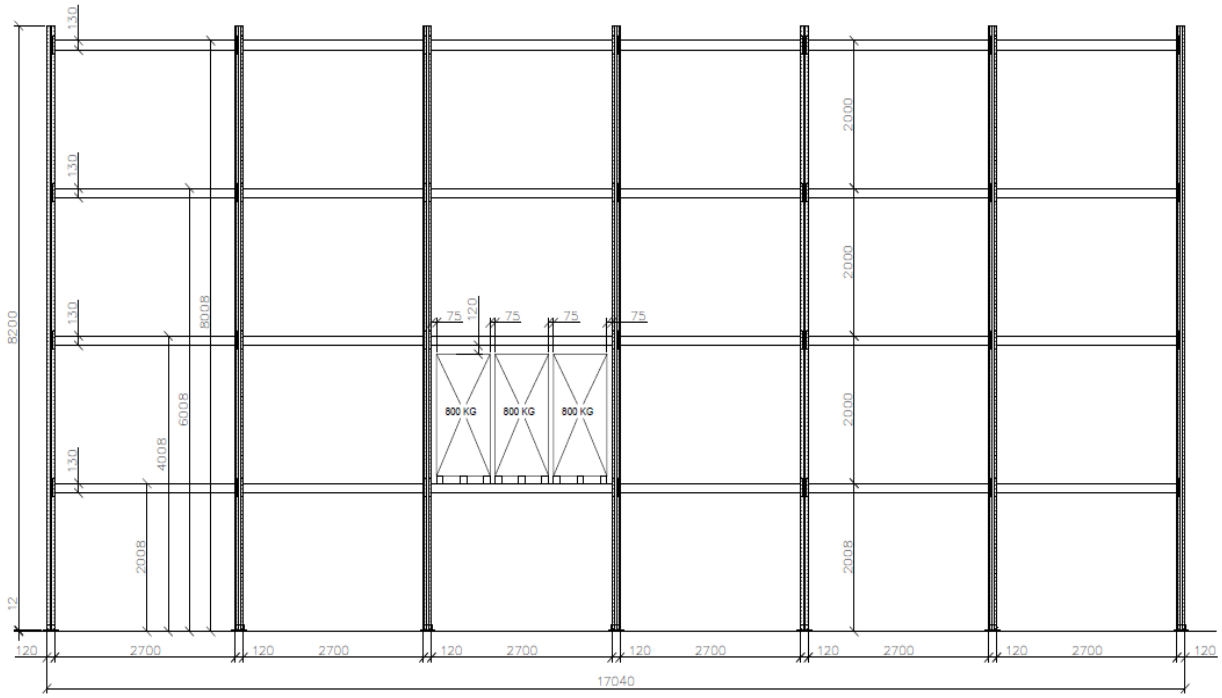

_ Plan view

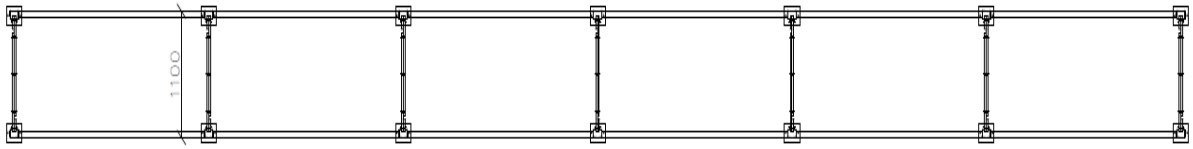

_ Cross-aisle view

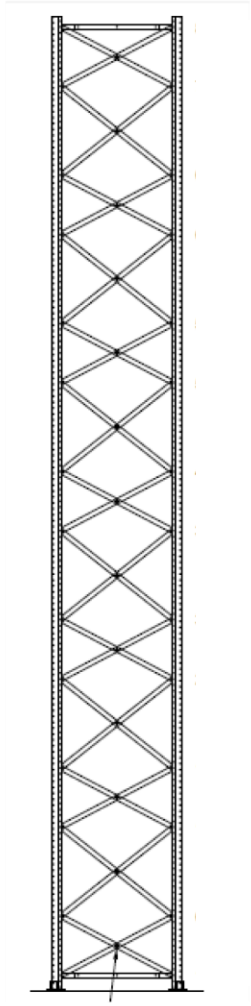

_Details of uprights and base plates

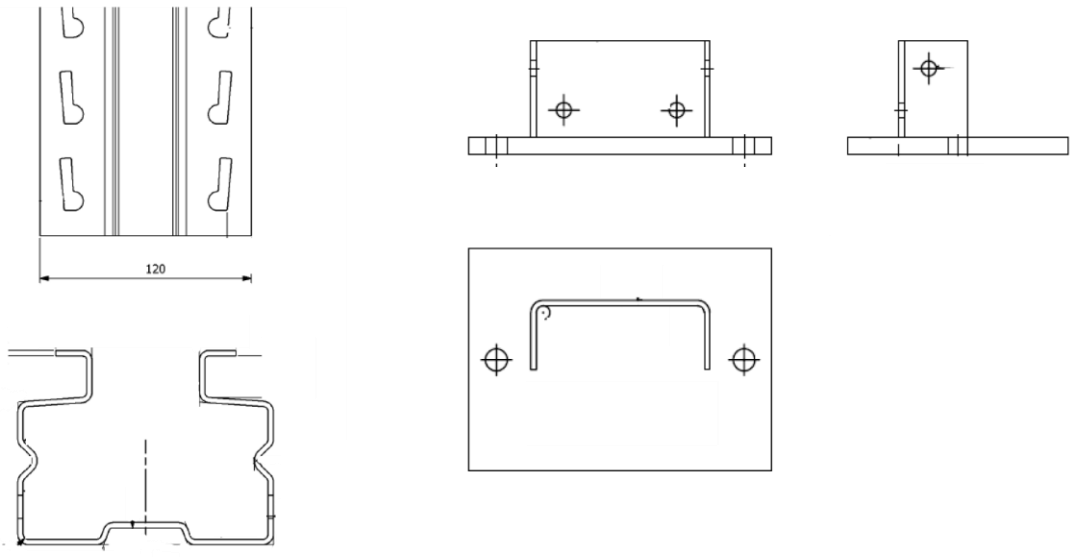

_ Beam end connections

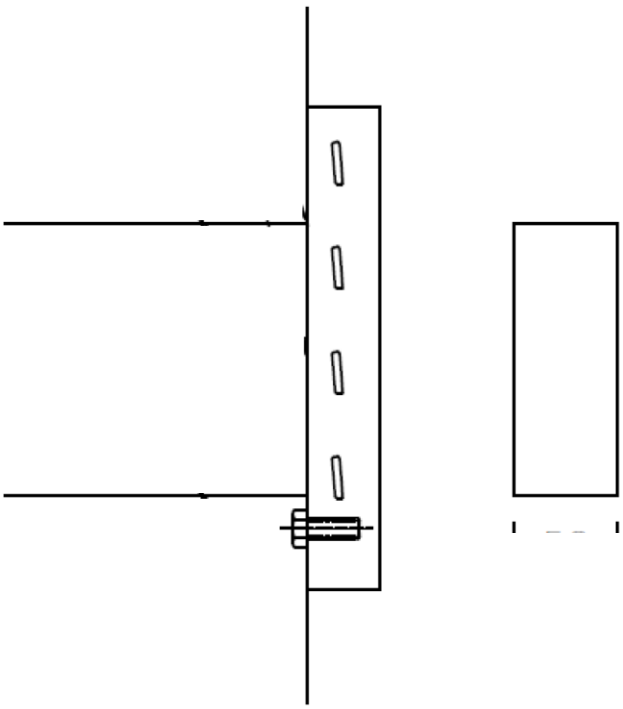

_ Diagonal bracing connection

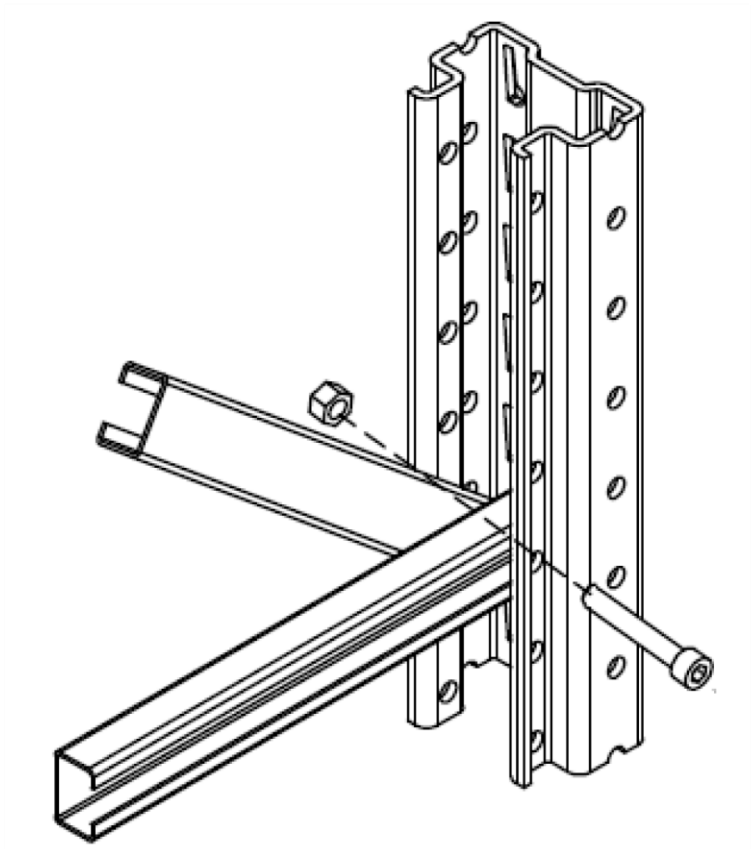

4.4.2 High seismicity

_ Longitudinal view

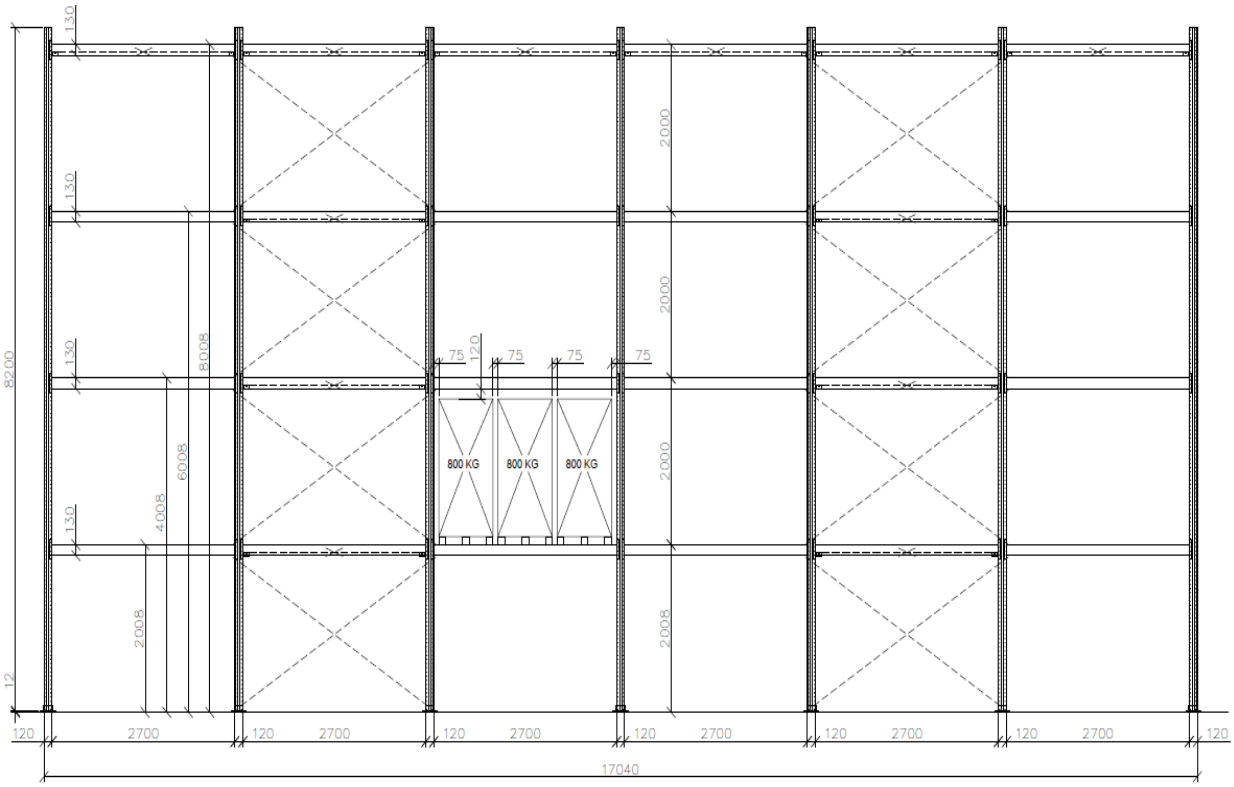

_ Plan view

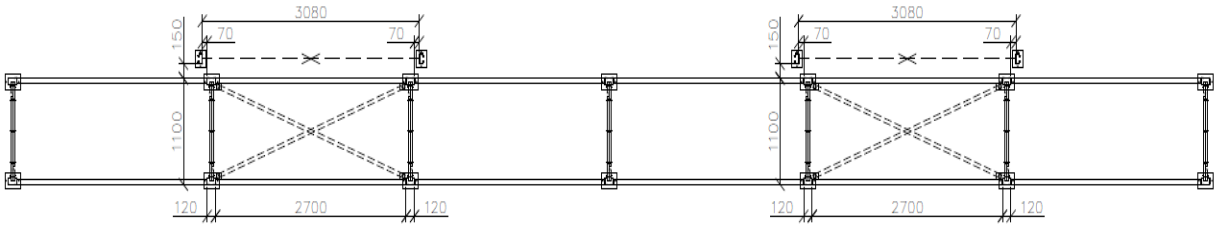

_ Cross-aisle view

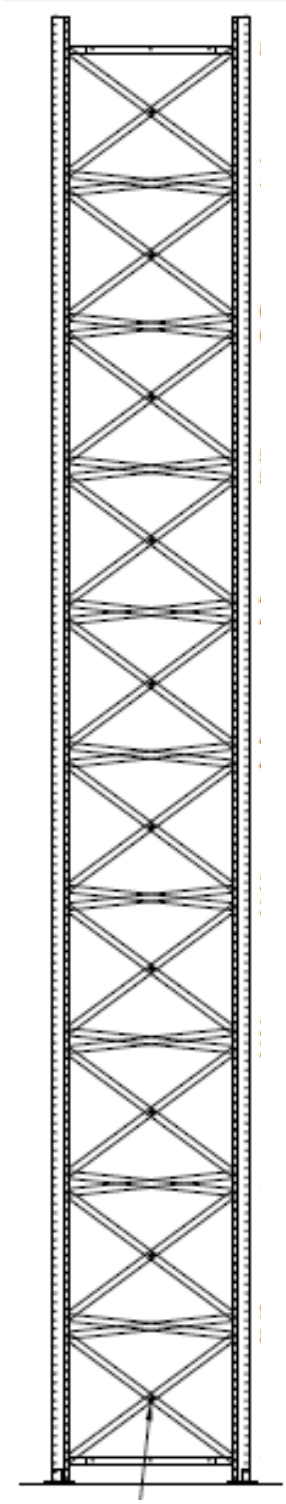

_ Rear bracing view

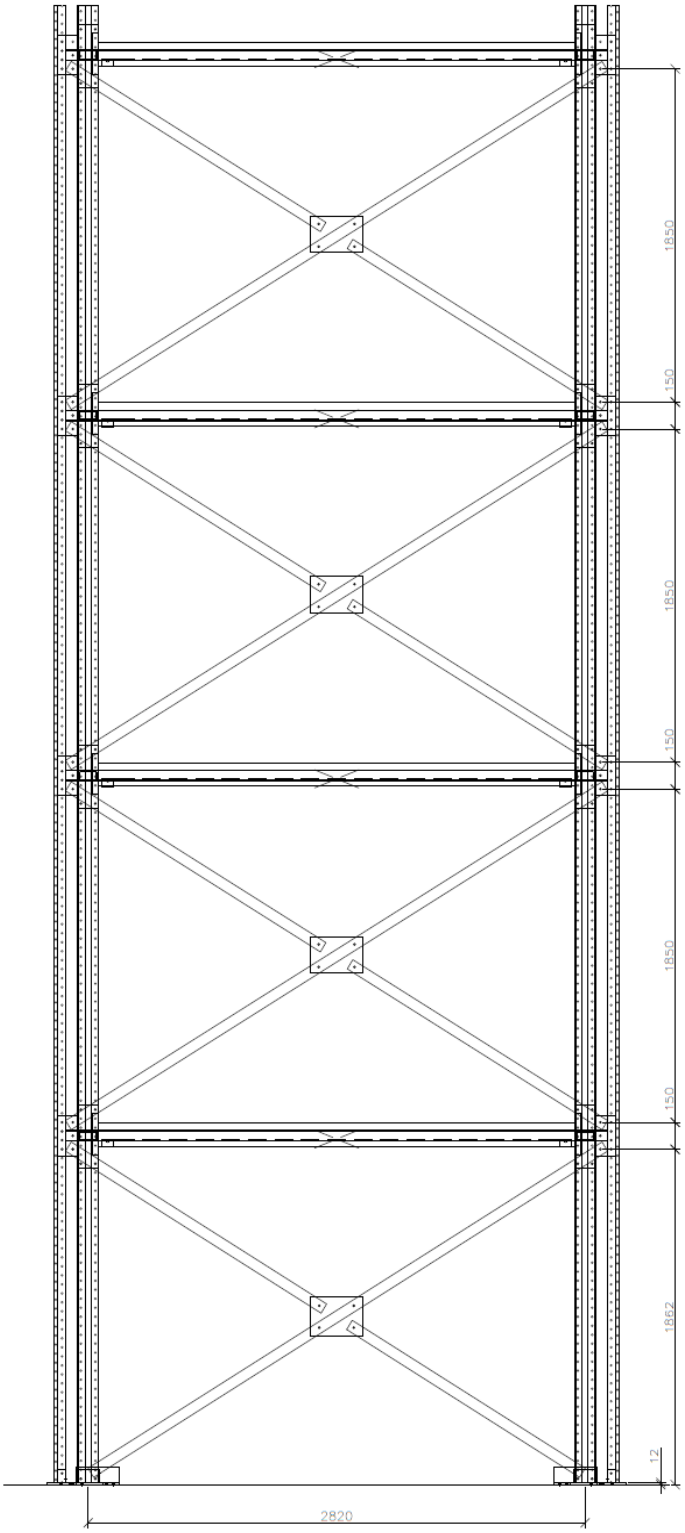

_ Uprights

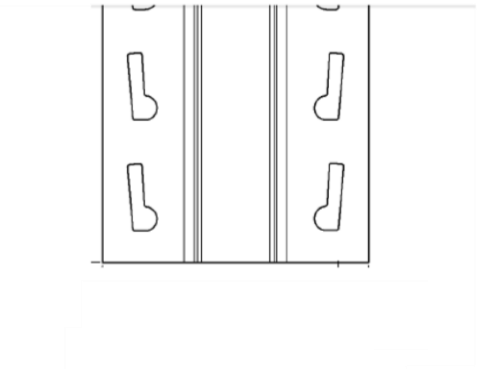

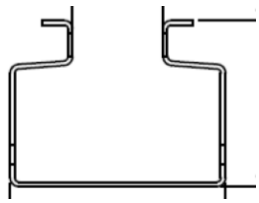

Type 1

Upright 120

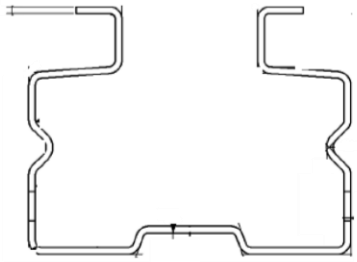

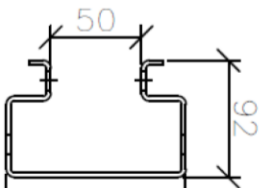

Type 2

Upright 100

_ Base plates

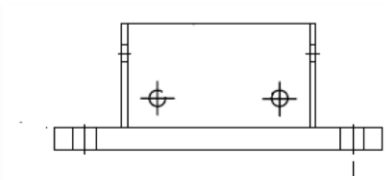

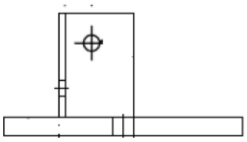

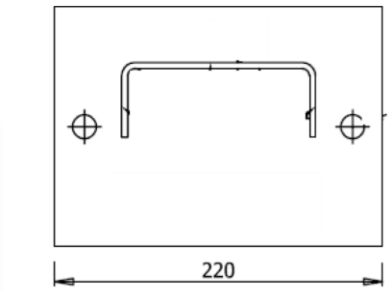

_ Footplate view (rear vertical bracing connection)

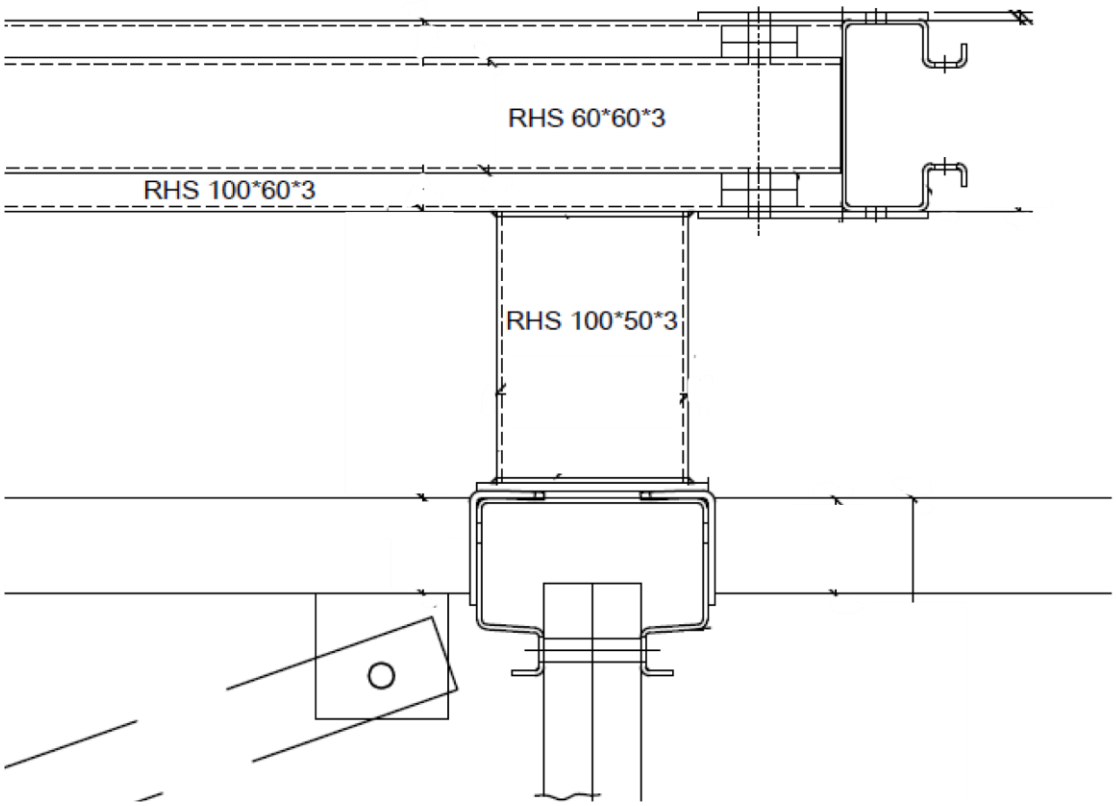

_ Diagonal connection

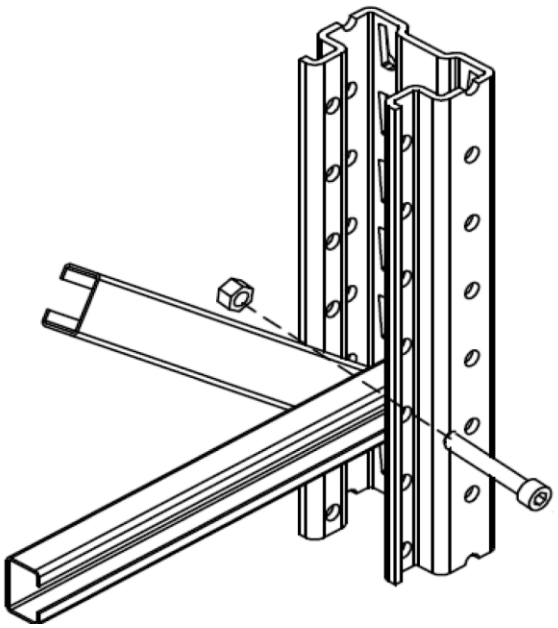

_ Beam end connections

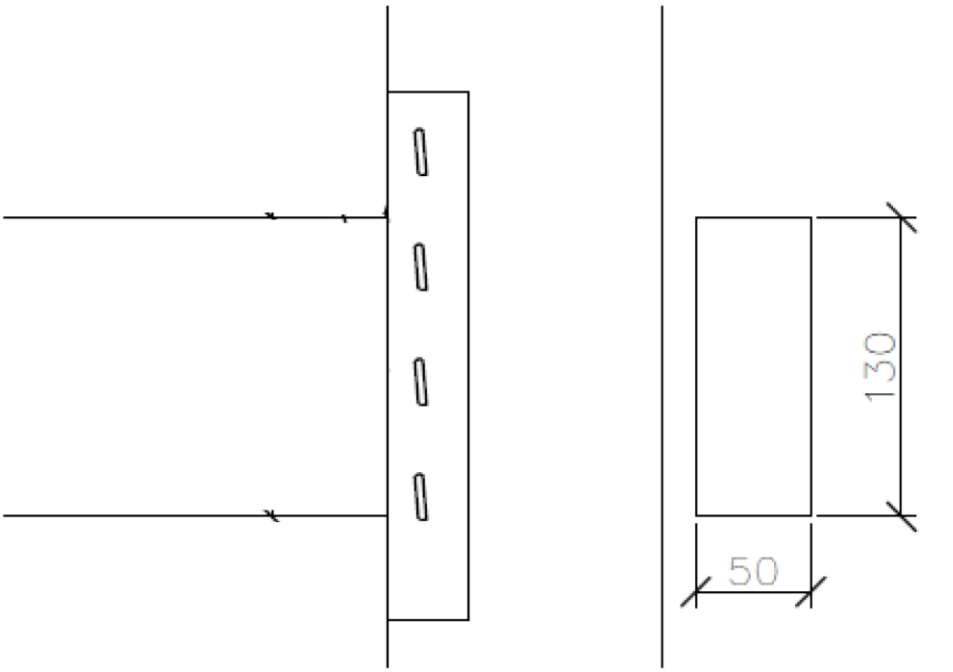

4.5 Table summarizing configurations, materials and basic section properties

	Company A		Company B		Company C	
seismicity	**medium**	**high**	**low**	**high**	**medium**	**high**
geometry-configuration*						
Symmetry in X axis	no	yes	no	no	yes	yes
Horizontal bracings	yes	yes	yes	yes	no	yes
_ location (bay/level)	4 / 4	1,6 /1,2,4	3 / 4	3 / 4	-	2,5 bays+4 level
_ Double horizontals (2X)	no	yes	no	no	-	no
_ Extra horizontals (IXI)	yes	yes	no	no	-	no
_ tension or tens/compress	T	T	T	T	-	T+C
Symmetric diagonals	yes	yes	no	no	yes	yes
Rear vertical bracing	no	yes	no	no	no	yes
_ location (bays)	-	1,6	-	-	-	2,5
materials						
uprights	S420 MC	S420 MC	S355	S355	S355 MC	S355 MC
beams	S355 MC	S355 MC	S275	S355	S235 MC	S235 MC
bracings	S235 JRC	S235 JRC	SE250	SE250	S355 MC	S355 MC
Section properties (mm)						
Uprights						
_ gross section area A						
_ effective area A_{eff}						
_ effective section modulus:						
Weff,y(sup, inf)						
Weff,z						
Bracings						
_ gross section area A						
Beams						
dimensions	45*150*1.5	45*120*1.5	40*110*1.5	50*130*1.5	50*130*1.75	50*130*1.75
_ gross section area A (mm2)	762	641	600	720	816	816
_ effective area A_{eff}	762	640	599	719	816	816
_ effective section modulus:						
Weff,y(sup,inf)	32670	22500	22729	28179	31270	31270
Weff,z,(left,right)	12114	9661	4290	6280	13120	13120
Design parameters						
design acceleration a [g]	0.12	0.25	0.135	0.25	0.20	0.30
soil type	C	B	C	C	C	C
spectrum type	2	1	2	1	1	1
importance factor	0.84	1.00	0.84	0.84	0.84	0.84
Loads						
Dead loads (kN)	15.4	19.2	11.5	17.6	17.2	24.9
Live (pallet) loads (kN)	576	576	576	576	576	576
(Dead+Live)/Area (kN/m^2	7.9	7.5	7.9	8.0	7.9	7.8

Chapter 5 simulation and results _ Company A

5.1. Introduction

As mentioned before, the data from three companies were used in order to create the case study models of this thesis. Each company provided with data concerning two types of structures: one for medium or low seismicity and another for high seismicity.
In the following units the configuration of each model/company will be presented. The geometry of each structure as well as the assignment of nodes, loads and elements with inelastic behaviour has already been described in the previous chapters 3 and 4. In this chapter, the experimental data used as reference for each connection are presented along with the results of the various analyses performed: application of vertical loads, modal analysis and pushover analyses in down-aisle and cross aisle direction.
Note that for each company the same links and hinges were used to simulate the respective connections in lack of more specific data. Therefore their properties are presented in the beginning of each company/unit.
The presentation of the first company is more thorough than the next two in order to avoid repetition.

5.2. Material nonlinearity (experimental data and simulation)

The non linear behaviour of the base plate connections was described with the following moment-rotation diagram.

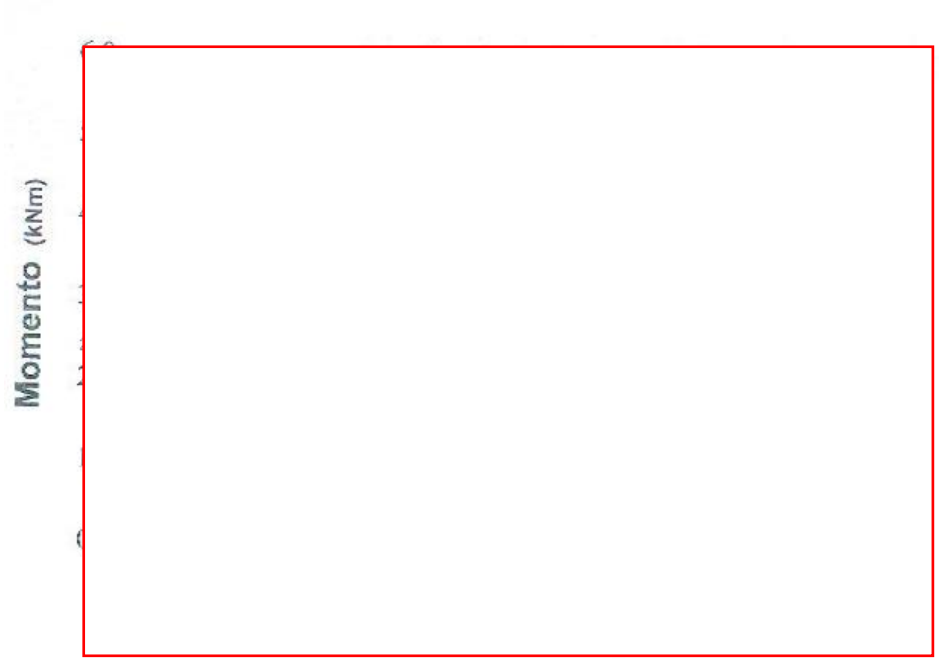

Figure 5.1: Base plate data

The previous graph was simulated with the following type of multi-linear plastic link in Sap2000.

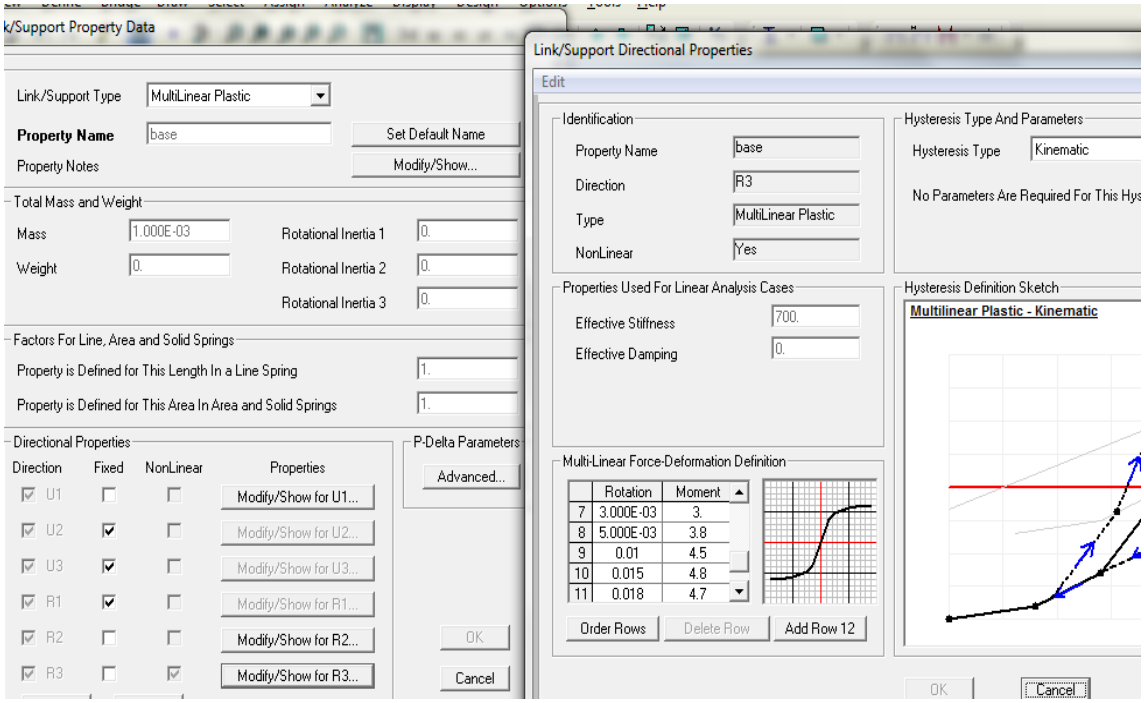

Figure 5.2: Base plate connection simulation

As far as the behaviour of the beam end connections is concerned, the experiments resulted in the following moment-rotation diagram.

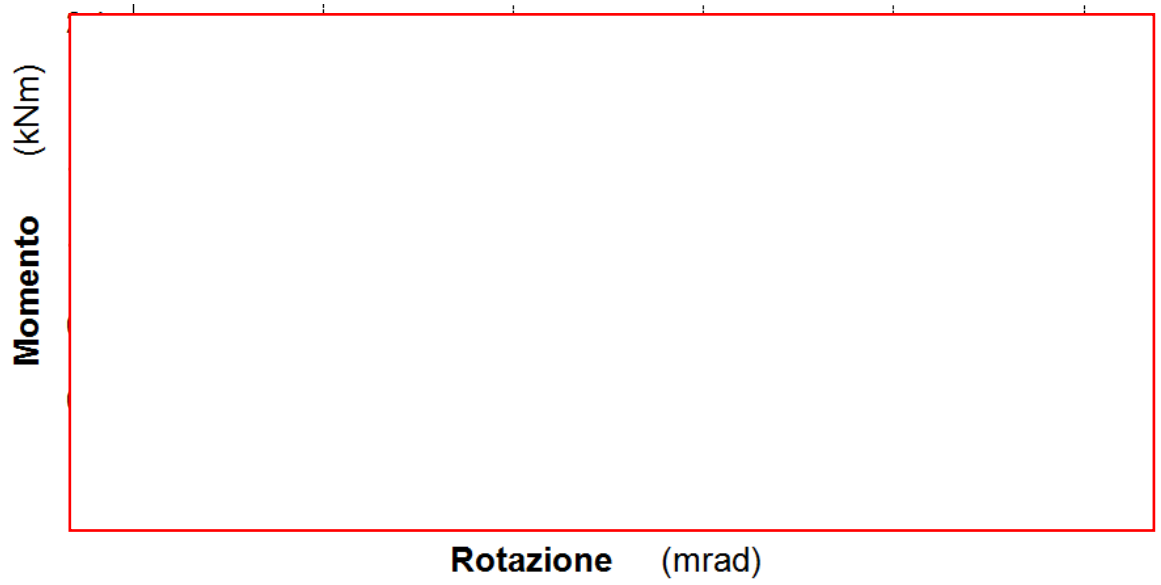

Figure 5.3: Beam end connector data

The previous graph was simulated with the following type of multi-linear plastic link in Sap2000. It can be noticed that the releases are different than in the case of base plate links.

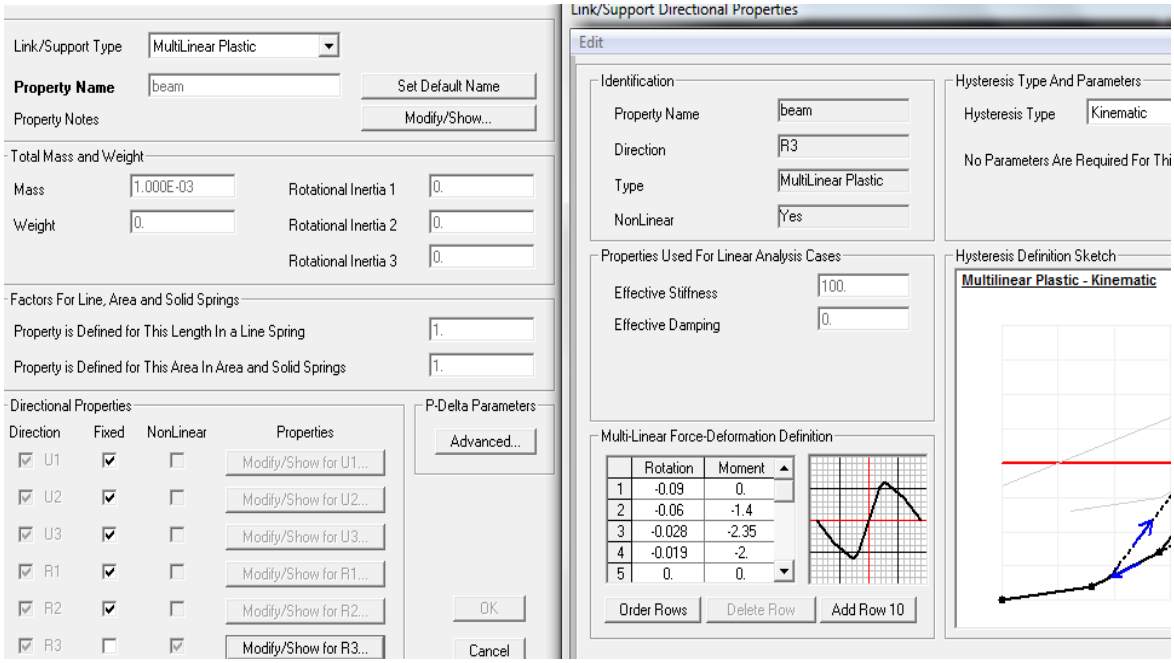

Figure 5.4: Beam end connectorsimulation

In the top of the columns of the lowest level, plastic hinges were assigned in order to simulate the failure modes indicated from previous research. As mentioned in Chapter 3, these hinges also enabled the control of the magnitude of the axial forces in the uprights and the interaction between these forces and moments. The type of plastic hinges used were "interacting P-M2" and hade the properties displayed in the figure. The interaction curve was defined with Pmax=175 kN and Mmax=7.5 (indicated by another software).

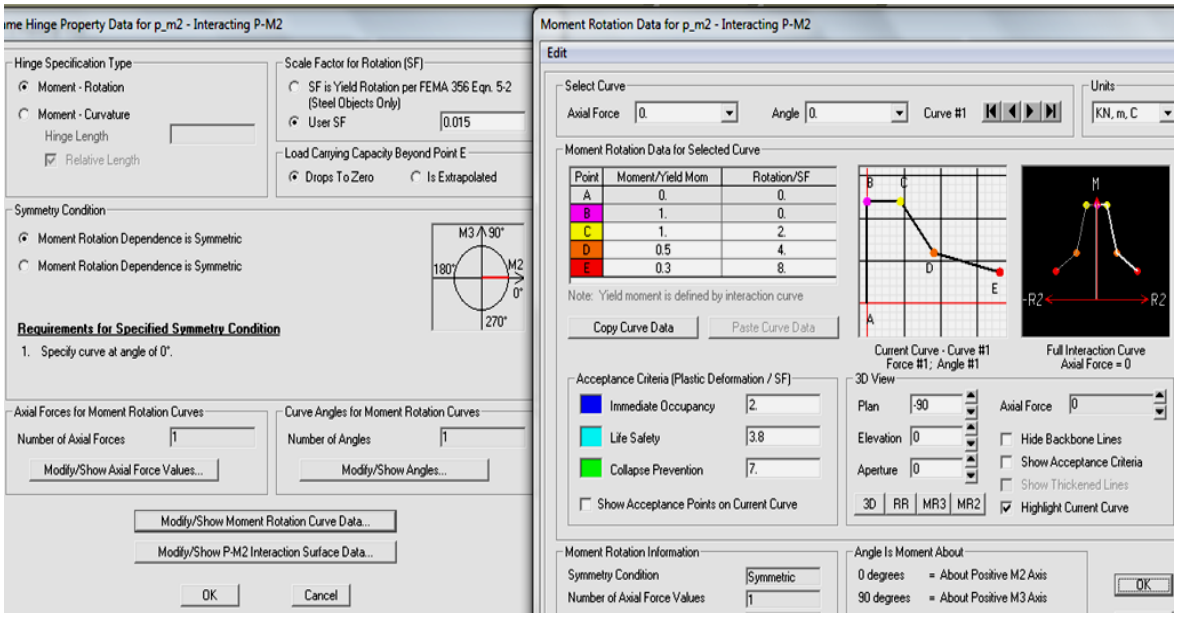

Figure 5.5: Plastic hinge on top of uprights

The plastic hinges assigned in the middle of each upright frame diagonal had the following properties. The values used were derived from the technical reports of the company and were

the critical amongst the buckling check of the member and the checks of the bolts (shear resistance and bearing resistance).

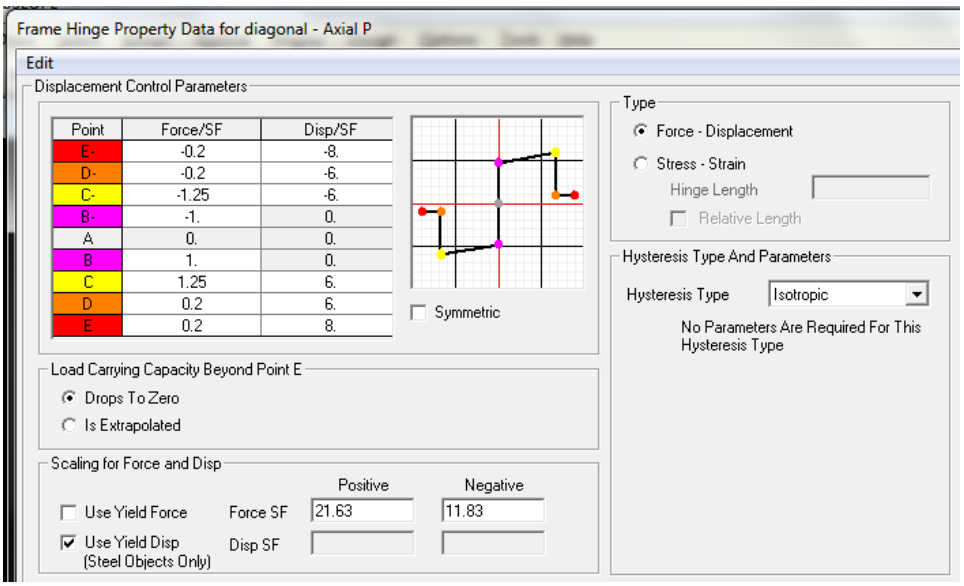

Figure 5.6: Plastic hinge assigned on diagonals

5.3. Medium seismicity model

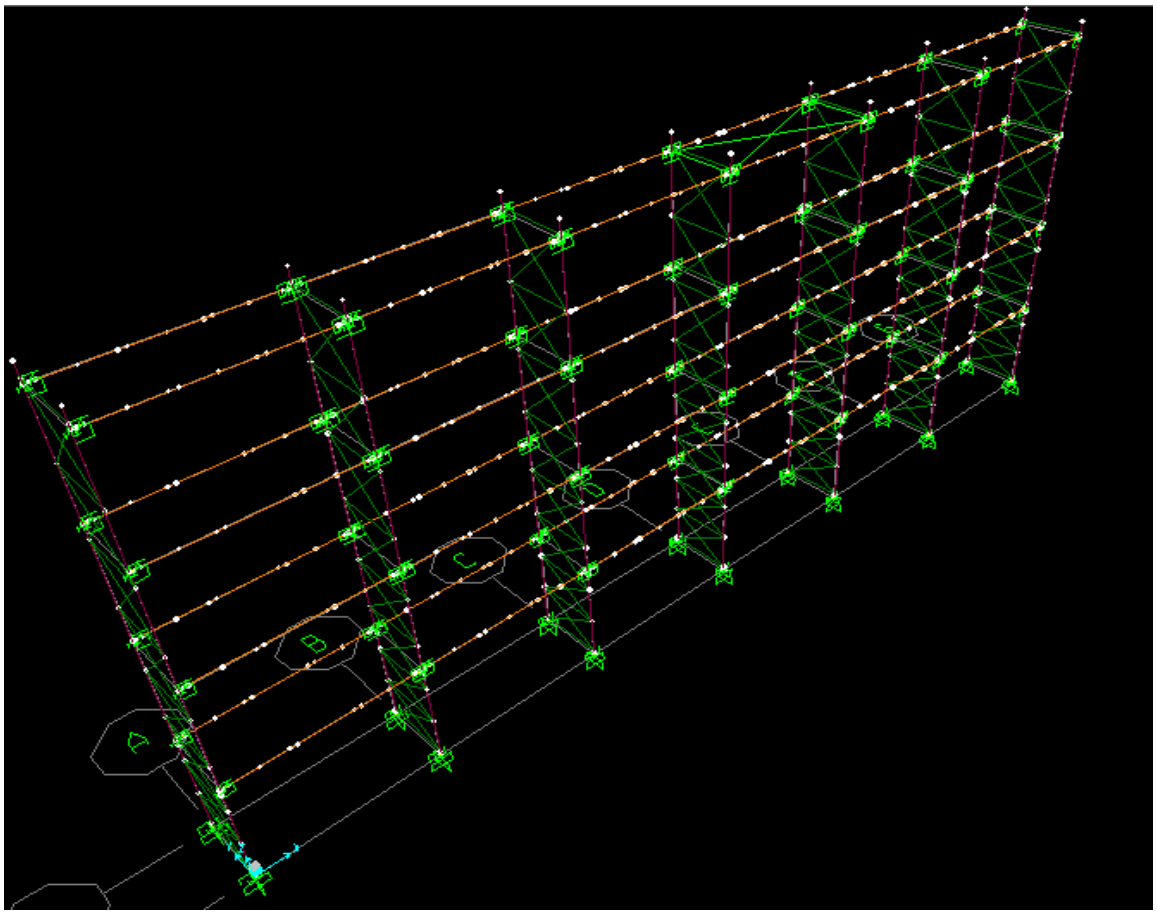

Figure 5.7: 3-D view of model

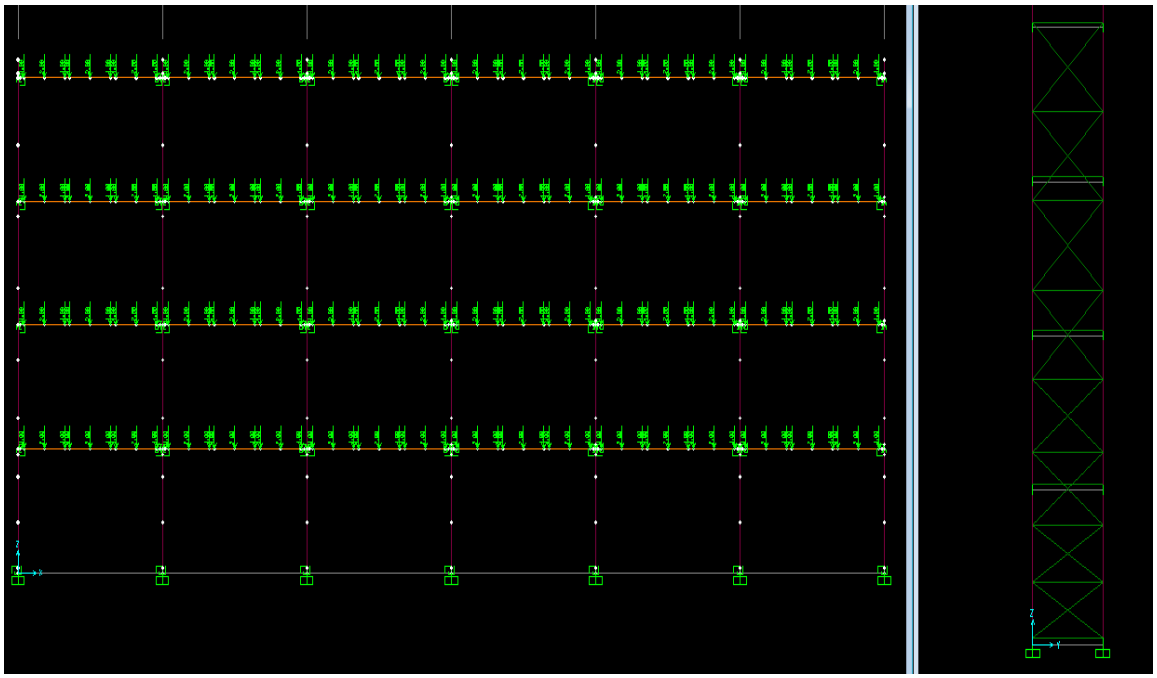

Figure 5.8: XZ (down-aisle) and YZ(cross-aisle) view of model- application of pallet loads

The assignment of vertical loads (dead and pallets) produced the following results in terms of internal moments and forces.

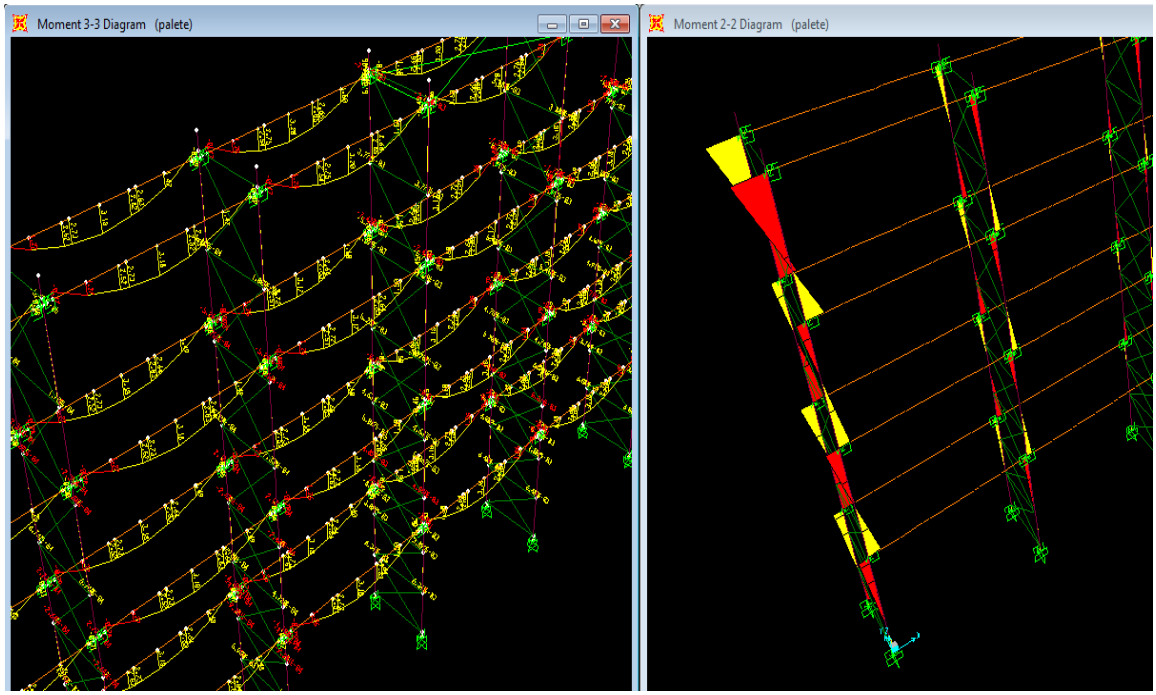

Figure 5.9: results of pallet loads- M3 main moments for beams and M2 main moments for columns

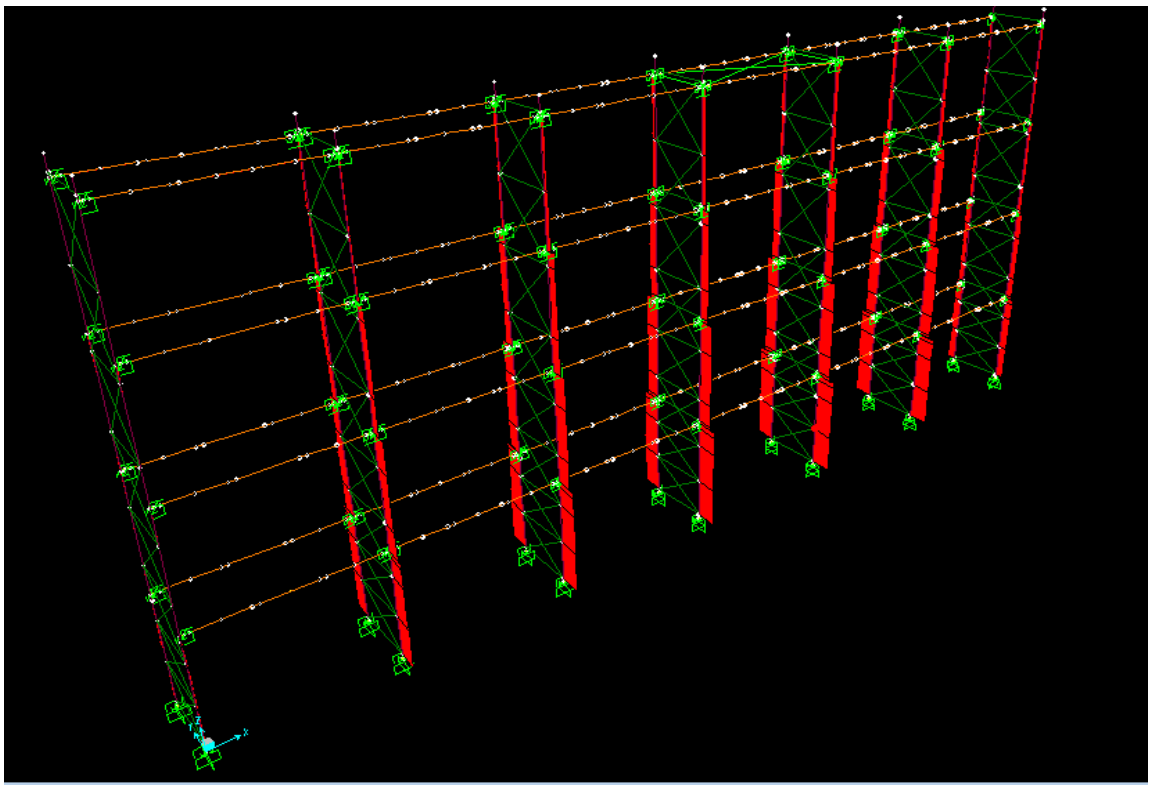

Figure 5.10: Axial forces from pallets- N_{max} = 48kN and N_{min}=21.3 kN

5.3.1. Modal analysis

The modal analysis resulted in the following. As it can be seen from the pictures, the first mode was translational in X axis (down-aisle direction) whereas the second mode was more obvious in Y axis. In the following table the first twenty modes are presented, along with their periods and the mass participation ratios.

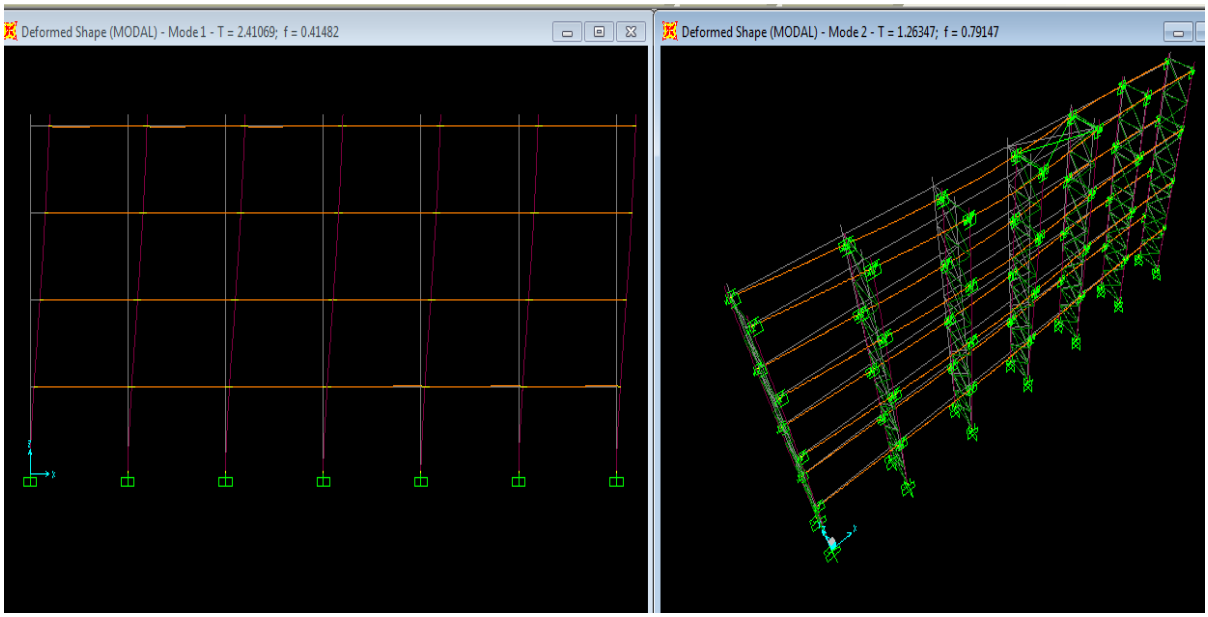

Figure 5.11: Modal analysis - first two modes

Table: Modal Participating Mass Ratios

StepNum	Period	SumUX	SumUY	SumUZ
	Sec			
1	2.410693	0.81438	5.195E-14	1.293E-14
2	1.263466	0.81438	0.46742	1.417E-14
3	1.251093	0.81438	0.69103	1.732E-14
4	1.123956	0.81438	0.77543	2.861E-14
5	0.958046	0.81438	0.78375	3.445E-14
6	0.853947	0.81438	0.79678	9.658E-14
7	0.738955	0.81438	0.81205	1.909E-13
8	0.662968	0.94086	0.81205	8.818E-13
9	0.611023	0.94086	0.81207	9.014E-13
10	0.504653	0.94086	0.81207	1.580E-12
11	0.498277	0.94086	0.81229	1.589E-12
12	0.492894	0.94086	0.81256	1.590E-12
13	0.490091	0.94086	0.81302	1.597E-12
14	0.489728	0.94086	0.81431	1.598E-12
15	0.488213	0.94086	0.81431	1.598E-12
16	0.487833	0.94086	0.81431	1.627E-12
17	0.487764	0.94086	0.81431	1.669E-12
18	0.467985	0.94086	0.81469	2.646E-12
19	0.466014	0.94086	0.81469	1.936E-10
20	0.455586	0.94086	0.81498	1.937E-10

Table 5.1: Modal analysis - first twenty modes and mass participation ratios

5.3.2. Pushover analyses

Pushover load cases were applied to the models in both X and Y directions. As mentioned before this pushover analyses were displacement based (monitored displacement at top of each structure) and had the form of a uniform acceleration applied at every joint. Hereby the capacity curves are displayed for each direction. The vertical axis refers to the base shear force (kN) and the horizontal axis refers to the top displacement (m). The horizontal forces used in the design (as mentioned in the company's technical report) are also shown.

Figure 5.12: Pushover in down-aisle direction, performance curve (and performance point)

Figure 5.13: Pushover in cross-aisle direction, performance curve (and performance point)

The performance points are calculated by the programme according to ATC 40. The parameters defined by the user are C_α, C_v and damping (3%). It is reminded that $C_\alpha = \alpha_g * S * n$ and $C_v = 2.5 * C_\alpha * T_c$ where S and T_c depend on the type of soil and the type of spectrum (see Tables 3.2 and 3.3 of prEN1998-1)

elastic response spectrum: **Type 1**

Ground type	S	T_B [sec]	T_C [sec]	T_D [sec]
A	1.0	0.15	0.4	2.0
B	1.2	0.15	0.5	2.0
C	1.15	0.20	0.6	2.0
D	1.35	0.20	0.8	2.0
E	1.4	0.15	0.5	2.0

Type 2

Ground type	S	T_B [sec]	T_C [sec]	T_D [sec]
A	1.0	0.05	0.25	1.2
B	1.35	0.05	0.25	1.2
C	1.5	0.10	0.25	1.2
D	1.8	0.10	0.30	1.2
E	1.6	0.05	0.25	1.2

Table 5.2: Parameters describing the elastic response spectrums in EC8

Pushover in down-aisle direction

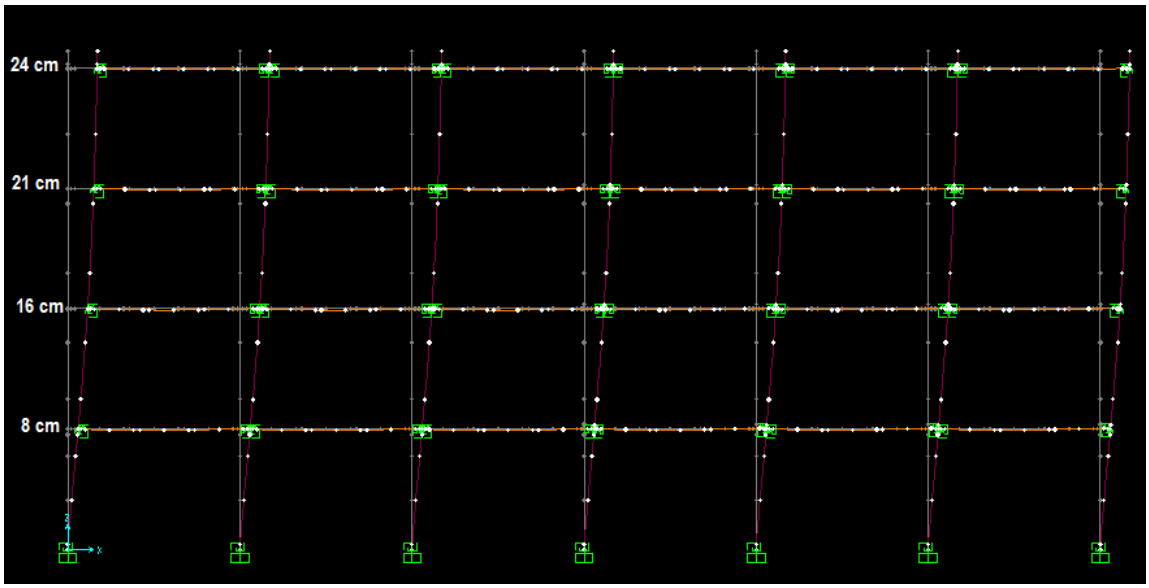

Figure 5.14: Deformed shape in Pushover final step (the displacements in each level are noted)

In the following two figures the response of the columns is summarized. As far as the base plate links are concerned, one can notice the step by step evolution of the moment/rotation relation as well as the failure point. As far as the hinges in the top of the columns are concerned, they were not activated (plastic rotation is equal to zero in the graph).

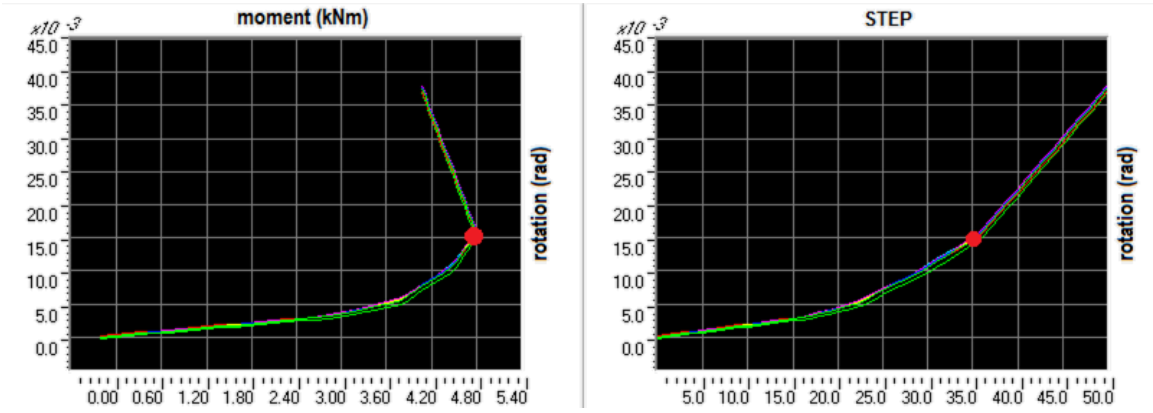

Figure 5.15: Behaviour of base links in terms of moment/rotation and rotation per step

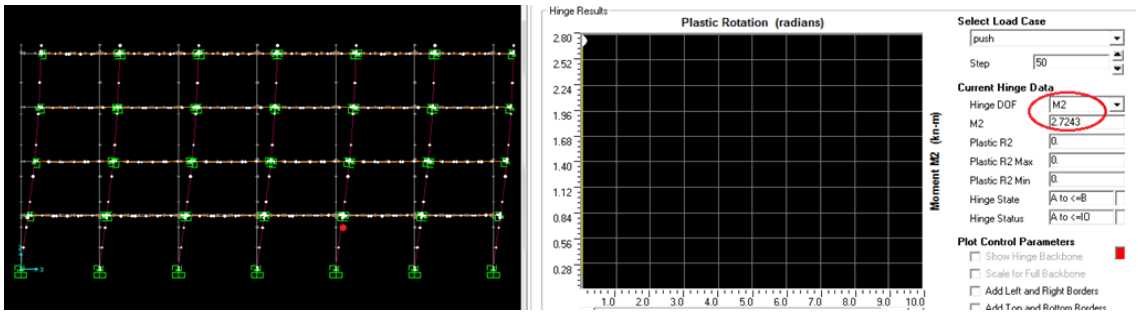

Figure 5.16: Behaviour of column hinges in the final step. No activation takes place.

The following figure summarizes the moment/rotation behaviour per step of the links simulating the beam-end connectors. The top row is for the connections in left and the other one for the connections in the right (most critical).

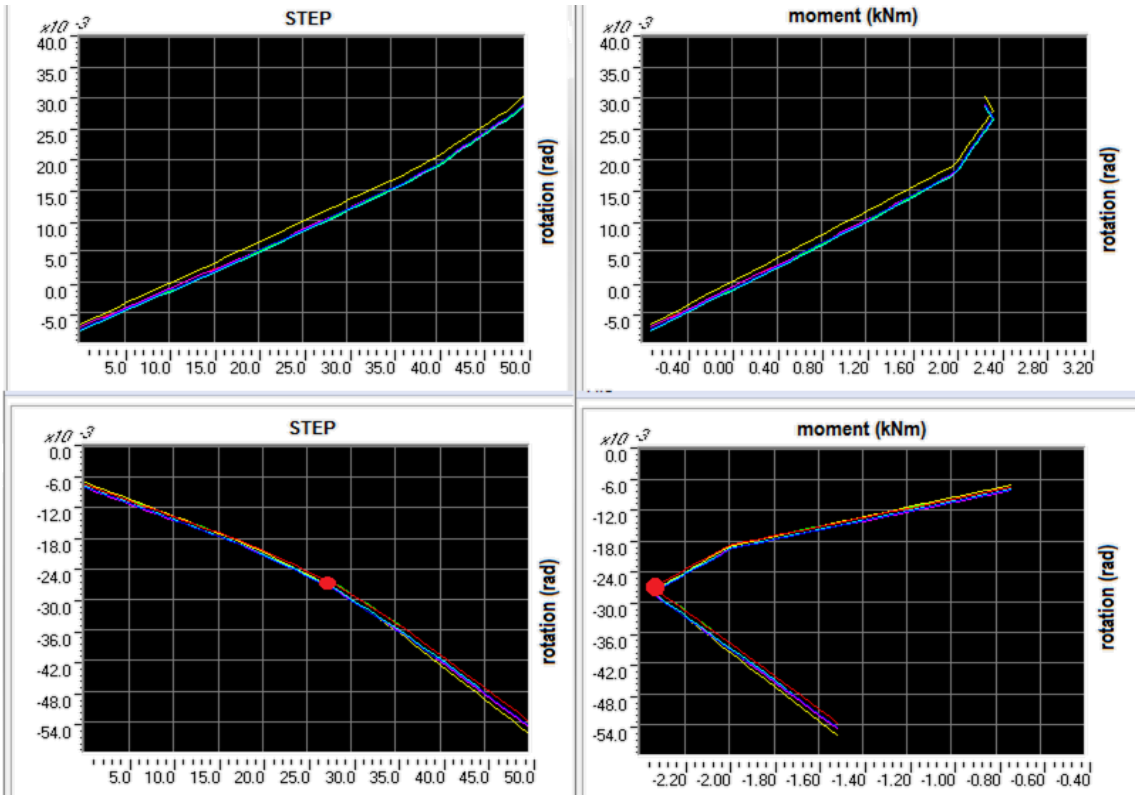

Figure 5.17: Behaviour of beam end connectors (left and right). Those in the right fail.

Pushover in cross-aisle direction

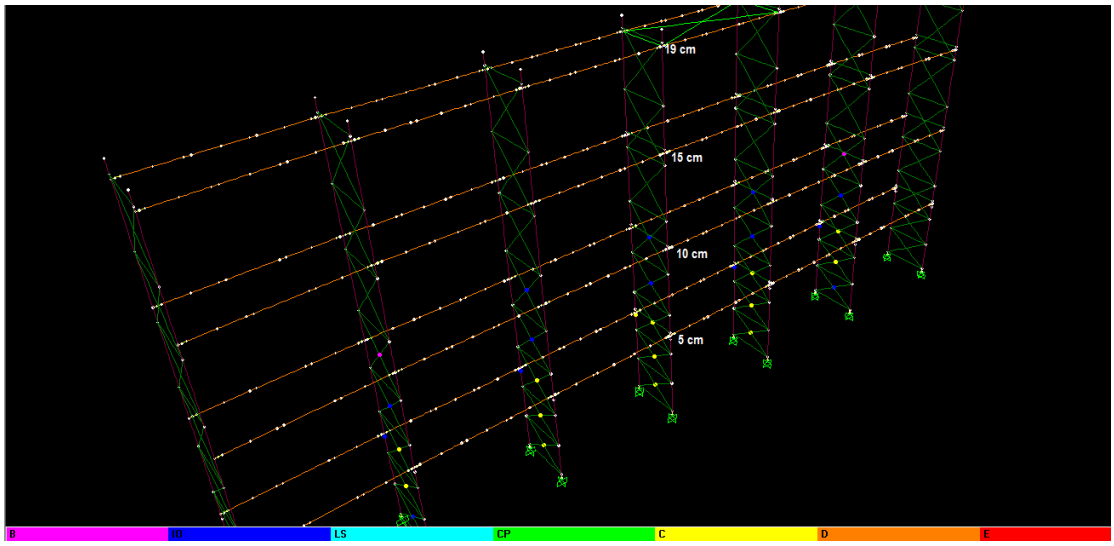

Figure 5.18: Deformed shape in Pushover final step (the displacements in each level are noted)

As can be seen from the picture above, many plastic hinges were activated in the diagonal members (coloured bullets and scale). In total 31 hinges out of the 203 assigned in the model were found with plastic deformations in the last step of pushover. In the following figure two hinges' responses in the middle upright frame of the structure are displayed.

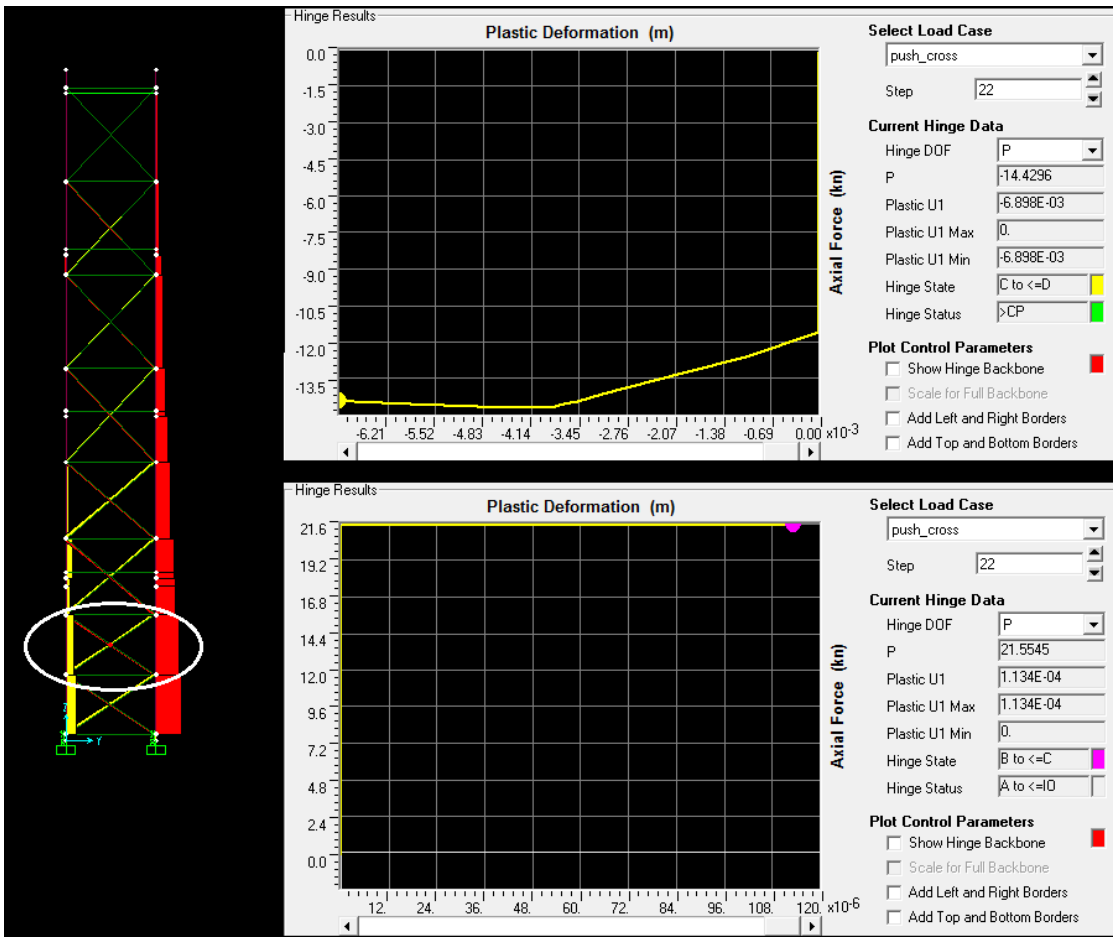

Figure 5.19: Pushover final step_ Plastic hinges in the middle upright frame (one diagonal in compression and another in tension)

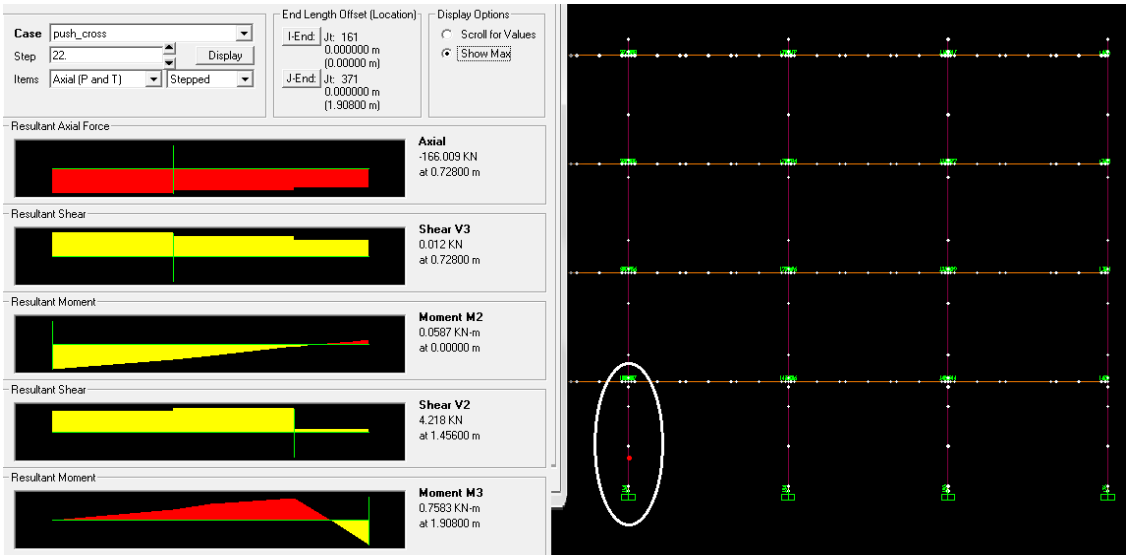

Figure 5.20: Pushover final step_ Internal forces in the most critical column

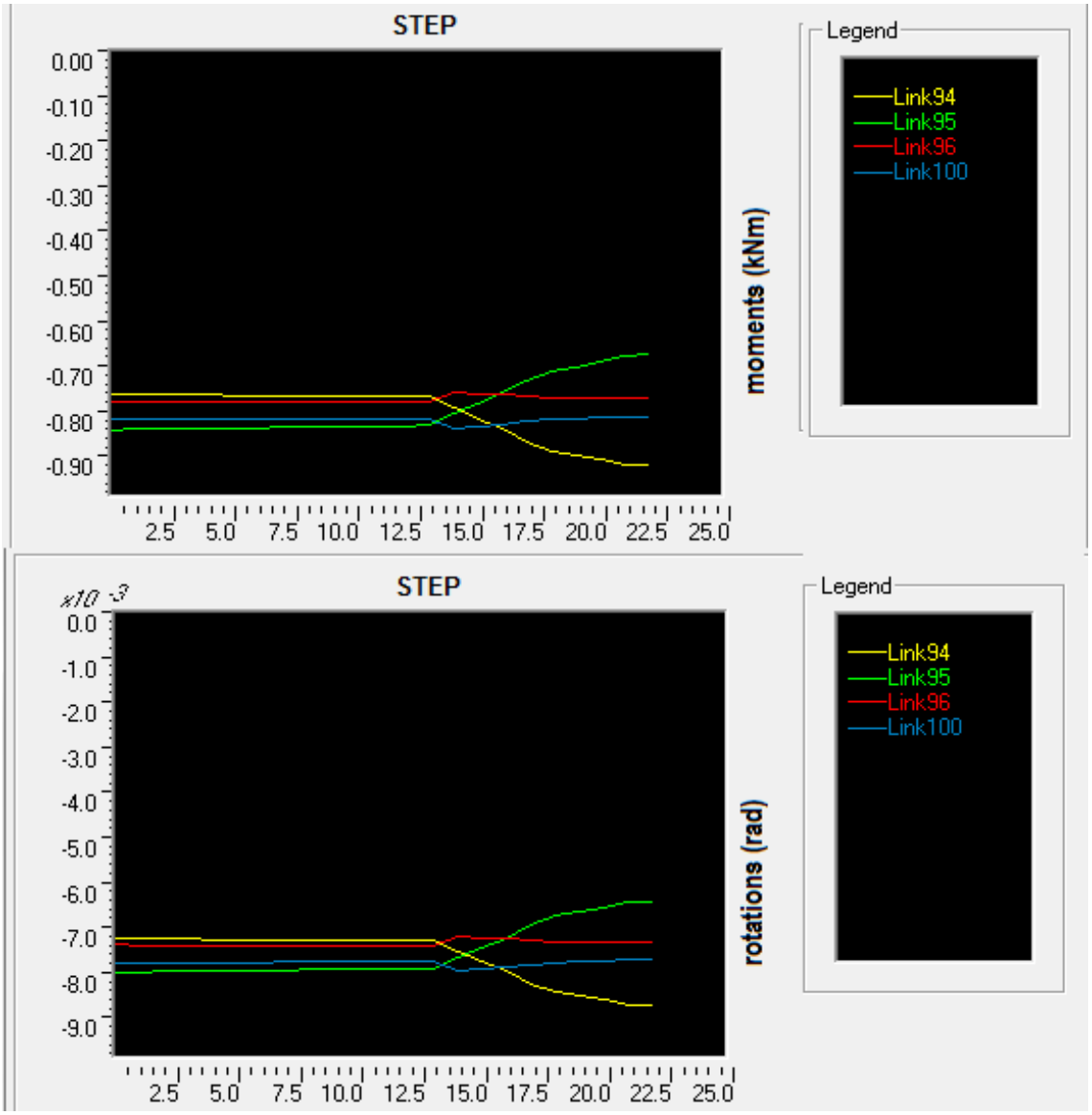

Figure 5.21: Behaviour of beam-end-connector links per step. No failure occurs.

5.4. High seismicity model

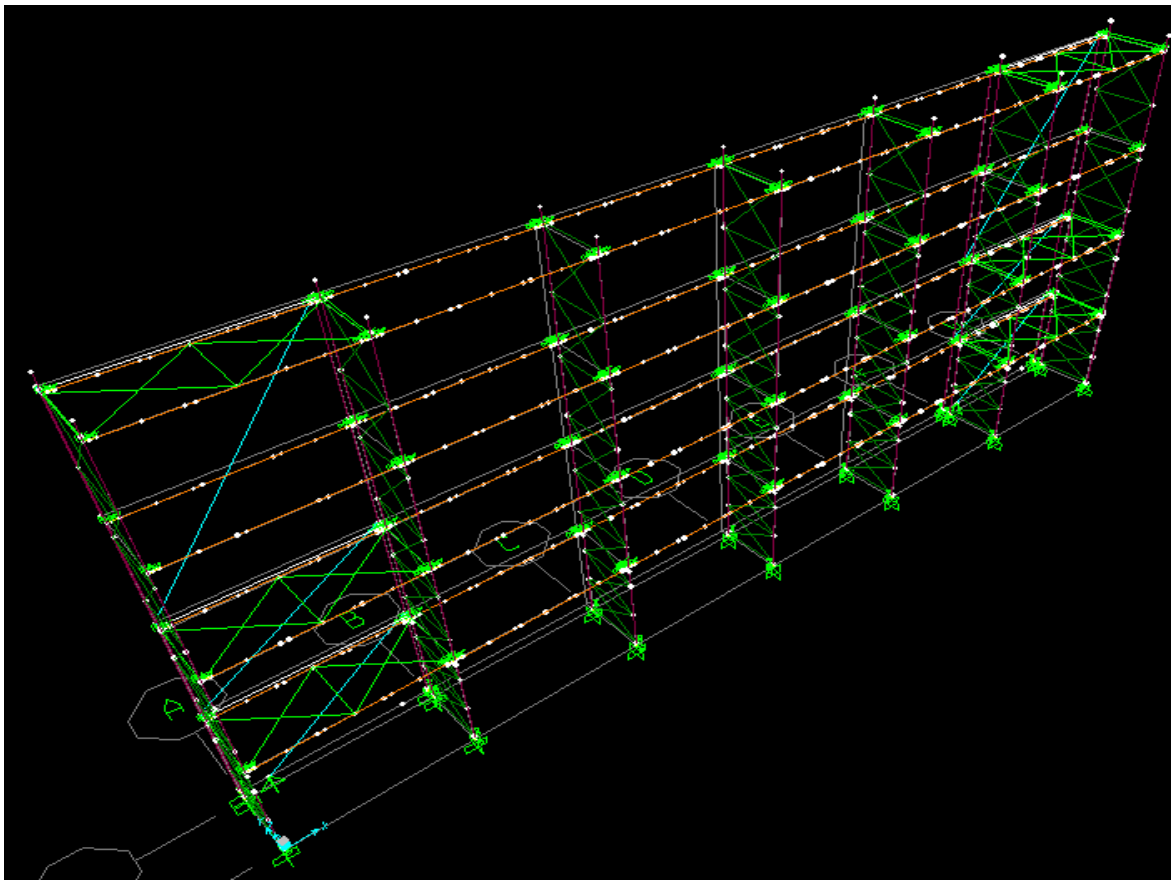

Figure 5.22: 3-D view of model

In the following figure the rear frame as well as the upright frame are depicted. Only the bracings of the rear frame that work in tension are taken into account in the simulation.

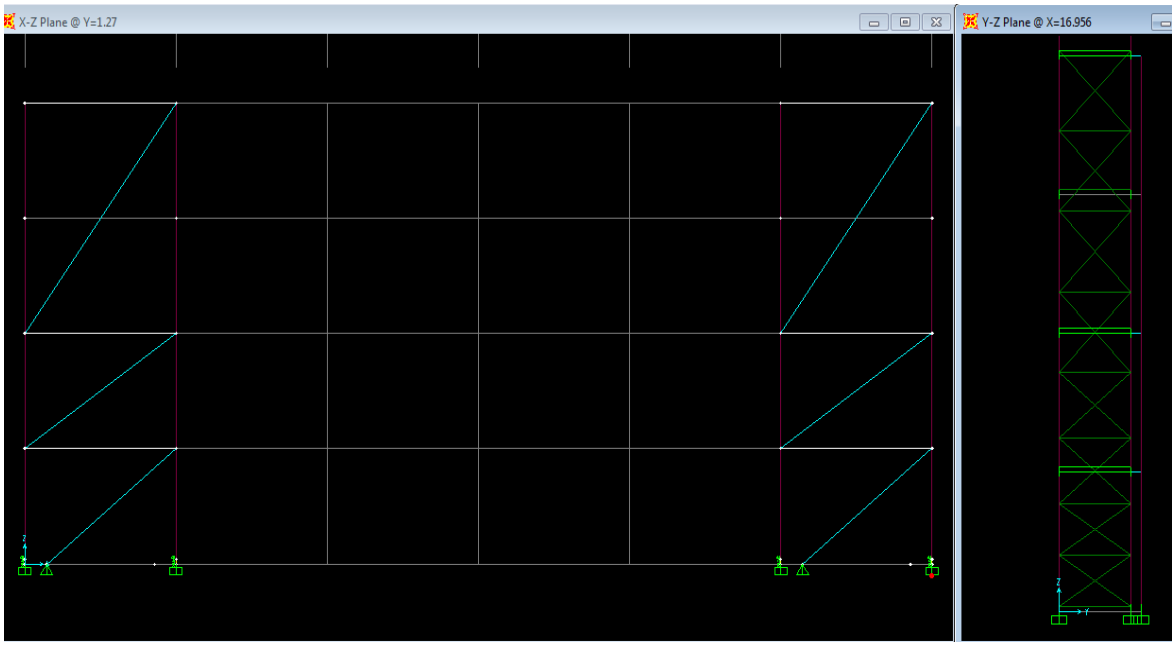

Figure 5.23: XZ elevation of rear frame and YZ (cross-aisle) view

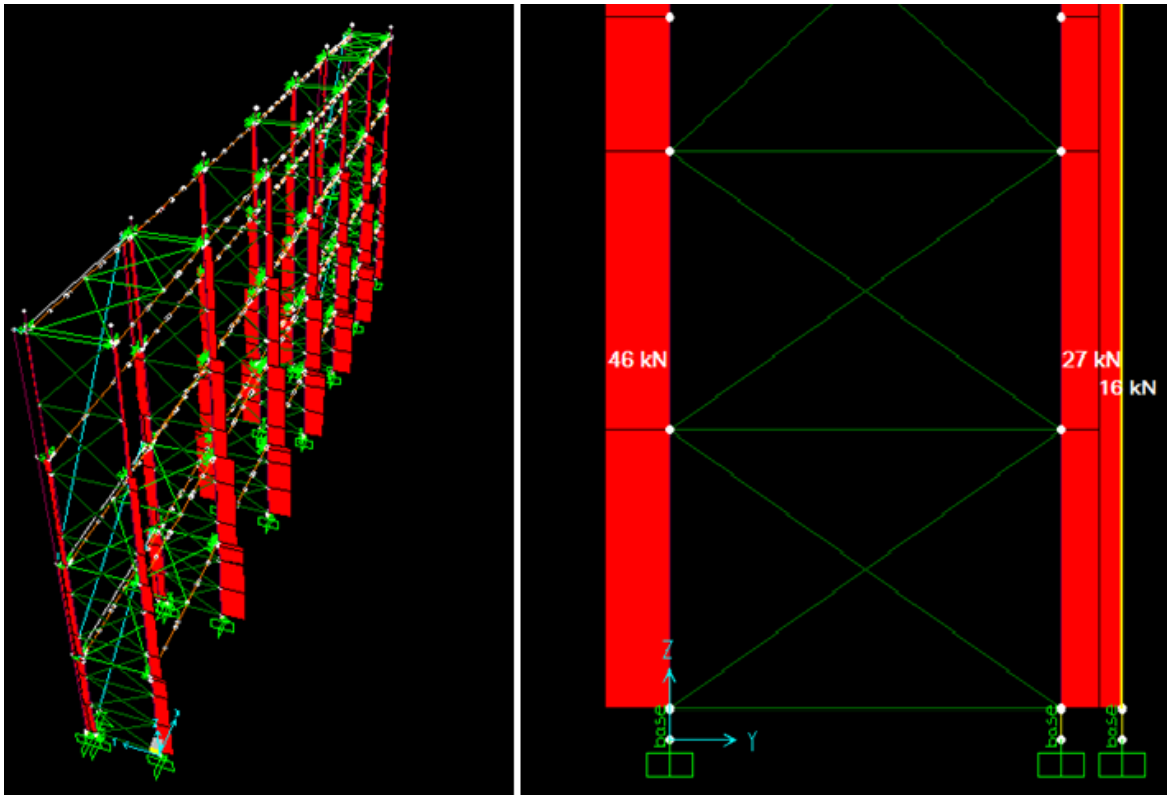

Figure 5.24: Axial forces from pallets and detail _ front frame: N_{max} = 48.9 kN and N_{min}=23.7 kN and rear frame: N_{max} =16 kN and N_{min}= 6 kN

5.4.1. Modal analysis

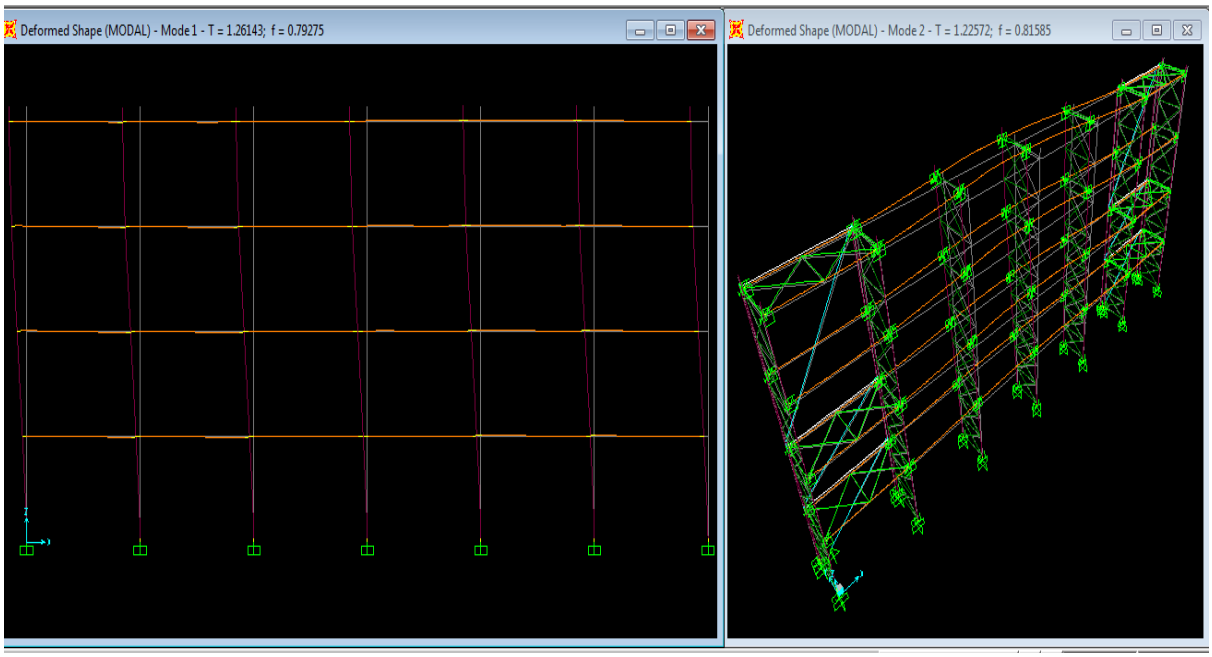

Figure 5.25: Modal analysis - first two modes

Table: Modal Participating Mass Ratios

StepNum	Period	SumUX	SumUY	SumUZ
	Sec			
1	1.261426	0.28246	0.00398	9.343E-08
2	1.225719	0.28786	0.52060	2.033E-06
3	1.003056	0.61856	0.55684	5.521E-06
4	0.977428	0.67592	0.82026	6.531E-05
5	0.840695	0.68645	0.82053	6.565E-05
6	0.615108	0.68662	0.82387	7.607E-05
7	0.594668	0.79004	0.82394	7.918E-05
8	0.538663	0.79004	0.82394	7.918E-05
9	0.526973	0.79025	0.82394	7.935E-05
10	0.516784	0.81672	0.82396	8.046E-05
11	0.498803	0.81673	0.82396	8.047E-05
12	0.485789	0.81675	0.82396	8.056E-05
13	0.480911	0.81688	0.82396	8.057E-05
14	0.476559	0.81782	0.82396	8.069E-05
15	0.468891	0.81782	0.82396	8.069E-05
16	0.460086	0.81813	0.83155	8.315E-05
17	0.456431	0.83558	0.83233	8.317E-05
18	0.431825	0.83571	0.83277	9.131E-05
19	0.421054	0.84399	0.83294	9.190E-05
20	0.417603	0.84409	0.91682	0.00011

Table 5.3: Modal analysis - first twenty modes and mass participation ratios

5.4.2. Pushover analyses

The capacity curves are displayed for each direction. The vertical axis refers to the base shear force (kN) and the horizontal axis refers to the top displacement (m).

Figure 5.26: Pushover in down-aisle direction, performance curve (and performance point)

Figure 5.27: Pushover in cross-aisle direction, performance curve (and performance point)

Pushover in down-aisle direction

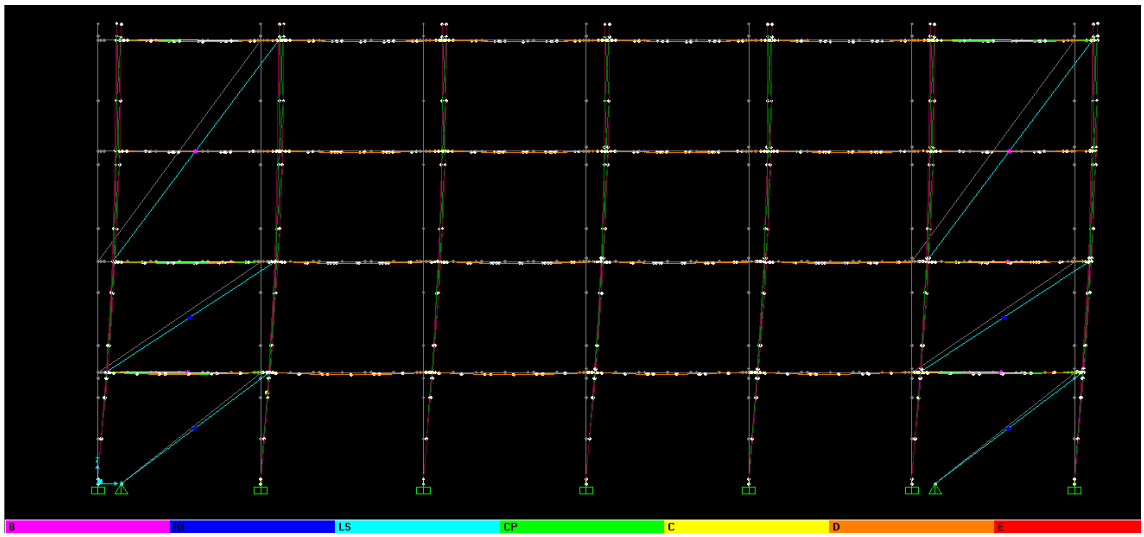

Figure 5.28: Deformed shape in Pushover final step. The colours signify the activation of hinges.

As shown in the picture above, some plastic hinges were activated in the rear frame of the structure. In total 10 out of the 229 plastic hinges were found with plastic deformations in the final step of the pushover load case. As far as the links simulating the base pates are concerned, it can be observed in the following figure that at some point they reached their ultimum moment and started losing strength.

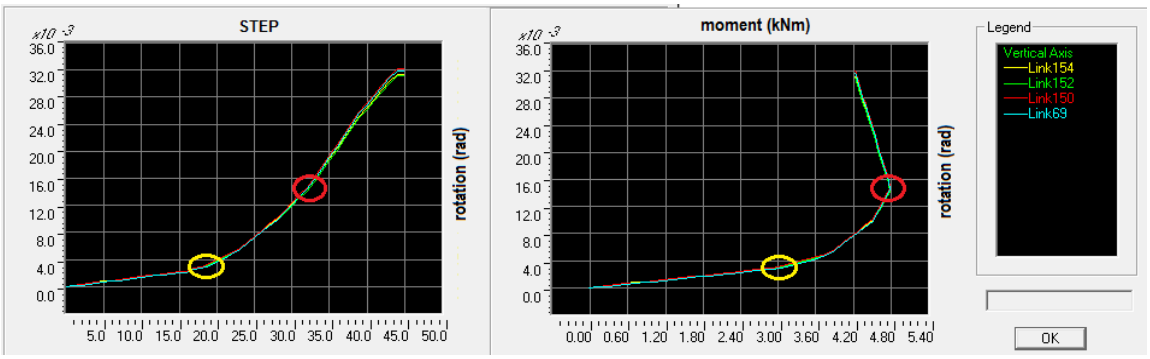

Figure 5.29: Behaviour of base links in terms of moment/rotation and rotations per step

The inelastic deformations of the top of the columns in the rear frame can be seen in the following picture. The plastic hinge displayed was type " interacting forces P- moments M" and the plastic deformation for both degrees of freedom are exhibited.

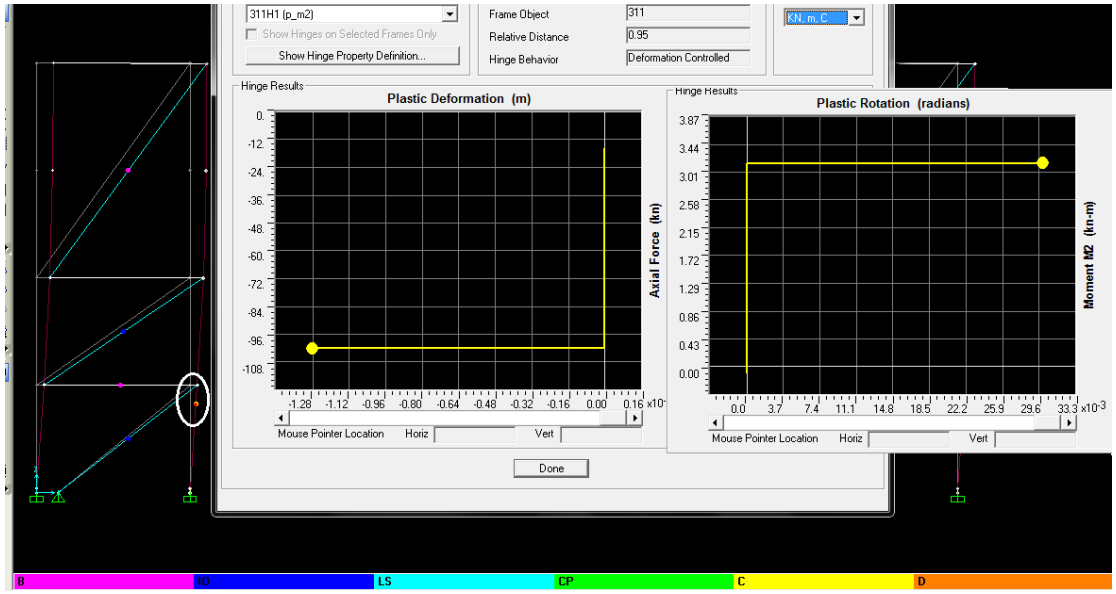

Figure 5.30: Plastic hinge activated in the uprighs of the rear frame

As far as the response of beams and their connections is concerned, they were reported to reach their moment limit before the final step of the pushover.

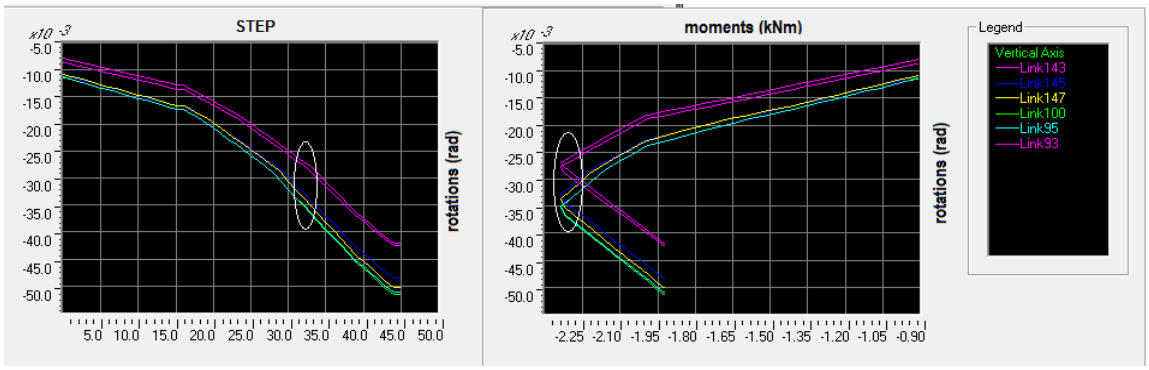

Figure 5.31: Moment/rotation behaviour of beam-end-connector links per step. Failure is noted.

The response of the uprights in terms of internal forces is presented in the following. Two upright examples are presented in the final step of pushover: the most critical upright in the main structure and the most critical one in the rear frame. It can be observed that the axial forces in the rear frame are significantly larger.

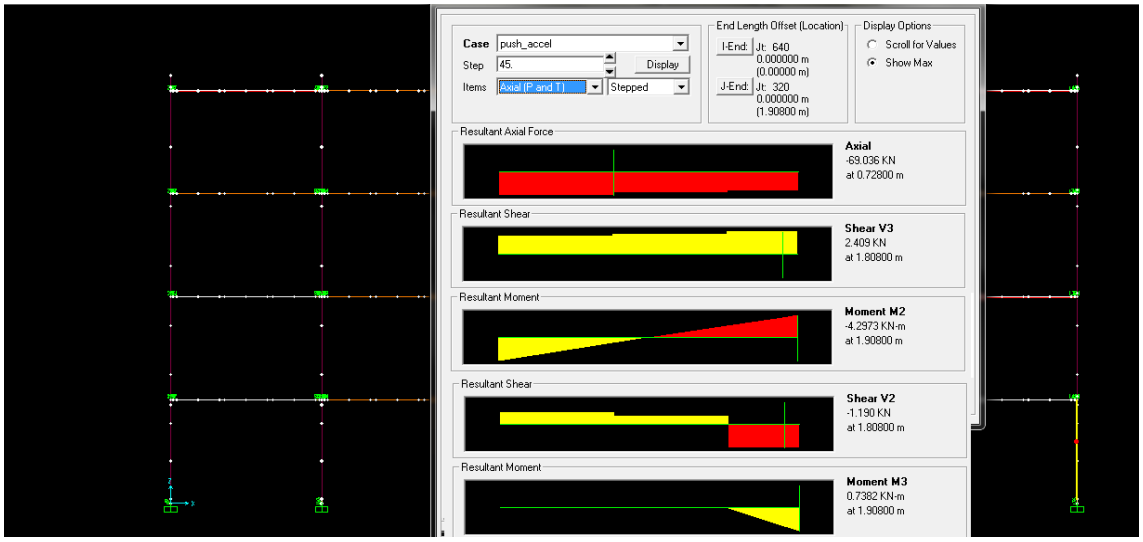

Figure 5.32: Pushover final step_ Internal forces in the critical uprigth of the main rack structure.

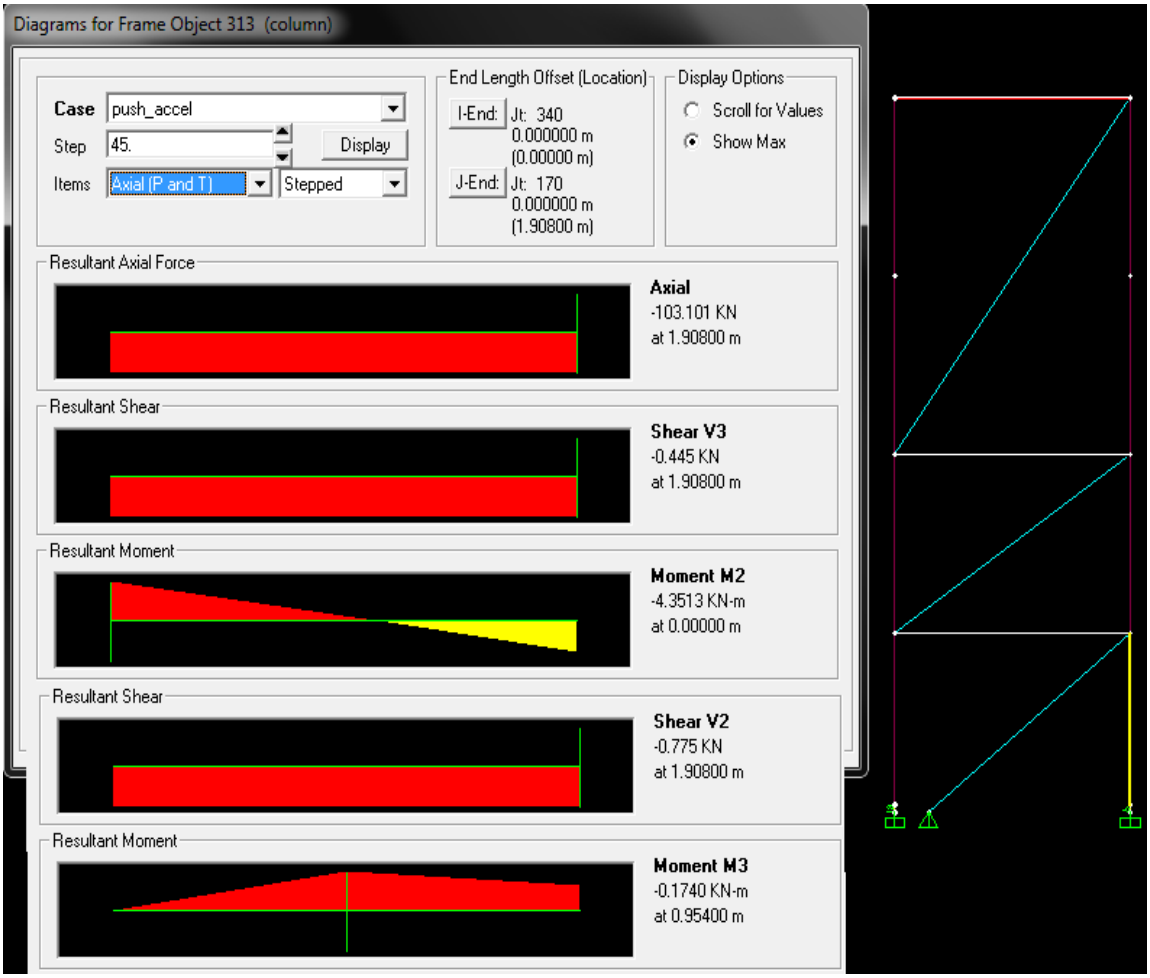

Figure 5.33: Pushover final step_ Internal forces in the critical uprigth of the rear supporting frame.

Pushover in cross-aisle direction

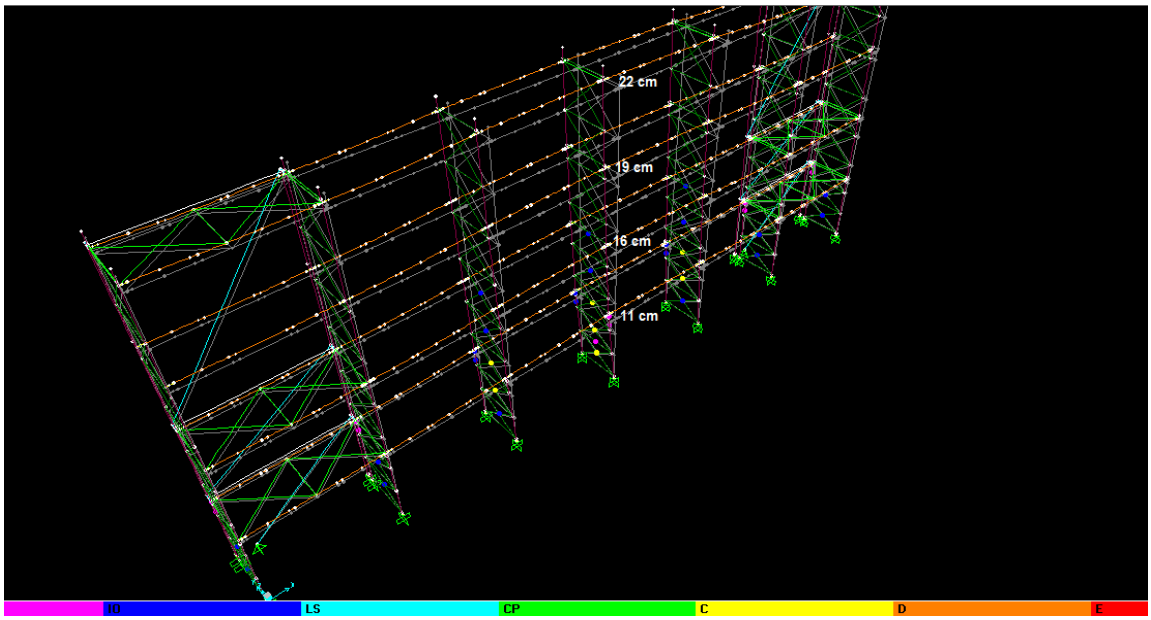

Figure 5.34: Deformed shape in Pushover final step. The colours signify the activation of hinges.

As can be seen from the picture above, many plastic hinges were activated in the diagonal members (coloured bullets and scale). In total 39 hinges out of the 229 assigned in the model were found with plastic deformations in the last step of pushover. On the other hand, the deformations of the multi-linear links assigned in the base plates and the beam-end connections were insignificant. In the following picture, the plastic deformations of the hinges assigned on the most adverse diagonals (in the lowest part of the middle frame) are presented. It can be noticed that the one diagonal is in tension and the other in compression, having different failure points.

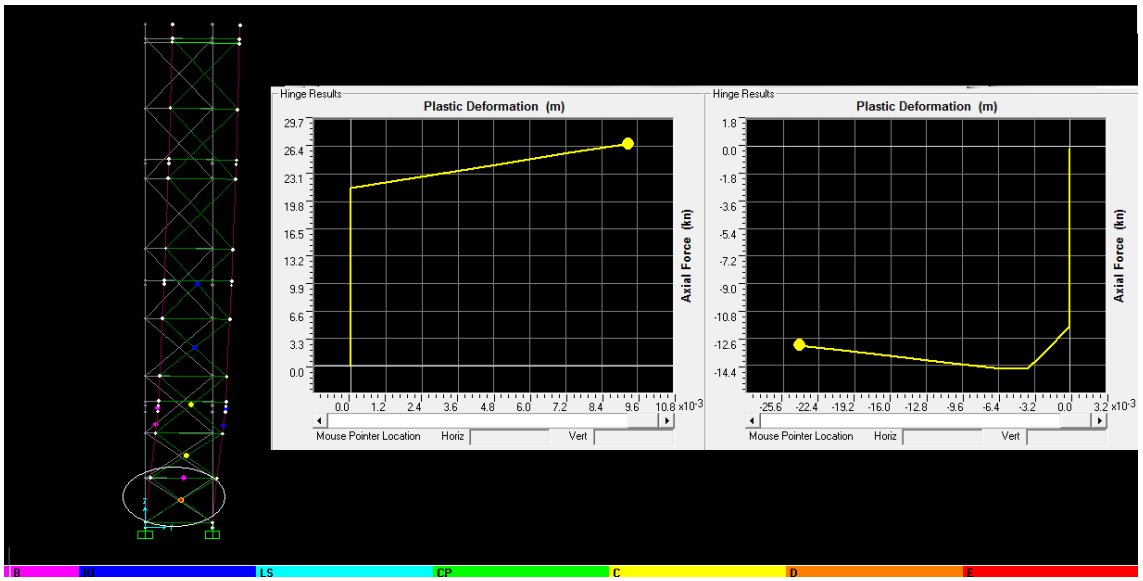

Figure 5.35: Pushover final step_ Plastic hinges in the middle upright frame (one diagonal in compression and another in tension)

In the following picture, the internal forces of the most adverse upright are displayed.

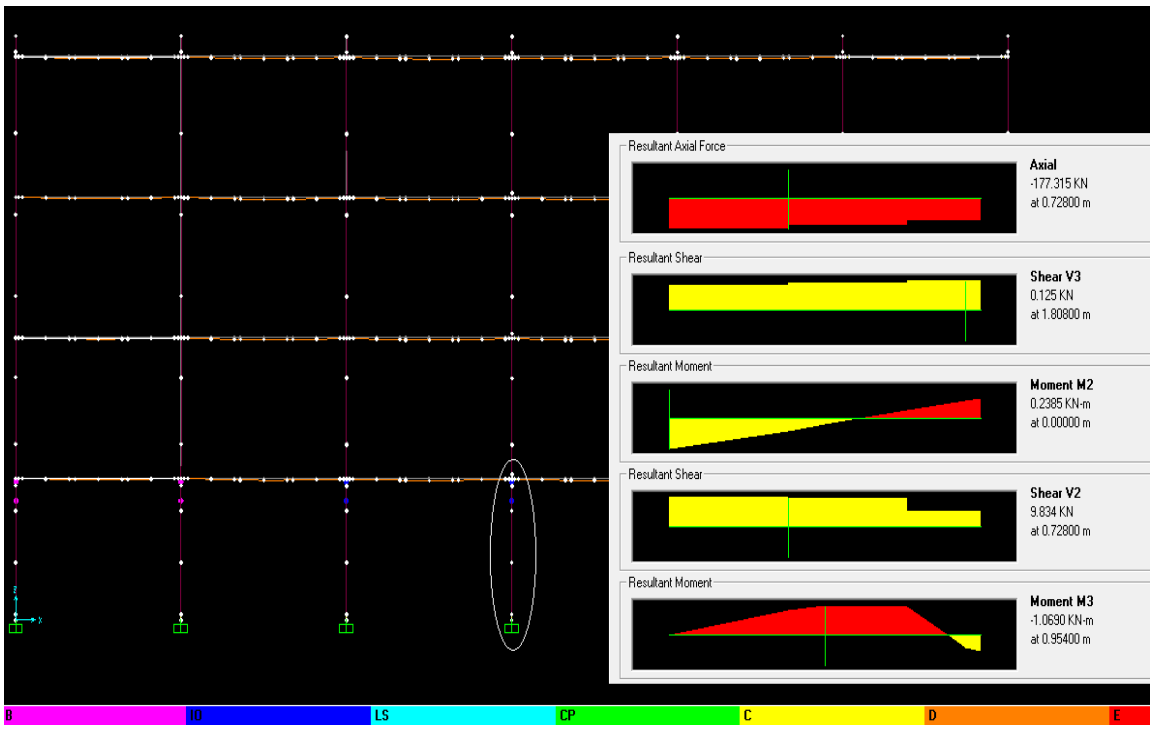

Figure 5.36: Pushover final step_ Internal forces in the most critical column

6.1. Material nonlinearity (experimental data and simulation)

In contrast with the other cases, no experimental data were available as far as the non linear behaviour of the base plate connections is concerned. However a technical report was provided by the company including values for the rotational stiffness that could be used in the bases of the columns, by means of the partial release/fixity option in Sap2000. The only available experimental data concerning the uprights were some compression test results.

Figure 6.1: Upright, compression test data

Due to the lack of data, no base plate links were used in this case. In order to simulate the inelastic behaviour of the uprights and their connections, plastic hinges and partial fixity springs were used. Instead of the base plate, a "moment M2" type of plastic hinge was assigned whereas on the top of columns in the lowest level, an "axial force P- moment M2" type was used. The P-M2 interaction curve of the latter was defined with P_{max}= 121 kN and M_{max}=5.53 kNm (values defined by another software).

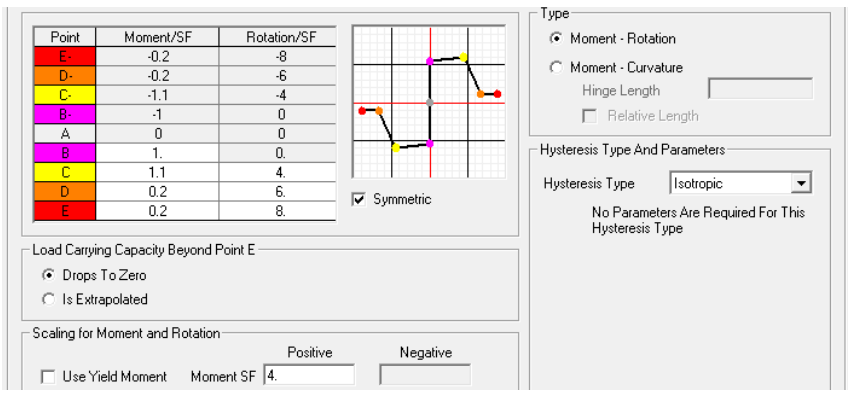

Figure 6.2a: Upright, Base hinges (moment M2)

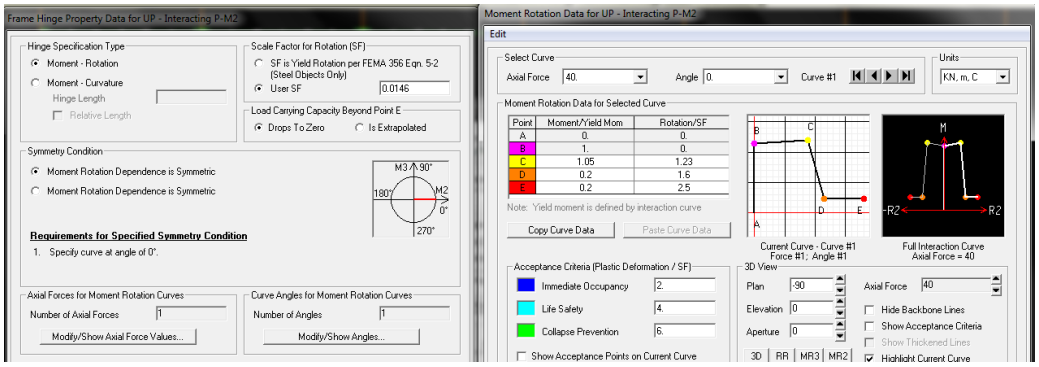

Figure 6.2b: Upright, top hinges (P-moment M2)

As far as the behaviour of the beam end connections is concerned, the experiments resulted in the following moment-rotation diagram.

Figure 6.3: Beam end connector data

The previous graph was simulated with the following type of multi-linear plastic link in Sap2000.

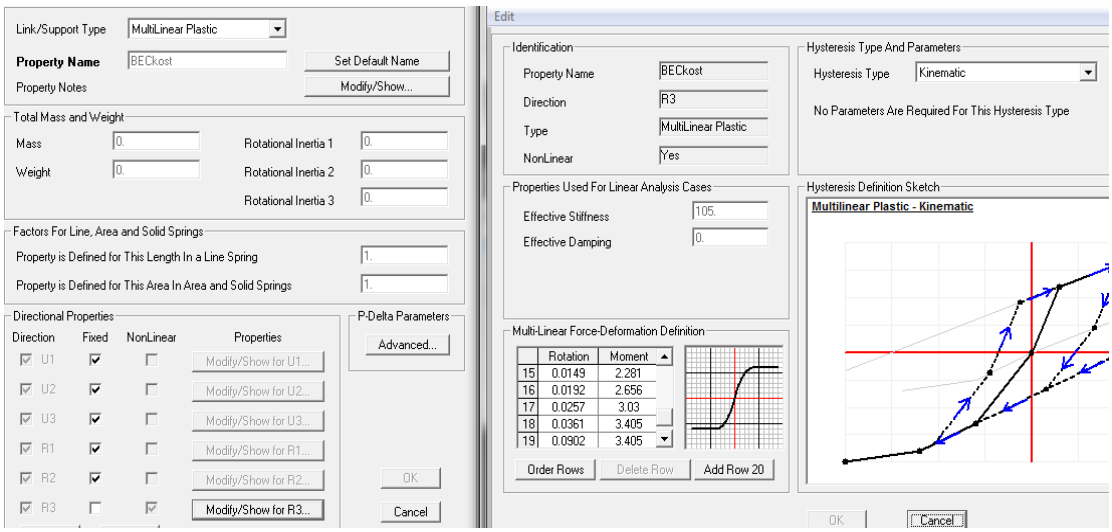

Figure 6.4: Beam end connector simulation

The plastic hinges assigned in the middle of each upright frame diagonal had the following properties. The values used were derived from the technical reports of the company and were the critical amongst the buckling check of the member and the checks of the bolted joints (shear resistance and bearing resistance).

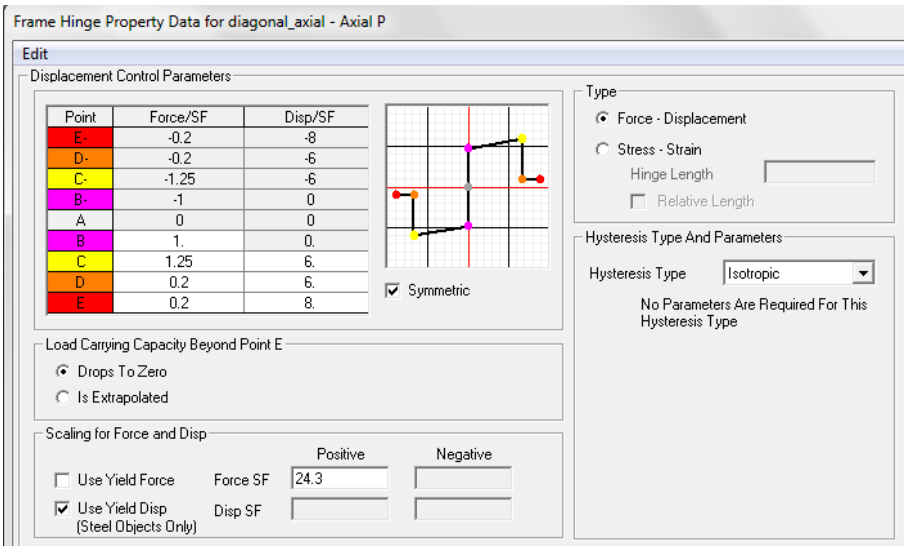

Figure 6.5: Plastic hinge assigned on diagonals

6.2. Medium seismicity model

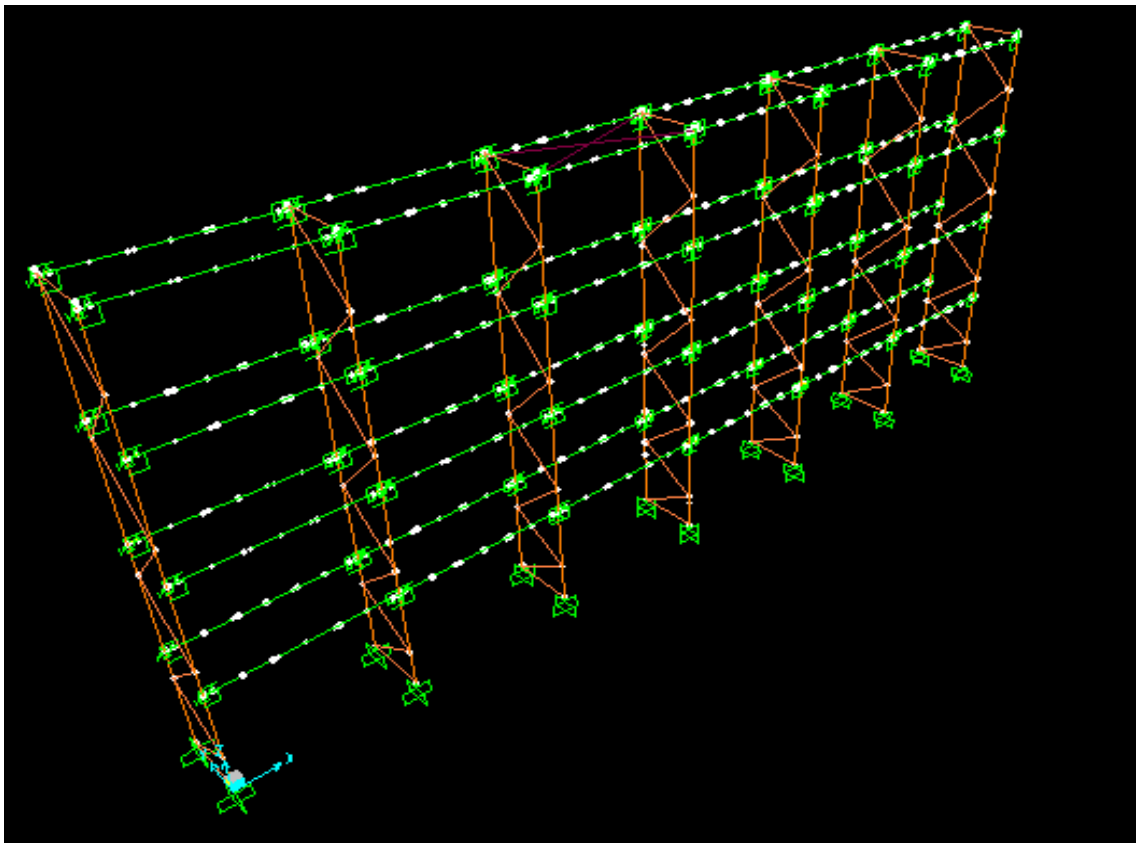

Figure 6.6: 3-D view of model

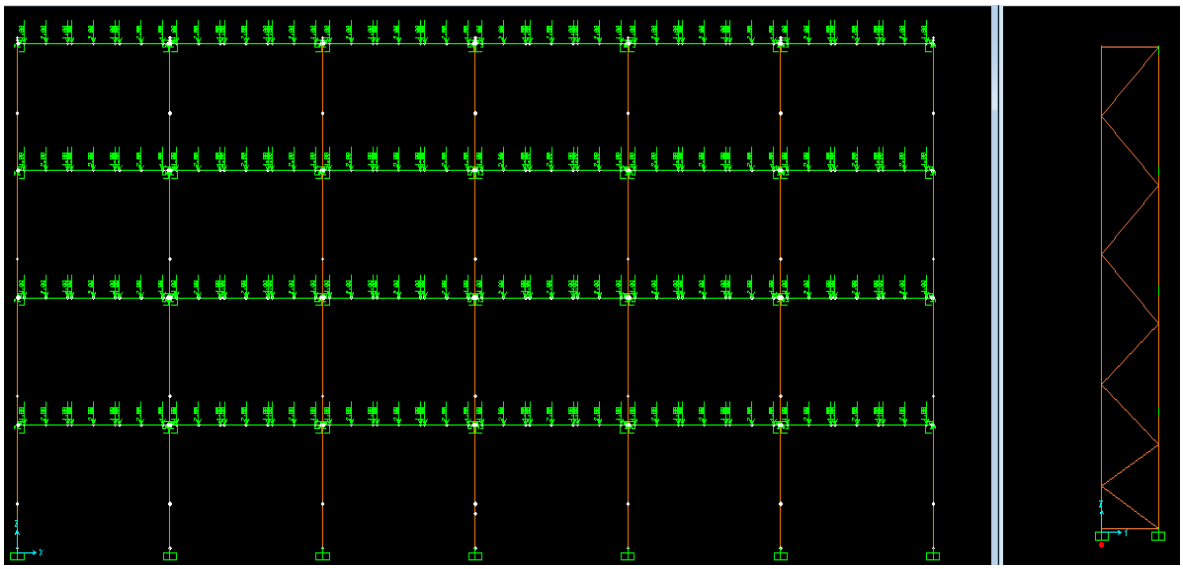

Figure 6.7: XZ (down-aisle) and YZ(cross-aisle) view of model- application of pallet loads

As in the previous case, the main moments for the beams are M3 moments whereas the main moments for the uprights are the M2 moments.
The internal forces under the vertical loading of pallets are shown in the following figure.

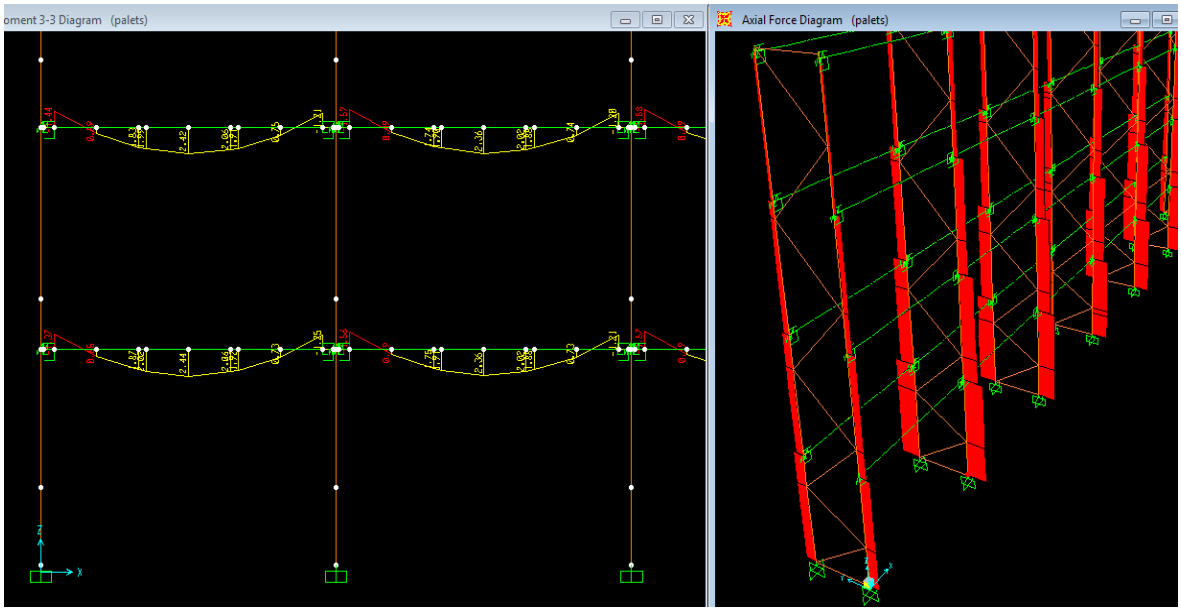

Figure 6.8: Pallet loads_ $M3_{max}$=2.44 kNm, N_{max}= 48.3 kN and N_{min}= 24.2 kN

6.2.1. Modal analysis

The modal analysis resulted in the following. As it can be seen from the pictures below, the first mode (on the left) was translational in X axis whereas the second mode (on the right) looks like an oscillation of both columns and beams in Z axis and in Y axis respectively.

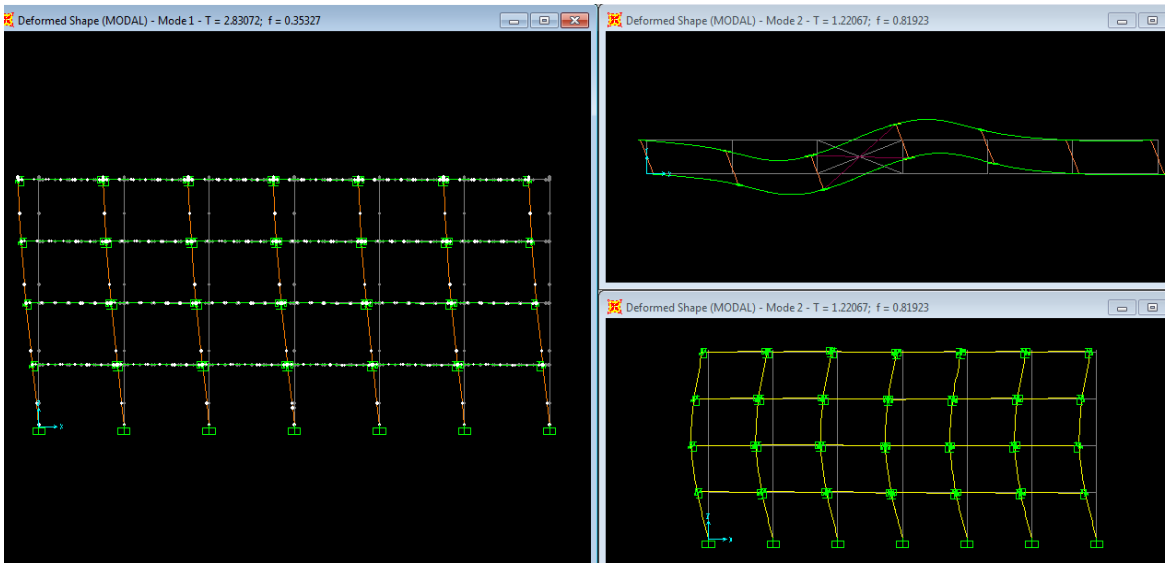

Figure 6.9: Modal analysis - first two modes

In the following table the first twelve modes are summarized, with their periods and the mass participation ratios.

Table: Modal Participating Mass Ratios

StepNum	Period Sec	SumUX	SumUY	SumUZ
1	2.830723	0.88000	1.563E-15	3.474E-17
2	1.220666	0.88000	0.00025	7.079E-11
3	1.031962	0.88000	0.73599	3.814E-07
4	1.021230	0.88000	0.74562	3.845E-07
5	0.982284	0.88000	0.76665	3.892E-07
6	0.914640	0.88000	0.76751	3.894E-07
7	0.823126	0.96989	0.76752	3.894E-07
8	0.812619	0.96990	0.78389	3.919E-07
9	0.706938	0.96990	0.78389	3.919E-07
10	0.665160	0.96990	0.78389	3.919E-07
11	0.662930	0.96990	0.78389	3.919E-07
12	0.662465	0.96990	0.78389	3.919E-07

Table 6.1: Modal analysis - first twelve modes and mass participation ratios

6.2.2. Pushover analyses

Pushover load cases were applied to the models in both X and Y directions. As mentioned before this pushover analyses were displacement. Hereby the performance curves are displayed for each direction. The vertical axis refers to the base shear force (kN) and the horizontal axis refers to the top displacement (m). The horizontal forces used in the design (as mentioned in the company's technical report) are also shown.
The performance points are calculated by the programme according to ATC 40 [chapter 5].

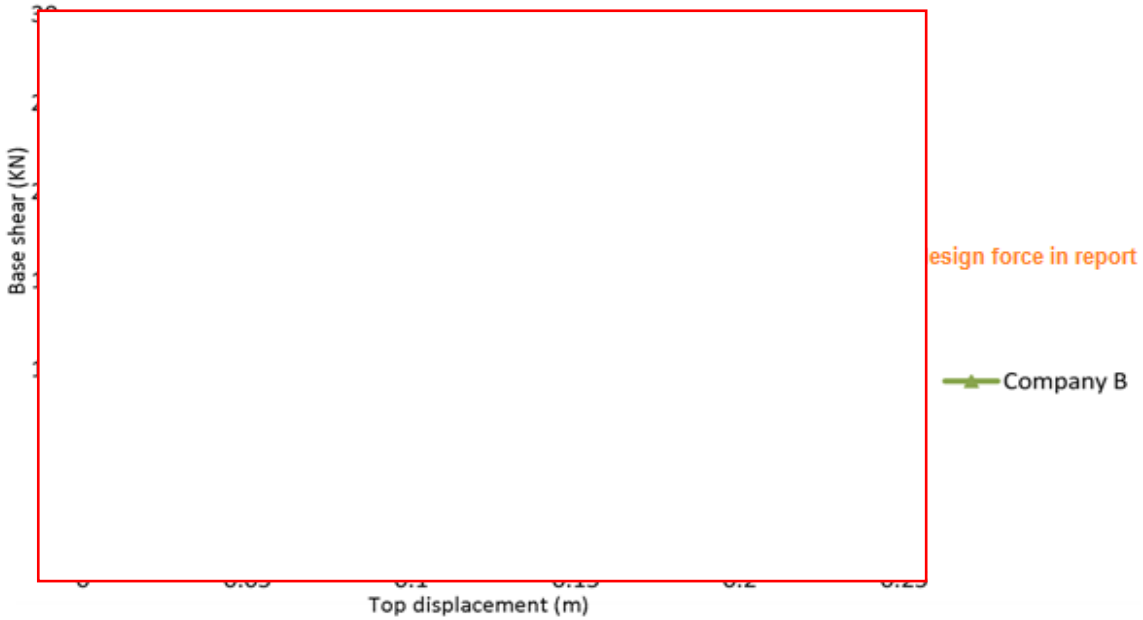

Figure 6.10: Pushover in down-aisle direction, performance curve (and performance point)

Figure 6.11: Pushover in cross-aisle direction, performance curve (and performance point)

Pushover in down-aisle direction

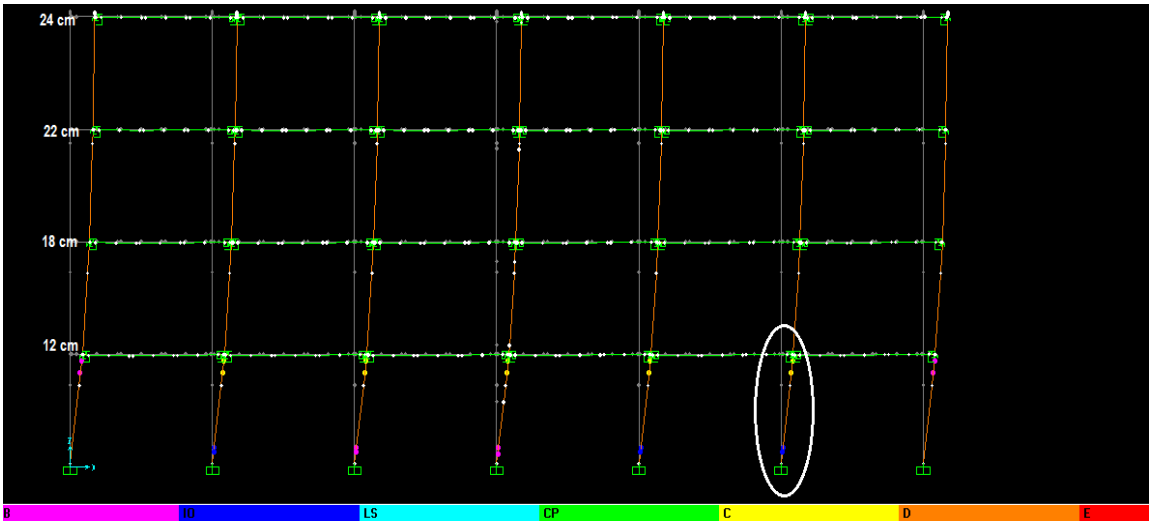

Figure 6.12: Deformed shape in Pushover final step and activated plastic hinges (colour scale). The displacements in each level are noted.

It should be reminded that in this company no base links were assigned to the uprights and two hinges (one at the base and one at the top of the lowest level) were used instead. In total 23 plastic hinges out of the 28 assigned were activated during the analysis. The most critical upright which failed earlier than the rest is the one circled in the figure above. Its response can be seen in the following picture.

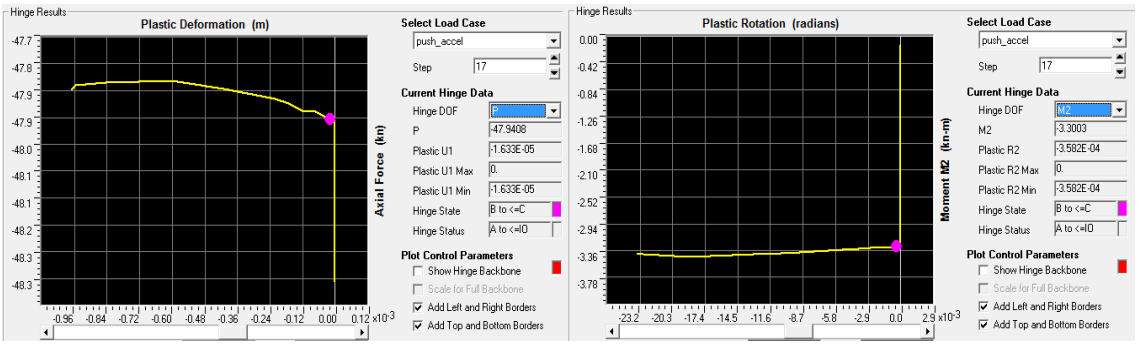

Figure 6.13: Plastic hinge (type P-M), at top of critical upright, activated first during pushover.

As far as the multi-linear links simulation the beam-end connections are concerned, failure also occurred. In fact many of them reached maximum moment in the middle of the pushover analysis. Their step-by-step behaviour can be observed in terms of moments/rotations in the following figure.

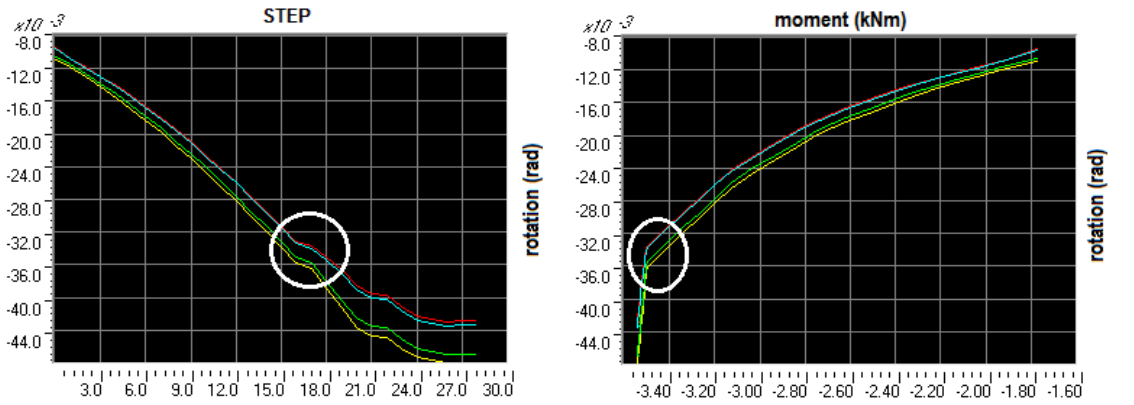

Figure 6.14: Moment-rotation behaviour of beam-end-connector links per step.

Pushover in cross-aisle direction

In the following picture, the deformed shape at the final step of the pushover analyses is displayed along with the measured displacements at each level in the middle of the rack and plastic deformations of the hinge that was activated first. In total 20 hinges out of the 98 created exhibited plastic deformations.

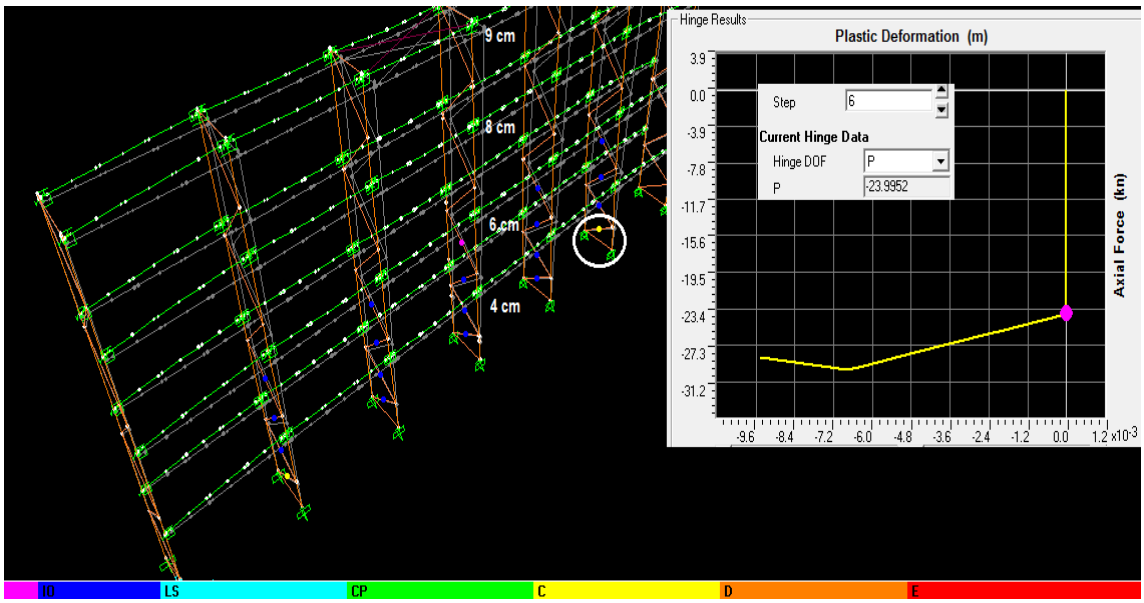

Figure 6.15: Deformed shape in Pushover final step and plastic deformations of first hinge

The beam-end-connector links exhibited relatively small deformation and therefore are not displayed. However, it could be useful to observe the internal forces in the most critical column.

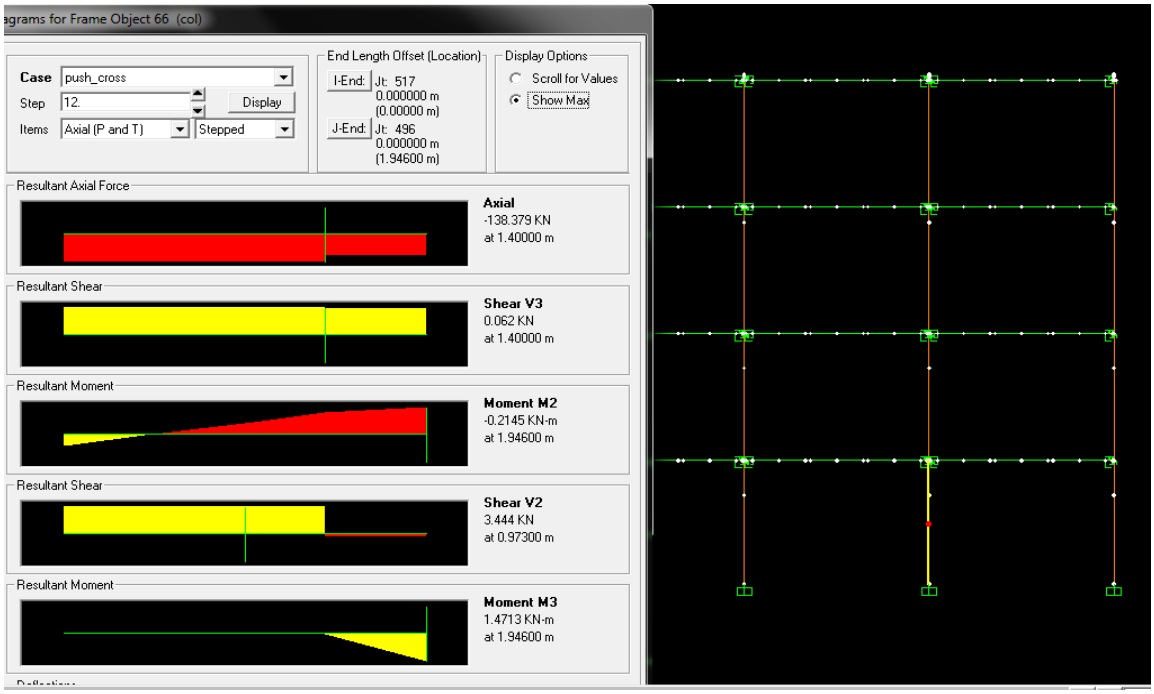

Figure 6.16: Pushover final step_ Internal forces in the most critical column

6.3. High seismicity model

As it can be noticed from the following figures, in this company's case the medium and the high seismicity model have no differences concerning their configuration. The geometry of the model is the same. However, the sections of the various elements differ.

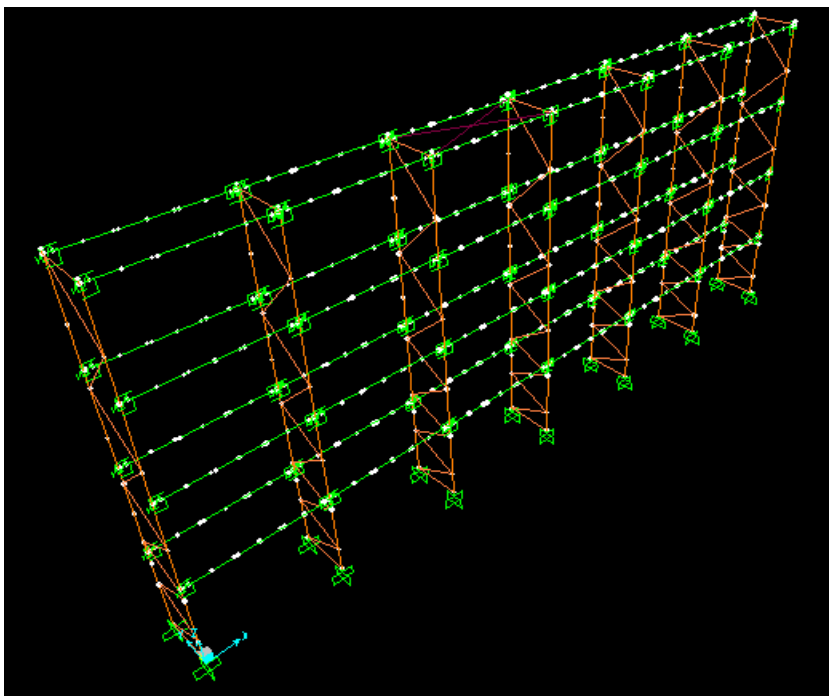

Figure 6.17: 3-D view of model

Due to similarity with the medium seismicity model, no other figures concerning the configuration and the results of the pallet loads are provided.

6.3.1. Modal analysis

As it was the case in the medium seismicity model, the first mode (on the left) was translational in X axis whereas the second mode (on the right) looks like an oscillation of both columns and beams in Z axis and in Y axis respectively.

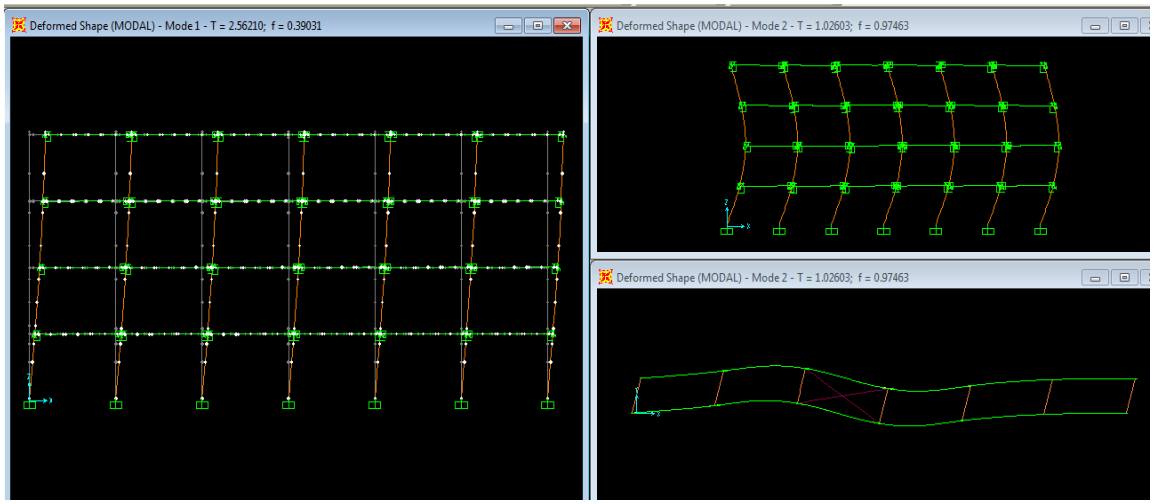

Figure 6.18: Modal analysis - first two modes

In the following table the first twelve modes are summarized, with their periods and the mass participation ratios.

Table: Modal Participating Mass Ratios

StepNum	Period	SumUX	SumUY	SumUZ
	Sec			
1	2.562096	0.88364	7.550E-12	3.331E-18
2	1.026034	0.88364	3.107E-05	3.728E-13
3	0.807058	0.88364	0.70063	3.513E-07
4	0.789399	0.88364	0.70323	3.529E-07
5	0.739010	0.88364	0.76335	3.714E-07
6	0.721643	0.97090	0.76335	3.714E-07
7	0.646621	0.97090	0.76360	3.716E-07
8	0.546448	0.97090	0.78733	3.775E-07
9	0.434568	0.97090	0.78741	3.784E-07
10	0.387094	0.97090	0.79078	3.817E-07
11	0.379313	0.97090	0.79079	3.821E-07
12	0.375163	0.97090	0.79079	3.821E-07

Table 6.2: Modal analysis - first twelve modes and mass participation ratios

6.3.2. Pushover analyses

Pushover load cases were applied to the models in both X and Y directions. Hereby the performance curves are displayed for each direction. The vertical axis refers to the base shear force (kN) and the horizontal axis refers to the top displacement (m).

Figure 6.19: Pushover in down-aisle direction, performance curve (and performance point)

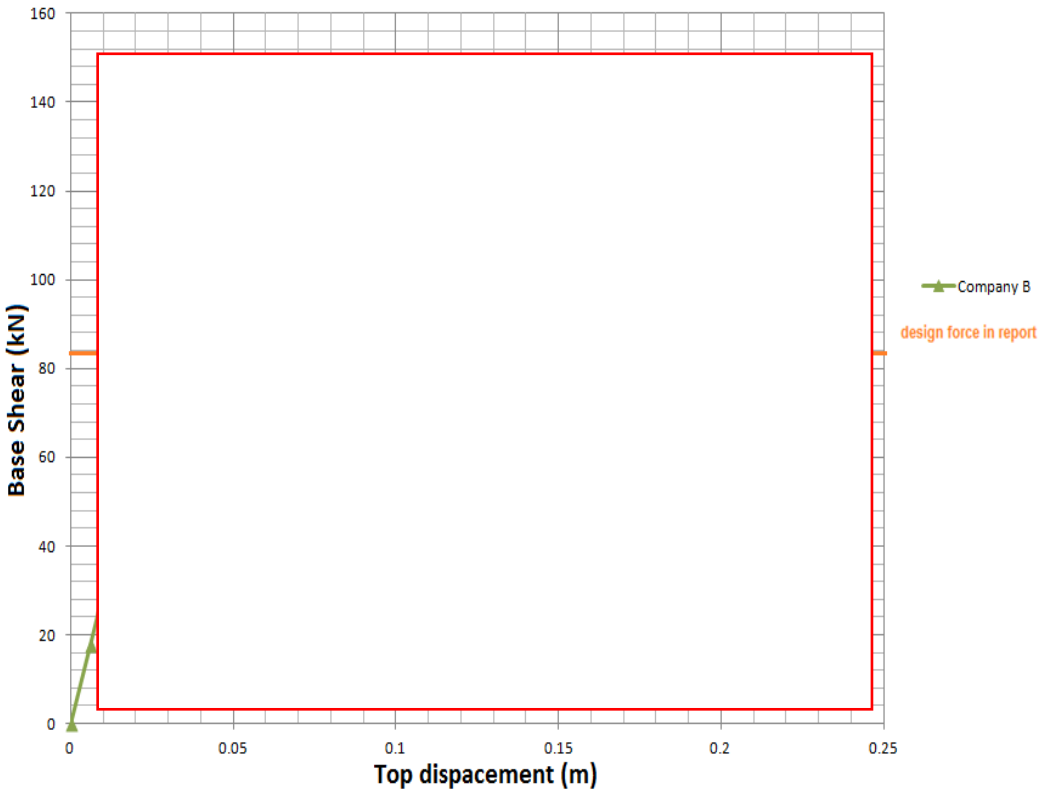

Figure 6.20: Pushover in cross-aisle direction, performance curve (and performance point)

Pushover in down-aisle direction

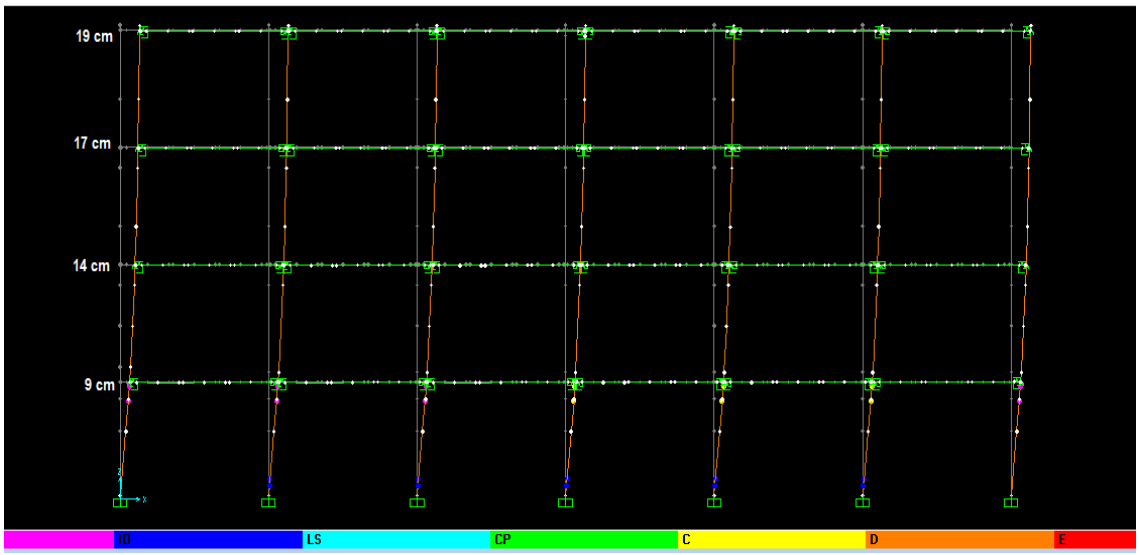

Figure 6.21: Deformed shape in Pushover final step and displacements at each level. The colours signify the activation of hinges.

In total 24 out of 28 plastic hinges were activated. In the following figures a column hinge response is displayed (in terms of axial force and bending moment), as well as the behaviour of the links simulating the beam-end-connections. Failure occurred in these links as well.

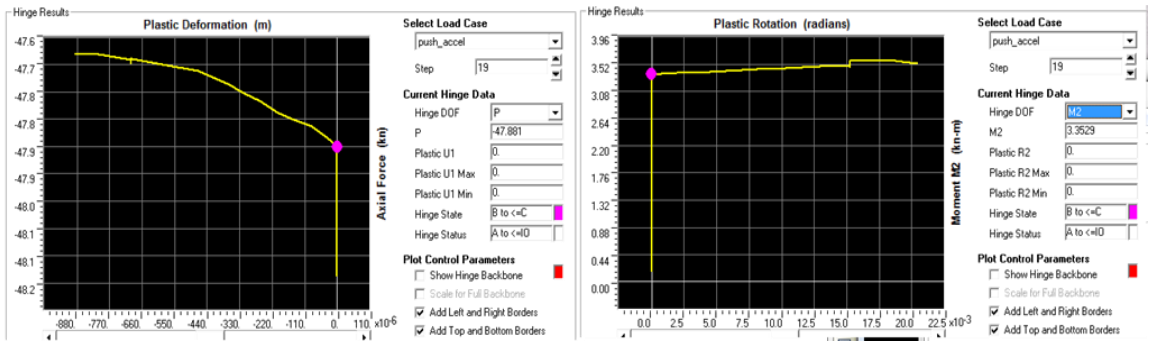

Figure 6.22: Plastic hinge (type P-M), at top of critical upright, activated first during pushover.

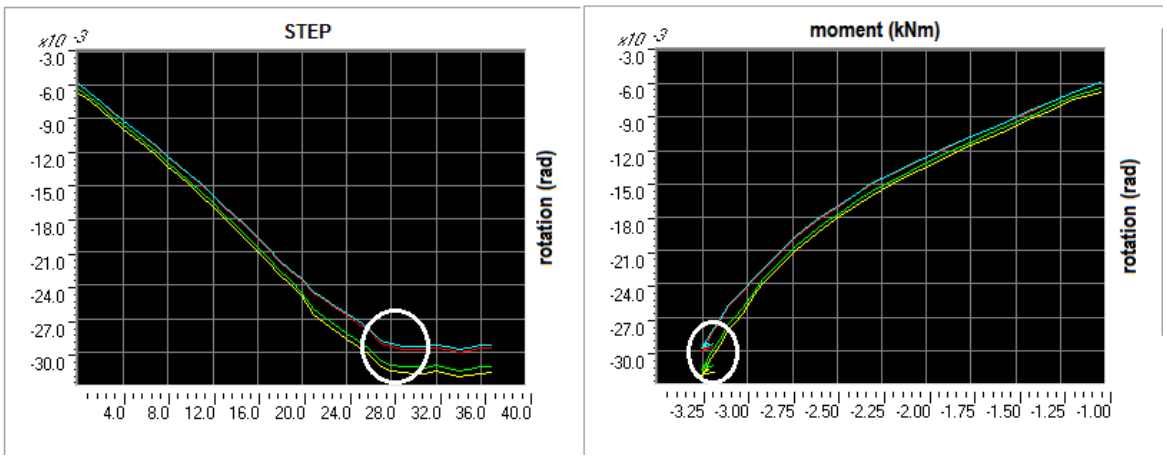

Figure 6.23: Moment/rotation behaviour of beam-end-connector links per step. Failure is noted.

Pushover in cross-aisle direction

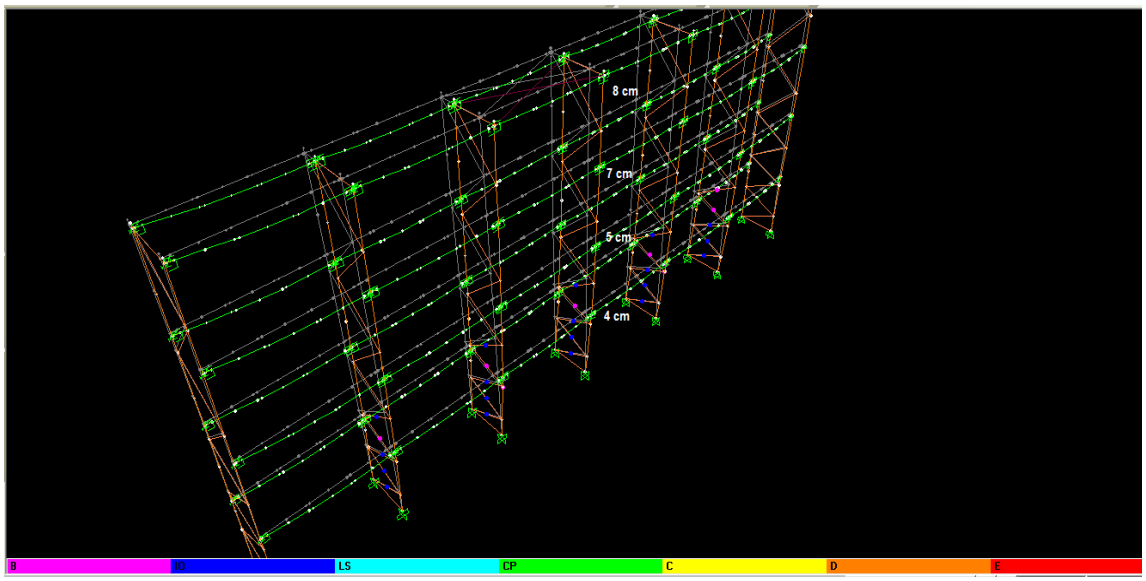

Figure 6.24: Deformed shape in Pushover final step and displacements at each level. The colours signify the activation of hinges.

In total 27 out of 112 plastic hinges were activated. The top displacement reached in this case is realtively small in comparison to the other companies (approximately 8 cm). The beam-end connector links did not exhibit significant deformations. In the following figure the internal forces of the most critical column are displayed, in the final step of the analysis.

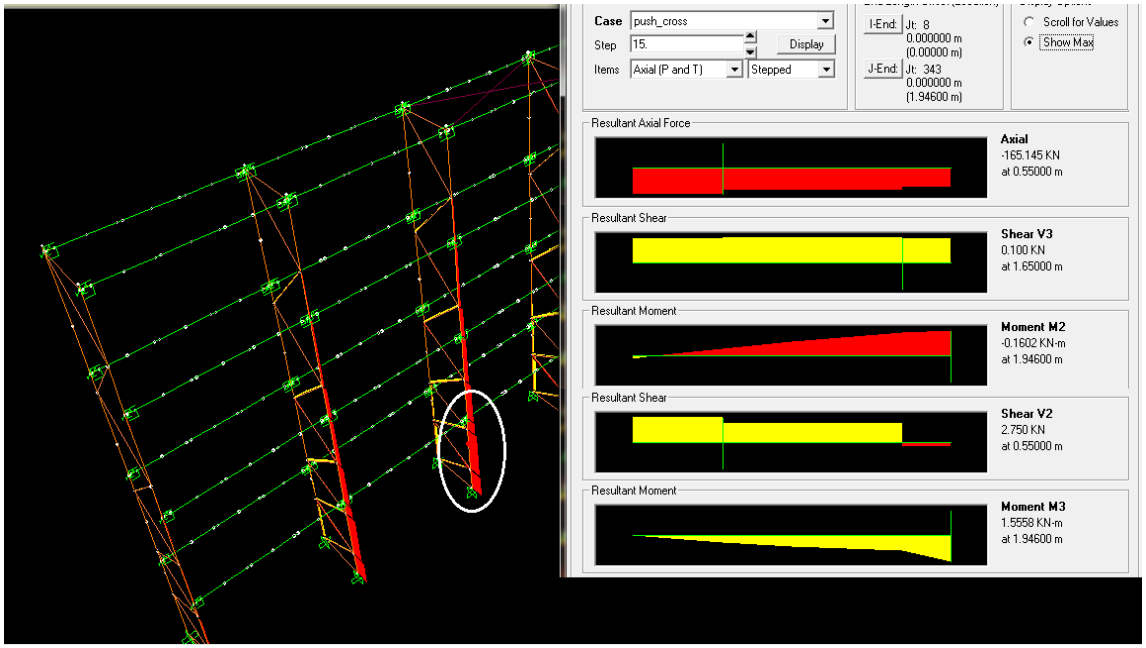

Figure 6.25: Pushover final step_ Internal forces in the most critical upright

Chapter 7 simulation and results _ Company C

7.1. Material nonlinearity (experimental data and simulation)

The non linear behaviour of the base plate connections was described with the following moment-rotation diagram.

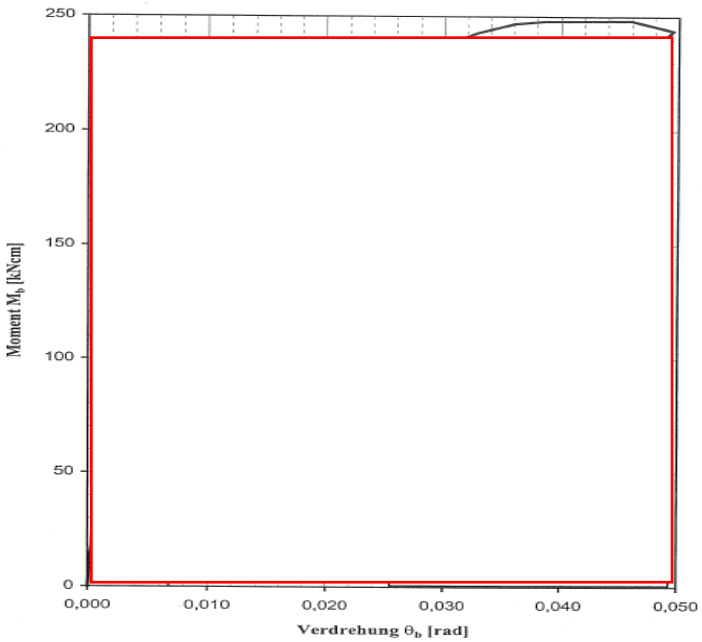

Figure 7.1: Base plate data

The behaviour described in the previous graph was simulated with the following type of multi-linear plastic link in Sap2000.

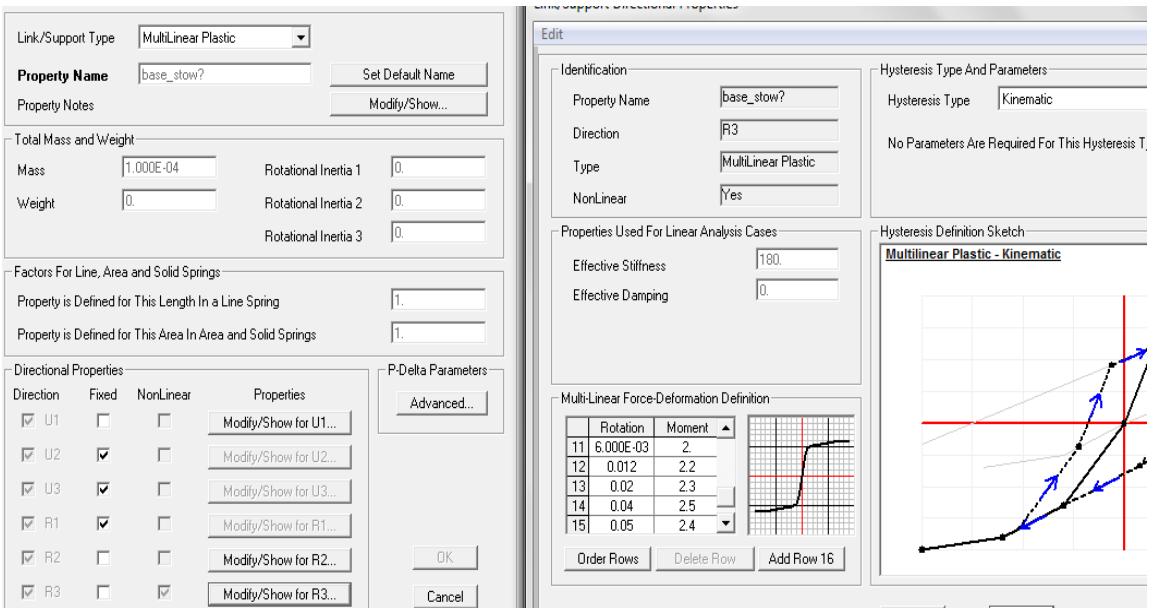

Figure 7.2: Base plate connection simulation

In the top of the columns of the lowest level, plastic hinges were assigned in order to simulate the failure modes indicated from previous research. These hinges are type "axial force P-moment M2" and enable the control of the magnitude of the axial forces in the uprights as well as the interaction between these forces and moments.

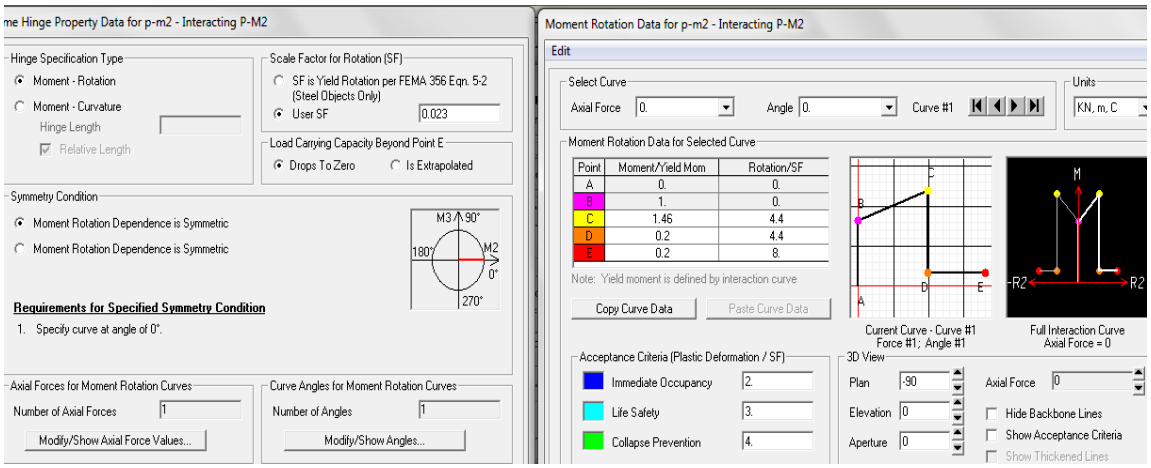

Figure 7.3: Plastic hinge on top of uprights

As far as the nonlinear behaviour of the beam end connections is concerned, in the following figures are displayed the experimental data resulted (moment-rotation diagram) as well as the simulation of the connectors in Sap2000.

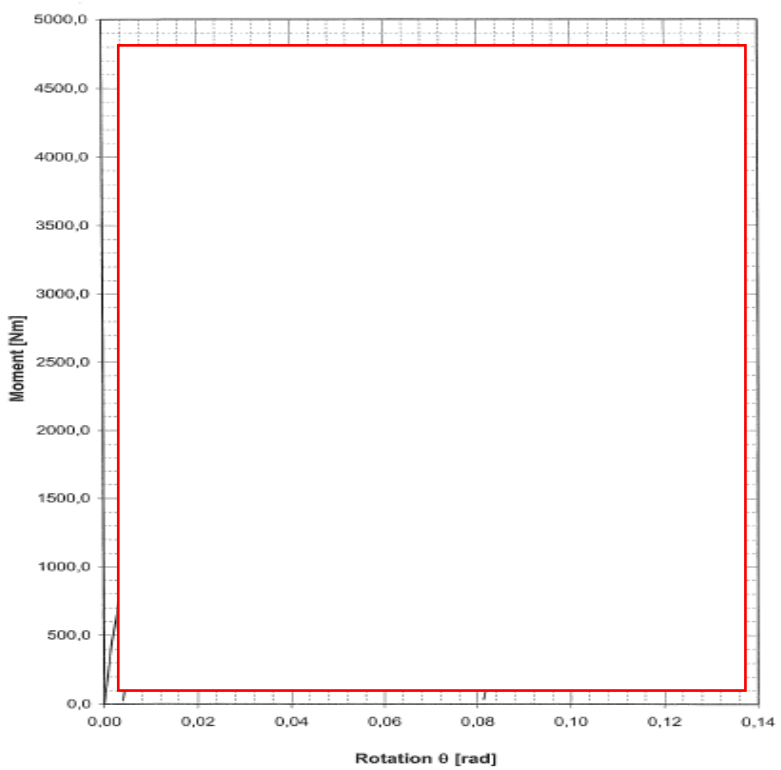

Figure 7.4: Beam end connector data

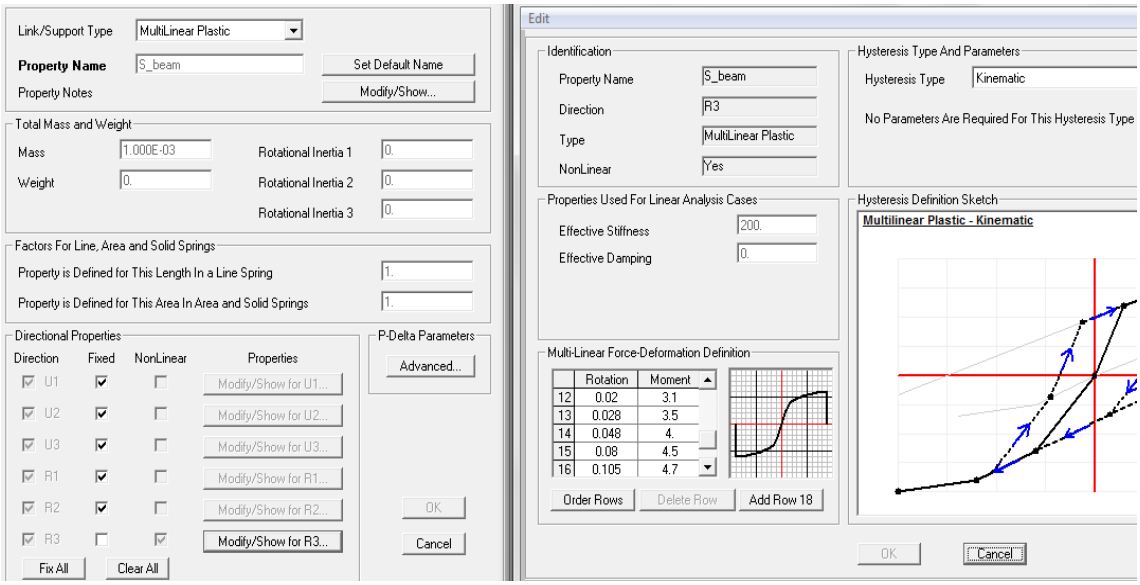

Figure 7.5: Beam end connector simulation

The plastic hinges (of type axial force P) assigned in every upright frame diagonal had the following properties. The values used were derived from the technical reports of the company and were the critical amongst the buckling check of the member and the checks of the bolts (shear resistance and bearing resistance).

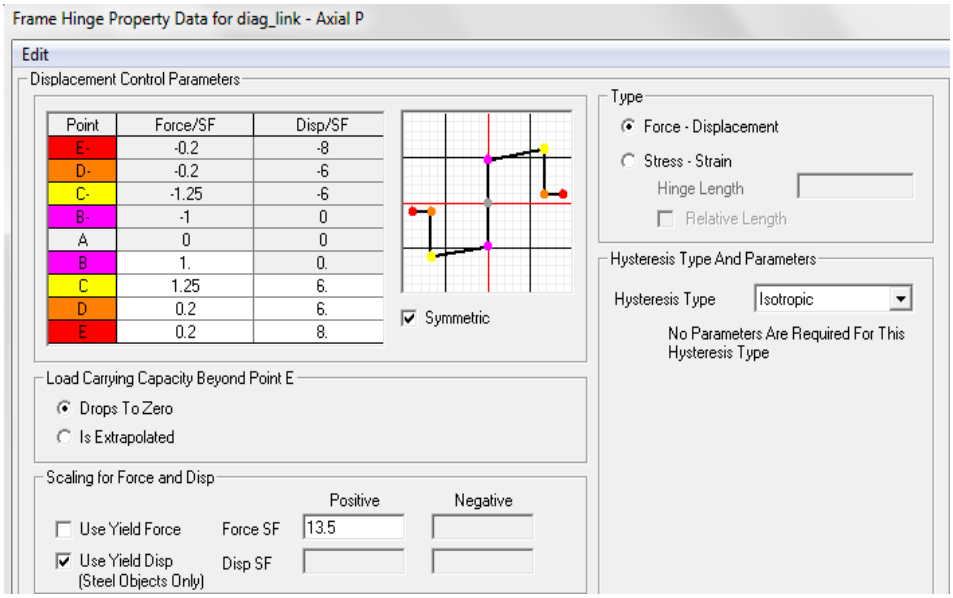

Figure 7.6: Plastic hinge assigned on diagonals

7.2. Medium seismicity model

As can be seen, this is the only case examined without any horizontal bracing.

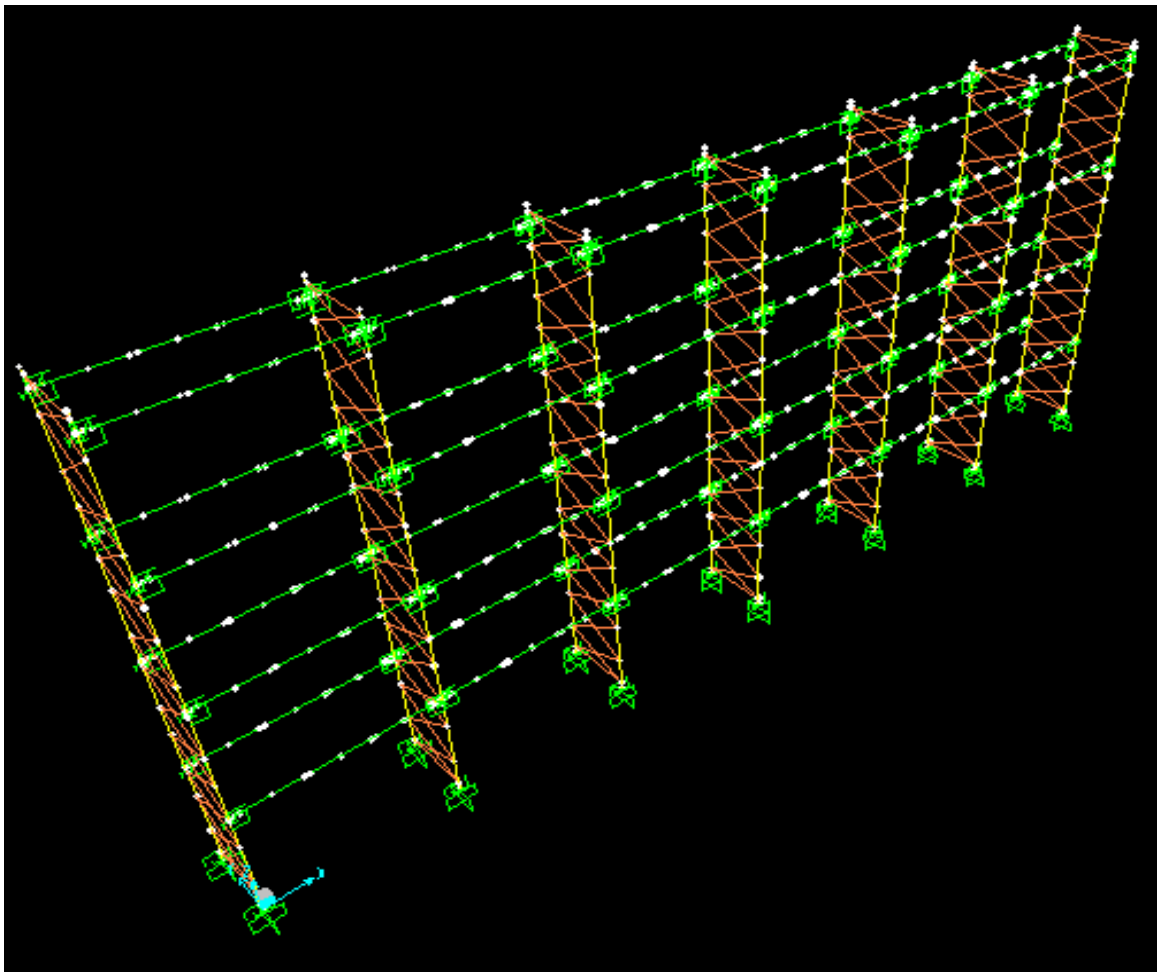

Figure 7.7: 3-D view of model

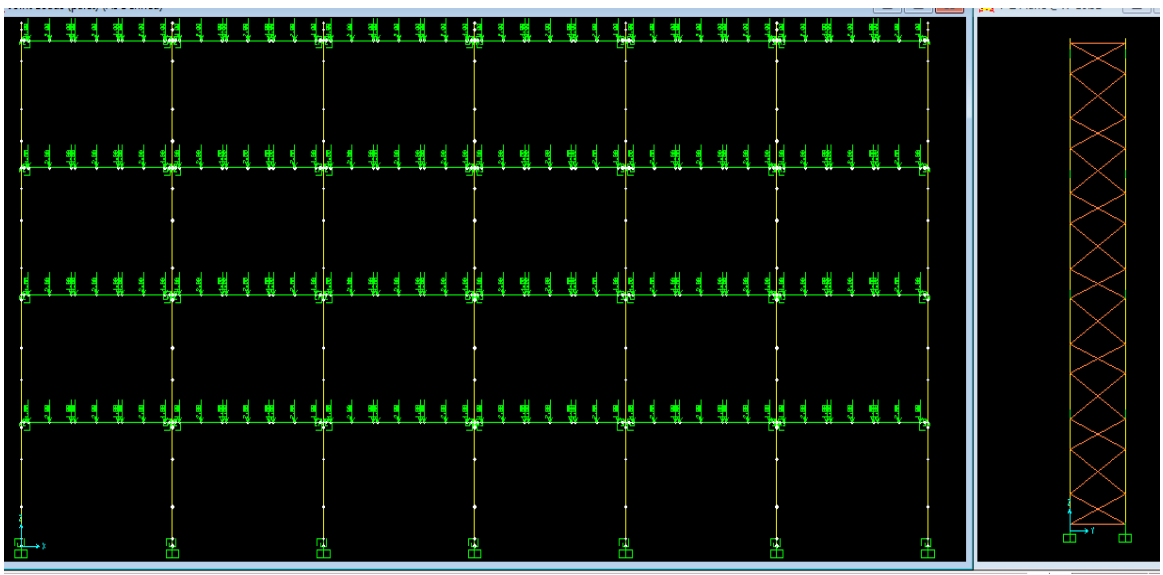

Figure 7.8: XZ (down-aisle) and YZ(cross-aisle) view of model- application of pallet loads

As in the previous case, the main moments for the beams are M3 moments whereas the main moments for the uprights are the M2 moments.
The internal forces under the vertical loading of pallets are shown in the following figure.

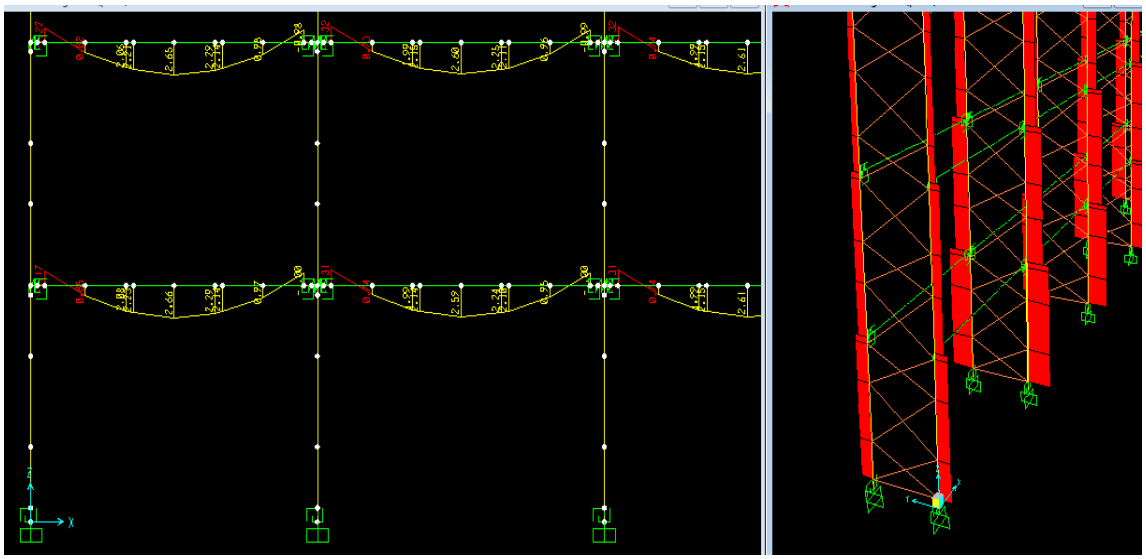

Figure 7.9: Pallet loads_ $M3_{max}$=2.66 kNm, N_{max}= 48.3 kN and N_{min}= 24.3 kN

7.2.1. Modal analysis

The modal analysis resulted in the following. As it can be seen from the pictures below, the first mode (on the left) was translational in X axis whereas the second mode (on the right) is rotational for the upright frames around the Z axis.

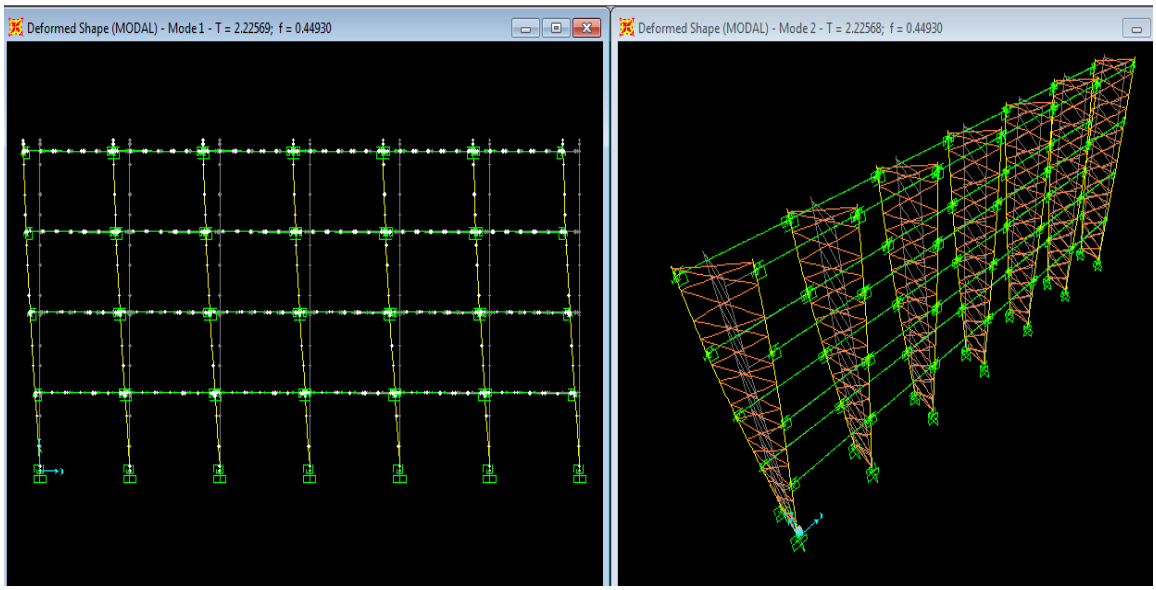

Figure 7.10: Modal analysis - first two modes

In the following table the first twenty modes calculated by the programme are summarized along with their periods and the mass participation ratios.

Table: Modal Participating Mass Ratios

StepNum	Period	SumUX	SumUY	SumUZ
	Sec			
1	2.225691	0.86476	0.00000	5.173E-16
2	2.225676	0.86476	3.733E-14	5.173E-16
3	0.917104	0.86476	0.70624	1.036E-15
4	0.906604	0.86476	0.70626	3.859E-15
5	0.853165	0.86476	0.76686	1.475E-14
6	0.749950	0.86476	0.76686	2.054E-14
7	0.646633	0.96220	0.76686	6.368E-13
8	0.646615	0.96220	0.76686	6.546E-13
9	0.628543	0.96220	0.79009	7.108E-13
10	0.518731	0.96220	0.79009	9.293E-13
11	0.460203	0.96220	0.79009	1.030E-12
12	0.456444	0.96220	0.79009	1.150E-12
13	0.455603	0.96220	0.79009	1.164E-12
14	0.455596	0.96220	0.79009	1.279E-12
15	0.455402	0.96220	0.79009	1.419E-12
16	0.455215	0.96220	0.79009	1.527E-12
17	0.455008	0.96220	0.79009	1.803E-12
18	0.439720	0.96220	0.79911	1.816E-12
19	0.422294	0.96220	0.80032	1.816E-12
20	0.418655	0.96220	0.80063	1.821E-12

Table 7.1: Modal analysis - first twenty modes and mass participation ratios

7.2.2. Pushover analyses

Pushover load cases were applied to the models in both X and Y directions. As mentioned before this pushover analyses were displacement based. Hereby the capacity curves are displayed for each direction. The vertical axis refers to the base shear force (kN) and the horizontal axis refers to the top displacement (m). The performance points are calculated by the programme according to ATC 40 (for the parameters used, chapter 5). The horizontal forces used in the design (as mentioned in the company's technical report) are also shown.

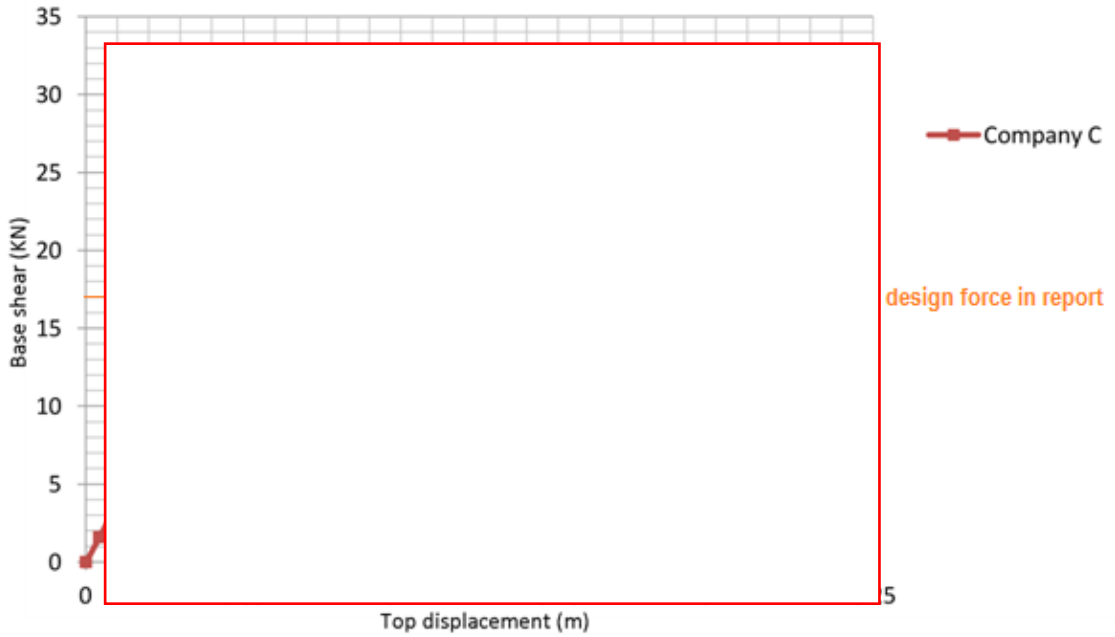

Figure 7.11: Pushover in down-aisle direction, performance curve (and performance point)

Figure 7.12: Pushover in cross-aisle direction, performance curve (and performance point)

Pushover in down-aisle direction

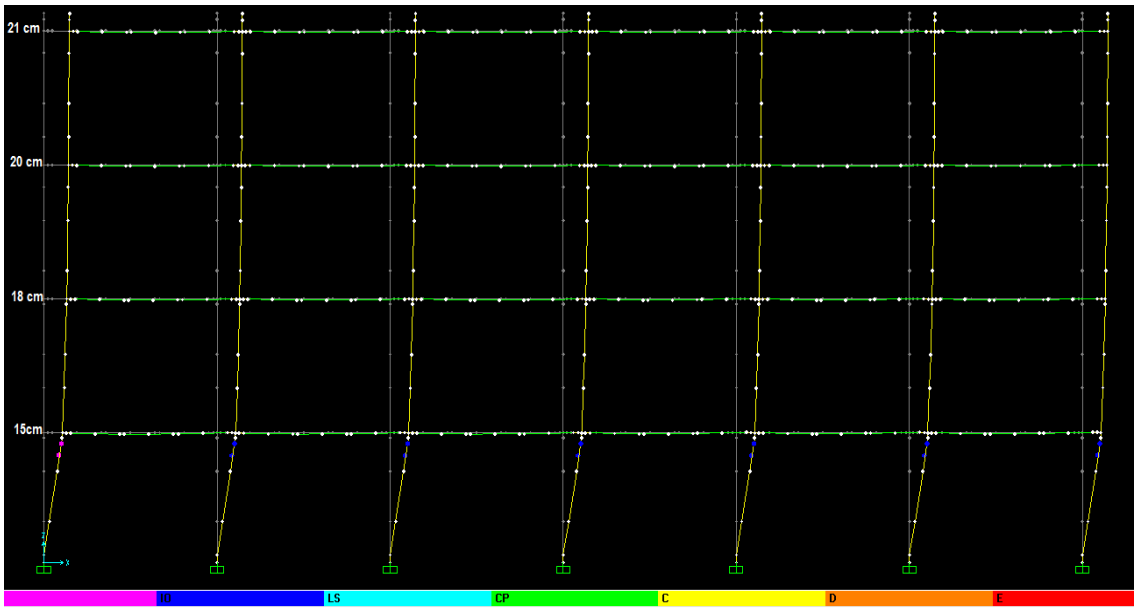

Figure 7.13: Deformed shape in Pushover final step and activated plastic hinges (colour scale). The displacements in each level are noted.

In total all 14 plastic hinges assigned on the uprights were activated during the analysis. The first link that was activated in the most critical upright is displayed in the following figure. Furthermore the links simulating the base plates reached their maximum moments as shown below. On the other hand, no failure occurred in the beam-end-connector links although those on the right side of the beams exhibited larger moments and rotations.

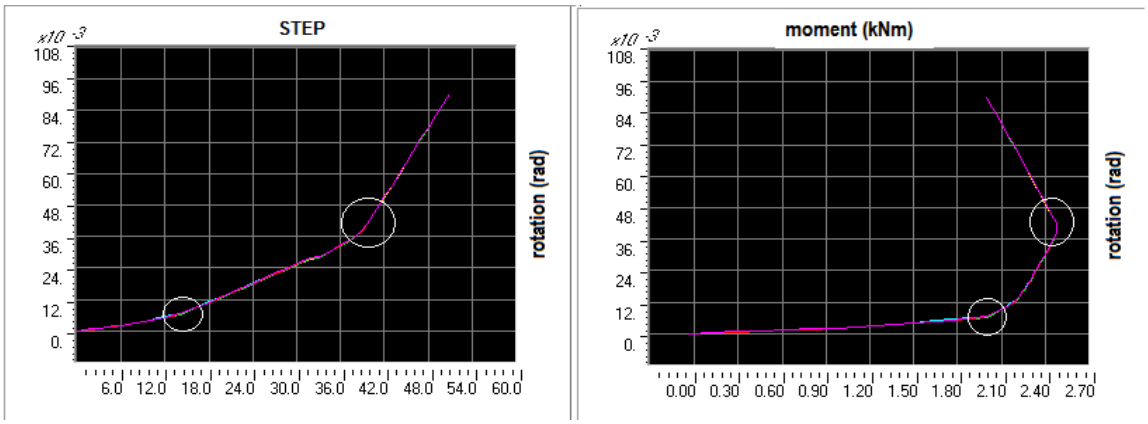

Figure 7.14: Moment-rotation behaviour of base-plate links per step. Failure is noted.

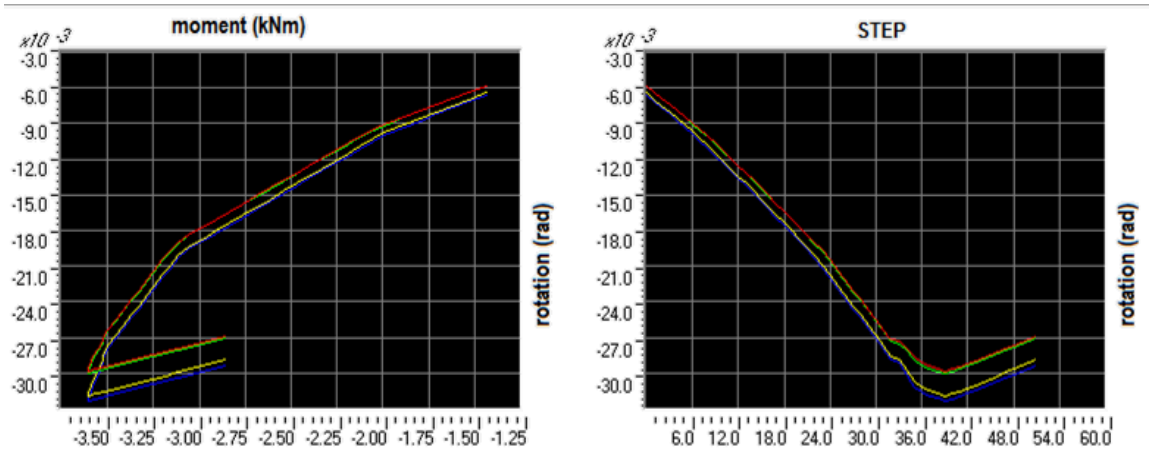

Figure 7.15: Moment-rotation behaviour of beam-end-connector links per step. No failure occurred.

In the following figure the inelastic behaviour of the hinge in the most adverse upright is exhibited, in terms of both axial forces and moments.

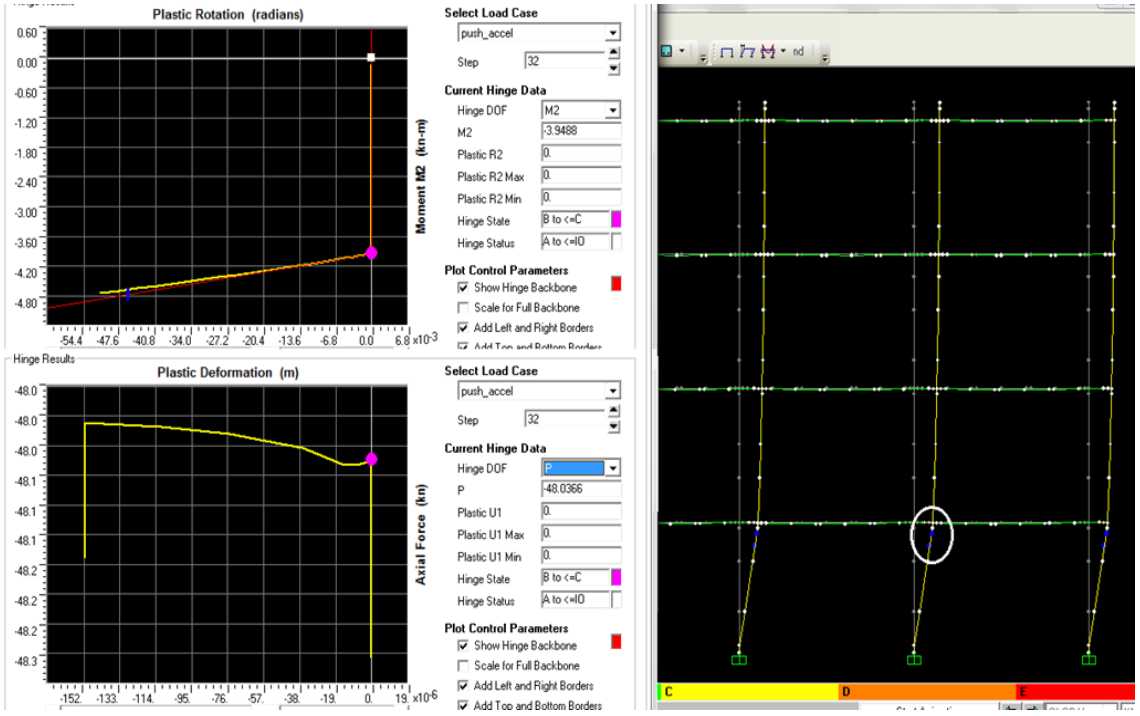

Figure 7.16: Plastic hinge (type P-M), at top of critical upright, activated first during pushover.

Pushover in cross-aisle direction

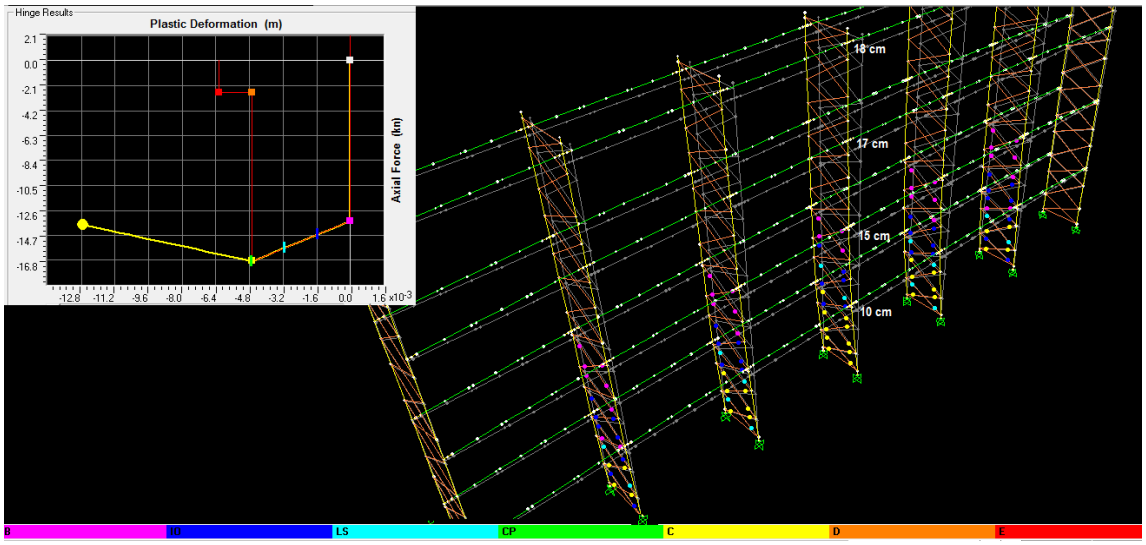

Figure 7.17: Deformed shape in Pushover final step with activated plastic hinges (colour scale). The diagram displays the behaviour of the first hinge activated in the middle upright frame.

In total 110 plastic hinges out of the 406 assigned in the model were activated. None of the links assigned simulating the base plates or the beam-end connectors was reported to fail. In the following figure the internal forces of the most critical upright during the final step of the pushover analysis, are displayed.

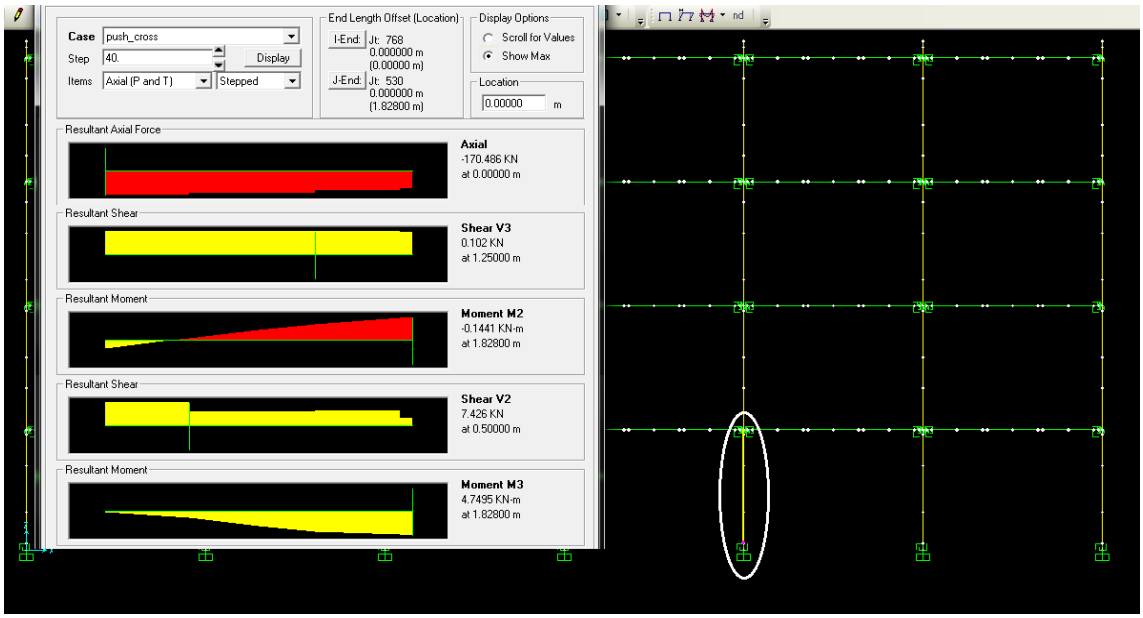

Figure 7.18: Pushover final step_ Internal forces in the most critical column

7.3. High seismicity model

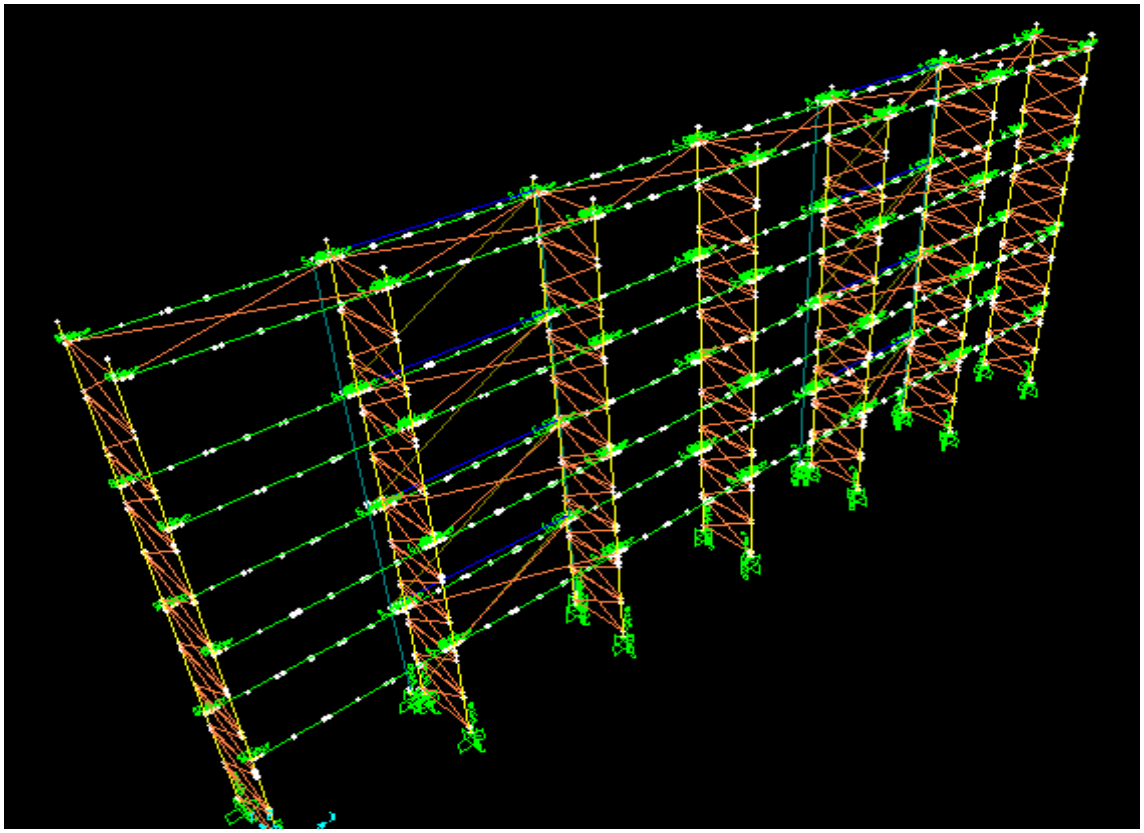

Figure 7.19: 3-D view of model

As shown in the previous picture this model is enforced with a rear frame in the second and the fifth bay, as well as with horizontal bracings in every level. The rear bracing and the upright frames are depicted more clearly in the following figure. Only the bracings of the rear frame that work in tension were taken into account.

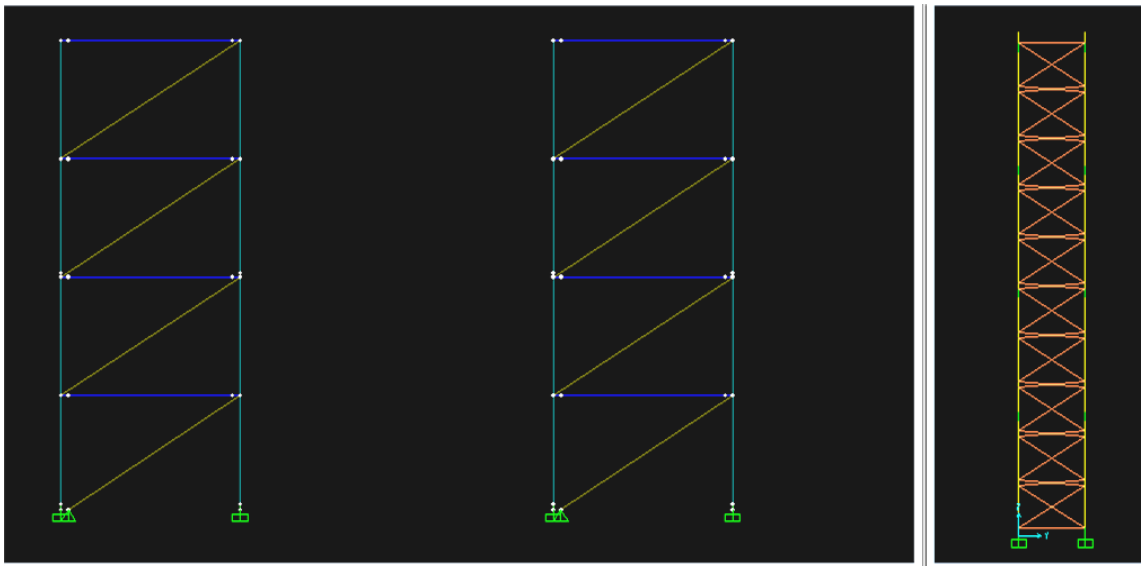

Figure 7.20: XZ elevation of rear frame and YZ (cross-aisle) view

The following figures display the distribution of the internal axial forces after the pallet load application. It can be seen that the extra rear braced frame lightens the situation of the former rear frame.

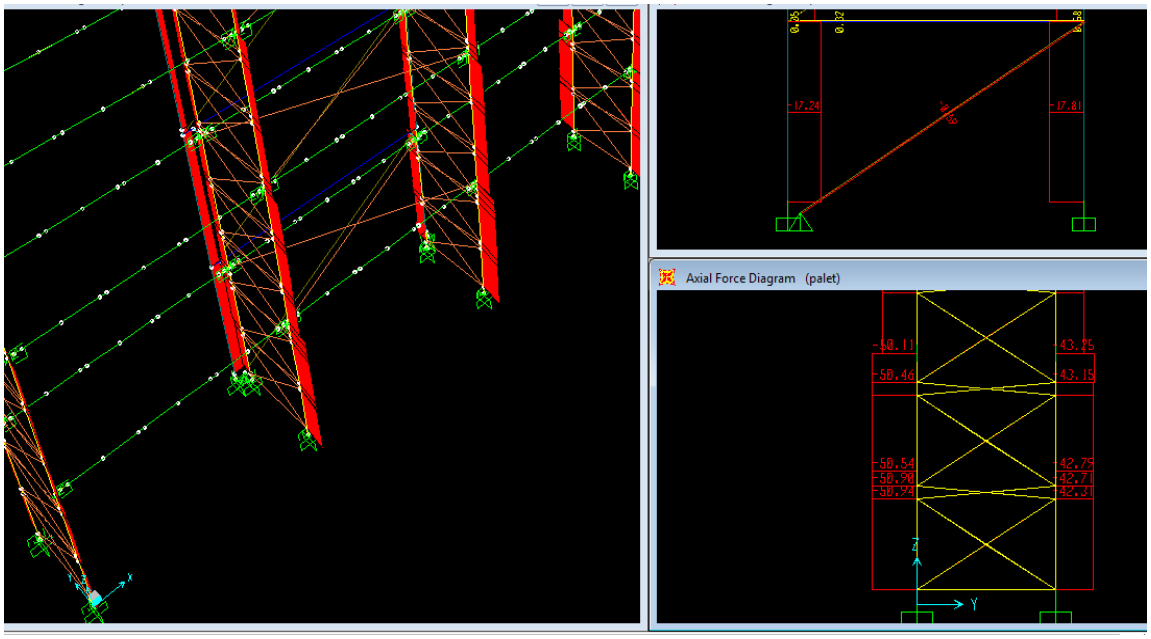

Figure 7.21: Axial forces from pallets and details _ front frame: N_{max} = 50.9 kN and N_{min}=27.3 kN and rear frame: N_{max} =17.9 kN and N_{min}= 17.2 kN

7.3.1. Modal analysis

In contrast with the previous cases, the first mode was translational in Y axis (cross-aisle direction). The second mode is torsional for the structure around Z axis.

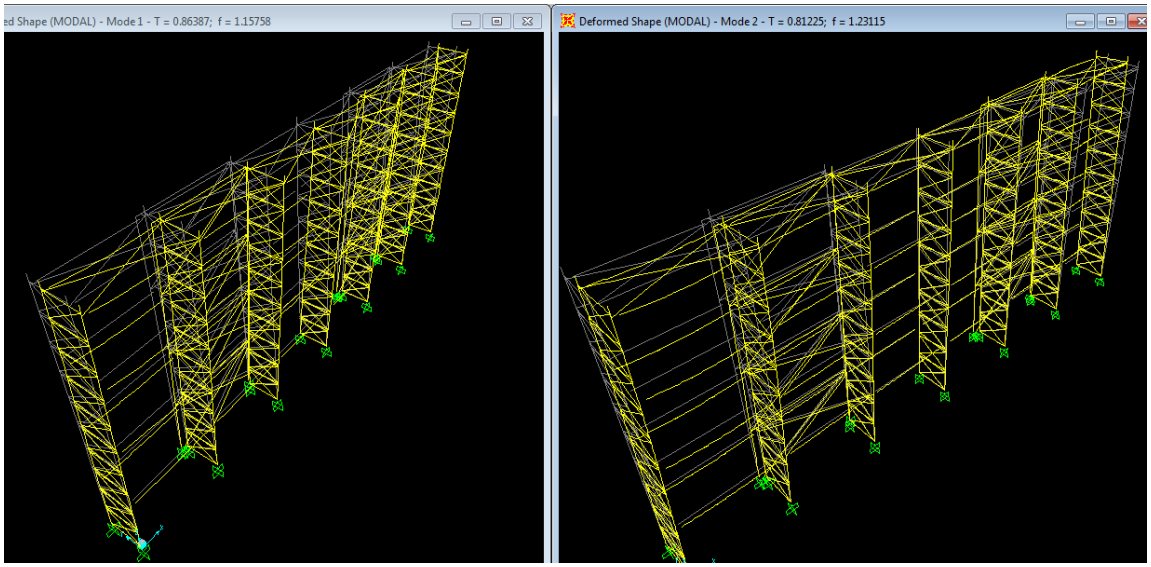

Figure 7.22: First two modes_ mode 1 on the left and mode 2 on the right

Table: Modal Participating Mass Ratios

StepNum	Period	SumUX	SumUY	SumUZ
	Sec			
1	0.863869	0.00198	0.80245	0.00011
2	0.812246	0.05489	0.80446	0.00011
3	0.564147	0.46565	0.80516	0.00013
4	0.523549	0.46566	0.80726	0.00013
5	0.468295	0.54776	0.80739	0.00014
6	0.457768	0.54789	0.80739	0.00014
7	0.455836	0.54790	0.80739	0.00014
8	0.455281	0.54790	0.80739	0.00014
9	0.443323	0.54846	0.80739	0.00014
10	0.430120	0.80246	0.80776	0.00019
11	0.423547	0.80278	0.81529	0.00019
12	0.418435	0.80278	0.81548	0.00019
13	0.416733	0.80278	0.81566	0.00019
14	0.379173	0.81737	0.81567	0.00019
15	0.345956	0.81779	0.81567	0.00019
16	0.341193	0.81779	0.81567	0.00019
17	0.330972	0.81793	0.85214	0.00026
18	0.322529	0.81913	0.85214	0.00026
19	0.319891	0.81954	0.85218	0.00027
20	0.314064	0.83043	0.85218	0.00027
21	0.303225	0.83074	0.85358	0.00027
22	0.303031	0.83265	0.86912	0.00031
23	0.296695	0.83270	0.86913	0.00031
24	0.296581	0.83273	0.86979	0.00031
25	0.294402	0.83301	0.91530	0.00039

Table 7.2: Modal analysis - first twenty-five modes and mass participation ratios

7.3.2. Pushover analyses

Hereby the capacity curves are displayed for each direction. The vertical axis refers to the base shear force (kN) and the horizontal axis refers to the top displacement (m). The performance point according to ATC40 as well as the design forces mentioned in the company's technical report, are also shown.

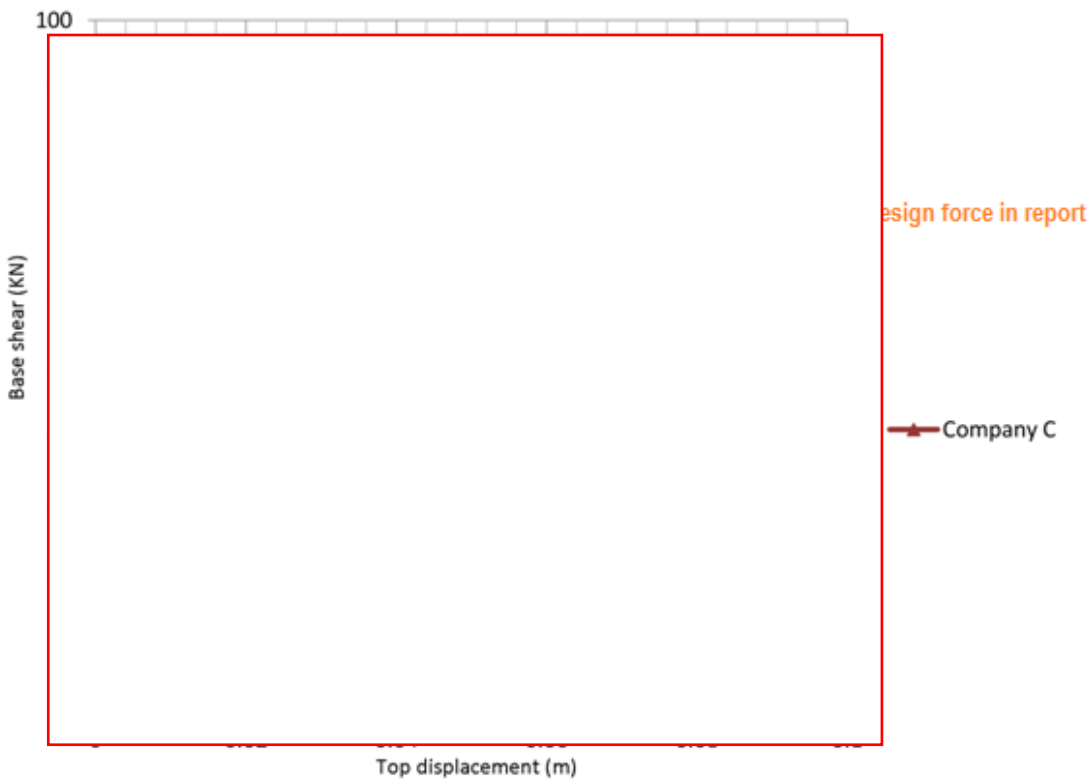

Figure 7.23: Pushover in down-aisle direction, capacity curve and performance point

Figure 7.24: Pushover in cross-aisle direction, capacity curve and performance point

Pushover in down-aisle direction

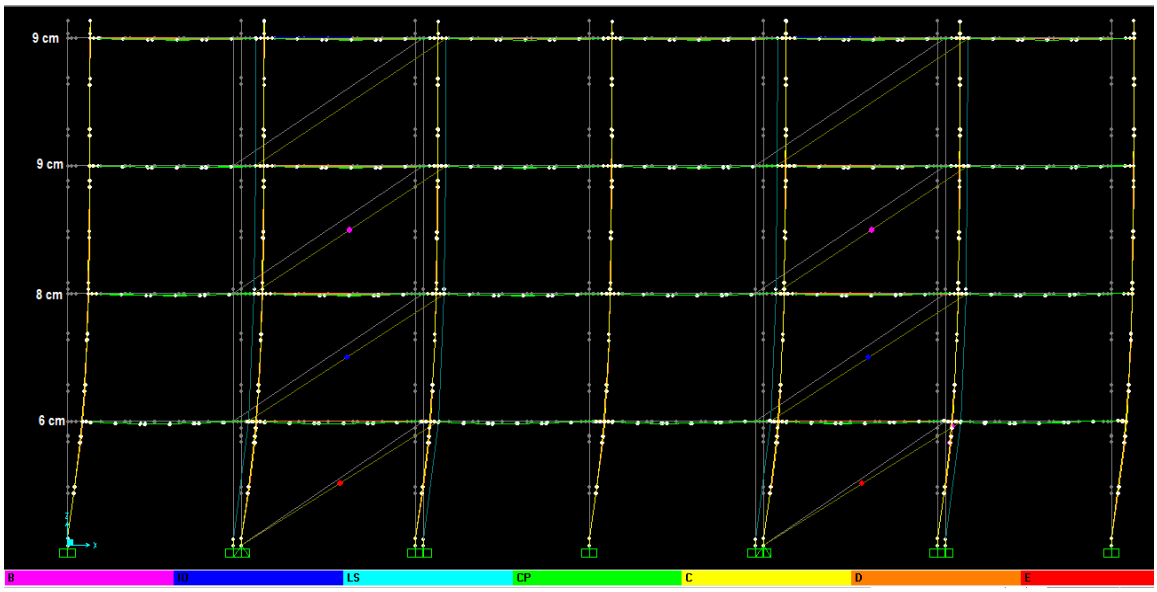

Figure 7.25: Deformed shape in Pushover final step and displacements at each level. The colours signify the activation of hinges.

It can be observed that in this case the top displacement at the end of the analysis was rather small, although it was supposed to be around 20 cm. In total 7 plastic hinges out of the 26 hinges assigned were activated, all belonging to the rear supporting frame except for one. In addition to this the links simulating the base plates almost reached their failure point in the step where the analysis was terminated. The internal forces, during the last step of the analysis, of the only upright in the main racking structure that exhibited a plastic hinge formation, as well as the inelastic behaviour of this hinge are also displayed below.

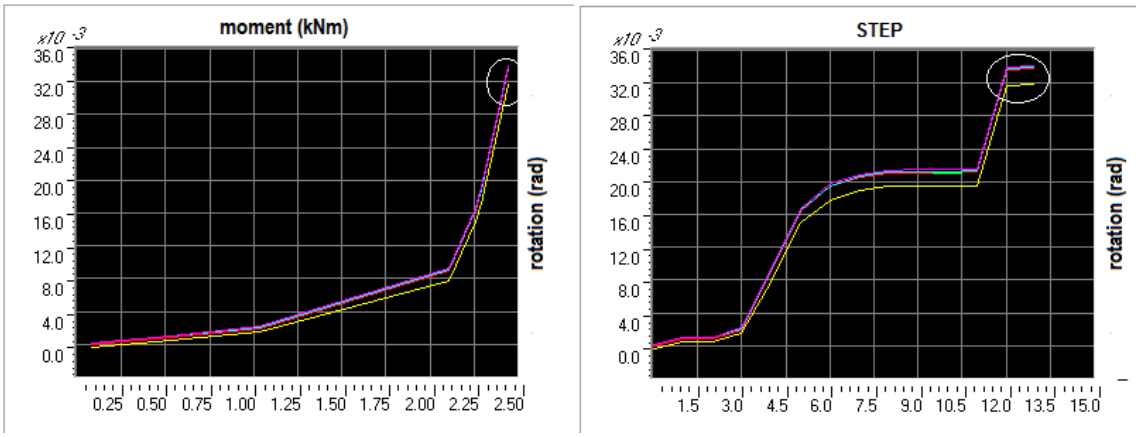

Figure 7.26: Moment-rotation behaviour of base-plate links per step. Failure is noted.

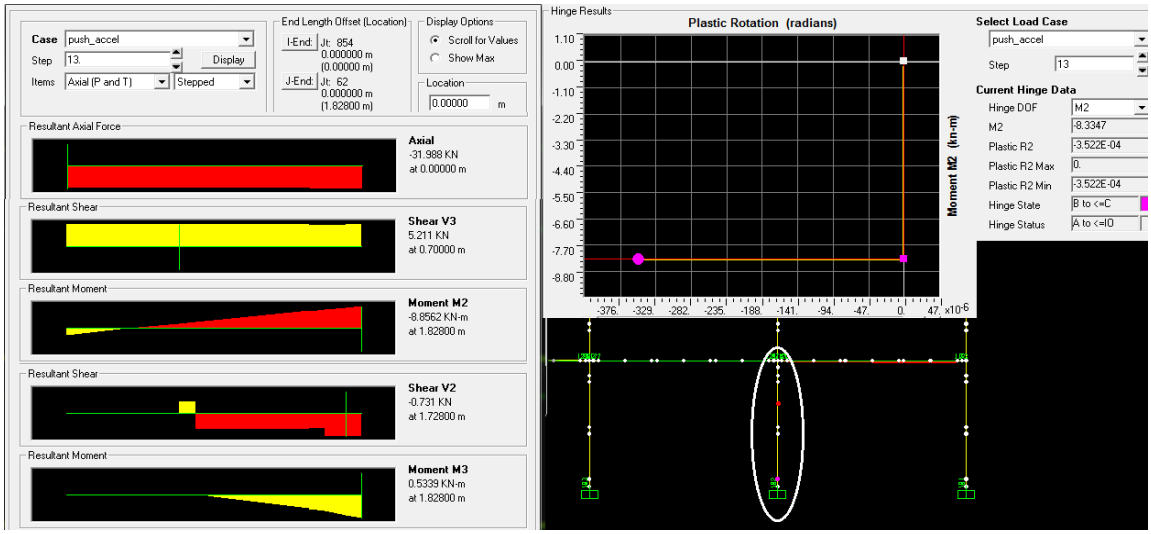

Figure 7.27: Pushover final step_ Internal forces and plastic rotations of column hinge

As far as the links simulating the beam-end-connectors is concerned, no failure was reported during the analysis. However in the following figure the step-by-step moment-rotation behaviour of the least favourable links is displayed.

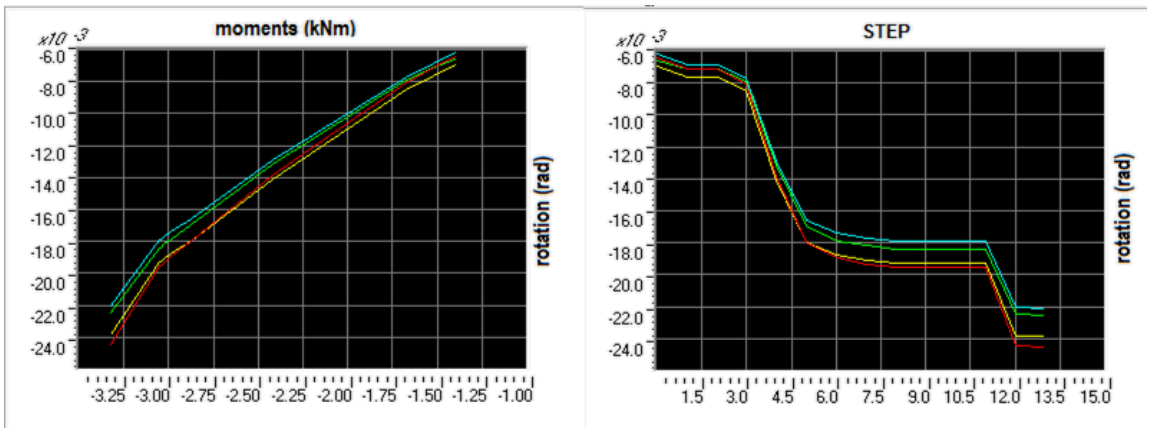

Figure 7.28: Moment/rotation behaviour of beam-end-connector links per step. No failure occurred.

Pushover in cross-aisle direction

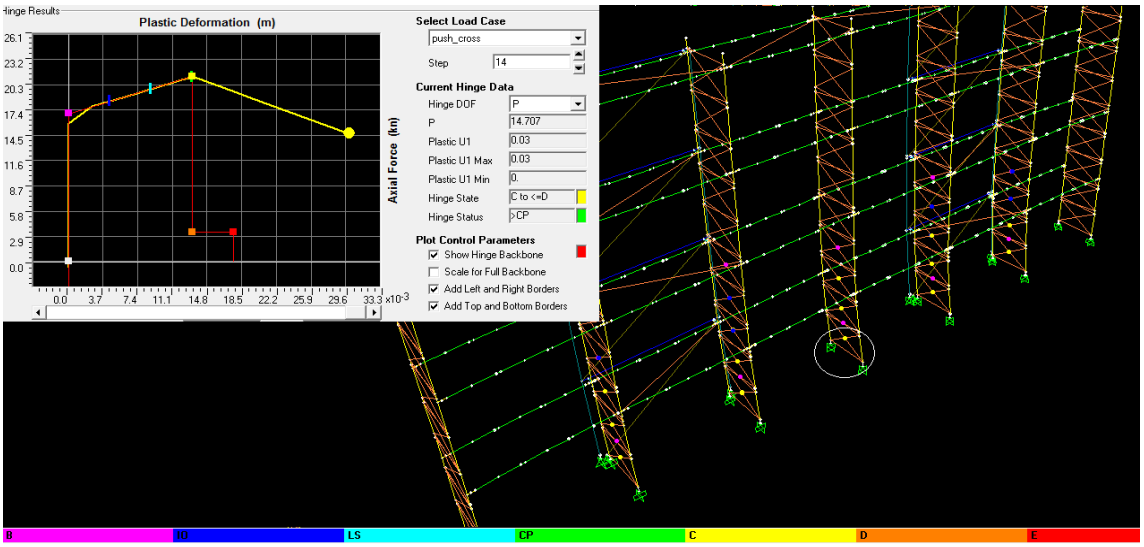

Figure 7.29: Deformed shape in Pushover final step with activated plastic hinges (colour scale). The diagram displays the behaviour of the first hinge activated in the middle upright frame.

In total 255 plastic hinges out of the 306 assigned in the model were activated. All of which belonged to the upright frame diagonals. The frame in the middle of the structure was the most unfavourable one. In the following figures, the internal forces of the most critical uprights are displayed: one in the rear frame and one in the main racking structure (which was reported to be the most unfavourable). As far as the rest of the links are concerned (base plates and beam-end connections) no failure occurred.

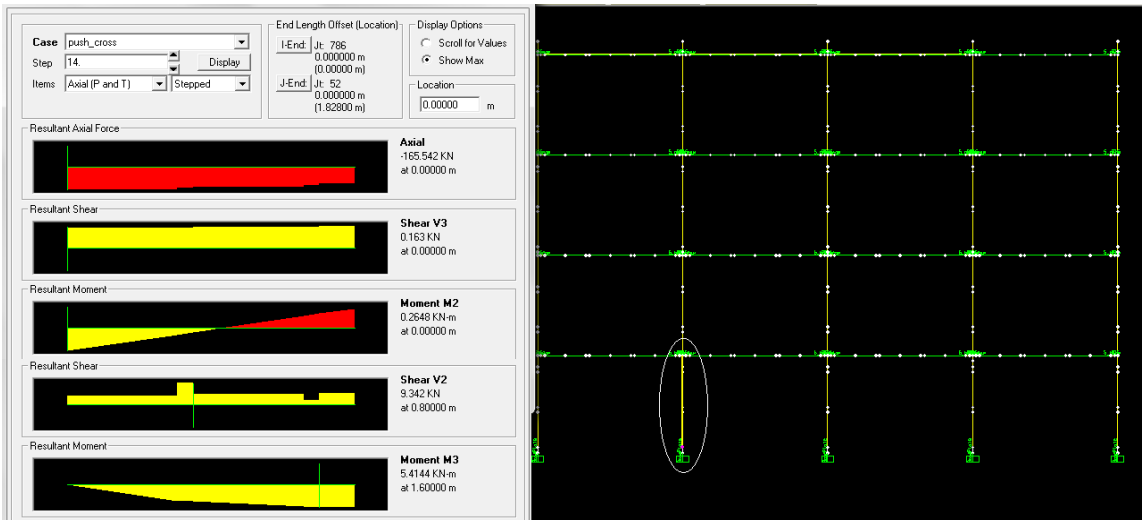

Figure 7.30: Pushover final step_ Internal forces of most critical upright

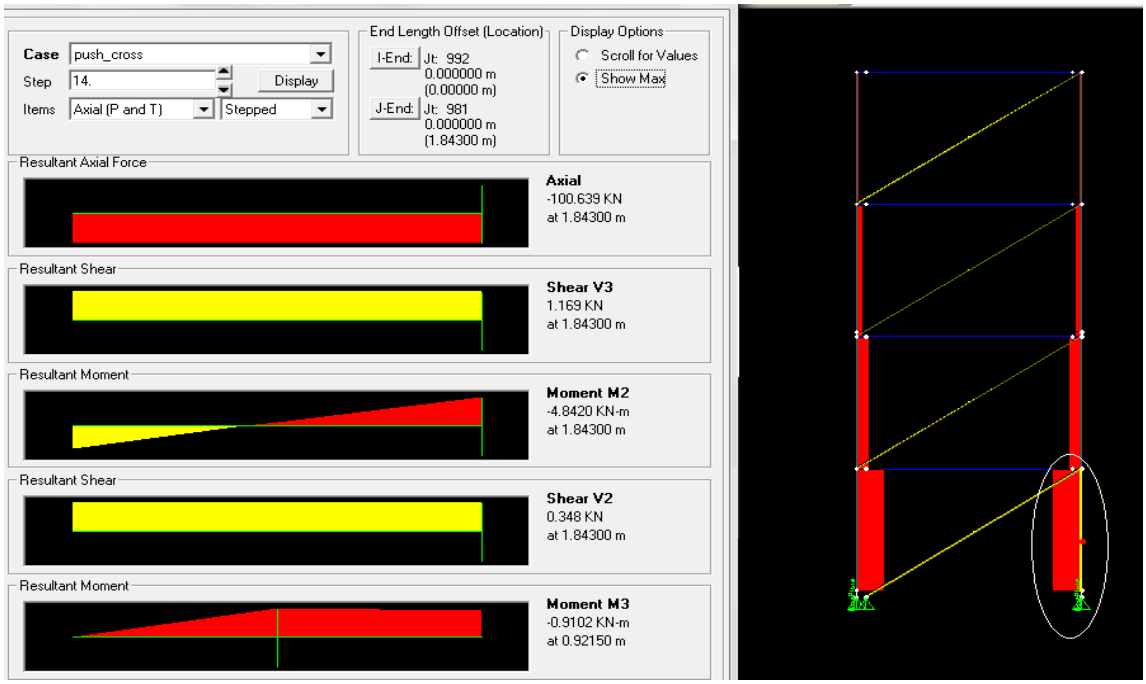

Figure 7.31: Pushover final step_ Internal forces of most critical upright in the rear frame

Chapter 8 conclusions

8.1. Summarizing the results

In this final chapter, the pushover curves of all the cases examined are superimposed in order to enable their comparison and the formation of general comments and conclusions. For each direction examined, the results are presented in groups. Comments are made concerning the response of each structure based on its stiffness, its configuration, its weight, its ductility, its performance point etc. As far as the factors calculated are concerned, most of them refer to a bilinear simulation of the capacity curve. Thus, the ductility, the overstrength and the q factor were estimated.
Apart from this, some other factors with similar meaning where calculated, in reference to the performance point mostly indicating its distance from yield. As a reminder, the P.P. is calculated by Sap2000 according to ATC40.
Furthermore, an alternative calculation of the q behaviour factor was attempted, based on the step of each pushover analysis that the Life Safety acceptance criterion is reached.

The inter-storey drifts for each case are presented and commented as well.
The results of the buckling analysis are also briefly presented in the beginning of this chapter in order to highlight the sensitivity of the nonlinear analyses, depending on the buckling factors and the geometric nonlinearities. Along with that, a brief reference is made to the alternatives concerning the lateral load application during the pushover analysis as encountered in Sap2000.

It should be reminded that despite of the general characterization of the structures as medium and high seismicity, their design parameters concerning the earthquake are not the same. Therefore the design accelerations (a) and the importance factor (γ) for each case are mentioned again, although these differences are presented in detail in Chapter 4.

In the following figures all the pushover curves for the down-aisle and the cross-aisle direction are superimposed. The performance points calculated are also displayed.
At first glance, it is obvious that the response of the structures in cross-aisle direction was more uniform than in down-aisle direction. Furthermore, it can be observed that in most cases in cross-aisle direction the structures appear to be stiffer and stronger since they undertake larger horizontal forces. This is in accordance with the experimental data from the previous Seisracks poject as also mentioned in unit 2.2.c.
On the other hand, as it was presented in the previous units, the behaviour of the racks in down-aisle direction is more dissipative since many plastic hinges were activated and many multi-linear links exhibited inelastic deformations and reached their failure point during the pushover analyses. The same did not apply for the pushover in cross-aisle direction when only the plastic hinges assigned on the diagonal members were activated due to their buckling, while most other components remained in the elastic range.

Figure 8.1: Pushover curves and performance points in down-aisle (DA) direction

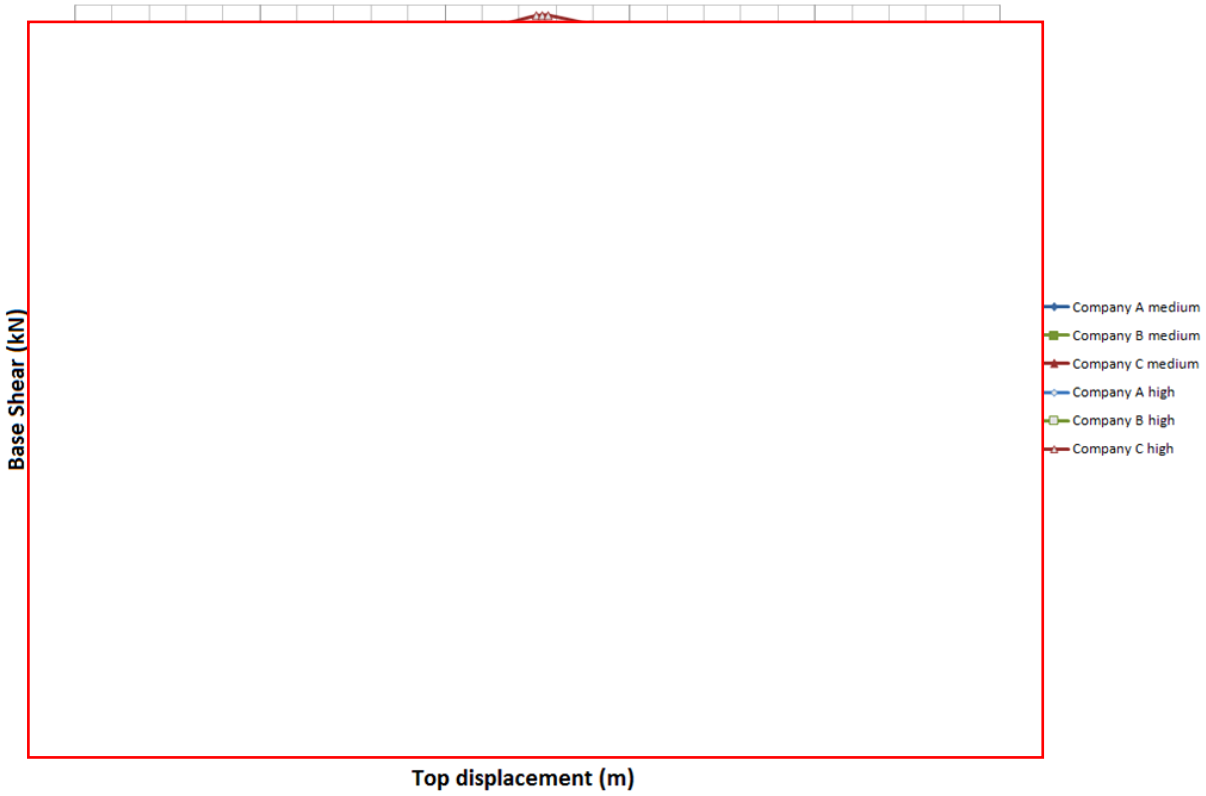

Figure 8.2: Pushover curves and performance points in cross-aisle (CA) direction

As far as the companies are concerned, it seems that Company C is the stiffest although its design parameters should also be taken into account as indicated in the following units.

8.2. Linear buckling analysis and sensitivity of structures due to p-delta effects

Steel members in compression often have stability problems especially as structures tend to get lighter for financial reasons. Their behaviour can be described with the factor $\rho=l*\sqrt{(N_{Ed}/E*I)}$ which indicates how second-order effects are increased either due to an increment of force or due to a reduction of stiffness.

These stability problems can be identified when defining the internal forces and moments of the structures' elements. This can be solved either with first-order analysis (using the initial geometry of the structure) followed by buckling checks or by using second-order analysis (taking into account the influence of the deformation of the structure).

In general, the results of second-order analysis as far as forces and deformations are concerned, are larger than those of first-order analysis. The effects of the deformed geometry shall be considered, only in case they increase the action effects significantly or modify significantly the structural behaviour. In practice, the second-order effects are usually neglected when they do not exceed the results of first-order analysis by more than 10%.

According to Eurocode 3 (En1993-1-1), first order analysis may be used for the structure when the increase of the relevant internal forces or moments or any other change of structural behaviour caused by deformations can be neglected. This condition may be assumed to be fulfilled, if the following criterion is satisfied:

$\alpha_{cr} = F_{cr} / F_{Ed} > 10$ for elastic analysis

$\alpha_{cr} = F_{cr} / F_{Ed} > 15$ for plastic analysis,

where

α_{cr} is the factor by which the design loading would have to be increased to cause elastic instability in a global mode

F_{Ed} is the design loading on the structure

F_{cr} is the elastic critical buckling load for global instability mode based on initial elastic stiffnesses.

It can be noticed that a greater limit is defined for plastic analysis. This happens because in plastic analysis structural behaviour may be significantly influenced by non linear material properties in the ultimate limit state (formation of hinges, non linear deformations from semi-rigid connections etc).

In case the above criterion is not fulfilled the influence of the deformation of the structure has to be taken into account and the structural stability must be verified considering imperfections and second-order effects.

Second order effects may be calculated by using an analysis appropriate for the structure (including step-by-step or other iterative procedures). However, in case the first sway buckling mode is predominant (and some other criteria concerning the configuration are met), first-order elastic analysis can be carried out with amplification of the relevant action effects (e.g. bending moments) by the factor: $1/[1-(1/\alpha_{cr})]$, provided that $\alpha_{cr} > 3.00$.

The aforementioned α_{cr} factor can be calculated in Sap2000 using the linear buckling analysis option. Linear buckling analysis in Sap2000 seeks the buckling modes of a structure when it withstands a user specified set of loads (in this case, dead and pallet loads). Each eigenvalue is

called buckling factor and it represents the scale factor that must be multiplied with the loads assigned in order to cause buckling, just like a safety factor. The buckling modes are different from the natural vibration modes.

In this thesis, the α_{cr} factors were calculated for each of the six different models examined. The results are displayed in the following table.

	Company A		**Company B**		**Company C**	
	medium	high	medium-low	high	medium	high
α_{cr}	3.9	13	2.4	2.9	4.1	22

Table 8.1: α_{cr} factors calculated during linear buckling analysis

The magnitude of the α_{cr} factor determines whether the pushover analysis as well as the application of vertical loads in the models in Sap2000 should be done by taking into account the p-delta geometric nonlinearity or none (first order analysis). Although in all simulation cases the p-delta option was chosen for the presentation of the final results, the same analyses were also run without geometric nonlinearity in order to examine the sensitivity of the results in each case. As indicated in the following figures, the differences between the pushover curves produced were particularly big whenever the α_{cr} factor was small. On the other hand, in the cases where the α_{cr} factor was relatively large, the differences between the analyses with the different geometric nonlinearities were not very significant.

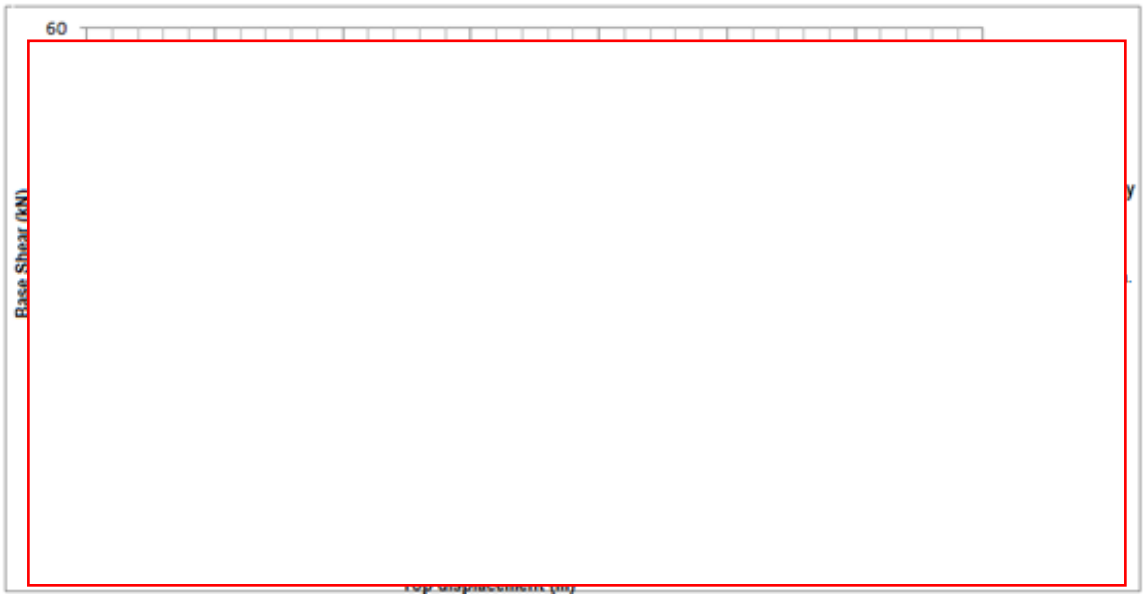

Figure 8.3: Pushover curves and performance points, with and without geometric nonlinearities when α_{cr} factor is small.

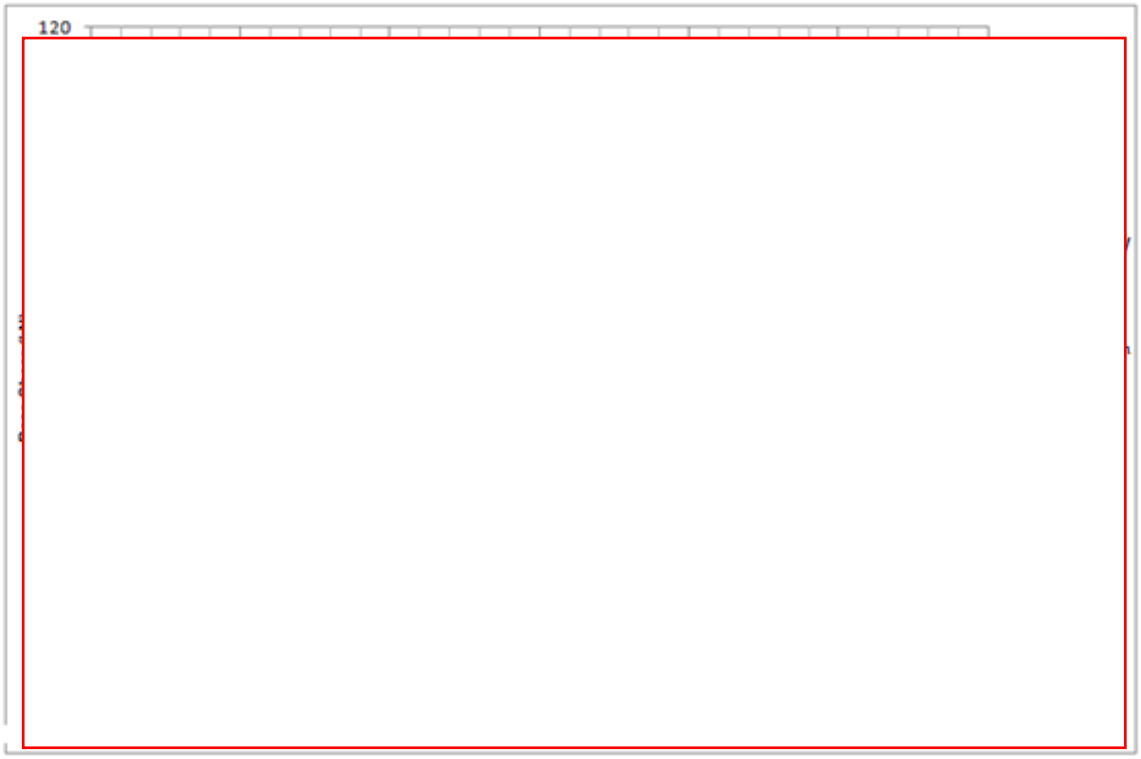

Figure 8.4: Pushover curves and performance points, with and without geometric nonlinearities when α_{cr} factor is large.

8.3. Different types of Pushover Load Case shape in Sap2000

As mentioned in unit 3, there are many ways to apply a pushover load in Sap 2000. For the purposes of this dissertation the following two were used:

_ application of a uniform pattern of accelerations on every joint, acting in a predefined direction (acceleration option)

_ horizontal load distribution among the different levels according to the first eigenvector (modal option)

The modal option usually resembles an inverted triangular force distribution, which is what will be probably used in the experiments. In general, the inverted triangle distribution and the uniform one are the two load patterns considered likely to result in the lower and upper bound of pushover curves, respectively. The first one tends to underestimate the capacity of a structure (not economic) whereas the latter overestimates it.

However in the cases of high seismicity models which are enforced with rear braced frames, it is very difficult to obtain a modal shape that resembles an inverted triangle, without torsional deformation of the racking system. This happens because these rear frames are very stiff and move the structure's centre of elastic rotation away from its centre of mass, thus causing the rack to rotate. Therefore the modal option for the pushover load cannot provide reliable results for all cases.

On the other hand, the application of a uniform load is more adverse than the inverted triangle, having the resultant force on a lower level (larger lever arm from top) and causing larger forces. However it is easier to control and it can be applied in all racking configurations in the same way. Thus in order to achieve uniformity in the results and enable comparison, this option was used for every case presented in this thesis.

As an example of the differences in the pushover curves obtained by a modal pushover analysis and a uniform acceleration one, the following figures are exhibited. Two medium seismicity models are presented, as more suitable. It is obvious that the forces are increased in the case of application of uniform load.

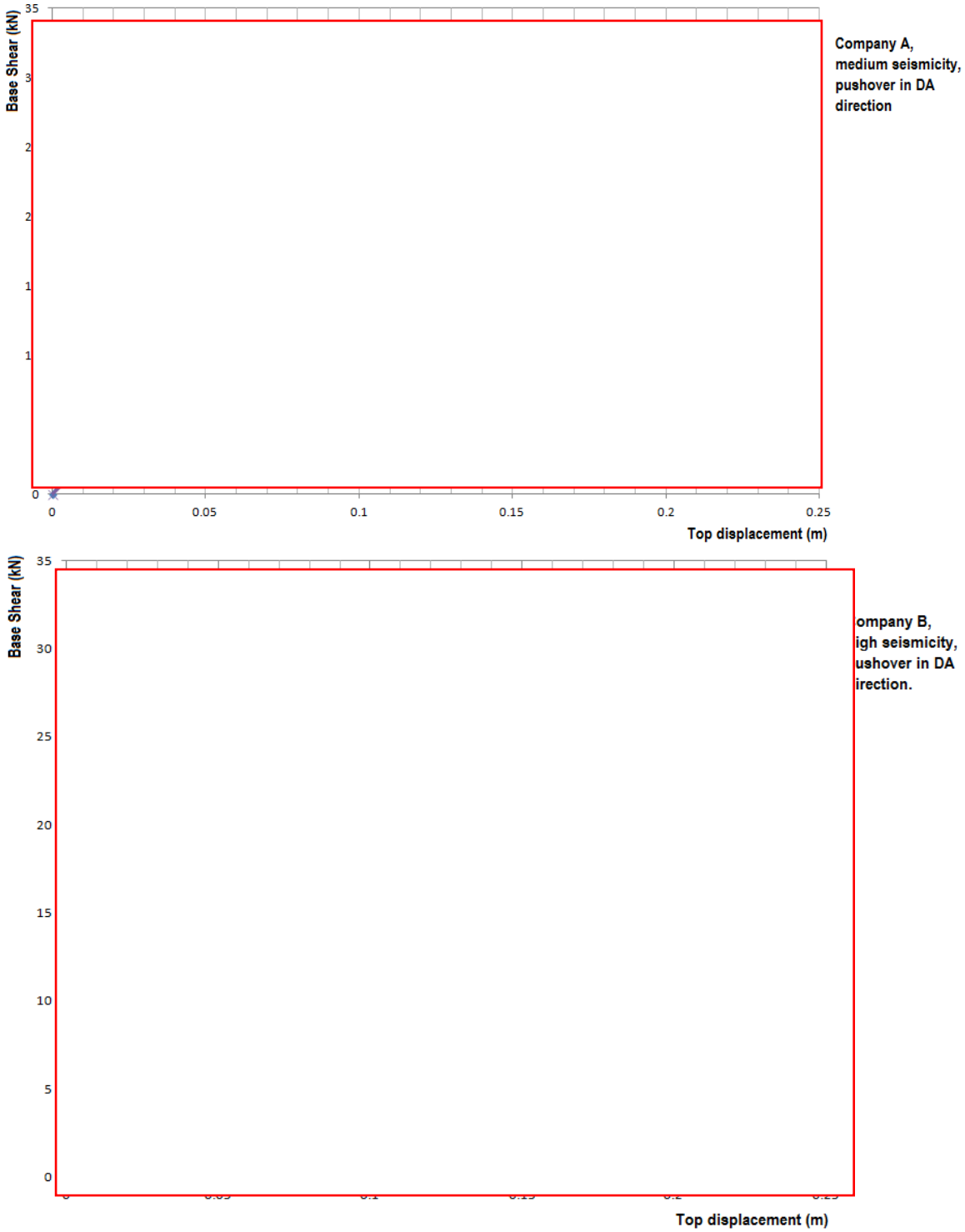

Figure 8.5: Pushover curves for uniform acceleration load application and modal shape load distribution

8.4 Interstorey drifts in performance point

As it was mentioned before, for each case the performance point was calculated by the software according to ATC40. The pushover step in which the performance point was reached was afterwards located and the deformed shape on this specific step was examined. The drifts during these specified steps were calculated for every analysis, using the following formula for each level: $\mathbf{(d_i-d_{i-1})/ H_i}$, where i = 4,3,2,1 , d is the horizontal displacement of the level in X or Y direction (depending on whether the pushover analysis is in down-aisle or cross-aisle direction accordingly), and H_i is the height of each floor. The results are presented graphically in the following figures.

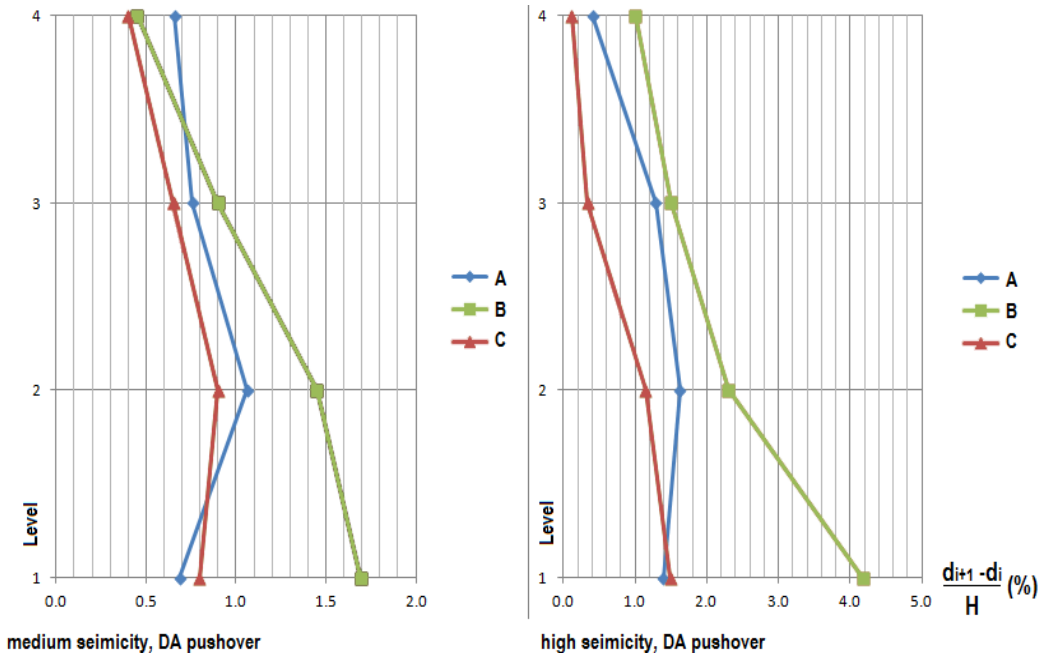

Figure 8.6: drifts for medium and high seismicity models in Down-aisle direction

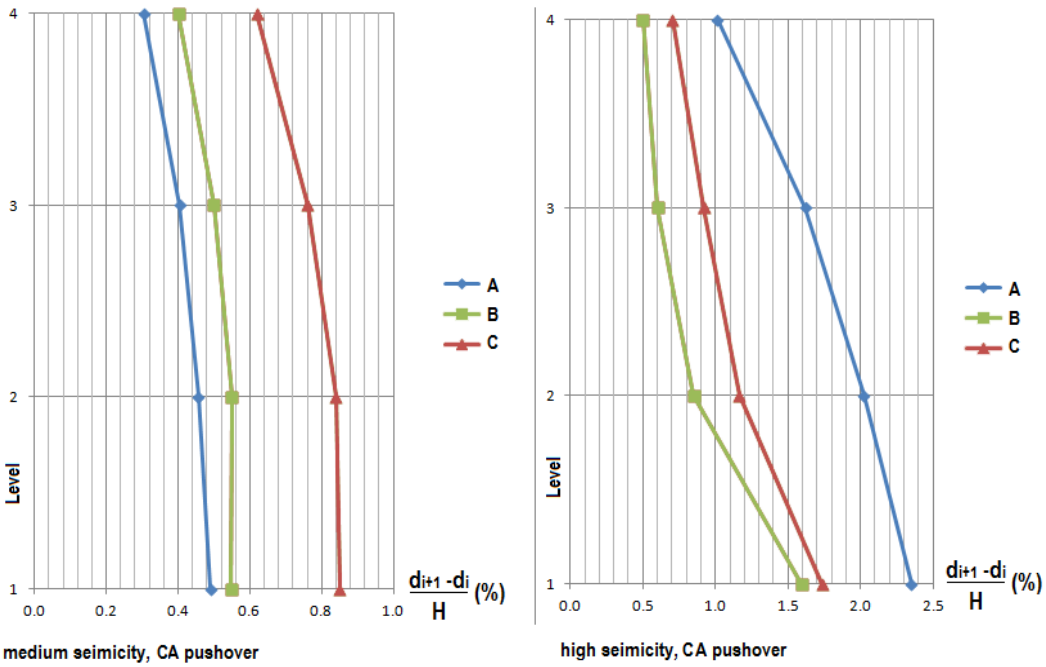

Figure 8.7: drifts for medium and high seismicity models in Cross-aisle direction

It can be noticed that in almost every case (with some exceptions regarding company A) the drifts of the first (lowest) level are the largest, indicating a possible "soft floor" mechanism (e.g. company B, high seismicity model, DA direction). Furthermore the drifts are increased in the high seismicity models.

8.5. Racks designed for medium or low seismicity

Figure 8.8: Pushover curves and performance points in down-aisle (DA) direction, racks in medium or low seismicity zone

Figure 8.9: Pushover curves and performance points in cross-aisle (CA) direction, racks in medium or low seismicity zone

Design parameters	Company A	Company B	Company C
a(g)*γ	0.12*0.84= 0.101 (g)	0.135*0.84= 0.113 (g)	0.2*0.84= 0.168 (g)

Table 8.2: Seismic design parameters (racks in medium or low seismicity zone)

Taking into account the design parameters in Table 8.1, the fact that Company C appears to be the stiffest one, is better understood. Apart from that, Company C appears was found to have the largest dead loads (17.2kN) whereas Company B had the lightest configuration (11.5kN). The magnitude of the dead loads is of course negligible in relation to the pallet loads but given the fact that the dimensions of the racks are similar, it provides a general idea about the configurations.

In addition to this it should be taken into account that Company B is the only one that did not use symmetric diagonals in the upright frames. This could have played a role in the fact that in pushover in cross-aisle direction it exhibited the lowest δ_y (yield) and δ_u (failure) top displacements.

8.5.1. Calculation of overstrength, ductility and q capacity factor

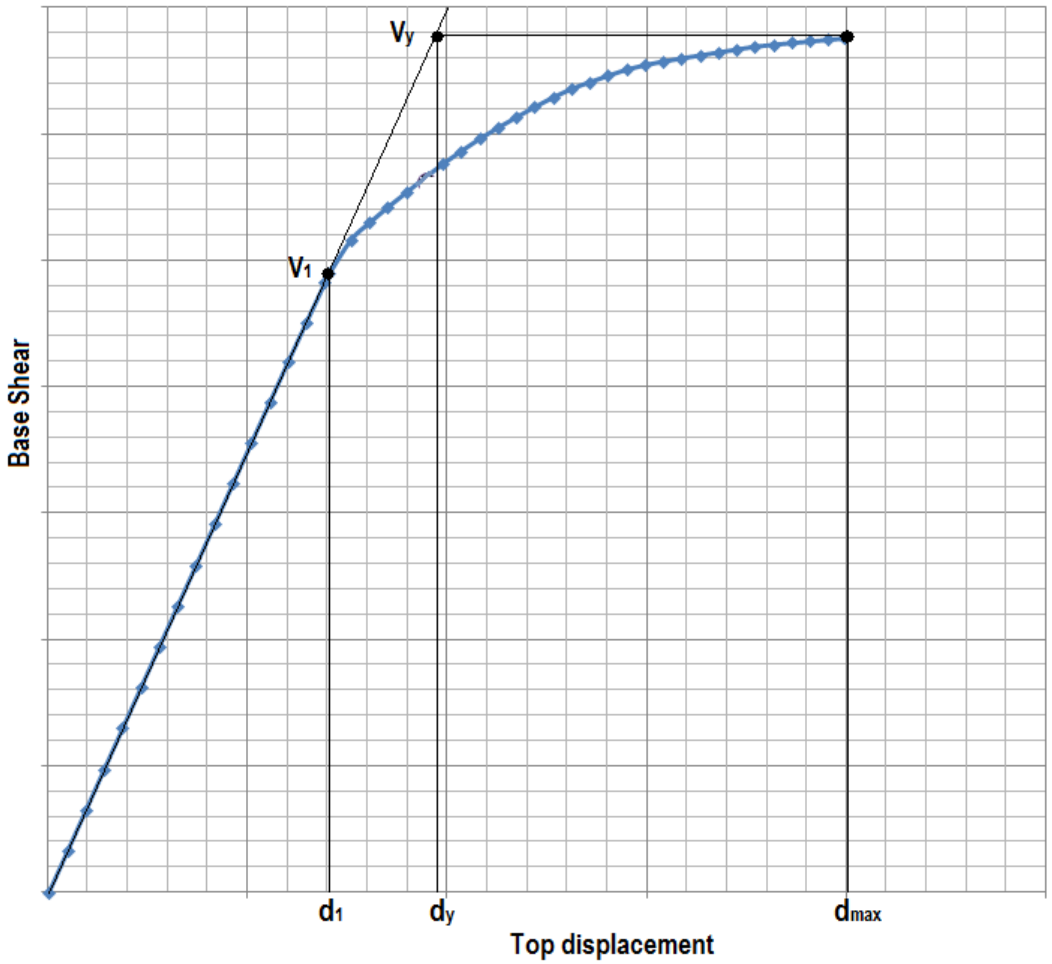

Figure 8.10: Bilinear approach of pushover capacity curve

As it can be seen from the above figure, every capacity curve was approached as bilinear for the specific calculations. The bilinear curve has an inclined part with the slope of the initial stiffness and a horizontal part. In each bilinear capacity curve, three points are noted as significant: the (d_1,V_1) point which represents the first significant yield and the apparent reduce of the structure's stiffness, the (d_y,V_y) point which is the intersection between the declined and the horizontal lines and represents yielding as well as the commencement of inelastic displacements and the (d_{max},V_y) point which represents the ultimate step (failure).
Three factors can be derived by the definition of the aforementioned points: the overstrength $\Omega=V_y/V_1$, the ductility $\mu= d_{max}/d_y$ and by combining these two the q capacity factor $q_{cap} = \Omega * \mu$.

Overstrength calculations

The overstrength is calculated as the ratio of the maximum base shear V_y over the base shear when the first yield occurs V_1. The ratio between the base shear of the performance point and V_1 was also calculated.

, pushover in down-aisle direction:
maximum force _ V_y/V_1 = 32/23 = 1.39
performance point_ V_{PP}/V_1 = 16/23 = 0.7
Company A, medium seismicity, pushover in cross-aisle direction:
maximum force _ V_y/V_1= 152/116 = 1.3
performance point_ V_{PP}/V_1 = 36/116 = 0.31

The calculations are made for each company in the same way and are summarized in the following table.

	Down-aisle direction			**Cross-aisle direction**		
	Company A	Company B	Company C	Company A	Company B	Company C
$\Omega = V_y/V_1$						
V_{PP}/V_1						

Table 8.3: Overstrength calculations (racks in medium or low seismicity zone)

It can be noticed that while in pushover in down-aisle direction the overstrength factor varies from 1.4 to 2.2, in cross-aisle direction it is smaller, around 1.2 for all cases.

Ductility calculations

The ductility μ is calculated in each case by dividing the maximum top displacement d_{max} with the top displacement d_y that refers to the yielding point of the bilinear curve: $\mu= d_{max}/d_y$. As far as the performance point is concerned, a similar factor d_{PP}/d_y was also calculated.

Company , , pushover in down-aisle direction:
ductility _ $\mu= d_{max}/d_y$ = 17/12.4 = 1.37
ductility of performance point_ $\mu_{PP}= d_{PP}/d_y$ = 6 / 12.4 = 0.48

Company A, medium seismicity, pushover in cross-aisle direction:
ductility _ $\mu = d_{max}/d_y = 18.5/12 = 1.54$
ductility of performance point_ $\mu_{PP} = d_{PP}/d_y = 2.8/12 = 0.23$

The calculations are made for each company in the same way and are summarized in the following table.

	Down-aisle direction			**Cross-aisle direction**		
	Company A	Company B	Company C	Company A	Company B	Company C
$\mu = d_{max}/d_y$						
d_{PP}/d_y						

Table 8.4: Ductility calculations (racks in medium or low seismicity zone)

Calculation of q capacity factor

As mentioned before the q capacity factor can be calculated by multiplying the ductility with the overstrength: $q_{cap} = \Omega * \mu$.
To be more specific, the capacity factor is actually given by the relationship $q_{cap} = q_d * q_o$ where q_d refers to ductility and q_o refers to overstrength (Ω). However for structures whose fundamental period is larger than 0.6 sec (flexible systems) the rule of equal displacements applies which means that $q_d = \mu$. In the other case (stiffer systems), the rule of equal energies applies which means that $q_d = \sqrt{(2\mu-1)}$. All the structures examined during in this thesis have T>0.6 sec so it is assumed that $q_d = \mu$.

The calculations are made for each company in the same way and are summarized in the following table.

	Down-aisle direction			**Cross-aisle direction**		
	Company A	Company B	Company C	Company A	Company B	Company C
$q_{cap} = \Omega * \mu$						

Table 8.5: q capacity and demand factors (racks in medium or low seismicity zone)

8.5.2. Calculation of q factor based on Life Safety (LS) performance criterion

An attempt was made to specify the q factor for each case. The calculating procedure was the following: In each case, the step of the pushover analysis in which the limit of Life Safety performance level was achieved, was noted. For this step, the top displacement of the rack was named δ_{LS}. Then the initial stiffness K_0 of each structure was calculated using the base shear and the top displacement of the first step in the pushover analysis. The magnitude of the elastic force that would cause the top displacement to be equal with δ_{LS} is $F_{el} = K_0 * \delta_{LS}$. In order to retrieve the q factor, this elastic force F_{el} was divided with the design force F_{Ed} that was indicated by the companies in their technical reports:

$$q = F_{el} / F_{Ed}$$

It should be noted that the structure was considered to reach the Life Safety performance level when either the plastic hinges activated or the multi-linear links used, reached a defined point in their inelastic behaviour. The defined point for the hinges was the middle of the distance between point B and C (see figure below). The selection of this point was indicated by FEMA 356 as shown in the following picture.

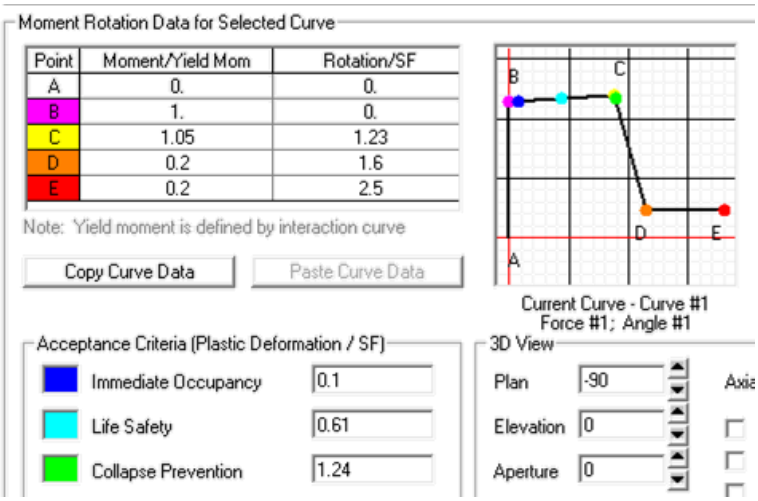

Figure 8.11: Definition of Acceptance Criteria for hinges

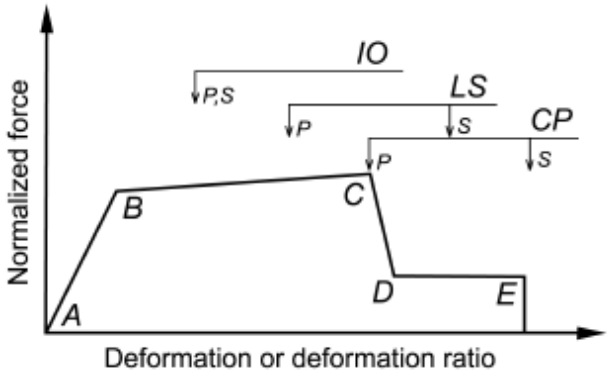

Figure 8.12: Acceptance criterion according to FEMA 356

As far as the links are concerned, the Life Safety performance point was approached with a graphic way. The moment-rotation graphs were plotted and they were simulated as bilinear, with the tangent of the second line being the one tenth of the initial stiffness. The first intersection point between the moment-rotation curve and the line of the reduced stiffness was considered to indicate the critical step. Usually this point coincided with the failure point. The q factors calculated are summarized in the following table. The q factor that was used by the companies during the design of the racks is also presented.

	Company A	Company B	Company C
Direction	DA CA	DA CA	DA CA
q factor calculated (LS)			
q in design			

Table 8.6: q factors for medium and low seismicity models in down aisle (DA) and cross aisle (CA) direction

8.6. Racks designed for high seismicity

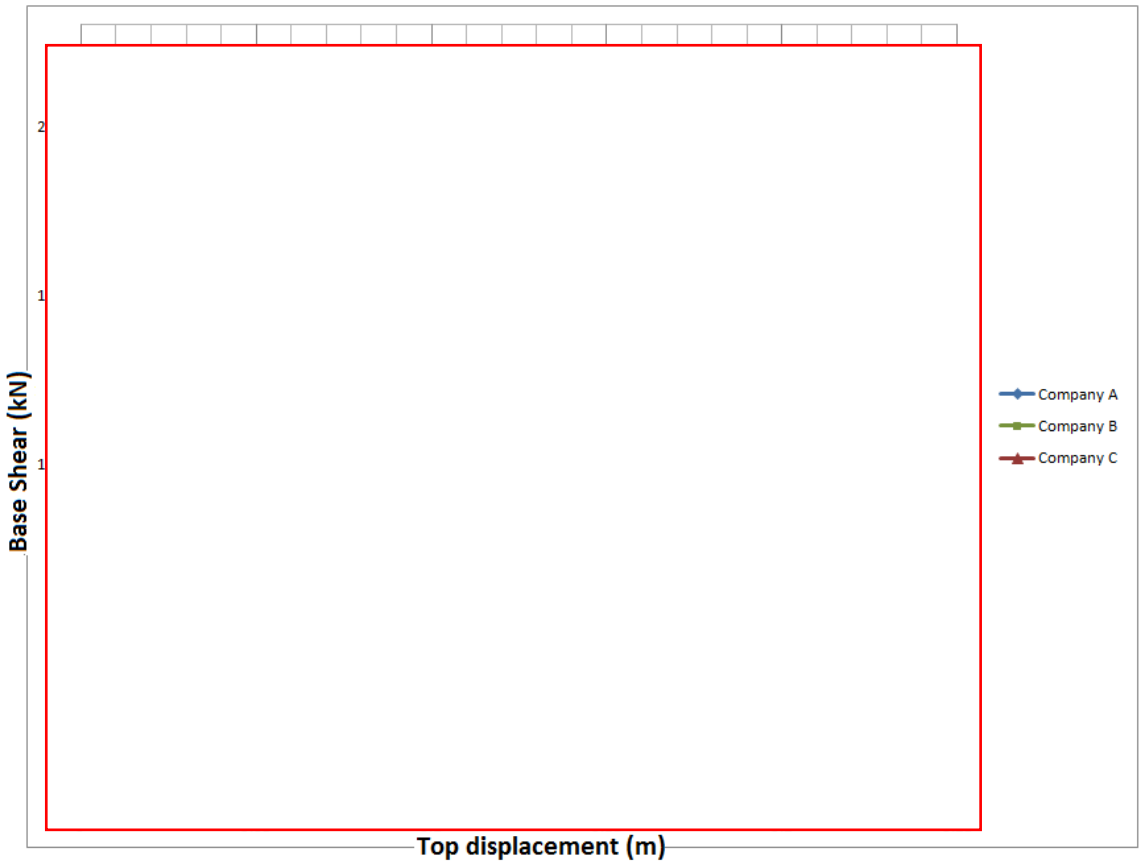

Figure 8.13: Pushover curves and performance points in down-aisle (DA) direction, racks in high seismicity zone

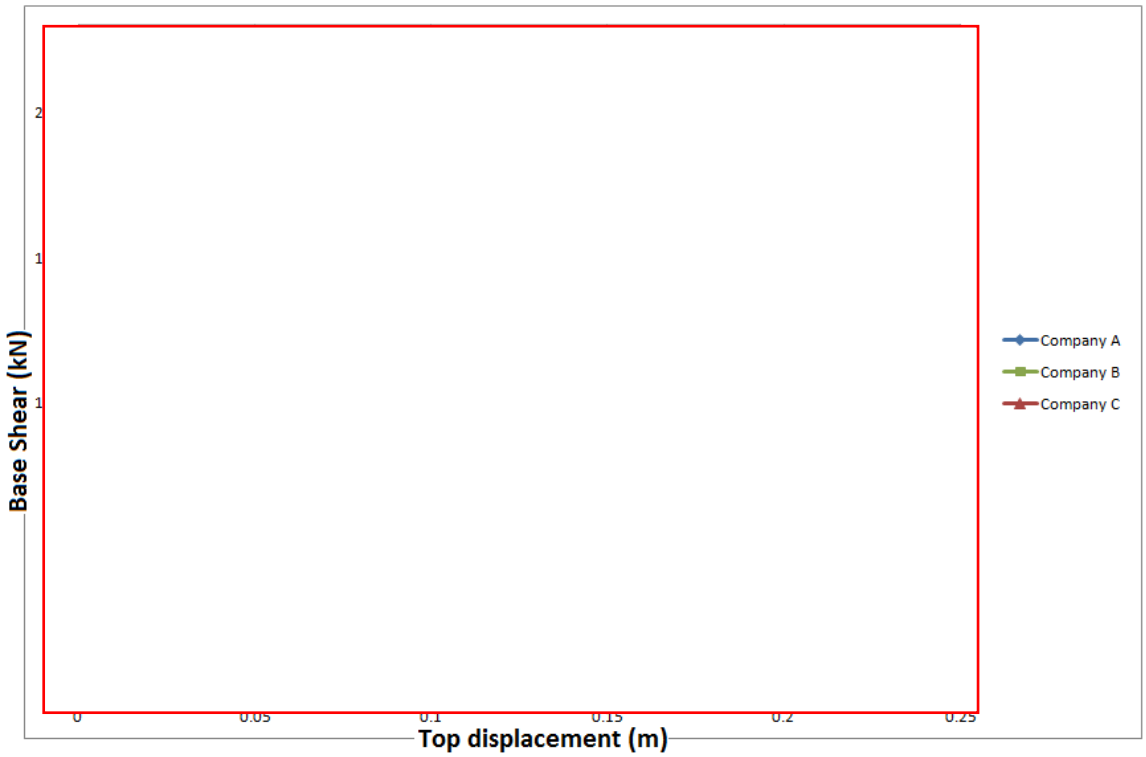

Figure 8.14: Pushover curves and performance points in cross-aisle (CA) direction, racks in high seismicity zone

Design parameters	Company A	Company B	Company C
a(g)*γ	0.25*1.00= 0.25 (g)	0.25*0.84= 0.21 (g)	0.30*0.84= 0.252 (g)

Table 8.7: Seismic design parameters (racks in high seismicity zone)

It can be observed in Table 8.3 that Company C's rack is designed to withstand larger seismic accelerations. Apart from that, the Company C rack has the largest dead loads (24.9kN) as it is designed to have the largest gross sections of uprights and beams [Chapter 4]. As a result the fact that it appears to be the stiffest one is not surprising.
On the other hand, Company B's rack is the lightest structure and also the only one without symmetric diagonals in the upright frames which affects its response in cross-aisle direction and could possibly play a role in its early failure. Apart from this, it does not have extra rear frames with vertical bracings, a fact that clearly affects its response in down-aisle direction and could partly explain the great difference (in the base shear measurements) between this company and the other two.

As far as the upright frame diagonals are concerned, Company C has the most "dense" configuration with forty (40) elements per upright frame, followed by approximately thirty (30) elements per frame in Company A, and only twelve (12) elements per frame in Company B. However in the case of Company B the few diagonals have almost the double gross section, compared to the other companies.
As far as the horizontal bracing are concerned, Company C appears to have the fewest (only one) and Company A appears to have the most, since it has double horizontal bracings in more bays as well as levels.

8.6.1. Calculation of overstrength, ductility and q capacity factor

As it was mentioned in unit 8.4.1, every capacity curve was approached as bilinear for the specific calculations [see figure 8.10]. The bilinear curve has an inclined part with the slope of the initial stiffness and a horizontal part. In each bilinear capacity curve, three points are noted as significant: the (d_1,V_1) point which represents the first yield and the apparent reduce of the structure's stiffness, the (d_y,V_y) point which is the intersection between the declined and the horizontal lines and represents yielding as well as the commencement of inelastic displacements and the (d_{max},V_y) point which represents the ultimate step (failure).

Three factors can be derived by the definition of the aforementioned points:
_the overstrength $\Omega=V_y/V_1$,
_the ductility $\mu= d_{max}/d_y$ and
_the q capacity factor $q_{cap} = \Omega * \mu$.

Overstrength calculations

, pushover in down-aisle direction:
maximum force _ $V_y/V_1 = 136/100 = 1.36$
performance point_ $V_{PP}/V_1 = 112/100 = 1.12$

, pushover in cross-aisle direction:
maximum force _ V_y/V_1 = 170/110 = 1.55
performance point_ V_{PP}/V_1 = 140/110 = 1.27
The calculations are made for each company in the same way and are summarized in the following table.

	Down-aisle direction			Cross-aisle direction		
	Company A	Company B	Company C	Company A	Company B	Company C
$\Omega = V_{max}/V_y$						
V_{PP}/V_1						

Table 8.8: Overstrength calculations (racks in high seismicity zone)

Ductility calculations

The ductility μ is calculated in each case by dividing the maximum top displacement d_{max} with the top displacement d_y that refers to the yielding point of the bilinear curve: $\mu = d_{max}/d_y$
As far as the performance point is concerned, a similar to ductility ratio (d_{PP}/d_y) was also calculated.

', pushover in down-aisle direction:
ductility _ $\mu = d_{max}/d_y$ = 20 / 9.6 = 2.08
ductility of performance point_ $\mu_{PP} = d_{PP}/d_y$ = 9.5 / 9.6 = 0.99
, pushover in cross-aisle direction:
ductility _ $\mu = d_{max}/d_y$ = 22 / 16 = 1.38
ductility of performance point_ $\mu_{PP} = d_{PP}/d_y$ = 13.6/ 16 = 0.85

The calculations are made for each company in the same way and are summarized in the following table.

	Down-aisle direction			Cross-aisle direction		
	Company A	Company B	Company C	Company A	Company B	Company C
$\mu = d_{max}/d_y$						
d_{PP}/d_y						

Table 8.9: Ductility calculations (racks in high seismicity zone)

Calculation of q capacity factor

As mentioned before the q capacity factor can be calculated by multiplying the ductility with the overstrength: $q_{cap} = \Omega * \mu$.
The calculations are made for each company in the same way and are summarized in the following table.

	Down-aisle direction			Cross-aisle direction		
	Company A	Company B	Company C	Company A	Company B	Company C
$q_{cap} = \Omega * \mu$						

Table 8.10: q capacity and demand factors (racks in medium or low seismicity zone)

8.6.2. Calculation of q factor based on Life Safety (LS) performance criterion

The q factors calculated according to the achievement of the Life Safety performance level, as it was described in unit 8.4.2, are summarized in the following table. The q factor that was used by the companies during the design of the racks is also presented. It can be noticed that in two cases (companies B and C) the q factor of the racks was overestimated by the companies.

	Company A		**Company B**		**Company C**	
Direction	DA	CA	DA	CA	DA	CA
q factor calculated (LS)						
q in design						

Table 8.11: q factors for high seismicity models in down aisle (DA) and cross aisle (CA) direction

8.7. Calculation of performance point' q factor

A behaviour factor concerning the performance point (P.P.) was also calculated. This q factor is given by the formula: $q_{PP}= V_{elPP} / V_1$, where V_{elPP} refers to the elastic force that would be demanded in order to obtain a top displacement equal to the target displacement (which means that $V_{elPP} = K_0 * d_{PP}$) and V_1 refers to the first yield as mentioned before.
The calculations were made for each case and are summarized in the following table for both medium-low and high seismicity models.

company/direction	**Company A**		**Company B**		**Company C**	
seismicity	DA	CA	DA	CA	DA	CA
medium-low						
high						

Table 8.12: q_{PP} factors concerning the Performance Point, for all cases examined

It can be noticed that the q_{PP} factors concerning the high seismicity models are relatively larger. That has to do with the fact that the Performance Point in all of these cases was estimated to be after the yielding of the structure.

8.8. Table summarizing the factors μ, Ω, q for all cases examined

medium seismicity	**Company A**		**Company B**		**Company C**	
	DA	CA	DA	CA	DA	CA
ductility **μ**						
overstrength **Ω**						
q = Ω*μ						
q used in design						

high seismicity	**Company A**		**Company B**		**Company C**	
	DA	CA	DA	CA	DA	CA
ductility **μ**						
overstrength **Ω**						
q = Ω*μ						
q used in design						

Final note:

Since the "Seisracks 2" research project is now in progress, these comments and results remain to be updated or corrected in the future. The experiments (full scale pushover tests) combined with new component/connection tests along with the computational approach through a more sophisticated software (which would also take into account the possible sliding of the pallets), should provide valuable information on the real properties of the structures' elements and connections as well as on the racks' seismic responses. Contributing thus to an optimized seismic design of this type of structures and to a more advanced background of relevant Codes and Regulations.

References

1. ATC 40, Seismic Evaluation and Retrofit of Concrete Buildings, Seismic Safety Commission, State of California, November 1996.

2. Carydis P., Castiglioni C.A., Lekkas E., Kostaki I., Lebesis N and Drei A., "The Emilia Romagna, May 2012 earthquake sequence: The influence of the vertical earthquake component and related geoscientific and engineering aspects", *Ingegneria Sismica: International Journal of Earthquake Engineering*, vol.2-3, July 2012.

3. Castiglioni C.A., *Seismic behaviour of steel storage pallet racking systems*, Structural Engineering Department of Politecnico di Milano, Milano, 2008.

4. CEN/TC 250, Eurocode 3: Design of steel structures - Part 1-1: General rules and rules for buildings. European Standard prEN 1993-1-1, final draft, December 2003

5. CEN/TC 250, Eurocode 8: Design of structures for earthquake resistance- Part 1: General rules, seismic actions and rules for buildings. European Standard prEN 1998-1, final draft, December 2003

6. Chung K.F., Building design using cold-formed steel sections: worked examples, the Steel Construction Institute (CSI), Berkshire, 1993.

7. Computers and Structures Inc., CSI Analysis Reference Manual for SAP2000®, ETABS®, and SAFE®, Berkeley, California, USA, 2010.

8. Degee H., Rossi B. and Jehin D., "Geometrically nonlinear analysis of steel storage racks submitted to earthquake loading", *International Journal of Structural Stability and Dynamics*, vol.11, no 5, 2011, pp 949-967.

9. Degee H. and Denoel V., Numerical modeling of storage racks subjected to earthquake, *ECCOMAS Thematic Conference on Computational Methods in Structural Dynamics and Earthquake Engineering*, Rethymno, Crete, Greece, June 2007.

10. Dubina D., Ungureanu V. and Crisan A. (2010), Experimental and numerical investigation of ultimate capacity of pallet rack members_ presentation of investigation program, ECCS TC7.5 Meeting, Barcelona, Spain, January 2010.

11. FEMA 356, Prestandard and commentary for the seismic rehabilitation of buildings, Federal Emergency Management Agency, November 2000.

12. FEMA 460, Seismic considerations for steel storage racks located in areas accessible to the public, Prepared by the Building Seismic Safety Council for the Federal Emergency Management Agency, National Institute of Building Sciences, Washington, September 2005.

13. FEM 10.2.02, The Design of Static Steel Pallet Racks, Federation Europeen de la Manutention, August 2000.

14. pr-FEM 10.2.08, Recommendations for The Design of Static Steel Pallet Racks under Seismic Conditions, final draft, Federation Europeen de la Manutention, December 2005.

15. FEM Racking and Shelving product group, European Racking Federation, Storage equipment information bulletin no.2: Latest developments in the harmonization of the design and use of storage equipment, *ERF Info : FEM 10 / I-02* , July 2010.

16. Godley M.H.R. and Beale R.G., Investigation of the effects of looseness of bracing components in the cross-aisle direction on the ultimate load-carrying capacity of pallet rack frames, *Thin-Walled Structures*, vol. 46, march 2008, pp 848-854. (www.sciencedirect.com)

17. Habibullah A. and Pyle S., Practical Three Dimensional Nonlinear Static Pushover Analysis, *Structure Magazine*, Winter, 1998.

18. Izadinia M., Rahgozar M.A. and Mohammadrezaei O., Response modification factor for steel moment-resisting frames by different pushover analysis methods, *Journal of Constructional Steel Research,* vol. 79, 2012, pp 83–90.

19. Khoshnoudian F. , Mestri S. and Abedinik F., Proposal of lateral load pattern for pushover analysis of RC buildings, *Computational Methods in civil Engineering*, vol. 2, 2011, pp 169-183. (http://research.guilan.ac.ir/cmce)

20. Sajjaa S.R., Beale R.G and Godley M.H.R., Shear stiffness of pallet rack upright frames, *Journal of Constructional Steel Research*, vol. 64, 2008, pp 867-874. (www.sciencedirect.com)

21. Schafer B.W., Thoughts on computational modeling of cold-formed steel, Coupled Instabilities in Metal Structures (CIMS), Sydney, Australia, 2008.

22. Βάγιας Ι., Dubina D., Σιδηρές Κατασκευές από λεπτότοιχες διατομές ψυχρής διαμόρφωσης, εκδόσεις Κλειδάριθμος, Αθήνα, 2004.

23. Βάγιας Ι., Ερμόπουλος Ι., Ιωαννίδης Γ., *Σχεδιασμός δομικών έργων από χάλυβα με βάση τα τελικά κείμενα των Ευρωκωδίκων*, εκδόσεις Κλειδάριθμος, Αθήνα, 2005.